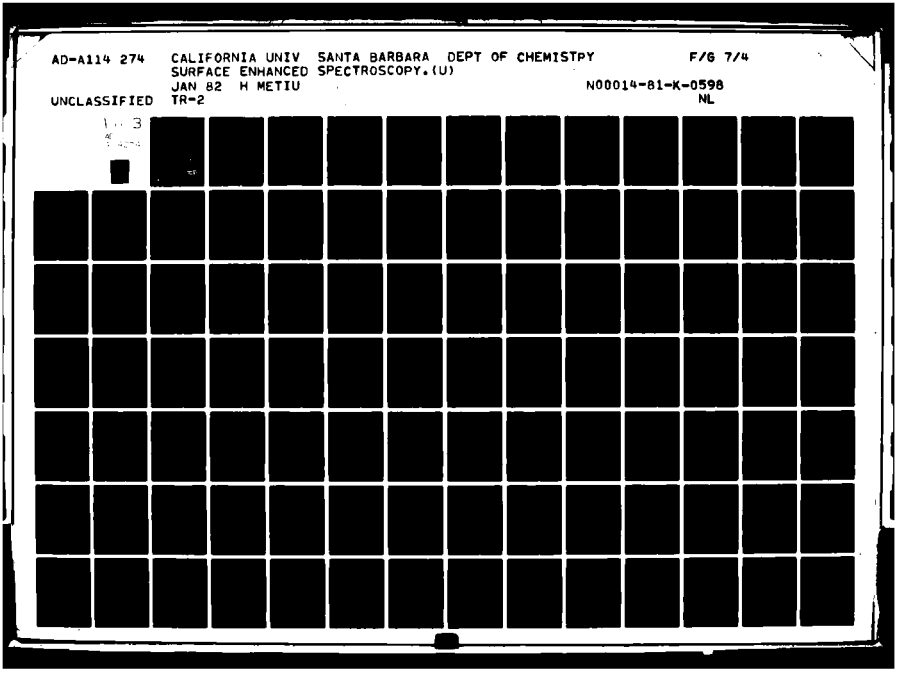
AD-A114 274
CALIFORNIA UNIV SANTA BARBARA DEPT OF CHEMISTPY
F/G 7/4
SURFACE ENHANCED SPECTROSCOPY.(U)
JAN 82 H METIU
N00014-81-K-0598
UNCLASSIFIED
TR-2
NL

SURFACE ENHANCED SPECTROSCOPY

Horia Metiu[a]
Department of Chemistry
University of California
Santa Barbara, California 93106

(a) Alfred P. Sloan Fellow and Camille and Henry Dreyfus Teacher-Scholar

OFFICE OF NAVAL RESEARCH

Contract N00014-81-K-0598

Task No. NR 056-766/4-21-81 (472)

TECHNICAL REPORT #2

SURFACE ENHANCED SPECTROSCOPY

by

Horia Metiu

Submitted for Publication

in

Progress in Surface Science

University of California, Santa Barbara
Department of Chemistry
Santa Barbara, CA 93106

January, 1982

SECURITY CLASSIFICATION OF THIS PAGE (When Data Entered)

REPORT DOCUMENTATION PAGE	READ INSTRUCTIONS BEFORE COMPLETING FORM
1. REPORT NUMBER: 2 — 2. GOVT ACCESSION NO.: AD-A114274	3. RECIPIENT'S CATALOG NUMBER:
4. TITLE (and Subtitle): SURFACE ENHANCED SPECTROSCOPY	5. TYPE OF REPORT & PERIOD COVERED: Interim Technical
	6. PERFORMING ORG. REPORT NUMBER:
7. AUTHOR(s): Horia Metiu	8. CONTRACT OR GRANT NUMBER(s): N00014-81-K-0598
9. PERFORMING ORGANIZATION NAME AND ADDRESS: University of California, Department of Chemistry, Santa Barbara, CA 93106	10. PROGRAM ELEMENT, PROJECT, TASK AREA & WORK UNIT NUMBERS: NR 056-766/4-21-81(472)
11. CONTROLLING OFFICE NAME AND ADDRESS: Office of Naval Research	12. REPORT DATE: January 1982
	13. NUMBER OF PAGES:
14. MONITORING AGENCY NAME & ADDRESS(if different from Controlling Office)	15. SECURITY CLASS. (of this report): Unclassified
	15a. DECLASSIFICATION/DOWNGRADING SCHEDULE:

16. DISTRIBUTION STATEMENT (of this Report)

This document has been approved for public release and sale; its distribution is unlimited.

17. DISTRIBUTION STATEMENT (of the abstract entered in Block 20, if different from Report)

18. SUPPLEMENTARY NOTES: Submitted for publication in Progress in Surface Science.

As the manuscript named above is a total of 267 pages, only the Table of Contents and Abstract have been submitted as part of this report.

19. KEY WORDS (Continue on reverse side if necessary and identify by block number)

Surface enhanced spectroscopy, colloids, fluorescence, Raman, absorption.

20. ABSTRACT (Continue on reverse side if necessary and identify by block number)

We review here the physical processes occurring when solid surfaces are used to modify in a substantial way the spectroscopic properties of molecules located nearby. This is achieved by enhancement of the local laser field, increase in molecular emission, and decrease in excited state life-time. We survey the use of flat surfaces, gratings, attenuated total reflection prisms, surfaces with small and large random roughness, isolated spheres and ellipsoids, and interacting solid surfaces. The spectroscopic

DD FORM 1 JAN 73 1473 EDITION OF 1 NOV 65 IS OBSOLETE

SECURITY CLASSIFICATION OF THIS PAGE (When Data Entered)

SURFACE ENHANCED SPECTROSCOPY

CONTENT PAGE

SURFACE ENHANCED SPECTROSCOPY

Horia Metiu[(a)]
Department of Chemistry
University of California
Santa Barbara, California 93106

ABSTRACT: We review here the physical processes occurring when solid surfaces are used to modify in a substantial way the spectroscopic properties of molecules located nearby. This is achieved by enhancement of the local laser field, increase in molecular emission, and decrease in excited state life-time. We survey the use of flat surfaces, gratings, attenuated total reflection prisms, surfaces with small and large random roughness, isolated spheres and ellipsoids, and interacting solid surfaces. The spectroscopic techniques surveyed are surface enhanced Raman, fluorescence, resonant Raman and absorption. The possibility of enhancing photo-chemical processes is also discussed. We have made an effort to present all these topics from an unifying point of view and to survey the experiments relevant to the concepts presented. The level of presentation is aimed at a non-expert or an experimentalist without extensive theoretical skills.

(a) Alfred P. Sloan Fellow and Camille and Henry Dreyfus Teacher-Scholar.

LIST OF ABBREVIATIONS

EELS - electron energy loss spectroscopy

DL - Drude Lorentz model

IR - Infrared

SEM - Scanning Electron Microscope

SRR - Small surface roughness

SERRS - Surface enhanced resonant Raman scattering

SERS - Surface enhanced Raman scattering

SES - Surface enhanced spectroscopy

UHV - Ultra-high vacuum

Erratum:

p. 13, line 14: life time → lifetime

p. 21, line 14: contsins → contains

p. 23, line 5: than → then

p. 44, lines 17, 18: oxydation → oxidation

p. 44, line 6 (from below): on the → of the

p. 49, line 9: expect[47] → expect[38,47]

p. 50, line 7: life time → lifetime

p. 50, Eq. (III.1): $(k_{11}^{sp})^2 \approx (\omega/c)^2 \, \mathrm{Re}\, \varepsilon(\omega) \left[1 + \mathrm{Re}\varepsilon(\omega)\right]^{-1}$ →

$$(k_{11}^{sp})^2 \approx (\omega/c)^2 \, \mathrm{Re} \left\{\varepsilon(\omega)\left[1 + \varepsilon(\omega)\right]^{-1}\right\} \simeq$$

$$(\omega/c)^2 \, \mathrm{Re}\, \varepsilon(\omega) \left[1 + \mathrm{Re}\, \varepsilon(\omega)\right]^{-1}$$

p. 51, line 13: tranlational → translational

p. 51, line 14: suppreses → suppresses

p. 51, line 9 (from below): funtions → functions

p. 52, line 2: life-time → lifetime

p. 52, line 14: wave-length → wavelength

p. 58, line 3: $\left(\Gamma_n f(y)\right)$ (in Eq. (16)) → $\left(\Gamma_n f(y)\right)$ in Eq. (16)

p. 58, line 15: ...wave length of light, than the wave length of the grating, and than the... → ...wavelength of light, the wavelength of the grating, and the...

p. 59, line 3 (from bottom): E_r^{Δ} → E_r^{s}

p. 60, Eq. (III.29): should be $K_1^2 = (\omega/c)^2 \mathrm{Re}\left\{\frac{\varepsilon(\omega)}{\varepsilon(\omega) + 1}\right\}$.

p. 60, Eq. (III.30): the right hand side of the equation is $\mathrm{Re}\left\{\varepsilon(\omega)/(\varepsilon(\omega) + 1)\right\}$

p. 65, line 10: plamon → plasmon

p. 68, line 17: Few... → A few...

p. 69, Eq. (III.32): $\mathrm{Re}\varepsilon(\omega) \left[1 + \mathrm{Re}\, \varepsilon(\omega)\right]^{-1}$ → $\mathrm{Re}\left\{\varepsilon(\omega) \left[1 + \varepsilon(\omega)\right]^{-1}\right\}$

p. 69, Eq. (III.33): $\mathrm{Re}\varepsilon(\omega) \, (1 + \mathrm{Re}\varepsilon(\omega))^{-1}$ → $\mathrm{Re}\left[\varepsilon(\omega)(1 + \varepsilon(\omega))^{-1}\right]$

p. 89, line 8: ...Eq. (44) parallel... → Eq. (44) contains parallel...

p. 158, line 6: coordinates[ ] → coordinates[108]

p. 158, line 7: Metiu[ ] → Metiu[122]

p. 189, line 3 (from bottom): gulk → bulk

p. 196, line 15: Compion → Campion

p. 196, line 15: Demuch → Demuth

p. 196, line 17: Ivan → Ivar

p. 196, line 2 (from bottom): R. Kohn → W. Kohn

p. 261, Ref [6]: should read T. E. Furtak

p. 262, Ref. [27]: Binning → Binnig

p. 262, bottom line: submieted → submitted

p. 255, Ref. [64]: L. Schlesinger → Z. Schlesinger

SURFACE ENHANCED SPECTROSCOPY

Horia Metiu[a]
Department of Chemistry
University of California
Santa Barbara, California 93106

(a) Alfred P. Sloan Fellow and Camille and Henry Dreyfus Teacher-Scholar

SURFACE ENHANCED SPECTROSCOPY

CONTENT PAGE

SURFACE ENHANCED SPECTROSCOPY

Horia Metiu[(a)]
Department of Chemistry
University of California
Santa Barbara, California 93106

ABSTRACT: We review here the physical processes occurring when solid surfaces are used to modify in a substantial way the spectroscopic properties of molecules located nearby. This is achieved by enhancement of the local laser field, increase in molecular emission, and decrease in excited state life-time. We survey the use of flat surfaces, gratings, attenuated total reflection prisms, surfaces with small and large random roughness, isolated spheres and ellipsoids, and interacting solid surfaces. The spectroscopic techniques surveyed are surface enhanced Raman, fluorescence, resonant Raman and absorption. The possibility of enhancing photo-chemical processes is also discussed. We have made an effort to present all these topics from an unifying point of view and to survey the experiments relevant to the concepts presented. The level of presentation is aimed at a non-expert or an experimentalist without extensive theoretical skills.

(a) Alfred P. Sloan Fellow and Camille and Henry Dreyfus Teacher-Scholar.

I. Introduction.

The purpose of this review is to explore the possiblity of modifying in a radical manner the spectroscopic properties of a molecule, by placing it near a solid surface. We are mainly interested in investigating those special circumstances under which the intensity and/or lifetime modifications are equal or larger than two orders of magnitude.

The solid may cause such effects electromagnetically, by modifying the laser field at the location of the molecule, as well as the lifetime and the emission intensity of the excited molecules. In addition, the binding of the molecule to the solid may affect the optical response of the molecule in a very substantial way. The relative importance of the electromagnetic and the molecular effects in producing a strongly modified signal is still a subject of debate and active research.

We have decided to concentrate mainly on electromagnetic effects because the theory is better developed, richer in consequences and has more predictive power. In pursuing the subject we have certain objectives that we would like to state explicitly.

(a) The electromagnetic effects can be discussed by solving Maxwell equations for an oscillating point dipole (the molecule) placed near a dielectric surface. The spectroscopic behavior of the molecule depends radically on the shape of the surface and its dielectric properties, as well as on the kind of spectroscopy performed. The research literature has developed explosively and generated an enormous amount of peculiar results, valid under peculiar conditions. We would like to show how all of them can be obtained from an unique theoretical scheme, built around few basic physical effects.

(b) Unfortunately the computational scheme mentioned above can be solved only for geometries which cannot yet be exactly produced in the laboratory, because we lack the ability of controlling precisely the surface shape and the surface-molecule distance. In those cases when a lot of care is taken to produce a certain configuration, we lack the means of proving to the disbeliever that the desired result has been achieved. So far we had to work with incompletely characterized surfaces or with surfaces for which no theory has been produced. For this reason, the experimental test of the theory is not a simple affair. We can form an opinion about the validity and the importance of the electromagnetic effects by examining, qualitatively or semi-quantitatively, a large number of trends expected to show up when the surface shape, the solid material, the molecule surface distance and the spectroscopic techniques are changed. This forced us to review extensively a large pool of data, which has been chosen for its power to illustrate various concepts and trends. We made no attempt to quote more experimental works than needed for such illustation.

(c) We have organized the material as required by a logical and readable presentation of the basic concepts and have made no attempt to pursue or even outline the historical development of the subject.

The material covered in the review should be of interest to several groups of people, having very different background and interests. (1) The molecular spectroscopists might want to learn how to use solid surfaces to modify and influence the spectroscopic signals of the molecules. (2) Surface scientists and electrochemists might be interested in the vibrational spectroscopy of surface molecules at rough surfaces or on small clusters. (3) People interested in the optical and electromagnetic properties of surfaces and small clusters might want to learn how to use molecular spectroscopy as a probe of these electromagnetic properties.

(4) Anyone with an interest in surface roughness will find here new ways to study it optically. (5) Curiosity seekers may find the topic amusing.

Since the subject is truly interdisciplinary, I made an effort to provide the required background as I went along. My aim has been to make the material accessible to non-experts and to those experimentalists who do not have a particularly strong training in theory.

Previous reviews[1-6] concentrated almost exclusively on surface enhanced Raman spectroscopy. Some[1-4] are already conceptually obsolete, but still contain a large and useful body of factual information. This article has practically no overlap with them. Otto's articles[5] present a point of view developed in his group which we have not discussed here since we had very little to add. Finally, the book edited by Chang and Furtak[6] has articles by leading experts and should nicely complement the present review.

II. General Theory

II.1. Statement of the problem

II.1A. A Broad Outline.

§1. Any theory of surface (or any other) spectroscopy must analyse three elements: the local electromagnetic field acting on each molecule, the molecular response to this field and the emission by the polarized molecule. To describe and interpret these processes we use, in most sections of this review, phenomenological models in which both the molecules and the solid are treated as polarizable objects. The phenomenology provides prescriptions for the computation of the polarization.

§2. The polarization of the solid. The polarization of the solid is computed by using the frequency dependent, complex dielectric constant $\epsilon(\omega)$. We assume[7-11] that $\epsilon(\omega)$ is the same at any point inside the metal and that it changes suddenly at the solid interface. Once this assumption is accepted, the involvement of the solid in the spectroscopy of surface molecules can be computed by solving Maxwell's equations.

This procedure has two, potentially severe, limitations. The dielectric response of the metal varies continuously through the interface and this variation can be treated as a sudden jump only if the location of the source causing the polarization and the location where the polarization field is measured, are both far from the surface.

In surface spectroscopy the molecules act (in the excitation process) as detectors of the local field while in the emission process they act as sources. If the surface-molecule distance is very small (~3- 5Å) the use of a discontinuous dielectric constant will introduce errors.

A further limitation appears when the polarization field varies rapidly in space. This is not the case for long wavelength photon fields but becomes a problem when the polarization source is a laser driven molecule located

at the surface, since this exerts on the metal a spatially inhomogeneous field. In such a case the polarization of the metal at a given location depends not only on the magnitude of the external field at that point (as assumed in the local, phenomenological theory)[7-11] but also on the magnitude of the field acting at each point of a neighbourhood of that location.

The consequences of the errors made in the phenomenological model, by ignoring the continuous variation of the dielectric response through the interface and the non-local character of the response, are analysed qualitatively in Section IV.

§3. The polarization of the molecule. In most of the present article we describe the molecular response to the local electromagnetic field by using point dipoles. In reality the induced charge distribution $\rho(\vec{r})$ has a finite size, extending over the dimensions of the molecule. Replacing this by a point dipole causes no problem if we consider the interaction of the molecule with the local field. The latter is smooth over distances equal to the molecular size and in such situations the response of the molecule is well approximated by a point dipole.[7-11] The interaction $\int e\,\rho(\vec{r})\,|\vec{r}-\vec{r}_e|^{-2}\vec{dr}$ between a metal electron of charge e, located at $\vec{r}_e$, and the molecular charge density $\rho(\vec{r})$ (induced by laser) can be replaced by the interaction of the electron with the induced dipole $\vec{\mu}(\vec{r}) = \int \vec{r}\,\rho(\vec{r})\,\vec{dr}$ only if the molecule-metal distance is larger than the molecular size. For adsorbed molecules this condition is not satisfied.

A further source of errors in the phenomenological models is the elimination of certain chemisorption effects that might play an important role in the polarization of the molecule. For example, as the laser drives

the molecular electrons, inducing thus an oscillating polarization charge, it is possible that the polarization process causes electron transfer back and forth between the molecule and the metal. If this happens the polarizability of the chemisorbed molecule may be substantially affected by the charge transfer. Another mechanism through which the polarizability of the adsorbed molecule may be augmented is due to the interaction between the electrons in the metal and the molecular nuclei. The dielectric response of the metal surface becomes a function of the amplitude of the molecular normal coordinates. Therefore the electrons in the metal surface will participate in the Raman scattering process in the same way as the molecular electrons, thus increasing the Raman signal.

Finally, for molecules close to the surface the excitation process is affected by the presence of the solid in many ways. Once excited the molecule can undergo a variety of processes. (a) It can emit a photon either into the vacuum or into the solid. The first process gives the natural line-width. The second one gives the broadening computed here through the "image field" model (to be discussed later). (b) When the molecule is close to the surface the excited electron can jump from the molecule into the solid. This process is likely if the molecular level occupied as a consequence of excitation is resonant with an empty state of the solid. The positive ion created by the charge transfer is then Auger neutralized.[12] (c) If the molecular orbital populated by the excitation process is resonant with a filled state of the solid, a metal electron can jump into the hole formed in the molecule by the excitation process and simultaneously eject the excited electron from the molecule.[12] Note that mechanism (a) and (c) are the Coulomb and exchange part of the same process of de-excitation.

The Coulomb one takes place at very large distances; the exchange part and the resonant ionization (process (b)) are short range processes. All of them contribute to the width of the upper level. The models used in the present review deal, in an approximate manner, with process (a) and ignore the others. They can be included by adding to the upper levels of the first layer molecules an additional width corresponding to a life-time of roughly 10^{-14} sec.

It is not yet clear to what extent the effects mentioned above are important, and how dangerous it is to leave them out, by using the phenomenological model. Here we take the view that when used with caution such a model yields semi-quantitative results. Since the experimental systems we are dealing with are rather imprecisely characterized this might be, as far as practical men are concerned, the proper level of description for many of the important aspects of the problems discussed here. If the effects ignored here are later understood quantitatively and shown to be important, they can be incorporated in the present framework without difficulty.

II.1.B. Once Over Lightly

§4. The local field. We consider a system consisting of a solvent, of surface molecules (adsorbed, chemisorbed or floating at some distance from the surface) and a solid surface (in most cases a metal). Since we discuss here laser generated processes only our model assumes that the spectroscopic

signal is generated because a given molecule, located at $\vec{r}_0$, is driven by a local electric field $\vec{E}_\ell(\vec{r}_0; t)$. This is written here as the sum of four terms,

$$\vec{E}_\ell(\vec{r}_0,t) = \vec{E}_i(\vec{r}_0, t) + \vec{E}_r(\vec{r}_0, t) + \vec{E}_{im}(\vec{r}_0, t) + \vec{E}_L(\vec{r}_0, t). \qquad (II.1)$$

The first term $\vec{E}_i(r_0,t)$ is the electric field caused by the incident laser beam in the absence of the "surface molecules" and of the solid surface, but in the presence of the solvent.

If the solid is present, a second field $\vec{E}_r(\vec{r}_0, t)$ appears because of the polarization of the solid by $\vec{E}_i$. Here $\vec{E}_r$ is called the reflected field while the sum $\vec{E}_p(\vec{r}_0, t) \equiv \vec{E}_i(\vec{r}_0, t) + \vec{E}_r(\vec{r}_0, t)$ is the primary field. The latter represents the total electric field established by the incident laser in the presence of the solid and solvent, but in the absence of the "surface molecules". Generally, we compute $\vec{E}_p$ by solving Maxwell's (and in special cases Laplace's) equations. In many cases the result is well known. For example if the surface is flat $\vec{E}_r$, and consequently $\vec{E}_p$, are given by Fresnel formulae [7-11].

The remaining two fields in Eq.(1) appear when the surface molecules are added to the system. First, consider the case when only the molecule placed at $\vec{r}_0$ is present. The molecule is polarized by the primary field $\vec{E}_p(\vec{r}_0, t)$ and as a result it acquires an induced dipole. The electric

field of this dipole polarizes the solid, which in turn produces an electric field at $\vec{r}_0$, denoted here as $\vec{E}_{im}(\vec{r}_0, t)$. For example, if the solid is a perfect conductor with a flat surface $\vec{E}_{im}(\vec{r}_0, t)$ can be computed very easily by using the so called image theorem, which shows that $\vec{E}_{im}$ is the field created by the image of the induced dipole with respect to the surface plane. Even though the image theorem cannot be generalized to hold for all practically interesting geometries and materials, we always refer to the polarization field $\vec{E}_{im}(\vec{r}_0, t)$ defined above as the <u>image field</u>.

Finally if we bring all the other molecules in place, they all get polarized (i.e. each acquires an induced dipole moment) and each causes an electric field at the point $\vec{r}_0$ where the local field is calculated. The sum of all these dipole fields is denoted here by $\vec{E}_L(\vec{r}_0, t)$ (this is the kind of field that appears during the derivation of the Lorentz-Lorenz formula).[11] In surface spectroscopy we need the dipole fields at $\vec{r}_0$ as modified by the presence of the solid surface (the dipole fields plus all the image fields). We call $\vec{E}_L(\vec{r}_0, t)$ the <u>Lorentz field.</u>

There is no compelling reason for using these names and/or this way of splitting the local field into a sum of terms. We do find it useful for all the applications discussed here and we hope that the nomenclature will be adopted by others; it seems that the advantage of having a common language outweighs whatever improvements one may obtain by continuously changing these names.

§5. <u>The spectroscopic role of these fields.</u> At this point it is necessary to anticipate later results and to point out that these fields play different roles in surface spectroscopy. The magnitude of the molecular response (i.e. the magnitude of the induced dipole) is proportional to the primary field $\vec{E}_p$.

The sum $\vec{E}_s(\vec{r}_0, t) = \vec{E}_{im}(\vec{r}_0, t) + \vec{E}_L(\vec{r}_0, t)$, which we call the secondary field, affects the induced dipole in a more subtle way, by modifying the effective polarizability of the molecule. Thus, if we consider a simple two level model the real part of the secondary field shifts the frequency needed to reach the upper level. This will affect the fluorescence frequency (both excitation and emission frequency) and the peak position in the resonant Raman effect. This shift is generally small. The imaginary part of the secondary field changes (increases) the width of the upper level. Thus it broadens the absorption line shape, shortens the fluorescence lifetime and lowers the resonant Raman intensity. While the image field $\vec{E}_{im}(\vec{r}_0, t)$ causes these effects at near zero surface coverage, the Lorentz field introduces in them a concentration (coverage) dependence.

It is very important to keep in mind that $\vec{E}_p$ and $\vec{E}_s$ affect different physical processes; if one looks at the right physical quantity one may neglect say $\vec{E}_s$ and compute only $\vec{E}_p$ (even though $\vec{E}_s$ might be larger than $\vec{E}_p$!), because the quantity being measured does not depend on $\vec{E}_s$. One such example is the intensity of the non-resonant (normal) Raman scattering, which does not depend on $\vec{E}_s$. An opposite situation is exemplified by the fluorescence lifetime, which depends on $\vec{E}_s$ only.

§6. The polarization of the molecule. The molecule located at $\vec{r}_0$ is under the influence of the local field $\vec{E}_\ell(\vec{r}_0, t)$ described at §4. We cannot simply assume that the induced dipole $\vec{\mu}$ is given by the molecular polarizability tensor dotted into $\vec{E}_\ell$. Some thought must be given to the fact that the terms composing $\vec{E}_\ell$ are of two kinds. The primary field $\vec{E}_p$ depends only on the incoming laser beam, the nature of the solvent and the nature and the positioning of the solid surfaces. In contrast, the secondary field $\vec{E}_s$ depends on the magnitude of the induced dipoles which we want to

compute in the first place. Therefore, we must be careful to compute $\vec{E}_s$ and $\vec{\mu}$ self-consistently.

The simplest way of doing this is to use the Drude-Lorentz equation. The details of the procedure will be discussed later. A reader with experience in this field will have no trouble in anticipating the general features of the result. If the incident electric field has the time dependence $\vec{E}_i(\vec{r}_0, t) = \vec{E}_i(\vec{r}_0)e^{-i\omega t}$ then the primary field has the form $\vec{E}_p(\vec{r}_0, t) = \vec{E}_p(\vec{r}_0)e^{-i\omega t}$ and the induced dipole has a time dependence given by

$$\vec{\mu}(t) = \overleftrightarrow{\alpha}_R \cdot \vec{E}_p(\vec{r}_0)e^{-i\omega t} + \overleftrightarrow{\alpha}_{RS} \cdot \vec{E}_p(\vec{r}_0)e^{-i(\omega-\omega_v)t} + \overleftrightarrow{\alpha}_{RA} \cdot \vec{E}_p(\vec{r}_0)e^{-i(\omega+\omega_v)t} \qquad (II.2)$$

The quantities α_R, α_{RS}, α_{RA} are the "effective" Rayleigh, Raman-Stokes and Raman Anti-Stokes polarizability tensors, respectively. They differ from the corresponding gas phase quantities due to modifications caused by the presence of the surface. We write the equation (2) as if the molecule has only one active Raman vibration of frequency ω_v, since the extension to the many-modes case is obvious.

§7. The emission process. In spectroscopic measurements we detect the light emitted by the surface and by the dipoles induced in each molecule. In most cases the light is scattered by the solid elastically; exceptions are the innelastic scattering caused by the thermal vibrations of the rough surface or the continuum bright "background" caused by the fluorescence of the rough surface. There are two ways in which emission experiments can be done. In steady state experiments the excitation source is kept on and the emission is monitored continuously. Examples are Raman or Rayleigh scattering. The main quantity measured is the emission yield, i.e. the ratio

of the emitted versus incident intensity. One can also carry out relaxation experiments in which the excitation source is turned off and the decay of emission intensity is monitored. The quantities measured in this way are the emission life-time and the magnitude of the intensity.

The molecular emission is modified by the presence of the solid surface in several ways. (a) The simplest, is a mirror effect. Photons that would not have reached the detector in a gas phase experiment, bounce from the surface and are sent to the detector. Some extra brightness is thus obtained and the process is not different from enhancing the luminosity of a candle by putting a mirror behind it. (b) If the emitting dipole couples to the electromagnetic resonances of the solid (e.g. surface plasmons, polaritons, excitons, etc.) and these are rapidly damped(e.g. by coupling to phonons or electron-hole pairs) or are incapable of radiating, the emission life time is shortened (in relaxation experiments) and the emission efficiency is diminished (in steady state experiments). (c) The coupling to the electromagnetic resonance can have different effects if the resonance is radiative. To understand how this happens one should remember that the electric field caused by an oscillating dipole is the sum of two kinds of terms[7]. One is the far field, which is transverse, carries energy away from the dipole and depends on distance like e^{ikr}/r. The other is the near field, which depends on distance like $(r^{-3}-ikr^{-2})e^{ikr}$ and is very large in the region around the dipole. This field does not carry energy away from the dipole and cannot be detected by a device placed far from the dipole. In case of a radio antenna (which is an oscillating dipole) the near field might be felt by the neighbours of the station but not by listeners located far away. If we place a solid surface very close to the emitting dipole, the solid interacts with the large near field. One consequence

of this is that the electromagnetic resonances (the radiative as well as the non-radiative ones) of the surface are excited. If the excitation of a radiative resonance is very effective, energy is transferred from the molecular near field to the radiative resonance and then emitted to the detector. This increases the amount of energy radiated per unit time. In a steady state experiment this must result in increased absorption, in order to conserve energy. In a relaxation experiment the balance of energy is more complicated.

In some cases further enhancement can be obtained if the shape of the surface is designed (e.g. gratings) to concentrate most of the radiated energy in a preferred direction.

The effects just listed separately work, in many cases, together. The near field of the molecular dipole excites both the radiative and the non-radiative resonances of the surface. Whether this brightens or quenches the emission depends on the competition between the excitation of various surface modes, the nature of the material, the kind of spectroscopic measurement performed, the shape of the surface and the molecule-surface distance. All these features are discussed later in detail.

§8. Surface enhanced spectroscopy. Before proceeding to expound on the behaviour suggested so far, we wish to point out the main ideas of surface

enhanced spectroscopy, in the context of the theoretical scheme already outlined.

(a) It turns out that by careful choice of material, surface shape and incident frequency it is possible to enhance substantially the reflected field $\vec{E}_r$. This can be done in two ways: (α) by exciting an electromagnetic resonance or by (β) giving the surface a large curvature. The first effect requires a material which damps electromagnetic resonances inefficiently (such as Ag, InSb, SiC, etc.). It is surface shape sensitive and takes place at specified incident frequency. The second is, to some extent, insensitive to the incident frequency.

(b) It is possible to design experimental conditions in which the molecular emission is also enhanced. This happens if the molecular dipole drives a radiative electromagnetic resonance of the solid. Some spectroscopic techniques, such as Raman scattering, benefit from both effects. Absorption spectroscopy is influenced by (a) and fluorescence by (b).

(c) The presence of the surface may, under certain conditions, quench very effectively the molecular emission from surface molecules. This is mostly done by coupling to non-radiative electromagnetic resonances in the solid. From the point of view of surface enhanced spectroscopy such effects are the other (darker) side of the coin. Few spectroscopists have made a living by quenching signals, but resonance Raman scattering might offer an exception. This technique has always been plagued by the presence of fluorescence, which can obscure the resonant Raman signal. Van Duyne[13] has recently deposited molecules on a rough surface which is a very effective fluorescence quencher and managed thus to sharpen considerably the resonance Raman lines. What can make a fluorescence devotee despair, may be a resonance Raman practitioner's delight.

(d) The effects discussed above are electromagnetic in nature. There is a good chance that the polarizability of the molecule might be enhanced when the molecule binds to a metal surface. This provides an additional source of enhancement.

One must keep in mind that all spectroscopic techniques measure intensity, which is the square of the electric fields discussed here. Furthermore the effect of various mechanisms is multiplicative. For these reasons several modest enhancements of the electric fields and induced dipoles may combine to give a spectacular total. For example, in Raman spectroscopy the intensity is the square of a product of the enhanced emission factor, Raman polarizability and the reflected field. A factor of 10 enhancement in each of these effects, gives a total of 10^6 in the measured intensity.

II.1.C Filling in some of the details.

§9. The key question in surface enhanced spectroscopy is how to manipulate the properties of the surface in order to enhance spectroscopic signals. In some rare cases we may also wish to quench some undesired effects. There are already many ways of doing this and there is a danger that examination of series of examples may obscure the fact that there are some general features common to all systems. In this section we try to express the model discussed so far in mathematical terms that underline these common and general features.

We divide, for ease of presentation, the basic aspects of the process into molecular and electrodynamic. The molecular problem is to sort out to what extent the optical response (e.g. polarizability) of a molecule is changed by chemisorption. The electrodynamic problem is to establish the modification of the local and emitted fields by the presence of the surface. While the "molecular theory" is in its infancy, the electrodynamic one is fairly well developed. For this reason the general discussion concentrates on the electrodynamic aspects.

§10. The primary field. If the response of the solid is linear we can always write the primary field, at a point $\vec{r}$ located outside the solid in the form

$$\vec{E}_p(\vec{r},\omega) = \vec{E}_i(\vec{r},\omega) + \vec{E}_r(\vec{r},\omega) = [\overleftrightarrow{I} + \overleftrightarrow{R}(\vec{r},\omega)]\cdot\vec{E}_i(\vec{r},\omega). \qquad (II.3)$$

We assume a harmonic incident field $\vec{E}_i(\vec{r},t) \equiv \vec{E}_i(\vec{r},\omega)e^{-i\omega t}$. In Eq. (3) $\overleftrightarrow{I}$ is the unit tensor and $\overleftrightarrow{R}(\vec{r},\omega)$, is a quantity which we call the reflection tensor. It depends on the shape and the dielectric properties of the solid, the position of the point $\vec{r}$ relative to the surface and the dielectric properties of the solvent. An analytic expression can be obtained in several cases

of interest, though most often it is given by a computer program which generates $\vec{E}_r$ when $\vec{E}_i$ is known.

The reflection tensor contains all the information concerning the electromagnetic resonances which can be excited by the incident field. The resonance manifests itself through a pronounced increase of the components of $\overleftrightarrow{R}$ when the incident frequency equals the resonance frequency.

§11. The emission. Another general electrodynamic problem in surface enhanced spectroscopy is the computation of the electric field $\vec{E}(\vec{r},t)$ caused at $\vec{r}$ by an oscillating dipole $\vec{\mu}(t)$ located at $\vec{r}_o$. If the time dependence of the dipole is $\vec{\mu}(t) = \vec{\mu}(\omega)e^{-i\omega t}$ then the emitted field has the form $\vec{E}(\vec{r},t) = \vec{E}(\vec{r},\omega)e^{-i\omega t}$. $\vec{E}(\vec{r},\omega)$ can always be written [14] as

$$\vec{E}(\vec{r},\omega) = \overleftrightarrow{G}(\vec{r}, \vec{r}_o;\omega)\cdot\vec{\mu}(\omega) = \{\overleftrightarrow{G}_o(\vec{r},\vec{r}_o;\omega) + \overleftrightarrow{G}_s(\vec{r},\vec{r}_o;\omega)\}\cdot\vec{\mu}(\omega) \qquad (II.4)$$

The dyadic Green's function $\overleftrightarrow{G}$ is a symbol for the set of operations required to obtain $\vec{E}$ from Maxwell's equations when $\vec{\mu}$ is known. In few cases these operations can be specified in an analytic form. In others, all we have is a computer program. The word dyadic calls attention to the fact that the rule embodied in $\overleftrightarrow{G}$ is tensorial; in other words the vector $\vec{E}$ has a different direction than $\vec{\mu}$.

The two terms $\overleftrightarrow{G}_o$ and $\overleftrightarrow{G}_s$ have the following physical meaning. $\overleftrightarrow{G}_o\cdot\vec{\mu}$ is the field caused by the dipole in the absence of the solid. The extra term, $\overleftrightarrow{G}_s\cdot\vec{\mu}$ is needed because the surface is there and modifies the dipole emission. For example, in the simple case of a flat surface [2, 14] the field $\overleftrightarrow{G}_s\cdot\vec{\mu}$ represents (at large distance from the dipole) the radiation of the dipole $(\epsilon(\omega)-1)(\epsilon(\omega)+1)^{-1}\ \vec{\mu}$ placed at a position which is the mirror image of the molecular location with respect to the surface plane.

If $\overleftrightarrow{G}$ is correctly computed it will contain both the near field (for

$\vec{r}$ close to the dipole or the surface) and the far (radiated) field (for $\vec{r}$ far from both the surface and the dipole). In scattering problems it is customary to simplify the calculations by eliminating the part of $\overleftrightarrow{G}$ which contributes to the near field only. Uncritical use of such expressions can give completely erroneous results when applied to compute the field at points close to the surface.

The important quantity, as far as surface enhanced spectroscopy is concerned, is $\overleftrightarrow{G}_s$. This contains all the effects of the solid surface on dipole radiation. It depends on the dielectric properties and the shape of the solid, the position of the dipole with respect to the surface and the placement of the detector. If the dipole excites the electromagnetic resonances of the solid this will be evident in the frequency dependence of $\overleftrightarrow{G}_s(\vec{r},\vec{r}_o;\omega)$.

§12. Drude-Lorentz theory of the molecular response. To make further progress we must have a prescription which gives the response of the molecule to the laser field, providing thus the magnitude of the induced dipole $\vec{\mu}$. This is strictly speaking a problem which requires calculations of the electronic structure of the chemisorbed molecule and the response of the electrons to time dependent electromagnetic fields. We circumvent the need for such formidable calculations by using the Drude-Lorentz model (DL).

This postulates that the dipole induced in a molecule located at $\vec{r}$ and interacting with an electromagnetic field $\vec{E}_\ell(\vec{r},t)$ is given by the following differential equation:

$$\frac{d^2\vec{\mu}}{dt^2} + \omega_o^2\vec{\mu} + \Gamma_o \frac{d\vec{\mu}}{dt} = (e^2/m)\overleftrightarrow{f}\cdot\vec{E}_\ell(\vec{r},t). \qquad (II.5)$$

Such equations were used before quantum mechanics was invented and it is

interesting to review the thinking that went with them. It was assumed that the molecule contains some polarizable effective charge e* which interacts with the "external field" $\vec{E}_\ell(\vec{r},t)$. This pulls the charge from its "equilibrium" (neutrality) position and the displacement thus induced is denoted $\delta\vec{r}$. If the charge has a mass m*, Newton's equation for the process is

$$m^* \frac{d^2\delta\vec{r}(t)}{dt^2} = -k\delta\vec{r}(t) - \Gamma^* \frac{d}{dt}\delta\vec{r}(t) + e^*\cdot\vec{E}_\ell(\vec{r},t) \qquad (II.6)$$

The first term at the r·h·s of (6) expressed the belief in the stability of the molecule: an elastic force prevented the charge from taking off or causing extremely large polarization. The second term was necessary to account for the fact that once the charge is set in motion it cannot oscillate forever. Radiation or interaction with other molecules, (leading ultimately to heating) will damp the oscillator. The term $\Gamma^* d\delta\vec{r}(t)/dt$ introduces an exponential damping of the amplitude when the driving field $\vec{E}_\ell(\vec{r},t)$ is shut off. The last term in the r.h.s. represents the force exerted by the field on the charge. The form chosen in Eq.(6)is too simple since it always gives an induced displacement parallel to the incident field. This is not consistent with the asymmetry of molecules or with the experimental fact that a molecule can depolarize elastically scattered light. The concept of oscillator strength is thus necessary. It is postulated that the force term is $e^*\overleftrightarrow{f}^*\cdot\vec{E}_e$ where $\overleftrightarrow{f}^*$ is a tensor called oscillator strength. Multiplying now Eq. (6) by e^* and recognizing that the induced dipole is $e^*\delta\vec{r}$ we obtain

$$d^2\vec{\mu}/dt^2 + (k/m^*)\,\vec{\mu}(t) + (\Gamma^*/m^*)\,\frac{d\vec{\mu}}{dt} = [(e^*)^2/m]\overleftrightarrow{f}^*\cdot\vec{E}.$$

Now defining $\Gamma_o \equiv \Gamma^*/m^*$, $(k/m^*) = \omega_o^2$ and $(e^2/m)\overleftrightarrow{f} = [(e^*)^2/m^*]\overleftrightarrow{f}^*$ we obtain Eq. (5).

This equation contsins only three known quantities: ω_o^2, Γ and $\overleftrightarrow{f}$ (e and m are the electron charge and mass, respectively). One way of finding what these quantities mean is to inquire into the spectroscopic properties of the induced dipole defined by Eq. (5). If the external field has the form $\vec{E}_\ell(\vec{r},t) = e^{-i\omega t}\vec{E}_\ell(\vec{r},\omega)$ then $\vec{\mu}(t) = \vec{\mu}(\omega)e^{-i\omega t}$ (assuming that Γ, ω_o and $\overleftrightarrow{f}$ are time independent!) and Eq. (5) gives:

$$\vec{\mu}(\omega) = \frac{(e^2/m)\overleftrightarrow{f}\cdot\vec{E}_\ell(\omega)}{\omega_o^2-\omega^2-i\omega\Gamma} \equiv \overleftrightarrow{\alpha}(\omega)\cdot\vec{E}_\ell(\omega). \tag{II.8}$$

This equation defines a frequency dependent polarizability $\overleftrightarrow{\alpha}(\omega)$.

If we inquire into the absorption cross section for this dipole we find[15] the extinction coefficient K to be

$$K = \frac{(\Gamma/4c)(fe^2/m)}{(\omega_o-\omega)^2+(\Gamma/2)^2}\rho \tag{II.9}$$

Here ρ is the number density of oscillators and c is the velocity of light. We have assumed a refractive index close to one and have taken an isotropic oscillator strength. We see now that $\omega_o[1-(\Gamma^2/4\omega_o^2)]^{1/2} \approx \omega_o$ is the absorption frequency and Γ is the width of the Lorentzian absorbtion line. The model embodied by Eq.(5) corresponds to a two level system and ω_o and Γ are the frequency and the width of upper level.

If we carry out a relaxation experiment we must compute the emission of the dipole after the interruption of the field $\vec{E}_\ell$. The solution of Eq. (5) in this case is

$$\vec{\mu}(t) = \vec{\mu}(0)\ \exp(-it\omega_o[1-(\Gamma^2/2\omega_o^2)]^{1/2})\exp(-t\Gamma/2). \tag{II.10}$$

Since the emitted intensity is proportional to the square of the dipole moment the rate of decay is proportional to $\exp(-\Gamma t)$ so that Γ^{-1} is the lifetime of the upper level.

§13. This "empirical" analysis defines the quantities appearing in the DL equation (5) in terms of spectroscopic observables. We can also understand the model if we compare it to the quantum theory. The dipole induced by an oscillating field $\vec{E}_\ell(t) = (1/2)\vec{E}_0[\exp(-i\omega t) + \exp(i\omega t)]$ in a molecule is

$$\vec{\mu}(t) = \langle \Psi(t) | e \sum_i \vec{r}_i | \Psi(t) \rangle , \qquad \text{(II.11)}$$

where $\vec{r}_i$ are the positions of the electrons and $\Psi(t)$ is the molecular wave function in the presence of the field $\vec{E}_\ell(t)$. Since we are interested in the linear response we can compute $\Psi(t)$ to first order in $\vec{E}_\ell$ by perturbation theory. We then compute $d^2\vec{\mu}/dt^2$ by taking derivatives of Eq. (11) Assuming that the molecule has only one excited state we obtain

$$\ddot{\vec{\mu}}(t) + \omega_o^2 \vec{\mu}(t) = \frac{2e^2\omega_o}{3\hbar} (\vec{\mu}_{12}\vec{\mu}_{12}) \cdot \vec{E}_o \qquad \text{(II.12)}$$

Here $\omega_o = (E_2 - E_1)/\hbar$ and $\vec{\mu}_{12} = \langle \Psi_2 | e\sum_i \vec{r}_i | \Psi_1 \rangle$ is the transition dipole between the time independent states 1 and 2. If we compare this to Eq. (5) we find that

$$\overleftrightarrow{f} = (2m\omega_o/3\hbar)\vec{\mu}_{12}\vec{\mu}_{12}. \qquad \text{(II.13)}$$

This derivation of the DL model from quantum theory supports the conclusions reached empirically and in addition provides an expression for the oscillator strength. The "friction" term Γ does not appear because the quantum theory used here is too primitive. Using Wigner-Weisskopf theory[16] introduces Γ in the problem

and the equation for $\vec{\mu}(t)$ is then exactly like Eq. (5). Use of methods described by Heitler[7] can provide quantum expressions for Γ.

§14. We have gone through this analysis to point out that the Drude-Lorentz equation is not a "classical theory" of the polarizability in the sense that it treats the electron motion in the molecules by using classical electrodynamics. It is a phenomenological theory which guessed the correct structure of the quantum equations, on the basis of a "classical" argument concerning the polarization of molecular charges. The DL model is very useful in surface spectroscopy because it allows us to understand how the electrodynamic properties of the surface can affect the molecular polarizability. Thus one can show that the image fields change ω_o and Γ thus affecting the position and the width of the upper states.

Furthermore, the model allows empirical incorporation of some surface effects. Chemisorption will change $\overleftrightarrow{f}$, ω_o and Γ and one must keep in mind that the values of these quantities might be different from those of the gas phase molecule. There are however effects which are not contained in this model, such as charge transfer between metal and molecule during the polarization process or metal electrons participation in Raman scattering by molecular vibrations (see Section V.2 for details).

§15. *Putting all the parts together:* Using the notation developed above we can write the equations describing surface spectroscopy in a compact form. The electric field caused by the molecular dipoles $\vec{\mu}_\alpha(t) = \vec{\mu}_\alpha(\omega)^{-i\omega t}$, $\alpha = 1, \ldots, N$, at the detector location $\vec{R}_d$ is

$$\vec{E}(\vec{R}_d; t) = \vec{E}(\vec{R}_d; \omega) e^{-i\omega t}, \tag{II.14}$$

with

$$\vec{E}(\vec{R}_d; \omega) = \sum_{\alpha=1}^{N} \overleftrightarrow{G}(\vec{R}_d; \vec{r}_\alpha; \omega) \cdot \vec{\mu}_\alpha(\omega) \tag{II.15}$$

Here N is the number of induced dipoles (i.e.the number of surface molecules).

The molecular dipoles are given by the DL equation (5) for $\vec{\mu}_\alpha(\omega)$ (located at $\vec{r}_\alpha$):

$$-\omega^2\vec{\mu}_\alpha(\omega) + \omega_o^2\,\vec{\mu}_\alpha(\omega) - i\omega\Gamma_o\vec{\mu}_\alpha(\omega) = (e^2/m)\overleftrightarrow{f}\cdot\vec{E}_\ell(\vec{r}_\alpha;\omega). \qquad (II.16)$$

We use a two level model and assume that all surface molecules have the same frequency ω_o, width Γ_o and oscillator strength $\overleftrightarrow{f}$.

The local field at $\vec{r}_\alpha$ is the sum of the four terms defined by Eq. (1) and discussed in §4 and §10. The primary field is given by Eq. (3) in terms of the reflection tensor $\overleftrightarrow{R}(\vec{r};\omega)$. The image field is given by the equation

$$\vec{E}_{im}(\vec{r}_\alpha;\omega) = \overleftrightarrow{G}_s(\vec{r}_\alpha, \vec{r}_\alpha;\omega)\cdot\vec{\mu}_\alpha(\omega) \qquad (II.17)$$

which has been discussed at §11. Note that only the $\overleftrightarrow{G}_s$ part of the dyadic Green function $\overleftrightarrow{G}$ is needed since we want the field caused by the fact that the dipole polarizes the metal. It is essential that $\overleftrightarrow{G}_s$ in Eq. (17) is computed by a procedure in which the near fields are included.

Finally, the Lorentz field $\vec{E}_L(\vec{r}_\alpha;t) = \vec{E}_L(\vec{r}_\alpha;\omega)e^{-i\omega t}$ is given by

$$\vec{E}_L(\vec{r}_\alpha;\omega) = \sum_{\beta\neq\alpha}^{N}\overleftrightarrow{G}(\vec{r}_\alpha, \vec{r}_\beta;\omega)\cdot\vec{\mu}_\beta(\omega) \qquad (II.18)$$

This contains the fields exerted at the point $\vec{r}_\alpha$ by the dipoles $\vec{\mu}_\beta$, located at $\vec{r}_\beta$. $\overleftrightarrow{G}$ must contain the usual dipole field (through $\overleftrightarrow{G}_o$), the effect of surface polarization (through $\overleftrightarrow{G}_s$) and the near and far fields as well.

§16. We can now put together all these equations by replacing the local field $\vec{E}_\ell(\vec{r}_\alpha;\omega)$ with the sum given by Eq. (1) and the expressions (3), (17) and (18) for $\vec{E}_p$, $\vec{E}_{im}$ and $\vec{E}_L$, respectively. The result is

$$-\omega^2\vec{\mu}_\alpha(\omega) + \omega_o^2\vec{\mu}_\alpha(\omega) - i\omega\Gamma_o\vec{u}(\omega) = (e^2/m)\overleftrightarrow{f}\cdot\{[\overleftrightarrow{I} + \overleftrightarrow{R}(\vec{r}_\alpha;\omega)]\cdot\vec{E}_i(\omega)$$

$$+ \overleftrightarrow{G}_s(\vec{r}_\alpha, \vec{r}_\alpha; \omega)\cdot\vec{\mu}_\alpha(\omega) + \sum_{\beta\neq\alpha}^{N}\overleftrightarrow{G}(\vec{r}_\alpha, \vec{r}_\beta; \omega)\cdot\vec{\mu}_\beta(\omega)\}. \qquad \text{(II.19)}$$

We have now a complete computational scheme which can in principle provide the emission produced by N "surface" molecules, "dissolved" is a solvent (which can be taken to be vacuum), in the presence of pieces of solid material with arbitrary surface shape. The driving force is the incident laser field $\vec{E}_i(\vec{r},t) = \vec{E}_i(\vec{r},\omega)e^{-i\omega t}$.

To perform calculations we must specify the following:

(1) The incident field $\vec{E}_i$ (its magnitude, frequency, polarization and direction of propagation);

(2) the position, shape and dielectric properties of the solid materials. This allows — in principle — the computation of $\overleftrightarrow{R}$ and $\overleftrightarrow{G}_s$;

(3) the molecular properties (i.e. resonant frequency ω_o, excited state width Γ_o, and oscillator strength $\overleftrightarrow{f}$);

(4) the position of each molecule or the probability that the molecule 1 is at $\vec{r}_1$ and ... the molecule N is at $\vec{r}_N$. Strictly speaking only the pair distribution function is needed.

Assuming that we know all these, we must carry out the following sequence of operations: (a) solve Maxwell's equations to find $\overleftrightarrow{R}$ and $\overleftrightarrow{G}$; (b) solve the system of linear equations (19) to obtain $\vec{\mu}_\alpha(\omega)$, $\alpha = 1, \ldots N$; (c) compute the electric field $\vec{E}(\vec{R}_d;\omega)$ at the detector position by using Eq. (15); (d) find the intensity I detected at $\vec{R}_d$ (at frequency ω and polarization direction $\vec{\eta}$), which is proportional to $|\vec{\eta}\cdot\vec{E}(\vec{R}_d;\omega)|^2$; (e) model the probability distribution of the particle positions, dipole phases and orientations and use it to average $|\vec{\eta}\cdot\vec{E}(\vec{R}_d;\omega)|^2$.

§17. A simplified model: This is a formidable program which is considerably simplified by making three approximations. (1) We neglect the Lorentz field. (2) We assume incoherent scattering. (3) We consider that the molecules are randomly distributed. The justifications for these approximations and their consequences are examined below.

(1) Taking $E_L = 0$ neglects (see Eq. (18)) the field caused by the surface molecules $\beta = 1, \ldots \alpha-1, \alpha+1, \ldots, N$ at the location $\vec{r}_\alpha$ of the molecule α. This corresponds to removing the sum in Eq. (19). Mathematically this results in an enormous simplification since the 3N x 3N system of equations (19) is reduced to a 3x3 one. Physically, the approximation removes the coverage dependence of the level shift and width. This approximation can be avoided by using methods already developed for the study of peak frequency dependence on coverage in the IR spectroscopy of surface molecules[18]. There is very little work in this direction in Raman spectroscopy[19].

(2) The incoherent scattering assumption is equivalent in this context with the statement that the phases of the oscillators are uncorrelated. The assumption is implemented in the following manner. The intensity of the photons with polarization $\vec{\eta}$ and frequency ω, detected at $\vec{R}_d$, is

$$I \propto \langle |\eta \cdot \vec{E}(\vec{R}_d;\ \omega)|^2 \rangle = \sum_{\alpha\beta} \sum \langle [\vec{\eta} \cdot \overleftrightarrow{G}(\vec{R}_d,\ \vec{r}_\alpha;\ \omega) \cdot \vec{\mu}_\alpha(\omega)] [\vec{\eta} \cdot \overleftrightarrow{G}(\vec{R}_d,\ \vec{r}_\beta;\ \omega) \cdot \vec{\mu}_\beta(\omega)] \rangle \qquad \text{(II.20)}$$

We have used here the expression (15) for the field at the detector. The meaning of $\overleftrightarrow{G}$ is discussed at §11.

The average implied by the angular brackets is over the position of the oscillators and their phases. If the oscillator phases are uncorrelated the averages $\langle \vec{\mu}_\alpha \vec{\mu}_\beta \rangle$ give zero if $\alpha \neq \beta$. The double sum reduces to a single one and the total intensity is the sum of the intensity emitted by each oscillator. In reality there are some correlations and the average $\langle \vec{\mu}_\alpha \vec{\mu}_\beta^* \rangle$ decays with the distance $|\vec{r}_\alpha - \vec{r}_\beta|$. The length over which this decay takes place is the phase correlation length.

In all the works on enhanced spectroscopy the possible effects of phase correlations have been ignored. Coherence effects, and the possible enhancement produced by them, have thus been eliminated. In our opinion this is probably justified in the case of surface enhanced Raman scattering. The "Raman dipole" $\vec{\mu}_R$ is $\vec{\mu}_R = \left(\frac{\partial \vec{\mu}}{\partial Q}\right)_{eq} (Q - Q_{eq})$ where Q is the normal coordinate amplitude and Q_{eq} is its value at equilibrium nuclear configuration. There are thus two phases to contend with, one of the induced dipole and the other of the nuclear oscillator. Even if we polarize the molecules with a coherent source and excite the dipoles $\vec{\mu}$ coherently, this will not affect the phases of the normal coordinates $\delta Q = Q - Q_{eq}$. In the highly disordered systems used in SERS it is unlikely that there are significant correlations between δQ_α and δQ_β so that taking $\langle \delta Q_\alpha \delta Q_\beta \rangle \cong \delta_{\alpha\beta}$ is justified. In other words, we do not expect coherence effects to contribute significantly to SERS because of the lack of correlation in the phases of the nuclear vibrations. The coherence is also destroyed in fluorescence spectroscopy if following the excitation of the molecule the emitting state is "prepared" by an internal relaxation process lacking "phase memory" (e.g. vibrational relaxations or radiationless transitions).

(3) Another difficult problem is deciding how to carry out averages over the molecular positions $\vec{r}_\alpha$. All works on surface enhanced spectroscopy assume that the molecules are randomly distributed, i.e. that the probability of finding a molecule in the volume element $d\vec{r}$ at the point $\vec{r}$ is given by $d\vec{r}/V$, where V is the total volume.

There are many ways of improving on these assumptions ranging from theoretical models to Monte Carlo simulations. We doubt that, at this time, this is a fruitful line to pursue. Since we use surfaces whose structure is poorly characterized we can only get a crude approximation for the electrodynamic quantities $\overleftrightarrow{G}(\vec{R}, \vec{r}_\alpha; \omega)$, $\overleftrightarrow{G}(\vec{r}_\alpha, \vec{r}_\beta; \omega)$ and $\overleftrightarrow{R}(\vec{r}_\alpha; \omega)$. It seems therefore excessive to try to average these quantities over $\vec{r}_\alpha$ and $\vec{r}_\beta$ with high accuracy.

§18. An "oversimplified" model: In many of the qualitative discussions that follow we use an oversimplified model in which we take $\overleftrightarrow{f} = f\hat{z}\hat{z}$, $\overleftrightarrow{G}_s \equiv \hat{z}\hat{z}$ and $(\overleftrightarrow{I} + \overleftrightarrow{R})\,\vec{E}_i \equiv E_p\hat{z}$. Here $\hat{z}$ is a unit vector perpendicular to the surface and pointing away from the solid. Mathematically these approximations turn the system of 3x3 equations (19) (the sum in (19) is the Lorentz field and it is neglected) into a scalar equation. We do this to avoid, in qualitative discussions, all the cumbersome details related to inverse matrices, etc. None of the qualitative conclusions are affected by this simplification.

Physically, the approximations are also tenable. Taking $\vec{E}_p \equiv (\overleftrightarrow{I} + \overleftrightarrow{R}) \cdot \vec{E}_i \equiv E_p\hat{z}$ is reasonable since the primary field (see §10) tends to be perpendicular to the surface due to the boundary conditions. Taking $\overleftrightarrow{f} = f\hat{z}\hat{z}$ implies that the molecule is located with its most polarizable direction perpendicular to the surface. Thus a perpendicular primary field will induce a perpendicular dipole. The parallel components of the dipole are neglected. Finally $\overleftrightarrow{G}_s(\vec{r}_\alpha, \vec{r}_\alpha; \omega) \simeq \overleftrightarrow{G}_s\hat{z}\hat{z}$ states that the image field of a perpendicular dipole, at the dipole location, is perpendicular to the surface; this is also reasonable.

Due to all these, the equation (19) becomes

$$\mu(\omega) = \{\omega_o^2 - \omega^2 - i\omega\Gamma_o - (e^2/m) f G_s(\vec{r}_\alpha, \vec{r}_\alpha; \omega)\}^{-1} (e^2/m)\, f\, E_p \qquad (II.21)$$

with $\mu(\omega)$ defined by $\vec{\mu}(\omega) \simeq \mu(\omega)\hat{z}$. We see that the image field (included through $G_s(\vec{r}_\alpha, \vec{r}_\alpha; \omega)$) "renormalizes" the frequency and the width of the upper level (compare to Eq. (8) where the image field is absent).

II.1.D. The final round. Enhancement sources for various spectroscopic measurements.

§19. Terms containing the electromagnetic enhancement. The theory is now simple enough and general enough to make it worthwhile to try to pinpoint possible sources of electromagnetic enhancement. These are introduced through two quantities, the reflection tensor $\overleftrightarrow{R}$ and the scattering part $\overleftrightarrow{G}_s$ of the dyadic $\overleftrightarrow{G}$. They have a simple physical meaning. (a) Reflected field enhancement. The reflected field $\vec{E}_r(\vec{r};\ \omega)$ is related to the incident field $\vec{E}_i(\omega)$ through $\vec{E}_r(\vec{r};\ \omega) = \overleftrightarrow{R}(\vec{r};\ \omega)\cdot\vec{E}_i(\omega)$; the quantity $\overleftrightarrow{R}$ tells us the extent to which the laser field is modified by the presence of the surface. In most cases $\overleftrightarrow{R}$ is of order unity and no significant increase of the field is observed. However for specially chosen surface shapes and solid materials, $\overleftrightarrow{R}$ has a resonant behavior at certain frequencies. The resonance enhances the reflected field around the surface and a molecule located there is polarized much more effectively. Another enhancement source in $\overleftrightarrow{R}$ is the presence of a large surface curvature, which increases the field nearby. (b) Emission enhancement. The quant $\overleftrightarrow{G}_s(\vec{R}_d,\ \vec{r}_\alpha;\ \omega)$ gives the electric field $\vec{E}_s(\vec{R}_d;\ \omega) = \overleftrightarrow{G}_s(\vec{R}_d,\ \vec{r}_\alpha;\ \omega)\vec{\mu}_\alpha$ caused by the fact that an oscillating dipole $\vec{\mu}_\alpha$ located at $\vec{r}_\alpha$ polarizes the nearby solid making it radiate. $\vec{E}_s$ is the field caused by the radiation of the polarization charges and currents. In most cases $\overleftrightarrow{G}_s$ is of order unity but special surface geometries and well chosen materials can produce a resonance in $\overleftrightarrow{G}_s$. The field $\vec{E}_s$ is correspondingly enhanced. We shall see shortly that $\overleftrightarrow{G}_s(\vec{r}_\alpha,\ \vec{r}_\alpha;\ \omega)$ affects the fluorescence lifetime while $\overleftrightarrow{G}_s(\vec{R}_d,\ \vec{r}_\alpha;\ \omega)$ modifies the emission intensity.

In what follows we examine how these enhancement sources act in different spectroscopic measurements.

§20. The effective polarizability. Many of the spectroscopic measurements discussed here require knowledge of the molecular polarizability. The presence of the surface modifies this quantity in two ways. Binding to

surface causes changes of the electronic structure, which affect polarizability. The dielectric properties of the solid modify the electromagnetic properties of the system which also affect the polarizability. In the DL model the former are incorporated by the choice of the constants ω_o, Γ_o and $\overleftrightarrow{f}$. The latter appear explicitly in what we call the effective polarizability. This is obtained by solving Eq. (19).

$$\vec{\mu}_\alpha(\omega) = \{\omega_o^2-\omega^2-i\omega\Gamma_o-(e^2/m)\overleftrightarrow{f}\cdot\overleftrightarrow{G}_s(\vec{r}_\alpha, \vec{r}_\alpha; \omega)\}^{-1}\cdot (e^2/m)\overleftrightarrow{f}\cdot\{\overleftrightarrow{I} + \overleftrightarrow{R}(\vec{r}_\alpha; \omega)\}\cdot\vec{E}_i(\omega) \tag{II.22}$$

$$\equiv \overleftrightarrow{\alpha}_{eff}(\omega)\cdot\vec{E}_i(\omega) \tag{II.23}$$

$$\equiv \{\omega_o^2-\omega^2-i\omega\Gamma_o-(e^2/m)\overleftrightarrow{f}\cdot\overleftrightarrow{G}_s(\vec{r}_\alpha, \vec{r}_\alpha; \omega)\}^{-1}\cdot\overleftrightarrow{f}_{eff}(\vec{r}_\alpha, \omega)\cdot\vec{E}_i(\omega)(e^2/m) \tag{II.24}$$

The effective oscillator strength is defined as

$$\overleftrightarrow{f}_{eff}(\vec{r}_\alpha; \omega) \equiv \overleftrightarrow{f}\cdot\{\overleftrightarrow{I} + \overleftrightarrow{R}(\vec{r}_\alpha; \omega)\}. \tag{II.25}$$

Two important electrodynamic effects appear in the effective polarizability tensor $\overleftrightarrow{\alpha}_{eff}$. One is the renormalization of the oscillator strength, which comes about from incorporating the reflection tensor $\overleftrightarrow{R}$ into $\overleftrightarrow{f}_{eff}$. Since $\overleftrightarrow{R}$ can be enhanced by manipulation of the solid surface (see § 19) the effective oscillator strength is enhanced accordingly. The other is the renormalization of the upper level, by changing both its width and frequency.

§ 21. The effect is more clearly seen in the "oversimplified" model (§18, (21)) where

$$\mu(\omega) = \{\omega_o^2-\omega^2-\Delta^2(\omega)-i\omega\Gamma_{eff}(\omega)\}^{-1}\cdot(e^2/m)\, fE_p \tag{II.26}$$

with

$$\Delta^2(\omega) \equiv +(e^2/m)f\mathrm{Re}G_s(\vec{r}_\alpha, \vec{r}_\alpha; \omega) \tag{II.27}$$

and

$$\Gamma_{eff}(\omega) \equiv \Gamma_o + (e^2/m\omega)\mathrm{Im}G_s(\vec{r}_\alpha, \vec{r}_\alpha; \omega) \qquad (II.28)$$

The resonant frequency is now

$$\omega_{res} \cong \omega_o\left[1 - \frac{\Delta^2(\omega_o)}{\omega_o^2} - \frac{\Gamma_{eff}^2(\omega_o^2)}{4\omega_o^2}\right] \simeq \omega_o \qquad (II.29)$$

if $\omega_o >> \Delta(\omega_o)$, $\Gamma_{eff}(\omega_o)$. The effective width of the level is

$$\Gamma_{eff} \simeq \Gamma_o + (e^2/m\omega_o)\mathrm{Im}G_s(\vec{r}_\alpha, \vec{r}_\alpha; \omega_o) \qquad (II.30)$$

Clearly both shifts are due to the image field effects embodied in $G_s(\vec{r}_\alpha, \vec{r}_\alpha; \omega)$ (see Eq. (17) and §15).

Certain spectroscopic processes (e.g. Raman and Rayleigh scattering) are carried out under the condition $\omega_o >> \omega$. In this case $\{\omega_o^2-\omega^2-i\omega\Gamma_o-(e^2/m)\overleftrightarrow{f}\cdot\overleftrightarrow{G}_s\}^{-1} \simeq \omega_o^{-2}$ and the effective polarizability becomes

$$\overleftrightarrow{\alpha}_{eff}(0) \cong (e^2/m\omega_o^2)\overleftrightarrow{f}_{eff}(\omega) \qquad (II.31)$$

In what follows this will be called the static effective polarizability. In the absence of the surface this is given by $(e^2/m\omega_o^2)\overleftrightarrow{f}$ and represents the response of the molecule to a static electric field or a field whose frequency is much lower than

§22. Surface enhanced Rayleigh scattering. This is the simplest spectroscopic process in which the light scattered by the molecules is detected at the incident frequency ω. The process is substantially simplified if $\omega << \omega_o$ so that absorption by the upper level is avoided. In this case the molecular response is given by the static polarizability Eq. (31). Combining Eqs. (2) with (20), assuming incoherent scattering, and using Eq. (31) gives

$$I_{Ra} \propto \sum_\alpha \langle |\vec{n}\cdot\overleftrightarrow{G}(\vec{R}_d, \vec{r}_\alpha; \omega)\cdot\overleftrightarrow{f}_{eff}(\vec{r}_\alpha; \omega)\cdot\vec{E}_i(\omega)|^2 \rangle \qquad (II.32)$$

We recall (§11, Eq. (4)) now that $\overleftrightarrow{G} = \overleftrightarrow{G}_o + \overleftrightarrow{G}_s$, where $\overleftrightarrow{G}_s$ is the part which takes into account the presence of the solid surfaces; furthermore $\overleftrightarrow{f}_{eff} = \overleftrightarrow{f}(\overleftrightarrow{I} + \overleftrightarrow{R}(\vec{r}_\alpha; \omega))$ where $\overleftrightarrow{R}$ includes the surface effects. Therefore,

I_{Ra} contains a purely surface term of the form

$$\sum_{\alpha} |\vec{\eta}\cdot\overleftrightarrow{G}_s(\vec{R}_d, \vec{r}_\alpha; \omega)\cdot\overleftrightarrow{f}\cdot\overleftrightarrow{R}(\vec{r}_\alpha; \omega)\cdot\vec{E}_i(\omega)|^2; \tag{II.33}$$

both $\overleftrightarrow{G}_s$ and $\overleftrightarrow{R}$ would be zero if no solid surface was present. As we mentioned in §21 both $\overleftrightarrow{R}$ and $\overleftrightarrow{G}_s$ can be enhanced by proper choice of experimental conditions. A factor of 10 in $\overleftrightarrow{R}$ and $\overleftrightarrow{G}_s$ leads to a 10^4 enhancement in the intensity.

§22 Surface enhanced Raman scattering. The theory for this process parallels that of Rayleigh scattering. The only difference[20] is that the "Raman dipole" is involved in emission. This is obtained by taking the derivative of the polarizability with the normal coordinate of interest. If $\omega << \omega_o$, to avoid resonant Raman scattering, we need[20] only the static effective polarizability (§20, Eq. (26). Thus, we have

$$\vec{\mu}_\alpha^{RS}(t) = \vec{\mu}_\alpha^{RS}(\omega-\omega_V)e^{-i(\omega-\omega_V)t} \tag{II.34}$$

with

$$\vec{\mu}_\alpha^{RS}(\omega-\omega_V) = \left(\frac{\overleftrightarrow{\partial\alpha}^o_{eff}(\vec{r}_\alpha; \omega)}{\partial Q}\right)_{eq}\delta Q_o\cdot\vec{E}_p \tag{II.35}$$

and

$$\delta Q(t) = \delta Q_o e^{i\omega_V t} \tag{II.36}$$

Here $\delta Q(t)$ is the normal coordinate displacement with respect to the nuclear equilibrium position. In the Drude-Lorentz model the nuclear coordinate enters[20] into the oscillator strength $\overleftrightarrow{f}$ and the level position ω_o. The derivatives $\partial\overleftrightarrow{f}/\partial Q$ and $\partial\omega_o/\partial Q$ are empirical parameters. The intensity of Raman scattering is therefore proportional to

$$I_{RS} \propto \sum_{\alpha}\langle|\vec{\eta}\cdot\overleftrightarrow{G}(\vec{R}_d, \vec{r}_\alpha; \omega-\omega_V)\frac{\partial}{\partial Q}\{\omega_o^{-2}\overleftrightarrow{f}\}_{eq}\delta Q_o\cdot(\overleftrightarrow{I} + \vec{R}(\vec{r}_\alpha; \omega))\cdot\vec{E}_i(\omega)|^2\rangle. \tag{II.37}$$

The average is over the nuclear displacement δQ_o and the molecular positions $\vec{r}_\alpha$. In the absence of the surface $\overleftrightarrow{G} \to \overleftrightarrow{G}_o$ and $\overleftrightarrow{R} \to 0$.

The electromagnetic enhancement of the Raman signal is again proportional to $|\vec{n}\cdot\overleftrightarrow{G}_s(\vec{R}_d, \vec{r}_\alpha; \omega-\omega_V)\cdot\overleftrightarrow{R}(\vec{r}_\alpha; \omega)|^2$ and it is roughly similar to the Rayleigh case. The only difference is that $\overleftrightarrow{G}_s$ is taken at the detected frequency $\omega-\omega_V$ and $\overleftrightarrow{R}$ at the incident frequency ω. If ω_V is much smaller than the width of the electromagnetic resonance than both $\overleftrightarrow{G}_s(\vec{R}_d, \vec{r}_\alpha; \omega-\omega_V)$ and $\overleftrightarrow{R}(\vec{r}_\alpha; \omega)$ can be resonantly enhanced simultaneously.

Note that from a practical point of view it is more convenient to work with surface enhanced Raman scattering than with the Rayleigh one. The frequency of the detected photons is different from that of the incident ones and (except for a "background continuum") there is no signal in the absence of the molecules.

§23. Resonant Raman. We use here a crude theory to evaluate the main features of the surface enhanced resonant Raman spectroscopy (SERRS). Some error is made when we decide to use Eq. (19) (or its "oversimplified" version Eq. (21)) since in obtaining it we have assumed that ω_o, Γ_o and $\overleftrightarrow{f}$ are time independent. The assumption was implicitly made while going from Eq. (5) to (16) (or equivalently, to (19)). Mathematically this leads to great simplifications since only values of $\vec{\mu}_\alpha(\omega)$ at the same frequency appear in the Eq. (19). This is not true if Γ, ω_o or $\overleftrightarrow{f}$ depend on time[21]. However, the dependence of Γ, ω_o and $\overleftrightarrow{f}$ on the normal coordinate δQ (and through it, on time) is essential; without it the DL model will not lead to a Raman effect. The way out of the dilemma is to assume that Γ, ω_o and $\overleftrightarrow{f}$ are independent on δQ, solve the DL equation for $\vec{\mu}_\alpha$ and then allow Γ, ω_o and $\overleftrightarrow{f}$ to depend on δQ. This "approximation" causes no trouble with normal Raman, but is not very good as far as resonant Raman is concerned[20,21]. We use it here, however, for exploratory calculations and for qualitative discussions. Furthermore, we use the "oversimplified" model, § 12, Eq. (21).

We can now compute the derivative $\partial\mu/\partial Q$ and then take $\omega = \omega_o$ to satisfy the resonance condition Eq. (29). Carrying this out yields:

$$\left(\frac{\partial\mu_\alpha}{\partial Q}\right)_{res} = -\frac{(e^2/m)}{i\omega_o\Gamma_{eff}}\left[\frac{\partial f}{\partial Q} + \frac{2\omega_o f(\partial\omega_o/\partial Q)}{i\Gamma_{eff}} - \frac{f}{\Gamma_{eff}}(\partial\Gamma_{eff}/\partial Q)\right]E_p \equiv \tilde{\alpha}E_p \qquad (II.38)$$

The effective width Γ_{eff} is given by Eq. (30) and E_p is the z-component of the primary field (see Eq. (3)).

Numerical calculations indicate that G_s becomes rather large if the particle is close to the surface. Therefore, it will overwhelm Γ_o and dominate Γ_{eff} (Eq. 28)). The leading term in $(\partial\mu_\alpha/\partial Q)_{res}$ is proportional to $(\Gamma_{eff})^{-1}$ For this reason we expect that the presence of surfaces diminishes the value of $\tilde{\alpha}$ as compared to the gas phase value. However, by proper choice of working conditions we can increase the value of E_p (by using a surface with high curvature or one that has an electromagnetic resonance at the excitation frequency. Further intensity enhancement can be obtained in emission, exactly like in the case of Raman or Rayleigh scattering (§30 and §21). The intensity is proportional to (similar to Eq. (37))

$$I \propto \sum_\alpha \langle|\vec{\eta}\cdot\overleftrightarrow{G}(\vec{R}_d, \vec{r}_\alpha; \omega-\omega_v)\cdot\hat{z}\left(\frac{\partial\mu_\alpha}{\partial Q}\right)_{res}\delta Q_o|^2\rangle$$
$$= \sum_\alpha |\vec{\eta}\overleftrightarrow{G}(\vec{R}_d, \vec{r}_\alpha; \omega-\omega_v)\cdot\hat{z}\tilde{\alpha}E_p\delta Q_o|^2\rangle \qquad (II.39)$$

Since we use the "oversimplified" model the dipole is perpendicular to the surface. If we chose the working conditions so that the dipole emission excites an electromagnetic resonance, then $\overleftrightarrow{G}_s(\vec{R}_d, \vec{r}_\alpha; \omega-\omega_v) >> \overleftrightarrow{G}_o(\vec{R}_d, \vec{r}_\alpha; \omega-\omega_v)$ and (see Eq. $\overleftrightarrow{G}(\vec{R}_d, \vec{r}_\alpha; \omega-\omega_v) \sim \overleftrightarrow{G}_s(\vec{R}_d, \vec{r}_\alpha; \omega-\omega_v)$. However $\tilde{\alpha}$ is inversely proportional to $\overleftrightarrow{G}_s$ so the enhancement obtained in emission is roughly cancelled by the decrease of $\tilde{\alpha}$ However, there is still some electromagnetic enhancement left through E_p which is roughly proportional to $|R|^2$. Since ω_v is small, the incident photons of frequency ω, will excite the electromagnetic resonance, if the emission frequency $\omega-\omega_v$ does.

It is interesting to compare this to the electromagnetic enhancement

for ordinary Raman scattering. Arguments based on reciprocity theorem[22] indicate that $|G_s|^2$ and $|R|^2$ are of comparable magnitude. Therefore the electromagnetic enhancement of the normal Raman signal (when the system is operated on an electromagnetic resonance) is of order $|R|^2|G_s|^2 \sim |R|^4$, while that of resonant Raman is of order $|R|^2$. We find therefore the following rule of thumb: the enhancement factor for resonant Raman scattering is roughly equal to the square root of the enhancement factor of Raman scattering. This result is independent of the kind of roughness as long as both measurements are carried out at the same electromagnetic resonance and $\omega_o\Gamma_o \ll (e^2/m)f\mathrm{Im}G_s$ and $G_s \gg G_o$. The last two conditions mean that the enhancement is large and the electronic band used to carry out resonant Raman is narrow. If $\omega_o\Gamma_o \gg (\frac{e^2f}{m})\mathrm{Im}G_s$ the enhancement factors for Raman and resonant Raman are of comparable magnitude.

§24. Absorption spectroscopy. There are many ways of describing an absorption experiment and most depend on the particular geometrical arrangement. For this reason we prefer to compute the energy dissipated per unit volume and time at a point $\vec{r}_\alpha$ in the sample, in a steady state experiment The energy balance for the system is (MKSA units)

$$\int_{\mathcal{S}} (\vec{E} \times \vec{H}) \cdot d\vec{A} = - \int_{\mathcal{V}} \{\varepsilon_o \vec{E} \cdot \dot{\vec{E}} + \mu_o \vec{H} \cdot \dot{\vec{H}} + \vec{E} \cdot \dot{\vec{P}}\} dV \qquad \text{(II.40)}$$

Here we consider a small volume $\mathcal{V}$ of surface $\mathcal{S}$ surrounding the point $\vec{r}_\alpha$. The properties of the liquid (or vacuum) in which the "surface molecules" are imbedded appear through the dielectric and magnetic susceptibilities ε_o and μ_o. The surface molecules enter through the polarization $\vec{P}$. At steady state the first two terms in the right hand side are zero; that is, the energy stored into the fields is constant. We are left with

$$\int_{\mathcal{S}} (\vec{E} \times \vec{H}) \cdot d\vec{A} = -\int_{\mathcal{V}} \vec{E} \cdot \dot{\vec{P}}\, dV \qquad \text{(II.41)}$$

which equates two different ways of writing the net energy lost in the volume V in unit time. At the left we have the difference between the energy entering the surface and the energy leaving it ($\vec{E} \times \vec{H}$ is the Poynting vector, i.e. the energy flux). Therefore we must identify

$$(d\varepsilon/dt) \equiv -\vec{E} \cdot \dot{\vec{P}} \qquad \text{(II.42)}$$

with the energy stored in the atoms plus the energy dissipated, per unit time and unit volume.

To simplify matters we consider now the "over simplified" model of §18. The field acting on the oscillators is the primary field $\vec{E}_p$. From Eq. (26) this is $E_p = (m/fe^2)\{\omega_o^2 - \omega^2 - \Delta^2(\omega) - i\omega\Gamma_{eff}\}\dot{\mu}(t)$. The polarization is $\vec{P}(\vec{r}_\alpha, t) = \vec{P}(\vec{r}_\alpha; \omega)e^{-i\omega t} = \rho(\vec{r}_\alpha)\mu_\alpha(t)$. Here $\rho(\vec{r}_\alpha)$ is the number of oscillators per unit volume at $\vec{r}_\alpha$. Using these equations we have (neglecting $\Delta(\omega)$, which is small)

$$\frac{d\varepsilon}{dt} = (m/fe^2)\{\omega_o^2 - \omega^2 - i\omega\Gamma_{eff}\}\mu_\alpha(t)\, \rho(\vec{r}_\alpha)\mu_\alpha(t) \qquad \text{(II.43)}$$

Now we can identify the energy E_{osc}, stored into the oscillator, by recognizing that $\mu_\alpha(t) = e\delta r(t) = \mu(\omega)e^{-i\omega t}$, where $\delta r(t)$ is the charge displacement (see §12), and that

$$\frac{dE_{osc}}{dt} = \frac{d}{dt}\left\{\frac{m(\dot{\delta r})^2}{2} + m\omega_o^2(\delta r)^2\right\} = \frac{m}{e^2}\{\omega_o^2 - \omega^2\}\, \mu_\alpha(t)\dot{\mu}_\alpha(t). \qquad \text{(II.44)}$$

This is the rate of change of the total energy (kinetic plus potential) stored into the oscillator; using Eq. (44) in (43) gives

$$\frac{d\varepsilon}{dt} = f^{-1}\left[\frac{dE_{osc}}{dt} - i\omega(m/e^2)\Gamma_{eff}\mu_\alpha(t)\dot{\mu}_\alpha(t)\rho_\alpha(\vec{r}_\alpha)\right] \tag{II.45}$$

The first term at the right hand side of (45) is elastically stored in the oscillators and the second term is the energy dissipated. This is the quantity of interest to us and to relate it to observable quantities we must period average it. We obtain for the period averaged rate of energy dissipation:

$$\left(\frac{d\varepsilon}{dt}\right)_{dis} = f^{-1}\rho(\vec{r}_\alpha)(m/2e^2)\Gamma_{eff}(\omega)\omega^2|\mu(\omega)|^2$$

$$= (1/2)\rho(\vec{r}_\alpha)\Gamma_{eff}(\omega)\omega^2\frac{(fe^2/m)\,|E_p|^2}{(\omega_o^2-\omega^2)^2 + \omega^2\Gamma_{eff}^2(\omega)} \tag{II.46}$$

The rate of energy dissipation is maximum at the resonance frequency given by Eq. (29), which in most cases is very close to ω_o. On resonance, the rate of dissipation is

$$(d\varepsilon/dt)_{dis} = (fe^2\rho(\vec{r}_\alpha)/2m)(|E_p|^2/\Gamma_{eff}(\omega)) \tag{II.47}$$

If we operate the system such that an electromagnetic resonance is excited, both the primary field E_p and Γ_{eff} are enhanced; E_p through the reflection tensor $\overleftrightarrow{R}$ (see §10) and Γ_{eff} through $\mathrm{Im}\overleftrightarrow{G}_s(\vec{r}_\alpha, \vec{r}_\alpha; \omega)$ (see Eq. (28)). If $\vec{r}_\alpha$ is very close to the surface $\overleftrightarrow{G}_s$ becomes large. Its distance dependence is proportional to z^{-3}, where z is the distance of the oscillator to the surface. (For very small values of z [few Å], the formula for G_s breaks down!) On the other hand $\overleftrightarrow{R}$ tends to decay very slowly with the distance (over 50 Å or more). In most specific examples, we find that generally $|R|^2$ exceeds $(\frac{e^2 f}{m})\mathrm{Im}G_s$ and therefore the rate of energy dissipation is enhanced if the frequency ω_o at which the absorption occurs is capable of exciting an electromagnetic resonance. The absorption enhancement

at 7-8 Å from surface is larger than that at 1-2 Å since at the larger distance G_s becomes small while R is still very large.

§25. Fluorescence enhancement. We are concerned here with a relaxation experiment, in which the oscillators are driven by a light source of frequency ω which is turned off at $t = 0$. We then follow the oscillator emission intensity as a function of time. The surface can modify both the emission lifetime and intensity.

A dipole driven at steady state by a source of frequency ω at $t = 0$ has the magnitude (for simplicity we use the "oversimplified" model of §18)

$$\mu(\omega;\ t = 0) = \{\omega_o^2 - \omega^2 - \Delta^2(\omega) - i\omega\Gamma_{eff}(\omega)\}^{-1}(e^2/m)fE_p \qquad (II.48)$$

Following the field shut-off at $t = 0$, the dipole relaxes according to (to lowest order in Δ/ω_o and Γ_{eff}/ω_o)

$$\mu(\omega;\ t) \simeq \mu(\omega;\ 0)e^{-i\omega_o t}\, e^{-\Gamma_{eff}(\omega_o)t/2} \qquad (II.49)$$

The field reaching the detector is

$$\vec{E}(\vec{R}_d;\ t) = e^{-i\omega_o t}\, e^{-\Gamma_{eff}(\omega_o)t/2}\, \vec{\vec{G}}(\vec{R}_d,\ \vec{r}_\alpha;\ \omega_o)\cdot \hat{z}\mu(\omega;\ o) \qquad (II.50)$$

Some simplifications are required to obtain these formulae but we do not discuss them here (see §103).

The emitted intensity is therefore proportional to

$$I \propto \sum_\alpha \langle|\vec{n}\cdot G(\vec{R}_d,\vec{r}_\alpha;\ \omega_o)\cdot\vec{\mu}(\omega;\ 0)|^2\rangle e^{-\Gamma_{eff}(\vec{r}_\alpha;\ \omega_o)t}$$

Note that in fluorescence experiments the emission frequency ω_o is not necessarily equal to the excitation frequency ω. If the minimum of the upper electronic energy surface is shifted with respect to the minimum of

the ground state, then the excitation at the frequency ω may be followed by intramolecular relaxation and subsequent emission at a different frequency ω_o. In such cases we need a more detailed model than the one used here. Two oscillators are involved, one which is excited by laser and the other which is emitting light. The two are coupled by an intramolecular relaxation rate. The case discussed in text corresponds to one oscillator which has a resonance excitation at ω_o and emits at ω_o, but may be excited with off resonance radiation ω. The qualitative conclusions concerning the enhancement are however valid for both cases.

If the excitation frequency ω corresponds to an electromagnetic resonance E_p is enhanced (through R, § 9, Eq. (3) and so is $\vec{\mu}(\omega;o)$. This enhancement contributes to the emission intensity a factor of order $|R(\omega)|^2\Gamma_{eff}^{-1}$. If the emission frequency ω_o coincides with a radiative electromagnetic resonance (these resonances are fiarly broad so that we may be able to excite the same resonance at ω and ω_o, if $\omega-\omega_o$ is smaller than the resonance width) the emission is enhanced through $\overleftrightarrow{G}_s$ (which is part of $\overleftrightarrow{G}$, see § 12, Eq. (4)). This enhancement is of order $|G_s(\omega_o)|^2$.

In the most favorable case, when both ω and ω_o correspond to radiative electromagnetic resonances, the intensity enhancement is thus of order $|R(\omega)|^2|G_s(\omega_o)|^2\Gamma_{eff}^{-1}$. However one should not overlook the exponential $e^{-\Gamma_{eff}(\omega_o)t}$. According to Eq. (28) Γ_{eff} contains a term proportional to $ImG_s(\vec{r}_\alpha, \vec{r}_\alpha; \omega_o)$ (corresponding to the "image field") which may become very large if the molecule is very close to the surface. Then Γ_{eff} is large and $e^{-\Gamma_{eff}t}$ decays extremely rapidly. When the molecule is very close to the surface the rate of decay of the exponential is faster than the rate of turning off the driving source (at t=0). Therefore we cannot measure the decay of the fluorescence signal unless it is shifted with respect to the excitation frequency. If the molecule

location $\vec{r}_\alpha$ is moved further from surface (e.g. $\sim$20 Å) Γ_{eff} is small enough to permit fluorescence measurements and $|R(\vec{r}_\alpha; \omega)\, G_s(\vec{r}_\alpha; \omega_o)|^2 \Gamma_{eff}^{-1}$ is still large enough to give fluorescence enhancement. The enhanced signal (with the exponential factor removed) is of the same order of magnitude as the electromagnetic enhancement in resonant Raman spectroscopy (see §23).

Interesting surface enhanced effects can also be observed in steady state fluorescence experiments. Consider the case in which an upper level, which is continuously pumped by a laser of frequency ω_A, undergoes molecular relaxation and emits from an electronic level B, with a broad band frequency centered around ω_B. The absorption process pumping up A is enhanced, as discussed at §24. The enhancement is substantial if the frequency ω_A excites an electromagnetic resonance. The excitation spectrum of fluorescence (i.e. the fluorescence intensity as a function of the incident laser frequency) is essentially proportional to the absorption spectrum of the combined molecule-surface system and it will strongly depend on the excitation spectrum of the electromagnetic resonance.

Assuming now that the molecular relaxation rate is unaffected by the presence of the surface, the enhanced population of A leads to an enhanced population of B. The emission from B is enhanced in proportion to $|G_s(\vec{R}_d, \vec{r}_\alpha; \omega)|^2$. Furthermore, the emission spectrum will have spikes whenever the emission frequency equals that of an electromagnetic resonance.

III. The application of the electrodynamic theory to various systems.

III.0. Introductory remarks.

§26. We have now a general electromagnetic theory which suggests that there are two sources of enhancement: (a) the local field $\vec{E}_p$ can be substantially enhanced by curvature effects and by the excitation of the electromagnetic resonances of the surface. These appear in the theory through reflection tensor $\overleftrightarrow{R}(\vec{r},\omega)$ (§10); (b) the emission of the molecular dipole can be substantially enhanced if its frequency is very close to that of an electromagnetic resonance of the surface. In that case the dipole near field excites a radiative resonance and through this mechanism the non-radiative energy of the near field is turned into radiation by the solid. The emission enhancement appears in the theory through $\overleftrightarrow{G}_s(\vec{R}_d, \vec{r};\omega)$ (see §11).

In certain spectroscopic techniques an equally important element is the upper level width $\Gamma_{eff}(\omega)$ or, equivalently, its lifetime $\Gamma_{eff}(\omega)^{-1}$. Γ_{eff} is always increased by the presence of the surface and the magnitude of this increase is controlled by the "image field" through $(e^2/m\omega)\mathrm{Im}\,\overleftrightarrow{G}_s(\vec{r};\vec{r};\omega)$ (see §20). This broadening of the upper level diminishes the absorption and makes it difficult to observe fluorescence (in time resolved, relaxation experiments) if the molecule is very close to the surface.

In the present chapter we pursue the implications of this general theory by applying it to various surface shapes, materials and spectroscopic techniques. We'll find that the magnitude of the effects mentioned above as well as all their properties can be radically altered by changing the nature of the solid and its shape. From a practical point of view this diversity can be used to attempt to extend the frequency range in which enhancement is produced and to design geometries which give a desired enhancement under specified conditions. Since it is very difficult to prepare surfaces that have specified shape, it is likely

that it will not be possible to make detailed and accurate comparison between theory and experiment. Therefore, in testing the electromagnetic theory it is important to verify its various qualitative predictions on a very large number of examples. The correctness of the theory will probably be established by the weight of the "circumstantial evidence" rather than through detailed and exhaustive quantitative study of one example. For these reasons we present a large number of cases, including some which are not spectacular in their enhancing properties.

We must also emphasize that we are not yet convinced that in all cases the "molecular" effects are negligible. At the present there is little hope that we can compute the magnitude of such effects with accuracy. Therefore it seems that the issue of their relative importance can be settled by studying with special care those very few systems (if any) that allow exact electromagnetic calculations and might also be prepared in the laboratory. The presence of large systematic discrepancies between theory and experiment might then be an indication of the presence of sizable molecular effects. This explains why in this chapter, certain systems, which, hopefully, might be amenable to such a treatment, have received considerably more attention than others.

III.1. Flat Surfaces.

III.1.1. § 27. Introductory remarks. The electromagnetic enhancement at flat surfaces can be easily computed.[23,24] The primary field $\vec{E}_p$ is given by the Fresnel equations and it is roughly twice as large as the incident one. The emitted field is the coherent sum of the electric field radiated by two dipoles: the induced dipole $\vec{\mu}$ and the dipole $(\epsilon(\omega)-1)\,(\epsilon(\omega)+1)^{-1}\mu\hat{z}$. If the former is located at a height d above the surface (d is much smaller than the wavelength of light) the latter must be placed at a distance d inside the solid. The emitted field is, roughly, twice that of the induced dipole in vacuum. The dependence of these factors and of the depolarization ratio on the angles of incidence and detection and on frequency, have been studied by Efrima and Metiu,[23,24]

III.1.2 Raman scattering.

§28. For Raman scattering the effects mentioned at §27 combine to an enhancement factor of roughly $(\bar{2}^2)x(2^2)=16$. If the molecule is chemisorbed with the most polarizable direction perpendicular to the surface, an additional enhancement occurs. This happens because the primary field is almost perpendicular to the surface[24] and therefore the most polarizable direction is lined up with the field. In liquids or gases the tumbling of the molecule makes this favorable situation rather improbable. If we decree that one might thus gain a factor of 2 in the intensity (one cannot calculate this factor without detailed information concerning the mode of binding to the surface and the tilting motion of the bound molecule) the total expected electromagnetic enhancement factor is of order 30. Further enhancement must come from a "molecular" mechanism, i.e., from polarizability changes caused by chemisorption.

§29. In principle, experiments on flat surfaces in UHV are ideal for addressing the thorny question of the magnitude of the molecular enhancement. Working with a good Raman scatterer and no enhancement other than the electromagnetic factor of 30, one can detect[25] Raman signals from a submonolayer. Usual surface

science techniques can give adequate information concerning coverage, surface binding sites and molecular position. Armed with all these one can get a safe estimate of the molecular enhancement. The most serious difficulty is created by our inability to provide proof that the surface is flat. LEED and optical techniques can miss small particles lying on surface. The resolution of the scanning electron microscope used so far in this field[26] is 250 Å. Other methods, like ion or atom scattering or tunneling through a vacuum gap[27] might be useful but have not been employed. The flattest surface used so far for Raman studies[26] might have 250 Å boulders lying on it, which can give sizable electromagnetic enhancement, making it impossible to separate the molecular factors from the electromagnetic ones.

§30. The first experiments which attempted to work with flat surfaces were carried out by Pettinger et.al.[28] They used an aqueous solution of 0.1 M KCl and 0.05 M pyridine and a Ag(111)[28a, b], or Ag(100)[28a], or a polycrystalline[28b] Ag electrode.

Unfortunately, the Raman spectrum of Py could not be observed unless the electrode was anodized. The anodization procedure consists in an oxydation-reduction cycle carried out at the Ag electrode. During oxydation Ag atoms are removed to form a AgCl film on the surface. During reduction AgCl is reversibly decomposed to deposit the Ag back on the Ag electrode. Faraday's law permits a very precise determination of the number of atoms thus removed and redeposited. Unfortunately some complications appear since the intensity-voltage curves for anodization process with and without Py differ from each other. The peak corresponding to the AgCl reduction is the same and is independent on the number of cycles. However, when pyridine is present a new peak appears which corresponds to the reduction of an unspecified Ag-Py complex and grows with the number of cycles.

The Raman intensity of the Py signal also grows with the number of cycles. A signal appears even when less than a Ag monolayer is removed and redeposited.

A maximum signal is obtained in a cycle which involves 10 Ag monolayers. In going from an oxydation-reduction cycle removing less than one monolayer to one that removes ten monolayers, the Raman intensity grows approximately 650 times.

This detailed description is given to make sure that it is understood that anodization is a disruptive process, both physically and chemically. It is generally believed[29] that redeposition of Ag will form metal boulders on the surface. This is clearly the case in the experiments carried out by Van Duyne et.al.[26] who studied the same Ag-Py system and examined the surface with a scanning electron microscope (SEM). Unfortunately Van Duyne used 20 mC/cm^2 which would correspond to 33 Ag layers (300 $\mu C/cm^2$ for a Ag monolayer[28b]) which is more than what Pettinger et. al.[28] use. So, one cannot draw from Van Duyne's work any "hard" conclusion concerning the surface used by Pettinger et. al.[28] However we feel that at least a propensity for forming boulders during reduction, rather than reconstructing a flat surface, is demonstrated.

To test whether their surface is flat Pettinger et.al.[28] carried out electro-reflectance measurements[28b], which indicated that the anodized surface does not permit the excitation of the Ag surface plasmon. One is inclined to think that this would mean that the surface is flat [30], but we are not absolutely sure that this is the case. The behavior of the reflectance depends on the type of roughness and we are not yet convinced that such measurements rule out the presence of roughness whose correlation length is much smaller than the wavelength of light. Some further work needs to be done to clarify this point.

§31. The above discussion illustrates two major difficulties: (1) in electrochemical cells it seems that one has to anodize the surface and this is a messy process which changes the surface and perhaps the adsorbed molecule as well. (2) One is not sure that the surface is flat. The first difficulty was removed by Van Duyne et.al.[26] who demonstrated that one can obtain an enhancement factor of 10^4 by using a polished polycrystalline Ag electrode with

no anodization. This is true for two systems, Ag |0.05 M pyridine |0.1 MKCl |H_2O and Ag |0.005 M Pt $(CN)_4^{-2}$ |0.1 M SO_4^{2-1} |H_2O, and allays the suspicion that the observation might be specific to pyridine or Cl^- ions. Furthermore, SEM measurements indicate that the surface has no asperities of a size larger than 250 Å. However, smaller ones might be present and they could be very effective enhancers.[31]

Surface anodization with one cycle of 20 mC/cm^2 (roughly 33 Ag monolayers removed and redeposited) creates surface boulders of roughly 500 Å diameter and enhances the Raman intensity by an additional factor of 100 (to a total of 10^6). A safe conclusion is that an enhancement factor of 10^4 is produced by a flat surface with boulders of less than 300 Å diameter, and an additional enhancement factor of 100 is caused by the larger boulders.

§32. A very important advance has been provided by recent work in UHV. Hemminger, Ushioda et.al.[32] managed to obtain the Raman spectrum of pyridine on a "smooth" Ag(100) surface in UHV. No proof of flatness has been provided other than the fact that these authors followed a standard procedure for polishing Ag single crystal surfaces. There is however an indirect indication that roughness is not playing a role in the enhancement. Using the ratio of the carbon to silver Auger intensity Ushioda et.al.[32] monitored the surface coverage. They find that they can see a Raman peak at 1004 cm^{-1} and one at 1032 cm^{-1} at 10L exposure (which corresponds to roughly 1.5 coverage, according to the Auger calibration). Further exposure does not add to the intensity of the 1004 cm^{-1} mode but it does lead to an increased intensity at 991 cm^{-1} and 1032 cm^{-1}. This suggests that the 991 cm^{-1} peak corresponds to pyridine molecules that are not in contact with the metal, while the 1004 corresponds to chemisorbed molecules. The intensity of the 1004 cm^{-1} peak indicates[32] that the enhancement factor for the chemisorbed molecules is 244. If the surface is flat, the electromagnetic enhancement is around 30[24] (see §27) so $|\partial\alpha/\partial Q|^2$ is enhanced about eight times (i.e., 244/30 ~8.1). This is reasonable since the pyridine binds to the metal which is an electron rich system.

Furthermore, under the assumption that the surface is flat each physisorbed layer has an enhanced signal of about 30 (assuming a favorable ordering, as discussed in §27). For 100 L (an estimated totalof 10 layers) the nine layers of physisorbed molecules should have a peak intensity for the 991 cm^{-1} line of 9 x 30 ~270 times larger than the gas phase intensity for the same layer thickness. Since the 1004 cm^{-1} peak is enhanced 244 times, the intensity of the 993 cm^{-1} peak at 100 L exposure should be somewhat (but not much) larger than that of the 1004 peak. This is confirmed by measurements. Therefore, the data is consistent with a molecular enhancement factor of 1.8 for the first layer and an electromagnetic and orientational factor of 30 for each layer.[23, 24]

If the enhancement was caused by "boulders" lying on the surface, the behaviour of the Raman spectrum would be different[33, 34] (see III.5). If the boulders are large, the enhancement extends at a large distance from the surface[33] and the Raman intensity of the 991 cm^{-1} peak would be much larger than that observed by Hemminger et. al.[32] If the boulders are small, the enhancement is short ranged but it is very large[34] and the Raman intensity of the 1004 cm^{-1} mode should be enhanced by more than 244 times and be much larger than that of the 991 cm^{-1} peak. Based on these qualitative arguments we conclude, that the data of Hemminger et. al.[32] is consistent with the assumption that the surface is flat. Unfortunately, there is a discrepancy between Van Duyne's result of an enhancement factor of 10^4 and Hemminger-Ushioda's factor of 244. The absolute calibration of the intensity is a notoriously difficult task so these numbers might not be accurate. There is also a possibility that some differences exist between the enhancement in electrochemical systems and in UHV ones. Or it may be that the "flat" surfaces have a different degree of roughness and that is the cause for different results. Furthermore, we have approached the whole issue from the point of view of the electromagnetic theory. The model proposed by Otto,[5] in which single silver

atoms located on the Ag surface play an important role, may also be used to rationalize these discrepancies.

§32. Very recently Campion et. al.[35] have obtained the Raman spectrum of nitrobenzene on Ni (111). They observe only a minor enhancement consistent (within the limits imposed by difficulties in accurate intensity calibration) with Efrima-Metiu[24] calculations. Since Ni is not a good enhancer the presence of some accidental roughness should not have a very large effect. Therefore it is likely that Campion et. al.[33] have observed the Raman spectrum of a monolayer with no molecular enhancement and only the "minor" electromagnetic enhancement discussed in Ref. 24. This development is a remarkable achievement, not only for its obvious chemical applications in surface science, but also for its potential of making a great impact on the understanding of SERS. We can now study the Raman spectrum of molecules adsorbed on all metals, for all surface preparations. Prior to this we were confined mainly to Ag Cu or Au, roughened to increase the signals above the limits imposed by insensitive detection schemes.

III.1.3 Fluorescence.

§33. The modification of the molecular fluorescence by the presence of flat solid surfaces has been reviewed by Chance, Prock and Silbey.[36] When the molecule is close to the surface the fluorescence lifetime is shortened since the image dipole term $(e^2 f/m\omega_0)\,\mathrm{Im}G_s$ is added to the natural width Γ_o (see §20, Eq. (28)). Experimental studies of lifetime dependence on the distance to the surface[37] provide a detailed confirmation[34] of the validity of the electromagnetic models on which this review is based. It is however clear that the image model must break down as the molecule-surface distance is diminished, since it predicts infinite fields for very small distances. Recent experiments[38-44] have attempted to diminish the molecule-surface distance to study the details of this break down. Calculations based on a microscopic electron gas model[45-48] (see Ch. IV), which remove some of the approximations that are responsible for the break down of Maxwell equations, have

predicted[45, 46] that the image dipole formula holds for dipoles located at a distance of roughly 10 Å from the surface. The number depends on the emission frequency, the nature of the metal and the assumptions of the model. With one exception[42] the experiments[36-41] tend to substantiate this prediction. However Brus and Rosetti[42] find that the image formula seems to break down when the molecule is located at distances of less than 125 Å from the surface. The measured lifetime for distances less than 125 Å is larger than the one predicted by the image formula. It is difficult to attribute this effect to roughness since one would expect[47] that the lifetime on a rough surface is shorter than the one expected for a flat surface. We feel that the results[46] might be erroneous, due to experimental problems with the determination of the molecule surface distance, combined perhaps with the fact that the surface is rough.

III.2. Methods of exciting the surface plasmon to carry out SES.

III.2.1 General remarks.

§34. As we have emphasized in Section II, the electrodynamic resonances are the key to the understanding of the electromagnetic theory of enhanced spectroscopy. When the incident field excites a resonance the molecule feels an enhanced electric field and has an excess polarization. If the molecular dipole emits at the frequency of a radiative electromagnetic resonance, its emission is brighter. Finally, the non-radiative electromagnetic resonances can lower substantially the life time of the emitting molecular dipole by taking energy from it.

The electrodynamic resonance sustained by a flat surface is the surface plasmon.[50] This is a surface excitation which corresponds to an electric field wave moving along the surface. The wave is evanescent, in the sense that its amplitude decays exponentially along a direction perpendicular to the surface. Its frequency ω and parallel wave vector $\vec{k}_{\parallel}^{sp}$ are related through the dispersion relation[50]

$$(k_{\parallel}^{sp})^2 = (\omega/c)^2 \, \mathrm{Re}\, \epsilon(\omega) \, [1 + \mathrm{Re}\, \epsilon(\omega)]^{-1} \qquad \text{(III.1)}$$

(we assume that one of the media bordering the interface is vacuum).

The electric field near the surface would be substantially increased if the surface plasmon could be excited by the incident light. However, this is not possible since the photon dispersion relation $k_{\parallel}^{ph} = (\omega/c)\sin\theta$ (θ is the angle of incidence with respect to the normal to the surface) is such that for any ω we have $k_{\parallel}^{sp} \neq k_{\parallel}^{ph}$. The excitation of the surface plasmon by the photon would violate momentum conservation, and it is therefore prohibited.

To excite the surface plasmon we must try to bypass this constraint. This can be done by various procedures. (1) By choosing carefully the medium that is in contact with the metal surface we can modify the momentum of the incident photon, so that it matches that of the

plasmon. Various experimental arrangements which do this are collectively called here Attenuated Total Reflection (ATR) methods. They are discussed in Section III.2.3.

(2) By changing the shape of the surface into a grating we can use diffraction to change the photon momentum from $k_{||}^{ph} = (\omega/c)\sin\theta$ to $k_{||}^{ph} \pm (2\pi n/L) = (\omega/c)\sin\theta \pm (2\pi n/L)$, $n = 1, 2, 3, \ldots$. At a given frequency and grating wavelength L we can vary the angle of incidence so that the parallel momentum of the diffracted photon matches that of the surface plasmon: $k_{||}^{sp}(\omega) = (\omega/c)\sin\theta + (2\pi\eta/L)$. Now momentum is conserved and the diffracted photon is allowed to excite the plasmon.

(3) We may choose to roughen the surface randomly so that momentum conservation is no longer required (parallel momentum conservation is a consequence of the tranlational invariance in direction parallel to the surface; roughening suppreses this invariance). The plasmon can now be excited and the consequences of this procedure are outlined in Sections III.2.4. and III.2.5

III.2.2. Surface enhanced spectroscopy on gratings.

§35. Introductory remarks. The interest in gratings is by no means recent. Rayleigh[51] developed a first order perturbation theory which solves Maxwell's equations and provides expressions for the electric field near a grating on which we shine light. Recent work[52-55] in the physics literature uses either Rayleigh's method[52-53] or an equivalent procedure based on Green's funtions.[54] The current status of the theory has been extensively surveyed.[56]

In the areas of enhanced spectroscopy there are three aspects of the electromagnetic theory that must be considered. We would like to know (a) under what conditions one can enhance the primary (i.e. the reflected) field (§10) and what is the magnitude of the enhancement. This problem has been considered by Jha, Kirtley and Tsang.[57] (b) We are interested in the magnitude and the properties of the enhanced emission (§11) and this has been considered by Aravind, Hood and Metiu.[58] (c) The problem of image field for an oscillating

dipole located near a grating, has not yet been discussed. As a consequence, we do not have a theory of the fluorescence life-time for a molecule emitting near a grating. It is, however, fairly straight forward to adapt recent work of Rahman and Maradudin[59] on electron scattering from rough surfaces and give a perturbative solution to the lifetime problem.

The experimental work[60-64] has been carried out on holographic gratings made on photoresist and covered with a thin Ag film. The SER spectrum[60-62] and the fluorescence[63-64] of molecules deposited on Ag have been measured.

§36. From the point of view of the theory, a grating provides a system with a well defined surface for which we can compute the electromagnetic effects fairly accurately. The gratings can be used in UHV and this allows better control of surface cleanliness. Or they can be used in solution or at the solid-solid interface, and this increases their usefulness. Recent work at IBM, Yorktown Heights[62] has used gratings with such a long wave-length (10,000 Å) that the grating surface had large single crystal patches. This provides an opportunity of doing enhanced spectroscopy on single crystals. Finally, since the enhancement is long ranged one can hope to do enhanced spectroscopy on systems whose dielectric properties are not able to give a large enhancement. For example, one might obtain the SER spectrum of molecules absorbed on small metal clusters, which are located on top of Ag gratings which provide the enhancement.

The gratings have two disadvantages that should be kept in mind. It has not yet been clearly established that the surface of the grating is smooth. Silver "boulders" may exist on the grating's surface or the grating's profile might have small random mountains and valleys. These will contribute to the enhanced spectroscopy in a complicated manner that would make the theoretical analysis as difficult as on poorly defined rough surfaces. Finally, on the practical side, the enhancement obtained on gratings is comparable to that

of ATR and smaller than on other systems.

III.2.2.a. The calculation of the primary field

§37. The geometry of the system and the main equations. We consider two semi-infinite media, one called the metal and the other the vacuum. The dielectric constant of the "metal" is $\varepsilon(\omega)$, and it is complex and frequency dependent. The interface profile (Figure 1) has the period L in the y-direction and it is unchanged in the x- direction (perpendicular to the paper plane). The shape of the profile is given by the equation

$$z = f(y) = f(y + L) \tag{III.2}$$

Here the z-direction is perpendicular to the mean grating surface and points toward the metal. We discuss the general theory of this system only briefly, in order to set the stage for explaining the perturbation theory and applying it to sinusoidal gratings. Since f(y) is periodic it can be expanded in a Fourier series

$$z = \sum_n \xi_n e^{-iK_n y} \tag{III.3}$$

with $K_n = 2\pi n/L$. For a sinusoidal profile we have

$$z = a \sin (2\pi y/L) \tag{III.4}$$

and therefore, $\xi_n = (a/2i)$ for $n = 1$, $\xi_n = -(a/2i)$ for $n = -1$ and $\xi_n = 0$ for $n \neq \pm 1$. Here a is the amplitude of the grating. In order to compute the electromagnetic properties of this system, we must solve Maxwell's equations

for harmonic fields:

$$\nabla \times \nabla \times \vec{E}\,(\vec{r};\omega) - (\omega^2/c^2)\,\varepsilon(\omega;\vec{r})\,\vec{E}\,(\vec{r};\omega) = 0, \tag{III.5}$$

$$\vec{B}(\vec{r};\omega) = (c/i\omega)\,\nabla \times \vec{E}(\vec{r};\omega). \tag{III.6}$$

and

$$\nabla \cdot \vec{E}\,(\vec{r};\omega) = 0, \text{ for } z \neq f(y). \tag{III.7}$$

We use the notation

$$\epsilon(\omega;r) = \epsilon(\omega)\,\theta(z-f(y)) + \theta\,(f(y)-z) \tag{III.8}$$

where $\theta(x) = 1$ for $x > 0$ and $\theta(x) = 0$ for $x < 0$.

Furthermore, the field must satisfy the usual boundary conditions,[11] requesting the continuity of the normal components of $\vec{D}$ and $\vec{B}$ and of the tangential components of $\vec{E}$ and $\vec{H}$ (in our case $\vec{H} = \vec{B}$). We write here only one boundary condition, namely:

$$\vec{n}_{12} \cdot (\vec{D}_2 - \vec{D}_1) = 0, \tag{III.9}$$

which we need in order to illustrate certain points concerning the calculation. Here $\vec{n}_{12}$ is the unit vector perpendicular to the surface, directed from the medium 1 to medium 2. $\vec{D}_2$ and $\vec{D}_1$ are the displacement vectors in the two media.

§38. The electric fields. The strategy for obtaining the solution for $\vec{E}$ consists in identifying physically the main fields, expanding them in the appropriate basis set and using Maxwell's equations and the boundary conditions

to determine the expansion coefficients.

In vacuum the electric field is

$$\vec{E}_v(\vec{r};\omega) = \vec{E}_i(\vec{r};\omega) + \vec{E}_r(\vec{r};\omega) + \vec{E}_d(\vec{r};\omega), \text{ for } z < f(y), \tag{III.10}$$

where $\vec{E}_i$ and $\vec{E}_r$ are the incident and the specularly reflected fields. They can be written as (for $z < f(y)$)

$$\vec{E}_i(\vec{r};\omega) + \vec{E}_r(\vec{r};\omega) = e^{i\vec{k}_{||} \cdot \vec{r}_{||}} \quad [E_i(\omega)\, e^{ik_\perp z} + F_r(\vec{r};\omega) e^{-ik_\perp z}]. \tag{III.11}$$

The parallel momentum has the components

$$k_{||,x} = (\omega/c)\, \sin\theta \cos \phi \tag{III.12}$$

and

$$k_{||,y} = (\omega/c)\, \sin\theta \sin \phi \tag{III.13}$$

and the perpendicular one is

$$k_\perp = (\omega/c)\, \cos\theta. \tag{III.14}$$

Here ϕ is the azymuthal angle.

The amplitude $E_i(\omega)$ is determined by the intensity of the incident laser, while $E_r(\omega)$ is as yet unknown.

The diffracted wave $\vec{E}_d$ must satisfy the Floquet-Bloch theorem,[56,65] because the surface is periodic. This means that

$$\vec{E}_d(x, y + L, z;\omega) = e^{ik_{||,y} L} \vec{E}(x,y,z;\omega). \tag{III.15}$$

Therefore, we must expand the diffracted field with respect to a basis set that automatically insures the validity of Eq. (15). One possibility[51] is

$$\vec{E}_d(\vec{r};\omega) = \sum_{n\neq 0} \vec{E}_n(\omega) e^{i\vec{k}_{||} \cdot \vec{r}_{||}} \quad e^{iK_n y} \quad e^{+\Gamma_n z} \tag{III.16}$$

with $K_n = 2\pi n/L$ and $n = \pm 1, \pm 2, \ldots\ldots$

The quantities Γ_n and E_n are unknown functions of ω, to be determined from Maxwell's equations and the boundary conditions. If Γ_n comes out imaginary, we get an outgoing diffracted wave. If Γ_n is complex or real, we get an evanescent wave (surface plasmon). In this case, we must have $\mathrm{Re}\Gamma_n(\omega) > 0$ so that $e^{\Gamma_n z} \to 0$ as $z \to \infty$.

One can make similar assumptions about the transmitted wave, penetrating inside the metal ($z > f(y)$):

$$\vec{E}_m(\vec{r};\omega) = \vec{E}_t(\omega)e^{i\vec{k}_{\parallel}\cdot\vec{r}_{\parallel}}\, e^{-\gamma z} + \sum_{n\neq 0} \vec{E}'_n(\omega)e^{iK_n y}\, e^{-\gamma_n z}\, e^{i\vec{k}_{\parallel}\cdot\vec{r}_{\parallel}} \qquad \text{(III.17)}$$

By requesting $\vec{E}$ of Eqs. (17) and (10), (11) and (16) to satisfy Eq. (5) inside the metal and in the vacuum, we obtain

$$\varkappa_n^2 - (\omega/c)^2 = \Gamma_n^2 \qquad \text{(III.18)}$$

$$k_{\parallel}^2 - (\omega/c)^2\varepsilon(\omega) = \gamma^2 \qquad \text{(III.19)}$$

and

$$\gamma_n^2 = K_n^2 - (\omega/c)^2\varepsilon(\omega). \qquad \text{(III.20)}$$

with

$$\varkappa_n^2 = (\vec{k}_{\parallel} + \vec{K}_n)\cdot(\vec{k}_{\parallel} + \vec{K}_n) \qquad \text{(III.21)}$$

The condition for obtaining an evanescent wave in the vacuum is $\varkappa_n^2 - (\omega/c)^2 > 0$, which gives a real value for Γ_n.

The use of Eq. (7) provides relationships between the amplitudes of various waves, which force them to be transverse. These equations are not given here.

§39. The calculations made so far are straightforward. However, when we try to use the boundary conditions, we run into some difficulties which we circumvent by using perturbation theory. It is possible to use non-perturbative, "exact" numerical methods and this direction is currently being pursued.[66]

One difficulty appears because the unit vector normal to the surface, $\vec{n}(y)$, varies from point to point on the grating surface. Using simple differential geometry allows us to derive the equation for the components of $\vec{n}(y) \equiv (n_x, n_y, n_z)$, namely $n_x = 0$, $n_y = [1 + \partial f/\partial y]^{-1/2}$ and $n_z = -(\partial f/\partial y)[1 + \partial f/\partial y]^{-1/2}$

The vector $\vec{n}(y)$ defined above is oriented from vacuum towards the metal. The boundary condition (III.9) gives

$$\vec{n}(y) \cdot [\epsilon(\omega)\, \vec{E}_m(x, y, f(y); \omega)] = \vec{n}(y) \cdot \vec{E}_v(x, y, f(y); \omega) \qquad \text{(III.22)}$$

We see that this relationship is highly non-linear in f(y), because of the presence of $\vec{n}(y)$ and because the expressions (10) – (16), for $\vec{E}_v$, and (17) for $\vec{E}_m$, place f(y) at the exponent. The Eq. (22), and the similar ones given by the other boundary conditions, provide us with a system of equations from which we must extract $\vec{E}'_n(\omega)$, $\vec{E}_n(\omega)$, $\vec{E}_r(\omega)$ and $\vec{E}_t(\omega)$. A little contemplation of Eq. (22) can convince one that the nonlinearity in f(y) makes life difficult.

However, if we assume that f(y) and $\partial f/\partial y$ are small, in some sense to be established later, we obtain a considerable simplification of the problem.

Consider, for example, $E_v(x,y,f(y);\omega)$. The coordinate $z = f(y)$ appears in the exponentials $e^{ik_\perp z} = e^{ik_\perp f(y)}$ and $e^{-ik_\perp f(y)}$ (in Eq. (11)), as well as in exp $(\Gamma_n f(y)$ (in Eq. (16)). We replace these by $1 + ik_\perp f(y)$, $1 - ik_\perp f(y)$ and $1 + \Gamma_n f(y)$, respectively. This is reasonable only if $|k_\perp f(y)| << 1$ and $|\Gamma_n f(y)| << 1$ for all values of y. If we use the Fourier transform of f(y), given by Eq. (3), these conditions become $|\xi_n k| << 1$ and $|\Gamma_n \xi_m| << 1$, for all values of n and m. For sinusoidal gratings they give $(k\, a/2) << 1$ and $|\Gamma_n a/2| << 1$, for all n.

The derivative $\partial f(y)/\partial y$ appears in $\vec{n}(y)$, under the square root sign. If $|\partial f/\partial y| << 1$ for all y, we can expand the square root so that the boundary condition is linear either in f(y) or in $\partial f/\partial y$. The condition $|\partial f/\partial y| << 1$ for all y is equivalent to $|2\pi \xi_n/L| \ll 1$ for all n, which becomes $(\pi a/L) << 1$ for sinusoidal gratings.

To summarize, the simplifications brought about by perturbation theory are possible if, roughly, the height of the sinusoidal grating is smaller than the wave length of light, than the wave length of the grating, and than the decay length Γ_n^{-1} of the evanescent wave.

§40. Expressions for the vacuum field. After making the expansions suggested above, we obtain simplified formulae for the fields given by the expressions (10), (11), (16), and (17). Inserting these in the boundary conditions yields equations from which we can determine all the unknown amplitudes. We quote here only those results that we need in order to illustrate how the resonances in the primary field can be used in surface enhanced spectroscopy.

It is useful to chose a system of unit vectors that will allow us to distinguish easily the p- and s-components of the electric vectors $\vec{E}$. We use $\hat{z}$ for a unit vector perpendicular to the xoy plane. This plane is the flat mean surface of the grating. The second one is $\hat{k}_{||} = \vec{k}_{||} / |\vec{k}_{||}|$ which is the projection of the incident wave vector on the plane xoy. The third is $\hat{k}_{||} \times \hat{z}$, which is parallel to the surface and perpendicular to the plane

of incidence. Of course, z and $k_{||}$ are contained in the plane of incidence.

We can write any electric vector $\vec{E}_\alpha$ ($\alpha \equiv$ i, r, n or t) or $\vec{E}'_n$ in the form

$$\vec{E}_\alpha = E^s_\alpha (\hat{k}_{11} \times \hat{z}) + E^p_{\alpha,||} \hat{k}_{||} + E^p_{\alpha,\perp} \hat{z} \qquad \text{(III.23)}$$

Here E^s_α is the electric field of the s-polarized wave and $E^p_{\alpha,||}$ and $E^p_{\alpha,\perp}$ are the components of the p-polarized wave.

As an example we give the expression of E^s_1 and E^p_1 which are the diffracted wave amplitudes E^s_n and E^p_n, respectively, for n = 1. The amplitudes for $n \neq 1$ are zero since the perturbation theory used here corresponds to a "single scattering" theory (Born approximation) in which the light beam and the grating interact once. Second order perturbation theory gives non-zero results for $\vec{E}_2$, etc.

We have[51,55,57]

$$E^p_{1,\perp} = 2(a/2i)\, K_1 k_1 \gamma_1 (1 - \epsilon(\omega))\, [k_{||}\ (\epsilon\Gamma_1 + \gamma_1)]^{-1} \cdot$$

$$\cdot \{(\delta(2\pi/L)k_{||} + \epsilon(\omega)k_{||}\, K_1 \gamma_1^{-1})\ (\epsilon(\omega)k_\perp + i\delta)^{-1} E^p_{i,\perp} \qquad \text{(III.24)}$$

$$- ik_{||}\ (\vec{k}_{||} \times \vec{K}_1)_z\ (k_z + i\delta)^{-1}\ E^\Delta_1\},$$

$$E^p_{1,||} = (i\Gamma_1/K_1)\, E^p_{1,\perp}, \qquad \text{(III.25)}$$

and

$$E^s_1 = -(\omega/c)^2\, ak_\perp (1-\epsilon(\omega))\, [k_{||}\ (\Gamma_1 + \gamma_1)]^{-1} \{\gamma(\vec{k}_{||} \times \vec{K}_1)_z\ (\epsilon k_\perp + i\delta)^{-1} E^p_{i,\perp}$$

$$+ ik_{||}(\vec{k}_{||} \cdot \vec{K}_1)\ (k_\perp + i\delta)^{-1} E^s_i\}. \qquad \text{(III.26)}$$

The amplitudes of the waves reflected specularly, that is E^s_r and E^p_r, are given by the Fresnel equations for a flat surface. As is well known, they do not contain any resonant behavior and lead to the "minor" enhancement discussed in Section III.1.

§41. Resonances in the refracted field. We can find whether we can resonantly enhance the field in the vacuum by examining the denominators appearing in the amplitudes of the refracted waves. For p-polarization, we use Eq. (24) and consider the term

$$I_p = (1 - \varepsilon)\gamma_1 / (\varepsilon\Gamma_1 + \gamma_1).$$

which appears in the expression for $E^p_{1,z}$. We multiply I_p with $1 = (\varepsilon\Gamma_1 - \gamma_1)(\varepsilon\Gamma_1 - \gamma_1)^{-1}$ and use Eqs. (18), (20) and (21), to obtain

$$I_p = (\gamma_1 - \varepsilon\Gamma_1)\tilde{\gamma}_1 \{\kappa_1^2(\varepsilon + 1) - (\omega^2/c^2)\varepsilon\}^{-1}. \qquad \text{(III.28)}$$

This has a resonance when

$$\kappa_1^2 = (\omega^2/c^2)\ \mathrm{Re}\varepsilon/(\mathrm{Re}\varepsilon + 1). \qquad \text{(III.29)}$$

comparing to Eq. (1) we find that the resonance condition is equivalent to the requirement that κ_1 equals the parallel monemtum $k_{//}^{sp}$ of the surface plasmon. According to Eq. (21) κ_1 is the parallel momentum of the diffracted photon, since $\vec{\kappa}_1 = \vec{K}_1 + \vec{k}_{//}$. Using Eqs. (13) and (14) and $\vec{K}_1 = (2\pi/L)\hat{y}$ ($\hat{y}$ is the unit vector in the y-direction) we can write the resonance condition (29) as

$$(\lambda/L)^2 + 2(\lambda/L)\sin\theta\sin\phi + \sin^2\theta = \mathrm{Re}\,\varepsilon(\omega)[\mathrm{Re}\,\varepsilon(\omega) + 1]^{-1}. \qquad \text{(III.30)}$$

For a fixed frequency (in most cases, the frequency is one of the four lines of the Ar^+ laser), given material (i.e. given $\varepsilon(\omega)$) and grating (i.e. fixed L) we can vary the azimuthal and polar angles of incidence (i.e. θ and ϕ respectively) of a p-polarized incident beam, until Eq. (30) is satisfied. When this happens the refracted field is enhanced and so is the spectroscopic signal (e.g. SER) from molecules located near the grating.

It is intuitively clear that whenever a resonance is excited, absorption occurs and the reflectance goes down. Therefore, the result found here can

be formulated as a simple rule: the illumination conditions that produce a dip in the reflectance must produce a peak in the Raman excitation spectrum. This statement has been verified experimentally.[60-62]

§42. We see that on resonance the quantity I_p (hence $E^p_{1,\perp}$ and $E^p_{1,\parallel}$) is inversely proportional to Im ϵ, which is typical of almost all electromagnetic resonances. A material provides a large enhancement if it has, at the resonance frequency, a small value for Im $\epsilon(\omega_{res})$.

§43. The excited wave (surface plasmon) is evanescent if Γ_1 is positive. This can be seen from Eq. (16) in which $z < 0$ corresponds to vacuum. Using the definition (19) of Γ_1 and the resonance condition (29) we find that

$$(\Gamma_1^2)_{\text{on res.}} = -(\omega^2/c^2)\ [1 + \text{Re}\epsilon]^{-1} \qquad \text{(III.31)}$$

The wave is evanescent if Re $\epsilon < -1$. If Reϵ is smaller than but closer to -1, the value of Γ_1 is larger than the inverse wave vector of the incident light. For a Ag grating Γ_1 is of order of 1000 Å or less. This long range is typical for most of the electromagnetic resonances and it is frequently present for surface shapes other than gratings. It plays an important role in identifying experimentally the existence of an electromagnetic enhancement.

§44. It is interesting to note that according to Eq. 24), the resonance in $E^p_{1,\perp}$ can be excited by both s- and p-polarized light. In principle, this permits a rather detailed test of the electromagnetic theory. One can compute the Raman intensities for s- and p-polarized incident radiation and then measure their ratio on the same sample. In a given system (i.e. grating and molecules), this ratio depends on the azimuthal and polar angles of incidence and the incident frequency. If the Raman scattered light is collected over a wide angle and its polarization is not measured, then the result for the ratio reflects mainly the properties of the primary field as expressed by the equations (24) through (26). Detailed

measurements of the angular distribution and polarization of the scattered photons will superimpose on this the properties of the emission of the Raman dipole, as modified by the presence of the grating. The effect of this emission modification on the intensity of Raman scattering has not been worked out in detail. Obtaining it and using it to test the theory would be a simple, worthwhile addition to the existing work.

In spite of the lack of a detailed theory that includes emission effects, one can use the existing equations and make some simple qualitative predictions. From Eq. (24) one can see that if $\phi=90^{o}$ (i.e. the angle of incidence is such that the wave vector is perpendicular to the grooves of the grating) then $(\vec{k}_{\|} \times \vec{K}_1)_z = 0$ and $E^{p}_{1,\perp}$ and $E^{p}_{1,\|}$ are independent on E^{s}_{i}. If we use an s- polarized beam ($E^{s}_{i} \neq 0$ and $\vec{E}^{p}_{i} \equiv 0$), we have $\vec{E}^{p}_{1} = 0$ and $\vec{E}^{s}_{1} \neq 0$. But E^{s}_{1} does not have a resonant behavior, therefore, when we vary θ the SER intensity does not peak and the reflectance does not dip. If $\phi = 90^{o}$ and the incident field is s-polarized, then $(\vec{k}_{\|} \times \vec{K}_1)_z \neq 0$ and $\vec{E}^{p}_{1}$ depends on $\vec{E}^{s}_{i}$. The proportionality factor between these (Eq. (24)) has a resonant character and the SER intensity dependence on θ peaks when the reflectance dips.

One can also infer[58] (§52) that the intensity of the s-polarized Raman scattered photons does not have a peak with respect to the polar angle of detection θ_d if the azimuthal angle of detection ϕ_d is 90^{o}. There will be a peak in the intensity of the p- polarized photons even if $\phi_d = 90°$. At $\phi_d < 90°$, both the s and p- polarized Raman intensity have at least one peak.[58]

§45. One should keep in mind that the conclusions reached so far are subject to the limitations imposed by the use of perturbation theory. For quantitative agreement, we must have $a/L \ll 1$, $a/\lambda \ll 1$ (λ is the wavelength of the incident light) and $\Gamma_1 a \ll 1$.

If this is the case only the diffraction peak n = 1 is important and the theory computes it accurately when we operate the system far from the resonance frequency. Even if the conditions discussed above are satisfied,

the resonance position and width are computed only approximately. The theory predicts that the resonance occurs at the frequency of the surface plasmon of the flat surface. However, the plasmon "collides" with the grating and both its frequency and width (life time or mean free path) are modified. If we compute the evanescent field to order a (therefore the intensity to order a^2) we should also include the plasmon shift and width to order a^2.

If we think of the plasmon as an elementary excitation interacting with the light through a grating, we must compute both its oscillator strength (which we do) and its self-energy caused by the interaction with the grating (which we do not). The real part of the self-energy is the shift in the flat surface plasmon frequency caused by grating; the imaginary part gives the shift of the plasmon width. Such calculations are available[67] in a different context, and we do not review them here. One should keep in mind that the real plasmon is broader than the one appearing in this simple perturbation theory, therefore, the enhancement is smaller than predicted. If the grating problem is solved "exactly" by using numerical methods,[66] the limitations mentioned above will disappear.

§46. Dipole emission near a grating. The theory of SERS on gratings is still incomplete since the effect of the grating on emission has not been taken into account. Emission calculations have been carried out by Aravind, Hood and Metiu[8] and their results indicate that the effect is substantial at special detection angles at which the surface plasmon, driven by the near field of the Raman dipole, radiates. However, their[58] calculation has not yet been incorporated into the theory of the Raman scattering. For this reason the existing comparison between theory and experiment will have to be re-examined when the full theory is completed.

§47. SERS experiments on gratings. There are a number of experimental papers concerning Raman spectroscopy of molecules deposited on gratings. The first paper, by Tsang, Kirtley and Bradley,[60] used a commercial grating on which a tunneling junction was deposited. This consists of an Al layer obtained by condensing Al vapors on the grating. The layer is then oxidized to form Al_2O_3. Then 4-Py COH is deposited on Al_2O_3 and a thin Ag film is condensed on top of it. The Raman spectrum is obtained by shining light at molecules through the Ag film which is so thin as to be practically transparent. The Raman emission is collected over 90^o as it comes out through the Ag film.

These experiments, even though carried out on a system that differs from that used for theoretical calculations, have reached some important conclusions. By using an incident p-polarized beam having $\vec{k}_{||}$ perpendicular to the grooves (i.e. $\vec{k}_{||} \equiv (0, k_y)$ they demonstrated an increase in the Raman intensity by a factor of 20 when the incidence polar angle equals that at which the reflectance has a dip. If $\vec{k}_{||}$ is parallel to the grooves and the beam is p-polarized, the enhancement goes down. For $\vec{k}_{||}$ perpendicular to the grooves and an s-polarized beam the Raman intensity is independent on the angle of incidence. The same qualitative conclusions have been reached by Girlando, Philpott, Heitman, Swalen and Santo[61] who used a sinusoidal holographic grating on which they deposited thick Ag films (3000-4000 Å), to make the system resemble closer the one used by the theory. The grating had a height of 163 Å and a wavelength of 4507 Å, so that the perturbation theory should give adequate results. The Ag film was covered with a thin film of polystirene whose 1000 cm^{-1} Raman band was monitored. The Raman intensity went up by a factor of 80, as the angle of incidence reached a value at which the reflectivity had a dip. There was no angle dependence for an s-polarized beam whose $\vec{k}_{||}$ was perpendicular to the grooves (Figure 2).

§48. The difference between the two experiments are by no means

worrisome. Both systems might have some additional roughness, since there was a SERS signal even when the plasmon was not excited through the grating. This extra roughness damps the plasmon and makes the enhancement corresponding to resonance angle smaller than the prediction of the theory. The damping might be different for samples prepared differently.

Furthermore, the system used by Tsang et.al.[60] consist of layers and the plasmon field extends over two or more layers. For example, it may extend over the Ag and the Al_2O_3 layer, in the tunneling junction. The dielectric constant of Al_2O_3 has a larger value of $Im\varepsilon$ than Ag and therefore the Al_2O_3 layer damps the plamon more effectively than if the whole system was made of Ag.

These two observations might explain why the enhancement in the two experiments is different.

§48. The most recent experiments with gratings have been carried out by Sanda, Warlaumont, Demuth, Tsang, Christman and Bradley[10]. They have used a sinusoidal Ag grating with 10,000 Å wavelength and 1000 Å height which had $\vec{K}_1$ along the (110) direction of the crystal ($\vec{K}_1$ is perpendicular to the grooves). The peaks and the valleys of the grating are so smooth that 90% of its surface is made of Ag(111) terraces. The crystal was covered with Py in UHV and the coverage was monitored with UPS.

The Raman spectrum of Py was taken in a back-scattering geometry at a collection angle of 45°. The dependence of the Raman intensity of the $990\,cm^{-1}$ symmetric ring breathing mode of Py on coverage was measured. It was found that if the angle of incidence is chosen to excite the surface plasmon, the enhancement of the Raman signal for the molecules in the first layer is $\sim 10^4$, while that for subsequent layers is $\sim 10^2$. The coverage dependence can be transformed into a distance dependence (by assuming a pyridine packing like in the Py crystal), which is found to be in qualitative agreement with the electromagnetic theory.

A quantitative fit of the data required the addition of a "molecular" enhancement mechanism, proposed by Jha, Kirtley and Tsang,[57] for the molecules located at the surface. One should keep in mind that the electrodynamic theory used for fitting the data[57] is incomplete since it does not include the emission effects. Furthermore, some other kind of roughness might be present on the surface, whose role is not taken into account by the calculations. Therefore, the conclusion that there might be a molecular enhancement for the molecules in the first layer is very interesting but still questionable. There is no doubt, however, that the qualitative features predicted by the e.m. theory are experimentally present.

§49, The study of SERS on gratings is theoretically very important, since we have a chance to deal with a controlled form of roughness. In principle, such a system will permit us to separate quantitatively the magnitude of electromagnetic effects from the molecular ones. This can be achieved only if some further progress is made: (1) we should experimentally insure that no undesired roughness is present on the grating's surface; (2) we should use non-perturbative solutions of Maxwell equations for both the primary field and the emission problem. It is especially necessary to "renormalize" the plasmon (i.e. to allow its interaction with the grating); (3) the grating should be thick enough so that the theory for a semi-infinite metal applies. Or better yet, the theory should be worked out for layered structures. The latter produce more diverse physical phenomena and introduce more experimentally known parameters (i.e. thicknesses of various films, their dielectric constants, etc.) whose variation allows a test of the theory; (4) the influence of the adsorbed molecules on the surface plasmon should be included in the theory, especially when many molecular layers are studied; (5) there is much information in the dependence of SERS intensity on the polar

and azimuthal angles of incidence and detection, and on the polarization of the incident and detected light. The theory could make very detailed predictions which should be tested.

§50. Fluorescence by molecules located near a grating. As we have already explained in §25 the theory and the practice of fluorescence depends on whether the experiments are carried out at steady state or if relaxation measurements are performed. In the first case we are basically interested in the emission intensity and the quantum yield. In the second case the intensity enhancement and the lifetime are the parameters controlling the process.

The lifetime depends on the magnitude of the imaginary part of the image field acting back on the molecule. This has not yet been computed for a grating. The enhanced emission has been examined.[58]

§51. An emitting dipole placed in the neighborhood of a flat surface couples to the solid and transfers energy either to electron hole pairs or to the unretarded surface plasmon (at frequency given by $\epsilon(\omega) = -1$). The lifetime is always shortened[36] but the effect is most dramatic when the dipole couples to the plasmon. There is little intensity enhancement, mainly a "minor" effect caused by the fact that the emitting dipole has a reasonably good mirror behind it.

In discussing the general theory of emission we pointed out that this can be enhanced if the dipole couples to a radiative electromagnetic resonance of the surface. On a flat surface the only resonance to which the dipole couples is the unretarded plasmon which is not capable of radiating. As a result, this coupling is a very effective energy loss mechanism which quenches the fluorescence.

If a grating is created on the flat surface, the plasmon can radiate and some of the energy which the dipole transferred to it is recovered as radiation. For a dipole located close enough to the surface it is the dipole near field which interacts stronger with the plasmon. The near field energy, which is not radiative, is

thus transferred to the surface plasmon, which can now radiate it through the grating. Parallel momentum conservation will very narrowly confine the angle of this emission. The grating is thus a device which transforms the nonradiant energy of the dipole near field into narrowly directed photon beams. Thus, a substantial emission enhancement results at well defined detection angles.

§52. This fluorescence mechanism was proposed and computed by Aravind, Hood and Metiu.[50] They considered a dipole perpendicular to xoy plane and computed its emission by using a perturbation theory in which the grating height is assumed small. This is basically the same type of theory as the one used for an incident planar wave. The difference comes from the fact that the dipole field, which in the present case plays the role of the incident field, is more complicated than a planar wave.

Numerical calculations indicate that the emission has angular resonances which can be observed as sharp intensity peaks appearing when the polar angle of detection θ is varied, at fixed values of the emission frequency and of the azimuthal angle of detection ϕ. Few examples are shown in Figures 3 and 4.

The calculations[58] point out the following qualitative features: (1) At small values of ϕ and ω there is a double resonance at two values of the polar angle θ. The peak located at the lower θ value disappears if either ϕ or ω are substantially increased. The resonance conditions can be obtained by inspection of the poles of the Green's functions propagating the fields.(58) For $\mathrm{Im}\varepsilon \ll \mathrm{Re}\varepsilon$, which is true for Ag in the frequency range of interest here, the resonance condition is given by Eq. (30), with slight

modification:

$$(\lambda n/L)^2 + \alpha(\lambda n/L)\ \sin\theta \sin\phi + \sin^2\theta = \mathrm{Re}\varepsilon(\omega)[1 + \mathrm{Re}\varepsilon(\omega)]^{-1}. \qquad \text{(III.32)}$$

We have inserted here the integer ($n = 1, 2, 3, \ldots$) which does not appear in the first order theory used to obtain Eq. (30) which is the result of a "single scattering" theory (only $n = \pm 1$ appears). The parameter α (with $\alpha = +1$ or -1) takes into account the fact that the diffracted field momentum is the photon momentum plus or minus a multiple of the grating parallel momentum.

For $n = 1$ and $\alpha = +1$ or -1, the Eq. (32) can have one or two solutions satisfying $0 < \theta < 90°$. Two solutions appear if $\phi < \phi_c$ with ϕ_c given by:

$$\sin\phi_c = \{1 - [\mathrm{Re}\ \varepsilon(\omega)\ (1 + \mathrm{Re}\ \varepsilon(\omega))^{-1} - (\lambda/L)^2]\}[2(\lambda/L)]^{-1}. \qquad \text{(III.33)}$$

This explains the presence of the double peaks in Figures 3 and 4. The peak at lower θ corresponds to $\alpha = -1$.

Obviously, the same analysis can be carried out for $n > 1$ by replacing L^{-1} with (n/L). Additional peaks, not predicted by the first order perturbation theory, will thus appear. Since the n=2 peak is obtained in second order perturbation theory we expect its intensity to be lower than that corresponding to n=2. Since the small parameter in which the field is expanded is $(a/2)\kappa_n$ (see Eqs. (18) - (21)), we expect the intensity of a $n = 2$ peak to be roughly $(a\kappa_2)^4/(a\kappa_1)^2$ times smaller than that corresponding to n=1. One should not forget that the resonance angles for the two peaks are different and therefore the exact intensity ratio differs from the one given above, which indicates the order of magnitude only. To get a more precise result one has to do second order perturbation theory.

Certain qualitative trends regarding peak heights and position have been suggested by the numerical results.[58] At fixed frequencies the polar angle θ corresponding to the peak position increases and the peak intensity goes down, as the azimuthal angle ϕ is increased. If ϕ is fixed, the peak intensity and the value of θ at which the peak appears go down with frequency.

Although the polarization of the emitted radiation has not been studied[58] one can guess certain propensity rules by using material discussed in this section. It is clear that if a photon of given characteristics cannot excite a plasmon, then an excited plasmon cannot emit a photon with those characteristics. From the equations (24) and (25) we see that a s-polarized photon can excite a plasmon if $(\vec{k}_{\|} \times \vec{k}_1)_z$ is non-zero. We have $(\vec{k}_{\|} \times \vec{k}_1)_z = (\omega/c)(2\pi/L) \sin\theta \cos\phi$ and therefore if the incident azimuthal angle is $\phi = 90^\circ$, $(\vec{k}_{\|} \times \vec{k}_1)_z = 0$. Hence, if a s-polarized photon is sent in a direction perpendicular to the grooves ($\vec{k}_{\|}$ is perpendicular to the grooves, hence along the y-axis) the plasmon is not excited. Conversely, a plasmon excited by the dipole will not emit an s-polarized photon in the y- direction (perpendicular to the grooves). The peak emission in that direction will be p- polarized. The emission in a direction along the grooves, or at any $\phi \neq 90^\circ$, will have an s-polarized component.

The emission intensity at the peak of the angular resonance depends on the distance from the dipole to the grating. For moderate distances, the intensity decays exponentially. We expect this on the basis of a simple argument. If we denote the plasmon electric field by $\vec{E}_{pl}(z)$, the coupling energy between the dipole and the plasmon is $\vec{\mu} \cdot \vec{E}_{pl}(z)$. In perturbation theory the efficiency of the plasmon excitation by the dipole depends on the square of the coupling energy. If the z dependence of $\vec{E}_{pl}(z)$ is of the form $e^{\Gamma_1 z}$ then the efficiency varies as $e^{2\Gamma_1 z}$ (z is negative in vacuum and Γ_1 is positive). If z becomes comparable to roughly a fourth of the wave length $2\pi c/\omega$, the distance dependence is altered dramatically and interestingly. The alteration is caused by the interference between the photons sent by the dipole directly to the detector and those which first reach the surface and then are scattered towards the detector.

Some of the details of the numerical results depend on the fact that perturbation theory has been used. The plasmon of the flat surface appears in the theory and the effects of the plasmon-grating collisions are not taken into account. Furthermore, in experimental situations the surface of the grating might have some residual roughness which will broaden the plasmon. For this reason we expect the measured resonance intensities to be smaller than the computed one.

An additional source of broadening is provided by the fact that the gratings made in laboratory might not have a perfectly sinusoidal profile. One can think of such a grating as a superposition of several sinusoidal gratings of slightly different wave length. The angular resonances produced by them are slightly shifted with respect to each other and are overlapping. The detector will give one "inhomogeneously broadened" resonance.

§53. Some of the predictions made by the theory have been verified experimentally by Adams, Moreland and Hansma.[63, 64] They used a nearly sinusoidal photoresist grating covered with a 300 nm Ag film. The grating height was 40 nm $\pm$ 20 nm and the length 846.5 nm. The grating was placed in a vacuum system and a N_2 layer was frozen on its surface. Through electron bombardment, metastable nitrogen atoms emitting at λ = 523 nm, were created in the N_2 layer. When the electron beam is turned off the long lived atoms continue to emit. The plasmon emission , due to the direct plasmon excitation by the incident electrons, is not detected since it has a very short lifetime and it disappears as soon as the electron beam is off. Thus, only plasmon emission resulting from energy transfer from the atom to the plasmon is observed.

The vacuum chamber was such that only the detection angles $4^\circ \leq \theta \leq 40^\circ$ and $\phi = 90^\circ$ were scanned. The theoretical predictions[58] were confirmed by these measurements. The peaks corresponding to n=1 and n = 2 were found at the

predicted angles and the emission was p- polarized. The intensity went down as the thickness of the N_2 layer was increased (i.e. thus increasing the distance between the emiting atoms and the grating). The peak widths are all about FWHM = 2.4° while the theory gives ∿0.5. However, the experimental width is instrumental. Furthermore, as argued in § 53, various inaccuracies in theory should make the observed width larger than the one obtained numerically. There are some complications caused by the fact that the theory assumes a steady state experiment while the measurement is a relaxation one. The intensity in the relaxation experiments depends on lifetime, which in turn depends on the distance. For example, Adams, Moreland and Hansma[63] find that the lifetime of the emission from a 10nm N_2 film is $\tau \sim 5$ sec. while a 30nm film gives $\tau \sim 20$ sec. Therefore, the intensity of the emission in a relaxation experiment at small distances from surfaces may be smaller than that at larger distances, due to lifetime effects. In order to test the intensity predictions made by the theory, the experiment should be run in a steady state arrangement.

In most cases we expect the emission due to direct plasmon excitation by the electron to be smaller than that due to formation of N atoms. An upper limit is given by the emission of clean gratings bombarded with electrons.

III.2.3. The use of Attenuated Total Reflection (ATR).

III.2.3(a). General Remarks.

§54. It is possible to excite the surface plasmon of a flat surface by placing it in contact with a transparent medium (usually a prism) whose refractive index n_p is chosen so that the parallel momentum in the material matches that of the surface plasmon:

$$(\omega n_p/c) \sin \theta_i = k_{||}^{sp}(\omega) \qquad \text{(III.34)}$$

This method was invented by Otto[68] and modified and improved by others.[69] Several reviews are available.[70] In what follows we use the name of Attenuated Total Reflection (ATR) for all such methods even if neither reflection nor attenuation is monitored.

The idea of using an ATR configuration in order to enhance the Raman and the Coherent Anti-Stokes Raman (CAR) spectrum of adsorbed molecules was proposed by Burstein et.al.[71] They worked out the theory and estimated the expected enhancement. The experimental studies[72, 73] are in qualitative agreement with the predictions of the theory.

The ATR configuration can also be used[74-79] to study the energy transfer from molecules fluorescing near a metal film, to the surface plasmon. If the film is placed on a prism the plasmon, excited by fluorescing molecules, can be made to radiate through the prism and the intensity of this radiation can be measured.

Finally, there is a large body of work concerning the use of the ATR to measure the surface plasmon dispersion, the dielectric constant of thin, absorbing organic films or the properties of metal-electrolyte interface in electrochemistry. We shall not review this work here, but give few of the early references.[80-85]

§55. Various ways of carrying out surface enhanced Raman or flouresence measurements with an ATR configuration are summarized in Figure 5. One usually starts by evaporating a Ag film on a quartz slide. The slide is then attached through an index matching fluid to a half-cylinder, giving the so-called Kretschmann configuration. The free face of the Ag film can then be covered with the molecule of interest, which is deposited either by a spinning technique or by placing the film in a solution containing the molecules. The molecule-surface distance can be varied by using the Langmuir-Blodgett technique,[86] in which fatty acid layers of known thickness are deposited on the surface. The molecules are then placed on the fatty acid film.

The incidence and detection scheme may vary. One can send light in along the pathway 1 (Figure 5a), and vary the incidence angle until the resonance condition Eq. (34) is satisfied. The surface plasmon is excited and this results in a lowering of the reflectance (measured with the detector at 4) and an increase of the electric field acting on the molecules. The latter causes an enhancement of the Raman intensity, which can be monitored at 2 or at 6. If fluorescence experiments are done, the fluorescent emission might be measured at 6 or 2. The reason for the difference between θ_f and θ_i is that the incident frequency differs from the emission frequency (by the vibrational frequency (in Raman) or by the fluorescence shift) and the resonance condition Eq. (34) gives different emission angles.

For Raman measurements the scheme incidence at 3 detection at 6 allows the use of the plasmon field in both excitation and emission. On the other hand the scheme incidence at 3 detection at 2 uses the plasmon for excitation only. Finally, the scheme incidence at 1 detection at 6 uses the plasmon to produce an angular resonance in emission. Similar comments can be made for fluorescence.

It is interesting to note that the prism can be replaced by a grating, as shown in Figure 5(b). The resonance condition Eq. (34) must then be replaced by Eq. (32) of §53. Finally, a combination of the type shown in Figure 5(c) can also be used. There are no experiments yet with (b) and (c).

III.2.3.(b). Raman spectroscopy with an ATR geometry.

§56. The theory for the use of ATR to enhance Raman signal has been briefly presented by Burstein et. al.[87] It is a standard ATR calculation which can be found, for example, in Ref. 81. It predicts that the enhancement factor will be in the range 100 to 150 and that only the p-polarized light can excite the plasmon and cause the enhancement.

The theoretical predictions were tested by Dornhaus, Benner, Chang and Chabay[73] who have carried out Raman experiments by using a Kretchman ATR configuration. They used a 57nm Ag film deposited on the flat part of a $SrTiO_3$ hemicylindrical prism. The experimental arrangement was that described in Figure 5(a) without any fatty acid spacers. The incident light was sent along 3 (see Figure 5(a)) and Raman scattering was detected at 2. Therefore, the effect of the surface plasmon on the primary field is observed, but not its effect on emission. In order to detect enhanced emission as well, the detector should have been placed at position 6 at which a plasmon of frequency $\omega - \omega_v$ would radiate through the prism.

The Raman intensity goes up by a factor of ten as the angle of incidence reaches the value needed to excite the surface plasmon. If the amount of Ag deposited on the half-cylinder corresponds to a 5nm film, the metal forms islands of several hundred Å size, which are better enhancers than the flat film, [88,89] even when the laser excites the flat film plasmon. Similar island Raman activity has been observed by other authors (see Section III.5). It is clear that the quantitative interpretation of the ATR Raman experiments can be made only if one is sure that the film used experimentally is flat. Islands or other roughening will cause additional signals that are very hard to interpret.

The experiments of Pettinger, Tadjeddin and Kolb[72] are very similar. They worked with the same Ag-prism arrangement, but the 50nm silver film was in contact with a pyridine containing electrolyte. The Raman signal was too weak to be detected unless a very mild anodization cycle was applied to the Ag film (for the role of anodization, see §30).

It was experimentally found that if the incident light is p-polarized with respect to the detection plane, the Raman intensity peaks at the angle of incidence where the reflectance (through the prism) has a dip caused by plasmon excitation. The resonant enhancement is ten times higher than that obtained when the incident laser is at an off resonance angle. The s-polarized light does not give a peak, in agreement with the predictions of the theory. Note that if the incident light was sent on the Ag through the electrolyte there was only a minor difference between the Raman intensity of the s- and p-polarized light (with respect to the plane of incidence).

The enhancement by a factor of 10 is smaller than the one expected theoretically. However, the existence of additional roughness probably broadens the plasmon and depresses its electric field intensity, hence the Raman signal.

III.2.3.(c). Fluorescence spectroscopy with an ATR configuration.

§57. The ATR configuration has been successfully used to study the rate of energy transfer from a fluorescing molecule to the surface plasmon of a film. If no prism is present and the film is thick enough to prevent the formation of a radiative plasmon, then the transferred energy is used to heat up the metal. If the rate of this transfer is Γ the lifetime is diminished from Γ_o^{-1} to $(\Gamma_o + \Gamma)^{-1}$.

If a prism is connected to the film like in Figure 5(a), the plasmon is able to radiate if the matching condition Eq. (1) is fulfilled. Thus, part of the energy transferred by the molecule into the film is recovered as plasmon radiation through the prism.

One can improve the experiment if the excitation is done from 1 or 3 and plasmon emission is measured at 6, while the fluorescence life-time is obtained at 2 (by turning off the laser and measuring the decay of the fluorescence). In this way one can obtain both the rate of energy transfer from the molecule to the solid and the rate of energy loss by plasmon radiation through the prism.

§58. The theory of this process is implicit in the early work on the rate of energy transfer from a dipole to a flat metal, as reviewed by Chance, Prock and Silbey.[36] The application to the present problem has been made by Weber and Eagen.[75]

Consider the case when the dipole is parallel to the surface. The total rate of energy loss by the dipole, divided by the rate of radiative energy loss when the surface is absent, is[36, 75]

$$b_{\parallel} = 1 + (3/4)q \ \mathrm{Im} \int_0^{\infty} [(u^2 - 1)\, r_p + r_s] \exp(4\pi (u^2-1)^{1/2} D/\lambda_1)(u^2-1)^{-1/2} u \, du \qquad \text{(III.35)}$$

Here q is the fluorescence quantum yield of the molecule in the absence of the surface, λ_1 is the wavelength of the photon in the medium in which the molecules are imbedded (dielectric constant ε_1, refractive index $n_1 = \sqrt{\varepsilon_1}$ and $\lambda_1 = \frac{2\pi c}{\omega n_1}$) and D is the surface-molecule distance. The quantities r_p and r_s are the Fresnel coefficients for a s- and p-polarized planar wave. For the discussion that follows we need only the expression for r_p which is given by[8, 11]

$$r_p = [\varepsilon_2(u^2 - 1)^{1/2} - \varepsilon_1(u^2 - (\varepsilon_2/\varepsilon_1)^{1/2})^{1/2}] \cdot [\varepsilon_2(u - 1)^{1/2} + \varepsilon_1(u - (\varepsilon_2/\varepsilon_1)^{1/2})^{1/2}]^{-1}. \qquad \text{(III.36)}$$

One should remember that the rate of energy transfer is proportional to the imaginary part of the image field (§20), which is in fact given by the Eq. (35). This is more complicated than the

result given by the customary image formula

$$b_{\parallel} \sim \mathrm{Im}\left[(\varepsilon_2 - \varepsilon_1)\ (\varepsilon_2 + \varepsilon_1)^{-1}\right](2d)^{-3}\ , \qquad \text{(III.37)}$$

which is valid only in the "electrostatic case" when $D/\lambda_1 << 1$ and retardation can be neglected. The Eq.(35) is valid at all distances and one can in fact show that it reduces to Eq. (37) if $D/\lambda_1 \to 0$.

The equation (35) is valid for a semi-infinite metal and it should be modified when applied to layered structures. The recipe is simple and requires the replacement of the Fresnel coefficients of the semi-infinite metal with those of the layered structure. If the Ag film is thick enough (e.g. 70-80nm) Eq. (35) is adequate for qualitative analysis.

§ 59. We can use Eq. (35) to try to understand how the plasmon emission depends on the molecule-surface distance. Note that the plasmon appears in Eq. (35) as a complex pole of the integrand. The value of u making $r_p \to \infty$ is given by

$$u^2_{\text{pole}} \approx \varepsilon_2(\omega)\ (\varepsilon_2\ (\omega) + \varepsilon_1)^{-1} \qquad \text{(III.38)}$$

Comparing this to the surface plasmon dispersion relation (§34)

$$k^{sp}_{\parallel}(\omega) = \left(\frac{\omega}{c}\right)\left[\frac{\varepsilon_1\varepsilon_2}{\varepsilon_2 + \varepsilon_1}\right]^{1/2} \qquad \text{(III.39)}$$

we find that

$$u_{\text{pole}} \approx k^{sp}_{\parallel}(\omega)/k_1. \qquad \text{(III.40)}$$

Here $k_1 = \left(\frac{\omega}{c}\right) n_1$ is the wave vector of the photon in the medium 1.

We can now investigate how the pole contributes to the rate of energy transfer $b_{\parallel}$. (1) If (D/λ_1) is very small Eq. (37) is valid and we have $b_{\parallel} \sim \mathrm{Im}\left[(\varepsilon_2 - \varepsilon_1)\ (\varepsilon_2 + \varepsilon_1)^{-1}\right]$. Large values of $b_{\parallel}$ are obtained if $\varepsilon_2(\omega) = -\varepsilon_1$. This corresponds to the excitation of a surface plasmon

having $k_{sp}^2 \to \infty$ (see Eq. (39)). Such a plasmon cannot be made to radiate by a prism since the condition Eq. (34) cannot be fulfilled; photon emission would violate parallel momentum conservation. Therefore, if D is very small, the rate of energy transfer to the solid is extremely high, but none of the transferred energy can be recovered as plasmon radiation through the prism. The intensity of plasmon emission is zero.

(2) If $D/\lambda_1 \gg 1$, the exponential $\exp[-4\pi(u^2 - 1)^{1/2} D/\lambda_1]$ in Eq. (35) cuts down the integration range to u smaller than roughly $(\lambda_1/D)^{1/2}$. Since only those values of u in the range $0 < u \lesssim \sqrt{\lambda_1/D}$ contribute to the integral, and since $u_{pole} = (k^{sp}(\omega)/k_1)$, r_p can have a pole only if the frequency is such that $0 < \mathrm{Re}(k_{\|}^{sp}(\omega)/k_1) < \sqrt{\lambda_1/D}$. Since the frequency ω of the emitter if fixed by our choice of molecule, the excitation of the plasmon is possible if $0 < \frac{\mathrm{Re}\epsilon_2(\omega)}{\epsilon_1 + \mathrm{Re}\epsilon_2(\omega)} \lesssim \sqrt{\lambda_1/D}$ (we have used (39) and $\mathrm{Im}\epsilon_2 \ll \mathrm{Im}\epsilon_1$, which is valid for Ag and many other materials). We see that as D is increased this restriction cannot be satisfied and the surface plasmon cannot be excited. This is not surprising, since as $D \to \infty$ the dipole radiation is practically a planar wave and the latter cannot excite the plasmons of the flat surface.

(3) Therefore, all the action occurs at intermediate values of (D/λ_1). Plasmons of small $k_{\|}^{sp}$ can be excited and the prism can make them radiate (since the radiation condition $\mathrm{Re}k_{\|}^{sp}(\omega) = (\omega/c)n_p \sin\theta_f$ is satisfied.

The qualitative discussion presented above implies that the plasmon emission must have an intensity maximum as a function of distance. The numerical calculations of Weber and Eagen [75] using Eq. (35) substantiate

this analysis and give the results presented in Figure 6.

§60. The experimental test of these predictions can be found in recent work.[74-79] We review here the experiments of Pockrand, Brillante and Mobius,[78] who used fatty acid spacers, to achieve a known molecule-metal film distance. The experimental arrangement is that described by Figure 5. The thickness of the Ag film is 55nm and the length of the fatty acid molecules used as spacers is 2.68nm. Making multilayer structure (§35) they fabricated fatty acid films of thicknesses varying between 2.68nm, and 24.12nm in steps of 5.36nm (0, 2, 4, 6 and 8 layers were used). A dye with an imposing name (5, 6, 5', 6' - tetrachloro-1, 1' - dioctadecyl-3, 3' - diethyl - benzimidazolo-carbocyanin-p-toluensulfonate) was deposited on the fatty acid film. This has a fluorescence peak at λ = 595nm and a fairly broad excitation band.

Pokrand et.al.[42,78] have used two excitation-detection schemes, which can be both described with the aid of Fig. 5.

Scheme I has the incident beam along the direction 1 of Fig. 5, with the electric vector polarized perpendicular to the detection plane (which is taken perpendicular to the axis of the half-cylinder). The incident light having the wavelength λ_o excites the dye, but also excites the plasmon through unavoidable film roughness. Therefore, two plasmons are excited and coexist in the film. One excited directly by the laser having the frequency $\omega_o = 2\pi c/\lambda_o$ and parallel momentum $k_{||}^{sp}(\omega_o)$; the other excited by the molecules, and having the frequency $\omega = 2\pi c/\lambda$ and $k_{||}^{sp}(\omega)$. They can both emit through the prism at angles given by $(\omega/c)\sin\theta_f = k_{||}^{sp}(\omega)$ and $(\omega_o/c)\sin\theta_f^o = k_{||}^{sp}(\omega_o)$. In Fig. 5a these are represented by the directions 4 and 6. The emission peaks at θ_f and θ_f^o but it is fairly broad (half width at half height $\sim 2^o$). If λ and λ_o are close, θ_f and θ_f^o are close. The emission

due to direct plasmon excitation by laser through roughness (at θ_f) is much stronger than that due to plasmon excitation by energy transfer from the excited molecules (at θ_f^o). For example,[78] for λ_o = 520.8nm and D = 18.76nm the plasmon emission at θ_f (and λ = 595nm) is a barely visible shoulder on the wing of the plasmon emission at θ_f^o (with λ_o = 520.8nm). It is therefore important to work with dyes for which $|\lambda - \lambda_o|$ is large and to anneal and sputter the films to make them as smooth as possible to cut down the emission at θ_f^o.

Scheme II places the incident beam along 3 and the detector along 6 (see Fig. 5a). The angle θ_i is chosen to satisfy Eq. (34) and excite the surface plasmon. The evanescent field of the plasmon (of frequency $2\pi c/\lambda_o$) excites the molecules which transfer energy and excite a plasmon of frequency $2\pi c/\lambda$. Both plasmons emit through the prism, but the emission is at different angles (i.e. 4 and 6 in Fig. 5(a)). In this arrangement both the molecular excitation step and the energy transfer from the molecules to the plasmon depend on the molecule-surface distance D. The dependence of the emission intensity on D is a convolution of these two effects.

The experimental results[78] are presented in Fig. 7 where the fluorescence intensity is plotted versus the molecule-surface distance.[78] Since it is believed that the dye has the transition moment parallel to the surface the experimental curves Fig. 7(a) and (b) should be compared to the lowest curve of Fig. 6 computed by Weber and Eagen.[75]

The theoretical predictions are plotted together with the experimental points. Since the absolute fluorescence intensity is not being measured, the theoretical curve is calibrated to be equal to the experimental point at 18.8nm. The agreement between theory and experiments is satisfactory.†

† We are grateful to Dr. Pockrand who provided the theoretical curves shown in Fig. 7.

III.2.4. The use of small random roughness (SRR).

III.2.4.a. Introductory remarks.

Another useful representation of a rough surface is the small random roughness (SRR) model. The general shape of such a surface is shown in Fig. 8. The mean surface plane is located at $z = 0$ and the deviation $z \equiv \xi(\vec{r}_{\parallel})$ of the real surface with respect to the plane is a random function. In other words, given a point $\vec{r}_{\parallel}$ we do not know the height of the surface at that point, but only the probability of having a given height ξ.

It is useful to analyse the model in terms of the Fourier transforms $\xi(\vec{k}_{\parallel})$ of the surface shape:

$$\xi(\vec{r}_{\parallel}) = \int \frac{d\vec{k}_{\parallel}}{(2\pi)^2} e^{i\vec{k}_{\parallel} \cdot \vec{r}_{\parallel}} \xi(\vec{k}_{\parallel}). \qquad \text{(III.41)}$$

We can think now of the irregular surface as superposition of gratings of wavelength $2\pi/|\vec{k}_{\parallel}|$, with the amplitude $\xi(\vec{k}_{\parallel})$. Obviously, since we know only the probability that $\xi(\vec{r}_{\parallel})$ has a certain value, we cannot specify the values of $\xi(\vec{k}_{\parallel})$ but only the probability of each given value.

Like in the case of gratings we would like to use perturbation theory to compute the electromagnetic properties of the surface. This can be done if (§ 39) $\xi(\vec{k}_{\parallel})|\vec{k}_{\parallel,i}| << 1$, $\xi(k_{\parallel})k_{\parallel} << 1$ and $k_{\parallel}\Gamma^{-1} << 1$. Here $\xi(\vec{k}_{\parallel})$ is the height of the grating with wavelength $2\pi/|\vec{k}_{\parallel}|$, $k_{\parallel,i}$ is the wave vector of the incident radiation and Γ^{-1} is the decay length of the amplitude of the surface plasmon excited at the incident frequency. Note that if the incident field is a planar wave, then $k_{\parallel,i} = (\omega/c)\sin\theta_i$ (θ_i = polar angle of incidence with respect to the normal to the surface). If the incident field has a more complicated spatial dependence then we Fourier transform it and $\vec{k}_{\parallel,i}$ is the wave vector labeling the Fourier components. If the incident field varies rapidly in space its Fourier transform has components with high $k_{\parallel,i}$ and the perturbation theory tends to break down.

AD-A114 274 CALIFORNIA UNIV SANTA BARBARA DEPT OF CHEMISTRY F/G 7/4
SURFACE ENHANCED SPECTROSCOPY.(U)
JAN 82 H METIU N00014-81-K-0598
UNCLASSIFIED TR-2 NL

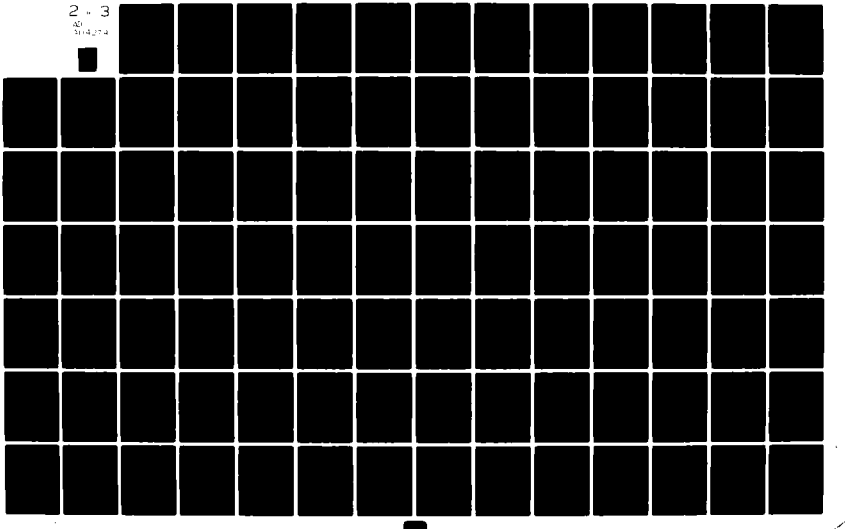

In order to define the model completely we must specify the statistical properties of the surface. Within perturbation theory we are only interested in the average values of $\xi(\vec{k}_{//})$ and $\xi(\vec{k}_{//})\xi(\vec{k}'_{//})$. These are given by

$$<\xi(\vec{k}_{//})> = 0 \qquad \text{(III.43)}$$

and

$$<\xi(\vec{k}_{//})\xi^*(\vec{k}'_{//})> = (2\pi)^2 \Sigma(\vec{k}_{//} + \vec{k}'_{//}) \Sigma^2 a^2 \exp[-(\frac{ak_{//}}{2})^2]. \qquad \text{(III.44)}$$

Here< > represents the average over the probability distribution for the surface height. The quantity Σ^2 is the mean square height and a is the correlation length of the roughness. The information conveyed by a is the following: consider two points $\vec{r}_{//}$ and $\vec{r}'_{//}$ on the surface. If $|\vec{r}_{//} - \vec{r}'_{//}| >> a$, the surface heights $\xi(\vec{r}_{//})$ and $\xi(\vec{r}'_{//})$ are statistically independent. Mathematically this means that $<\xi(\vec{r}_{//})\ \xi(\vec{r}'_{//})> = 0$. The physical consequence is that the scattering of radiation by such two points does not contribute to the scattering intensity. Another way to formulate this is to state that the roughness cannot change the momentum of the scattered photon by more than 1/a.

§62. It is believed that a physical realization of such a surface might be achieved by working with CaF_2 films.[83-86] The CaF_2 crystalites protrude through the film surface giving it a rugged aspect. The height of these protuberances increases with the film thickness. If a Ag film is deposited on the CaF_2 layer, its surface will have the same coarse aspect. Careful annealing can be used to smooth out the surface to some extent.

§63. The theory for light scattering by small random roughness has been developed by a number of authors.[54, 55] They all use perturbation theory and obtain, by different procedures, very similar results.

The application to surface enhanced spectroscopy is still incomplete. Aravind and Metiu[94] computed the intensity of the emission by a dipole located near the rough surface. The calculation assumes a steady state experiment in which the dipole is continuously driven by the incident laser. The results are relevant to all the spectroscopic techniques involving emission, such as Raman, fluorescence and Resonant Raman. Note however that the emission calculation solves only a part of these problems. For the fluorescence and resonant Raman spectroscopy the dipole must be modified to include the image field effects. This has been done by Arias, Aravind and Metiu.[49] For Raman scattering one must include the fact that the induced dipole is proportional to primary field (§22), which is affected by roughness. For this reason the induced dipole will have the same frequency and distance dependence as the primary field.

Finally, the theory of light emission by tunneling junctions[95,96,99] having SRR surface has been developed by Laks and Mills.[54c] Experiments by Tsang, Kirtley and Bradley[60] have shown that the roughness dependence of the Raman intensity of molecules placed in a tunneling junction is related to the intensity of light emitted by the rough junction[96] as a consequence of excitation by the fluctuations in the tunneling current.[97] The relationship will be discussed below.

§64. The enhancement generated by small random roughness is the least impressive compared to other methods of roughening. Therefore, the subject is not central to surface enhanced spectroscopy. However, it is important in those areas where a detailed comparison between experiment and theory is sought. One such situation appears in the experimental work[38-44]

that attempts to determine the molecule-surface distance at which phenomenological electrodynamics (i.e. local dielectric response and discontinuous boundary) becomes inaccurate. One way of probing this is to determine the fluorescence life time of molecules located at known distance from the surface and to test whether it agrees with the phenomenological formula for flat surfaces. Deviations can be caused by a breakdown of the theory or by the fact that the surface is not flat and some small roughness is present. Since there is no experimental technique to detect the presence of such roughness (light scattering will detect only small roughness with long correlation length), we must know how this roughness affects life time. If the observed lifetime differs from the one predicted by the phenomenological theory, the breakdown of the phenomenological equations is conclusively established only if the effect of roughness has either been ruled out or taken into account.

III.2.4.b. The intensity of the emission by a dipole near a surface with SRR.

§65. The theory is rather complicated and we give here only an outline of the procedure. An oscillating dipole $\vec{\mu}(t) = \vec{\mu}(\omega)\, e^{-i\omega t}\, \delta(z-z_o)\delta(x)\delta(y)$ located at $\vec{r}_o \equiv (0, 0, z_o)$ is equivalent[7] to the current density $\vec{j}(\vec{r},t) = -i\omega\vec{\mu}(\omega)\, \delta(z-z_o)\delta(x)\delta(y)\, e^{-i\omega t} \equiv \vec{j}(\vec{r},\omega)\, e^{i\omega t}$.

The electric field

$$\vec{E}(\vec{r},t) = \vec{E}(\vec{r};\omega)e^{-i\omega t} \qquad \text{(III.45)}$$

produced by this current is obtained by solving Maxwell's equation:

$$\nabla \times \nabla \times \vec{E}(\vec{r};\omega) - \varepsilon(\vec{r};\omega)(\omega/c)^2\, \vec{E}(\vec{r};\omega) = 4\pi(\omega/c)^2 \vec{j}(\vec{r};\omega) \qquad \text{(III.46)}$$

The dielectric constant $\varepsilon(\vec{r};\omega)$ is given by

$$\varepsilon(\vec{r};\omega) = \begin{cases} 1 & \text{for } z > \xi(x,y) \\ \varepsilon(\omega) & \text{for } z < \xi(x,y) \end{cases} \qquad \text{(III.47)}$$

where $z = \xi(x,y)$ is the position of the vacuum metal interface and $\varepsilon(\omega)$ is the dielectric constant of the metal.

We can write $\varepsilon(\vec{r};\omega)$ as

$$\varepsilon(\vec{r};\omega) = \varepsilon_o(\vec{r};\omega) + \Delta\varepsilon(\vec{r};\omega) \tag{III.48}$$

where $\varepsilon_o(\vec{r};\omega)$ is the expression (47) for the case of a flat surface located at the mean surface plane (i.e. $\xi(x,y) = z = 0$).

We can formally define a dyadic Green function $\overleftrightarrow{D}(\vec{r};z_o;\omega)$ which gives

$$\vec{E}(\vec{r};\omega) = \overleftrightarrow{D}(\vec{r};z_o;\omega)\ 4\pi(\omega/c)^2\ (-i\omega)\cdot\vec{\mu}(\omega). \tag{III.49}$$

The exact calculation of $\overleftrightarrow{D}$ for a rough surface is difficult. However, we know the dyadic Green's function $\overleftrightarrow{D}_o(\vec{r};z_o;\omega)$ for the flat surface (i.e. for $\Delta\varepsilon \equiv 0$) and if we assume that $\Delta\varepsilon$ is small, we can get $\overleftrightarrow{D}$ for the SRR surface by perturbation theory. [54] To the first order in $\Delta\varepsilon$ the perturbation theory gives

$$\overleftrightarrow{D} = \overleftrightarrow{D}_o + \overleftrightarrow{D}_o\ \Delta\varepsilon\ \overleftrightarrow{D}_o \tag{III.50}$$

A tedious calculation [94] starting with Eq. 46) provides an expression for $\overleftrightarrow{D}$. Using that in(49) gives the electric field radiated by the dipole.

§66. It is useful at this point to leave the mathematical description and develop an equivalent physical picture. The calculation here is very similar to the one used in light scattering from critical fluctuations [100] or a system undergoing spinodal decomposition. [101] There, the density fluctuates and its instantaneous value is $\rho = \rho_{eq} + \delta\rho$, where q_{eq} is the equilibrium value. Since the dielectric constant depends on density we have $\varepsilon = \varepsilon_{eq} + \left(\frac{\partial \varepsilon}{\partial \rho}\right)_{eq} \delta\rho$. The dielectric constant fluctuation $(\partial\varepsilon/\partial\rho)\delta\rho \equiv \delta\varepsilon$ scatters light and within the first order perturbation theory the intensity of the elastic scattering is determined by

$$\langle \delta\varepsilon(\vec{k})\ \delta\varepsilon(\vec{k}') \rangle = (2\pi)^3 \delta(\vec{k} + \vec{k}') \langle \delta\rho(\vec{k})\delta\rho^*(\vec{k}) \rangle \left| \left(\frac{\partial \varepsilon}{\partial \rho}\right)_{eq} \right|^2 \tag{III.51}$$

We can now regard suface roughness as a "density fluctuation" about the flat surface situation. The latter is the analog of the equilibrium density in the example discussed above. The "fluctuation" of the dielectric constant is $\Delta\varepsilon$ and the correlation function of $\Delta\varepsilon$ is proportional to Eq. (43) which is the analog of (51). There is a basic difference between the two situations since in our problem the scattering is from the surface, while in Eq. (51) it is from the bulk. Because of this the Eq. (44) parallel momenta only. Another difference appears because the surface does not move, while the density fluctuations do. In our case the time does not appear in the correlation function and for this reason the phenomenon is analogous to the elastic light scattering by fluctuations and no Brillouin peaks are present.

The analogy between the Eqs.(43)and (51) tells us that the correlation function in Eq.(43) acts as the structure factor of the rough surface The likelihood that the surface can change the parallel momentum $\vec{k}_{\|,i}$ of the incident wave into the parallel momentum $\vec{k}_{\|,f}$ of the scattered wave, is proportional to $\exp[-(|\vec{k}_{\|,f} - \vec{k}_{\|,i}| \frac{a}{2})^2]$. If $|\vec{k}_{\|,i} - \vec{k}_{\|,i}| a \lesssim 1$, this likelihood is high. The quantity $|\vec{k}_{\|,f} - \vec{k}_{\|,i}|$ is constrained by the fact that $k_{\|,i} = (\omega/c) \sin\theta_i$ and $k_{\|,f} = (\omega/c) \sin\theta_f$ where θ_i and θ_f are incident and final polar angles. Therefore, $|\vec{k}_{\|,i} - \vec{k}_{\|,f}|$ is of order (ω/c). As a result, if $\omega a/c \lesssim 1$ the roughness contribution to scattering by the surface is important. If $\omega a/c \gg 1$ the Gaussian is practically zero and only little roughness induced scattering occurs. For this reason a rough surface scatters differently from a flat one only if the correlation length of the roughness is of the same order or larger than the wavelength of the incident photon.

If the incident wave is not a planar one, but the spherical wave (including the near field) of a point dipole, we can still use the above discussion if we Fourier decompose the incident field in a superposition of planar waves. Each such planar wave is substantially scattered by roughness if its parallel wave vector $k_{\|}$ satisfies $k_{\|} a \lesssim 1$. The total scattered

light is given by the integral over the scattering of each incident planar wave, that is, by an integral over the parallel wave vectors.[94]

§66. Numerical calculations using the theory described above were performed by Aravind and Metiu.[94] To present their results we denote with I the intensity radiated by the dipole when a SRR surface is present, and with I_o the intensity radiated when the surface is flat and is located at z=0. In Fig. 9 we plot $I_{rough}/I_{flat} = (I - I_o)/I_o$ as a function of frequency. The metal is Ag, the mean height is $\delta = 30$ Å, the angle of detection is 45^o and the dipole is perpendicular to the mean surface. The mean surface-dipole distance is 2Å. It is obvious that the emission intensity is enhanced by roughness only if the correlation length a is small. A brief discussion of the role of a and d in the emission process is given in the Ref. [94] and we do not reproduce it here.

III.2.4.c. The change of fluorescence life time by the presence of a SRR surfac

§67. As explained in the introductory section (§ 20), the change in lifetime produced by roughness can be computed if the change in the image field is known. This has been examined by Arias, Aravind and Metiu [49] who used the work of Rahman and Maradudin.[102] They find[49] that the effect of roughness extends at fairly large distance from the surface and it is most pronounced if the frequency of the emitter is close to that of the surface plasmon. In Fig. 10 we represent the ratio between the rate of energy transfer to a rough surface versus that to a flat surface. The metal is Ag and the roughness is characterized by $\delta = 20$ Å and a = 60 Å More information can be found in the original paper.[49]

III.2.4.d. Light emitting tunneling junctions with SRR surfaces.

§68. We do not review in this article the light emitting tunneling junctions[95 - 99] to the extent they deserve, but confine ourselves to pointing out how they are related to surface enhanced spectroscopy. The model used to compute the photon emission assumes[91] that the tunneling electrons cause a fluctuating current in the junction. This current differs from the one generated by an excited molecule (Eq. (34)) in its magnitude, location and frequency dependence. However, it has the same electromagnetic effect: it drives the structure causing it to radiate in a manner that depends on the roughness. The electric field of the radiation is given by Eq. (49). The dyadic Green's function $\overleftrightarrow{D}$ depends on the junction's structure only[54c] but not on the properties of the driving current. For this reason the emission by the junction ought to have many of the characteristics that one would observe if the junction is doped with a dye and the dye fluorescence or Raman spectrum is studied. The same Green's function, but a different current, gives the electric field of the molecular emission. The general resemblance between the Raman spectrum of molecules located in a roughened junction[60] and the light emitted by that junction when driven by a voltage[95-96] has been observed by Tsang, Kirtley and Bradley.[60]

III.2.5. Excitation of surface plasmon by depositing metal particles on a flat surface

§69. Another way of exciting the surface plasmon, by avoiding the restrictions imposed by the conservation of the parallel momentum, is to deposit small particles on the flat surface. Translational symmetry along the surface is thus broken and momentum conservation is no longer a kinematic requirement.

Such particle deposition can be achieved, for example, by condensing small amounts of metal vapor on the flat surface of interest. Due to the nucleation process the condensed vapor forms small islands whose dimensions depend on the average amount of material per unit area.[103,104] (see Section III.5). Another method[105] consists of cooling the surface in a vacuum chamber and condensing molecules on it, to form a matrix. Simultaneously a noble gas beam containing metal spheres is directed towards the surface. During the condensation the matrix traps the spheres near the surface forming the system of interest. This can be used to carry out surface enhanced spectroscopy on the molecules of the matrix. Finally, we can deposit spheres on a surface by spinning a colloidal solution and then evaporating (if necessary) the solvent.

§70. The properties of these systems are modeled here by considering the electrodynamic properties of a small sphere located above a flat surface.[31,106,107] We present here results obtained for a perfectly conducting sphere[106] The case of dielectric sphere[107] is discussed in Section III.4.2., which is concerned with the interaction between two electromagnetic resonances.

The qualitative electrodynamic properties of the system can be understood by considering first the case of large sphere-surface separation. The incident field plus the field reflected by the flat surface polarize the sphere, inducing a dipole moment μ. If the external field frequency satisfies the condition Re $\varepsilon_1(\omega) = -1$ ($\varepsilon_1(\omega)$ is the dielectric constant of the semi-infinite

solid) the dipole μ excites the surface plasmon. The excitation is exclusively due to the presence of the sphere and it would not occur if the laser interacts with the flat surface only.

When the sphere is brought closer to the surface it suffers additional polarization due to the image field. Since the sphere-plane distance is small the image field varies rapidly in space. As a result, the sphere acquires both a dipole and a quadrupole moment which both can excite the surface plasmon, etc.

It is important to realize that the polarized sphere not only permits the excitation of the plasmon but also interacts with it and modifies it. As a result the combined sphere-plane system has new resonances whose complex frequencies are given by[106]

$$\exp\left[(2n+1)\,\mu_o\right] = (\epsilon_1(\omega) - \epsilon_o)\,(\epsilon_1(\omega) + \epsilon_o)^{-1} \qquad \text{(III.52)}$$

Here ϵ_o is the dielectric constant of the half-space in which the sphere is located, $\epsilon_1(\omega)$ is that of the semi-infinite material whose flat surface sustains the resonance, $\mu_o = [\cosh(1+\lambda)]^{-1}$ with $\lambda \equiv D/R_o$, D is the minimum distance between the flat surface and the surface of the sphere, and R_o is the radius of the sphere.

The resonance frequency depends on the geometry (through λ only) and on the dielectric properties of the flat material. This is illustrated in Table 1 where the resonance frequencies are given for a flat SiC surface, for various values of λ. As λ is diminished more than one resonance is present. By changing the geometrical parameter λ we can vary the resonance position between 878 cm^{-1} and 944 cm^{-1}. The width of these resonances are not given here; in most cases they are broad and cannot be experimentally resolved. One exception is SiC.

§71. The nature of these resonances is illustrated by computations of

$$\tilde{I} = (\vec{E} \cdot \vec{E}^*)/(\vec{E}_i \cdot \vec{E}_i^*) \ , \qquad \text{(III.53)}$$

which gives the ratio of the local laser "intensity" versus the intensity of the incident field in the absence of the solids. The factor $\tilde{I}$ is a measure of the magnitude of the primary field enhancement. The spatial extent of $\tilde{I}$ is characterized by two distances ξ_1 and ξ_2. These are taken along a line C defined as follows: it is contained in the plane of incidence of the laser; it is parallel as follows: it is contained in the plane of incidence of the laser and it is parallel to and located at one Å from the flat surface. ξ_1 is the distance, along C, from the rotational symmetry axis of the system to the point where $\tilde{I}$ is five times larger than the value of $\tilde{I}$ given by Fresnel equations (which are valid when the sphere is absent). ξ_2 is the distance measured along C, from the symmetry axis to a point where the presence of the sphere does not affect $\tilde{I}$. Both ξ_1 and ξ_2 are "measured" along C towards the light source. The values of ξ_1 and ξ_2 are shorter when they are "measured" in the opposite direction, in the "shadow of the sphere." From Table 2 we see that $\tilde{I}$ is enhanced substantially even at distances of an order of 150Å from the symmetry axis; the effect of the sphere disappears entirely at distances of order 300Å. Further calculations[106] show that $\tilde{I}$ is very large and practically constant along the rotational symmetry axis (in the space between the sphere and the plane). Therefore, the resonances excited in this system are very localized in space between the plane and the sphere, as if the polarized sphere acts on the surface plasmons and forms a localized wave packet.

§72. In order to give a feeling for the magnitude of the local field enhancement in the region between the sphere and the plane, we give in Table ? the resonance values of $\tilde{I}$ calculated at a point on the symmetry axis, at 1Å from the flat surface. The position of this point is not essential since $\tilde{I}$ is practically constant along the symmetry axis.

We find that the values of $\tilde{I}$ are much larger than those for the isolated sphere or than the intensities obtained by exciting the surface plasmon of the flat surface by using ATR or a grating. For SER the total enhancement is roughly $\tilde{I}^2$ since by the reciprocity theorem[22] the emission enhancement is comparable to the primary field enhancement. Thus using a Ag surface and a perfectly conducting sphere we would obtain, at $\omega = 3.2$ eV a Raman enhancement factor of 7.4×10^7. The enhancement factor $\tilde{I}$ in the case when the flat surface is made of SiC and InSb and p-polarized infrared light is used, is of order 10^4.

The elementary excitation of the planar surface, which is used by the sphere to build up the localized resonance producing the enhancement, does not have to be a surface plasmon. In the case of SiC it is a surface polarition, for an organic substrate (e.g., anthracene) it is a surface exciton and for Ag and InSb it is a surface plasmon. It is interesting to note that in the case of a semi-conductor the surface plasmon frequency, hence the resonance frequency of our system, can be modified by doping. The resonance frequency for InSb, for example, can be varied by doping between 200 cm^{-1} and 1100 cm^{-1}.

From the Table 2 it is clear that the p-polarized light is a more effective excitation source. Such a dramatic difference between p- and s-polarized light is not uncommon in surface spectroscopy and can be used to develop polarization modulation schemes that improve sensitivity even if large background signals are present.

III.3.1 Enhanced spectroscopy on spheres.

III.3.1.a. Introductory remarks.

§73. The spherical particles are the most convenient of the regular shapes since they are characterized by only one parameter, the radius. This compares favorably with ellipsoids, where two lengths are involved and we must average over their distribution as well as over the orientation of the ellipsoids with respect to the incident field. This proliferation of parameters and averages, over quantities which are hard to control or measure experimentally, introduces uncertainties which one would like to avoid if the purpose of the work is a detailed test of the theory. On the other hand, if the purpose is the generation of large enhancements over a large frequency range, a distribution of ellipsoids is preferable to one of spheres.

§74. In this section we review the existing theoretical and experimental work with spherical systems. It turns out that the largest enhancements are obtained for small particles (the Rayleigh limit). This is fortunate, since the theory for them is simplest and their preparation is not any more difficult than that of large particles. For these reasons we review the work with small particles in detail. For larger spheres we only select few results, to give a feeling for the trends expected as the radius is increased.

The experimental work has been carried out with colloidal solutions or particles prepared in gas phase and then frozen in a matrix. This is also reviewed in detail.

III.3.1.b. Electromagnetic properties of small spheres.

§75. The electrodynamic properties of small spheres have been computed by Rayleigh and his results can be found in many standard books.[7-11, 109] Several recent papers[110-117] have used Rayleigh theory to discuss the electromagnetic enhancement in SERS.

As explained in Section II we are interested in the electromagnetic fields caused by the polarization of the small sphere driven by the electric field of the incident laser

$$\vec{E}_i(\vec{r},t) = \vec{E}_i(\omega)e^{-i\omega t}e^{i\vec{k}\cdot\vec{r}}, \tag{III.54}$$

or by that of an oscillating dipole[7] located nearby:

$$\vec{E}(\vec{r},t) \equiv \overleftrightarrow{T}(\vec{r})\cdot\vec{\mu}e^{-i\omega t} = e^{i\vec{k}\cdot\vec{r}} = (3\hat{r}\hat{r}-\overleftrightarrow{I})\cdot\frac{\vec{\mu}}{r^3}e^{ikr}e^{-i\omega t} \tag{III.55}$$

Here $\vec{r}$ is the distance from the dipole to the field point $\hat{r} \equiv \vec{r}/r$, $\overleftrightarrow{I}$ is the unit tensor, $|\vec{k}| = \omega/c$ and the dyadic $\hat{r}\hat{r}$ acts on $\vec{\mu}$ according to the rule $(\hat{r}\hat{r})\cdot\vec{\mu} = \hat{r}(\vec{\mu}\cdot\hat{r})$.

The main advantage in working with objects smaller than the wavelength of the incident radiation is that retardation can be neglected and, as a consequence, the electric field can be computed by solving an electrostatic problem. If the object has a size d, the maximum variation of the phase of the incident field across the object is e^{ikd}. If $kd = 2\pi d|N|/\lambda$ (N is the complex refraction index and λ is the wavelength) is much smaller than one, $e^{ikd} \simeq 1$. Because of this, we make a small error if we take $kd = \omega d/c \to 0$. Since the frequency and the size are experimentally fixed, this limit corresponds to $c \to \infty$, (i.e., neglect of retardation). If we take $c \to \infty$ in Maxwell's equations we find that the electric field is fully determined by the scalar potential Φ, which in turn satisfies Laplace's equation.[7-11] Thus, we can get a good approximation for the electric field by solving an electrostatic problem.

Of course one cannot compute the radiation from the system by using electrostatics. The trick is to compute the dipole induced in the system and then assume that the observed radiation is that of the computed dipole.

These qualitative arguments are reinforced by rigorous studies [8,9,11] in which the problem is solved for a sphere of arbitrary radius and the solution in the limit $d|N|/\lambda \to 0$ is determined. The leading term of both local and radiated field in this limit is identical to the result obtained from the electrostatic calculation.

In what follows we present the equations necessary for discussing surface enhanced spectroscopy. We need (see Section II) the reflected field (i.e., the reflection tensor $\overleftrightarrow{R}$, §10), the radiation from the solid (i.e., the dyadic Green function $\overleftrightarrow{G}_s(\vec{R}_d;\vec{r}_\alpha;\omega)$, §11) and the image field (i.e., $\overleftrightarrow{G}_s(\vec{r}_\alpha,\vec{r}_\alpha;\omega)$, §20).

§76. Reflected field enhancement. As defined in §10 the reflected field $\vec{E}_r$ is the field caused by the incident laser field Eq. (54) in the presence of a sphere of radius a, when the surface molecules are absent. Since $ka \ll 1$ the laser field is uniform across the sphere and we need (§75) the solution of the Laplace equation in this uniform field. This is readily available [8] and indicates that $\vec{E}_r(\vec{r};\omega)$ equals the field caused by the dipole $\vec{p}(t) = \vec{p}(\omega)e^{-i\omega t}$, with $\vec{p}(\omega)$ given by:

$$\vec{p}(\omega) \equiv \beta(\omega)\vec{E}_i(\omega) = (\epsilon_1(\omega)-\epsilon_2)(\epsilon_1(\omega)+2\epsilon_2)^{-1}a^3\vec{E}_i(\omega), \qquad \text{(III.56)}$$

located at the center of the sphere (which is at the origin of the coordinate system). Here $\epsilon_1(\omega)$ is the complex, frequency dependent dielectric constant of the sphere and ϵ_2 is the dielectric constant of the surrounding medium, $\beta(\omega)$ the polarizability of the sphere and a is its radius.

Using Eq. (55) with the dipole $\vec{p}$ given by Eq. (56) we get $\vec{E}_r(\vec{r};\omega)$. Comparing to Eq. (II.3) we obtain the reflection tensor $\overleftrightarrow{R}$:

$$\overleftrightarrow{R}(\vec{r};\omega) = \beta(\omega)(3\hat{r}\hat{r}-\overleftrightarrow{I})\,r^{-3} \qquad \text{(III.57)}$$

and the reflected field

$$\vec{E}_r(\vec{r};\omega) = \overleftrightarrow{R}(\vec{r};\omega)\cdot\vec{E}_i(\omega). \qquad \text{(III.58)}$$

The primary field is

$$\vec{E}_p(\vec{r};\omega) = (\overleftrightarrow{I} + \overleftrightarrow{R}(\vec{r};\omega)) \cdot \vec{E}_i(\omega) \tag{III.59}$$

§77. There are two ways in which $\vec{E}_r$ (hence $\vec{E}_p$) can be enhanced. We could make the sphere as large as possible to increase the term a^3. However, this is limited by the requirement that $(a/\lambda)\,|N|<<1$, which assures the validity of Eq. (56). Increasing a beyond the limits imposed by this inequality takes us into the Mie regime, in which Eq. (56) breaks down and the enhancement is smaller than in the Rayleigh case.

The field can also be enhanced by choosing the light frequency equal to ω_{res} given by

$$\text{Re}\ \epsilon_1(\omega_{res}) = -2\epsilon_2. \tag{III.60}$$

In this case $\overleftrightarrow{R}(\vec{r};\omega_{res})$ becomes (from Eqs. (56) and (57))

$$\overleftrightarrow{R}(\vec{r};\omega_{res}) = (3\hat{r}\hat{r}-\overleftrightarrow{I})(a/r)^3\,[1 + 3i\,\epsilon_2/\text{Im}\,\epsilon_1(\omega_{res})] \tag{III.61}$$

If $\text{Im}\epsilon_1(\omega_{res})$ is very small relative to $\text{Re}\,\epsilon_1(\omega_{res})$ then R could be considerably enhanced.

This enhancement corresponds to the excitation of an electromagnetic resonance in the sphere. If $\epsilon_1(\omega)$ satisfies Drude equation $\epsilon_1(\omega) = 1-(\omega p/\omega)^2$, the resonance is located at $\omega_{res} = \omega_p(1+2\epsilon_2)^{-\frac{1}{2}}$. If the sphere is surrounded by vacuum $\omega_{res} = \omega_p/\sqrt{3}$.

§78. The search for materials yielding large primary field enhancement must look for two elements. In some frequency range the real part of the dielectric constant must be negative, so that Eq. (60) could be satisfied. Furthermore, at the resonant frequency Im $\varepsilon_1(\omega_{res})$ must be as small as possible. In Table 3 we present (in the line n=1) the values of resonance frequencies (from Eq. (60)) and $\mathrm{Im}\epsilon_1(\omega_{res})^{-1}$ for Ag and Au. Since the primary field appears squared in all formulae for enhanced spectroscopy, $\mathrm{Im}\epsilon_1(\omega_{res})^{-2}$ gives a feeling (since $E_p \sim R \sim \mathrm{Im}\,\varepsilon_1(\omega)^{-1}$) for the relative enhancing ability of these materials. The resonance frequency is the laser frequency at which maximum enhancement occurs.

Note that non-metallic materials and excitations other than plasmons can be used. Finally, it is important to realize that the plasmon frequency in semi-conductors can be varied by doping, resulting in some modest "tunability." For example the InSb plasmon frequency can be shifted roughly between 100 cm^{-1} and 1000 cm^{-1}.

§79. The calculations presented here assume that the small spheres have the same dielectric constant as the films used for dielectric measurements. This is not necessarily the case. The electron mean free path is of the order of 300 Å and therefore collisions with the surface of the sphere (which is unavoidably rough) have the same effect as the collisions with impurities do in bulk.[117] they shorten the relaxation time, hence increase the imaginary part of the dielectric constant. This results in smaller resonant enhancement of $\vec{E}_r$. Another effect of smallness can be simply understood in terms of an electron gas model. The energy levels of a free electron confined to a sphere of finite size are discrete and depend on size.[118] The Fermi level is also different. This alters the dielectric response, as compared to that of the bulk material, even in the absence of surface impurities or surface corrugation.

§80. The predictions made by the calculations presented above are semi-quantitative and they become reliable only if the dielectric constant is measured <u>in situ</u> and electron microscopy is done to ensure that the shape is spherical. Comparison to experiments requires the knowledge of the size distribution and some assurance that the spheres are isolated (i.e., once they are polarized their polarization charges do not interact).

In the absence of such a thorough test it is useful to have some understanding of how the features of the reflected field are related to optical quantities that are easy to measure. Chang et. al.[113] have computed the frequency dependence of the near field intensity Q_{NF}, absorption cross section Q_{ABS} and scattering cross section Q_{SCA}. Their graphs are reproduced here as Figures 11. As one can see the frequencies corresponding to the absorption, extinction or local field peaks do not necessarily coincide. This is true both in the Rayleigh and Mie limit.

It has been often stated in the literature that the Raman excitation spectrum of molecules located near a sphere must follow the extinction spectrum of the sphere. The excitation spectrum follows the local field (i.e., $\vec{E}_p$) excitation whose peak coincides with that of the extinction coefficient only for Ag in the Rayleigh limit, but not for Ag in the Mie case or for Cu and Au for all sizes. Therefore, extinction measurements are useful if interpreted with some care, that is, with the aid of detailed calculations.

§81. <u>Emission enhancement.</u> As we have already discussed, the second important source of enhancement is the effect of the sphere on the molecular emission. For exemplification we use the case of Raman scattering; other spectroscopic measurements can be discussed similarly, by following the general outline presented here.

In Section II the key quantity, as far as emission is concerned, is $\overleftrightarrow{G}_s(\vec{R}_d, \vec{r}_\alpha; \omega)$ defined at §11. We need to compute it for a small sphere.

For Raman scattering the source of the emission is the "Raman" dipole

$$\vec{\mu}_{RS}(t) \equiv \vec{\mu}_{RS}(\omega-\omega_v)e^{-i(\omega-\omega_v)t} \equiv \overleftrightarrow{\alpha}_{RS}\cdot\vec{E}_p(\omega)e^{-i(\omega-\omega_v)t} \tag{III.62}$$

induced by the primary field (see §6). An expression for $\vec{\mu}_{RS}(\omega)$, within the Drude-Lorentz model, is given at §22.

The electric field of the radiation from this dipole, in the absence of the sphere, is[7]

$$\vec{E}_o(\vec{R}_d;t) \equiv \overleftrightarrow{G}_o(\vec{R}_d,\vec{r};t)\cdot\vec{\mu}_{RS}(t) = k^2 \frac{e^{ikR_d}}{R_d} e^{-i(\omega-\omega_v)t}\overleftrightarrow{(I-\hat{R}_d\hat{R}_d)}\cdot\vec{\mu}_{RS}(\omega) \tag{III.63}$$

where $\vec{R}_d$ is the detector position, $\hat{R}_d \equiv \vec{R}_d/R_d$, $k = (\omega-\omega_v)/c \equiv \omega_{RS}/c$, and c is the velocity of light. The coordinate system is at the center of the sphere and $\vec{r}$ is the dipole position. $\overleftrightarrow{R}_d$ appears everywhere, instead of $|\vec{R}_d-\vec{r}|$, since $|\vec{R}_d| >>> |\vec{r}|$.

The more interesting problem is the computation of the radiation emitted because the electric field created by $\vec{\mu}_{RS}(\omega)e^{-i(\omega-\omega_v)t}$ polarizes the sphere. This computation is carried out by using Laplace's equation (see §75) to compute the scalar potential Φ. Analysing the multipole expansion of Φ we can identify the dipole $\vec{p}$ induced on the sphere by the molecular dipole $\vec{\mu}_{RS}$ driving it. The radiation of the sphere is assumed to be that produced by the dipole $\vec{p}e^{-i(\omega-\omega_0)t}$.

The same calculation also gives us the image field acting back on $\vec{\mu}$ because the sphere is polarized. This field is of importance for resonant Raman scattering, fluorescence, electronic absorption and photo-chemistry.

§82. We only outline the calculation of Φ since the procedure follows that used to compute the potential of a sphere and point charge, which is given by Stratton[8] (pp. 201-207). The dipole field can be constructed from two charges q of opposite sign separated by an arbitrarily small distance ℓ. The dipole moment is directed from the negative to the positive charge and has the magnitude $|q|\ell = \mu$. For simplicity we take the dipole $\vec{\mu}$ oriented along the z-axis, and located at the point $z=\xi$. The potential caused, by the sphere polarization, in the space outside the sphere is represented by

$$\Phi_2(\vec{r}) = \sum_{n=0}^{\infty} b_n \frac{P_n(\cos\theta)}{r^{n+1}} \quad . \tag{III.64}$$

Here P_n is the Legendre polynomial of order n and θ is the polar angle of $\vec{r}$. Inside the sphere the potential is

$$\Phi_1(\vec{r}) = \sum_{n=0}^{\infty} a_n r^n P_n(\cos\theta) \tag{III.65}$$

These two expressions are solutions of the Laplace equation. They are chosen so that $\Phi_2 \to 0$ as $r \to \infty$ and $\Phi_1 \to 0$ at $r \to 0$. The coefficients a_n and b_n are unknown and are determined from the boundary conditions

$$\Phi_0 + \Phi_2 = \Phi_1 , \quad \text{for } r = a$$

and

$$\epsilon_2 \frac{\partial}{\partial r}(\Phi_0 + \Phi_2) = \epsilon_1 \frac{\partial \phi_1}{\partial r} \quad , \text{ for } r = a. \tag{III.66}$$

The radius of the sphere is denoted a. Φ_0 is the potential (in MKSA units) due to the dipole μ at a point $\vec{r}$ (for which $|\vec{r}| < \xi$) and it is given by

$$\Phi_0(r) = -\frac{\mu_{RS}}{4\pi\epsilon_2} \sum_n \frac{(n+1)r^n}{\xi^{n+2}} P_n(\cos\theta) \qquad \text{(III.67)}$$

A simple computation yields

$$\Phi_2(\vec{r}) = \frac{\mu_{RS}}{4\pi\epsilon_0} \sum_{n=0}^{\infty} \frac{a^{2n+1}}{\xi^{n+2}} \frac{n(n+1)(\epsilon_2-\epsilon_1)}{[n\epsilon_1 + (n+1)\epsilon_2]} \frac{P_n(\cos\theta)}{r^{n+1}} \qquad \text{(III.68)}$$

We can compare this to the multipole expansion of the potential[8] to find that the dipole of the sphere can be expressed as

$$\vec{p}(\omega-\omega_v) = \beta(\omega-\omega_v)\,\vec{E}_{dip} \qquad \text{(III.69)}$$

where $\vec{E}_{dip}$ is the electric field caused by the molecular dipole $\vec{\mu}$ at the center of the sphere. The polarizability β of the sphere is given by Eq. (56).

One can generalize this result for the case when the dipole is located at an arbitrary point $\vec{r}$. The dipole induced in the sphere is given by Eq.(69) with $\vec{E}_{dip} = \overleftrightarrow{T}(\vec{r}) \cdot \vec{\mu}_{RS}(\omega-\omega_v)$ and T defined by Eq. (55). Hence

$$\vec{p}(\omega-\omega_v) = \beta(\omega-\omega_v)\overleftrightarrow{T}(\vec{r} \cdot \vec{\mu}_{RS}(\omega-\omega_v) \qquad \text{(III.70)}$$

Note that β is the same polarizability that appears in the computation of the dipole induced in the sphere by a spatially homogeneous laser field. One should not however conclude that the sphere polarization is independent on the driving source.

If a homogeneous ($2\pi a/\lambda << 1$) laser field $E_i(\omega)$ acts on the sphere the total polarization field is that caused by the dipole $\vec{p} = \beta \vec{E}_i$, located at the center of the sphere. If a dipole field $E_{dip} = \overleftrightarrow{T} \cdot \vec{\mu}_{RS}$ acts on the sphere, the total polarization is given by the potential Φ_2 of Eq. (68). However, the radiation produced by the polarized sphere is that of the dipole $\vec{p} = \beta \vec{E}_{dip} = \beta \overleftrightarrow{T} \cdot \vec{\mu}_{RS}$, located at the center of the sphere.

The molecular dipole $\vec{\mu}_{RS}$ excites all the multipoles of the sphere but only the dipole radiates. The non-radiative multipoles do influence the rate of energy transfer from $\vec{\mu}_{RS}$ to the sphere, hence the lifetime of $\vec{\mu}_{RS}$ (§133-132). The laser field excites only the dipole of the sphere.

§83. The total electric field radiated by the molecular dipole and the sphere (both at the frequency $\omega - \omega_v$) is given by the radiation of the dipole $\vec{\mu}_{RS} + \vec{p}$. This is

$$\vec{E}(\vec{R}_d;\omega-\omega_v) = \overleftrightarrow{G}_o(\vec{R}_d,\omega-\omega_v)\cdot(\vec{\mu}_{RS}(\omega-\omega_v) + \vec{p}(\omega-\omega_v)) \qquad \text{(III.71)}$$

Using Eqs. (70) and (71) we obtain

$$\vec{E}(\vec{R}_d;\omega-\omega_v) = \overleftrightarrow{G}_o\cdot\vec{\mu}_{RS} + \overleftrightarrow{G}_s(\vec{R}_d;\omega-\omega_v)\cdot\vec{\mu}_{RS} \equiv \overleftrightarrow{G}(\vec{R}_d;\omega-\omega_v) \cdot \vec{\mu}_{RS}(\omega-\omega_v) \qquad \text{(III.72)}$$

with

$$\overleftrightarrow{G}_s(\vec{R}_d,r;\omega-\omega_v) \equiv \overleftrightarrow{G}_o(\vec{R}_d;\omega-\omega_v)\beta(\omega-\omega_v)\cdot\overleftrightarrow{T}(\vec{r}) \,. \qquad \text{(III.73)}$$

We have thus obtained an expression for G_s (for a general definition see §11) for the particular case when the solid is a small sphere. This quantity controls the enhanced emission through $\beta(\omega)$, which can have an electromagnetic resonance (see §77).

§84. Raman Scattering intensity. We have now carried out all the electrodynamic calculations needed in the study of the enhanced spectroscopy caused by a sphere. Some additional calculations are required to obtain the absorption line shape and the resonant Raman cross section, and they are discussed later (§ 106-113).

The reflection tensor $\overleftrightarrow{R}(\vec{r};\omega)$ is given by Eq.(57) and the scattering part $\overleftrightarrow{G}_s(\vec{R},\vec{r}_\alpha;\omega)$ of the dyadic Green function $\overleftrightarrow{G}$, by Eq.(73). They are expressed in terms of the sphere polarizability $\beta(\omega)$ and the dipole propagator $\overleftrightarrow{T}(\vec{r})$ (Eq. (55)). The electromagnetic resonances appear through β and the dependence on the molecule sphere distance through $\overleftrightarrow{T}$.

The emitted intensity is obtained from Eq.(II.37). Using,(in Eq.(II.37)), the Eqs.(72) and (73) (for $\overleftrightarrow{G}$, and $\overleftrightarrow{G}_s$), Eq.(II.35) (for $\vec{\mu}_{RS}$) and Eqs.(58,59) for the primary field E_p, we can write

$$I_{RS} \propto \sum_\alpha \left\langle \left| \overleftrightarrow{G}_o(\vec{R}_d;\omega-\omega_v) \cdot \{\overleftrightarrow{I}+\beta(\omega-\omega_v)\overleftrightarrow{T}(\vec{r}_\alpha)\} \left(\frac{\partial \overleftrightarrow{\alpha}^{(o)}_{eff}}{\partial Q}\right) \delta Q \cdot \{\overleftrightarrow{I}+\beta(\omega)\overleftrightarrow{T}(\vec{r}_\alpha)\} \cdot \vec{E}_i(\omega) \right|^2 \right\rangle \tag{III.74}$$

§ 85. Let us now examine the electromagnetic enhancement given by this theory. The term $\beta(\omega)\overleftrightarrow{T}(\vec{r}) \equiv \overleftrightarrow{R}(r;\omega)$ gives the reflected field enhancement and $\beta(\omega-\omega_v)\overleftrightarrow{T}(\vec{r})$ gives the enhanced emission.

When the incident frequency is on resonance (i.e., when Re $\varepsilon_1(\omega) + 2\varepsilon_2 = 0$) $\beta(\omega)$ and $\beta(\omega-\omega_v)$ become large, especially if Im $\varepsilon_2(\omega)$ is small (see §77). The resonance is broad enough so that both $\beta(\omega)$ and $\beta(\omega-\omega_v)$ could be on resonance simultaneously. The largest contribution to the intensity (Eq. (74) comes from the term

$$\left| \overleftrightarrow{G}_o \cdot \beta(\omega-\omega_v)\overleftrightarrow{T}(\vec{r}) \cdot \beta(\omega)\overleftrightarrow{T}(\vec{r}) \cdot \left(\frac{\partial \overleftrightarrow{\alpha}_o}{\partial Q}\right) \delta Q \cdot \overleftrightarrow{E}_i(\omega) \right|^2 \tag{III.75}$$

and this will dominate SERS intensity.

This equation yields the following important predictions. (a) Distance dependence. The intensity depends on the molecule surface distance d through the dipole propagator $\overleftrightarrow{T}(\vec{r})$. The dimensionless parameter characterizing this dependence is $[a/(a+d)]^3$ (see Eqs. (56, 57)). The a^3 term comes from polarizability β (Eq.(56)) and $(a+d)^3$ from $\overleftrightarrow{T}$. The intensity (Eq.(75)) varies like $[a/(a+d)]^{12}$.

Table 4 shows that this quantity varies rather slowly with d. For example, for a sphere of radius a = 300 Å the enhanced Raman signal from a molecule located at 30 Å from the surface of the sphere is only 0.32 times smaller than that of a molecule located at the surface.

So far only the electromagnetic model predicts the existence of such a long range enhancement. This is why the Bell Labs experiments,[112-114] which were the first to demonstrate the existence of this phenomenon, provide strong evidence for the importance of the electromagnetic enhancement.

(b) Enhancing capability. As we have already mentioned (§7.7) the primary field and the emission can be enhanced if the laser frequency satisfies the equation $\mathrm{Re}\epsilon_1(\omega) = -2\epsilon_2$. This excites the dipolar electromagnetic resonance of the sphere, which enhances its polarizability β (and through it $\overleftrightarrow{R}$ and $\overleftrightarrow{G}_s$, i.e., the primary field and the emission, respectively). At resonance $\beta \sim [\mathrm{Im}\,\epsilon_1(\omega_{res})]^{-1}$, and since the enhanced intensity is proportional to β^4 (see Eq. 75)) this gives an intensity proportional to $\sim[\mathrm{Im}\epsilon_1(\omega_{res})]^{-4}$. This explains why apparently small differences in $\mathrm{Im}\epsilon_1$ can give substantial differences in SERS intensity. Going from $\mathrm{Im}\epsilon_1 = 0.2$ to $\mathrm{Im}\epsilon_1 = 0.1$ changes $(\mathrm{Im}\epsilon_1)^{-4}$ from 625 to 10,000.

(c) The excitation spectrum of SERS is a complicated function of frequency. (The excitation spectrum is the dependence of the Raman intensity of a given line on the incident laser frequency). If the customary ω^4 dependence is removed, the intensity still depends on ω through the dielectric properties of the sphere (entering in Eq. (75) through β). The Eqs.(75) and (56) give

$$\omega^{-4} I_{RS}(\omega) \propto \left|(\epsilon_1(\omega-\omega_v)-\epsilon_2)(\epsilon_1(\omega-\omega_v)+2\epsilon_2)^{-1}\right|^2 \left|(\epsilon_1(\omega)-\epsilon_2)(\epsilon_1(\omega)+2\epsilon_2)^{-1}\right|^2 \quad \text{(III.76)}$$

We have assumed that resonant and pre-resonant Raman[20] scattering is avoided, therefore no frequency dependence is introduced through the molecular polarizability. If this requirement is satisfied then all the Raman lines of all the molecules deposited on the same surface should have essentially the same excitation spectrum. The only difference comes from the fact that different lines have different values of ω_v. This prediction provides a very simple and important test of the purely electromagnetic theory and should be performed whenever possible. Furthermore, the ratio of two excitation spectra of the same molecule on spheres made of two different materials depends only on the dielectric constants of the spheres; more precisely the ratio can be computed by using the Eq. (76).

(d) Dependence on the radius of the sphere. The Raman intensity for a molecule located at a distance d from the surface of the sphere is proportional to $[a/(a+d)]$.[12] Integrating over all the molecules makes the intensity proportional to $\int_a^\infty \frac{x^2 dx\, a^{12}}{(a+x)^{12}}$ which gives proportionality to a^3. Experimentally, it is rather difficult to either measure or control the radius accurately. As the art evolves it might become possible to test this prediction.

§85 Systems consisting of small spherical metal particles are excellent candidates for a study of the mechanism of surface enhanced spectroscopy since the electromagnetic enhancement can be computed rather accurately. A comparison to experiments will allow us to establish whether other enhancement mechanisms are present and find out (by subtraction of the computed electromagnetic enhancement) their properties. Unfortunately, there are a number of difficult requirements that the experiment must meet in order to make such a program meaningful. These are discussed below.

(1) Colloidal particles tend to coagulate and form aggregates whose properties cannot be treated as if they are just a larger sphere. Recent calculations by Aravind, Nitzan and Metiu[122] show that the excitation spectrum and the local fields for two small (Rayleigh limit) spheres, separated by small distances, are very different from any obvious superposition of the single sphere behavior. A new resonance appears at a lower frequency than that of the single sphere case, and the square of the local field between the sphere is (for Ag) an order of magnitude larger than that for a single sphere. Since emission enhancement is also expected to increase[22] by a factor of 10, the enhanced Raman spectrum of a molecule located between two Ag spheres could be a hundred times larger than that of a molecule located near a single sphere. The point is that particle coagulation can alter radically the electrodynamic behaviour of the system and that it should be avoided in measurements which intend to provide a test of the theory.

(2) The dielectric properties of small colloidal particles might be different from those of the bulk metal. Differences might be caused, for example, chemically by impurity incorporation in the particle in the course of its growth. Or they might be due to the effects discussed at §78. One would like to have surface enhanced spectroscopy data from samples for which the dielectric constant of the spheres is measured in situ by detailed light scattering studies.

(3) The shape of the particle is important. The resonant behaviour of small spheroids[115-116, 123] is different from that of spheres. Electron microscopy combined with light scattering should be used to attempt to find preparation methods that yield spheres. A size histogram is also needed.

(4) As we have already emphasized it is important to study the enhanced Raman over as wide a frequency range as possible. The electromagnetic theory makes specific and striking suggestions concerning the behaviour of the excitation spectrum, which ought to be tested.

(5) A detailed study of the relative intensity of different lines of the same molecule, and especially of its frequency dependence, could be very revealing (§84).

§86. The first measurements on colloidal systems were carried out by Creighton et. al.[124] They were quickly followed by the work of Kerker et. al.,[125] Wetzel and Gerischer[126] and Chang et.al.[127] The only work with metal spheres trapped in a solid matrix has been reported by Moscovits et. al.[105] Since the conditions and the results of these works are rather different, we have to discuss them almost one by one.

§87. One of the problems in working with colloidal systems is their tendency to aggregate. This is generally prevented by the electric charges present around the colloids or by intentional addition of polymers. The addition of a neutral molecule such as pyridine and its subsequent adsorption removes some of the ions from the metal spheres. The repulsion between spheres is thus diminished and Brownian motion aided by the rather large van der Waals interactions[129] causes coagulation. The particles form bead strings[130-131] or irregular structures.[127]

Transmission electron microscopy is the obvious tool for the study of this phenomenon. However, in its absence, optical methods are rather suggestive. This is illustrated by Creighton's [124] results. His silver sols, prepared by reduction of $AgNO_3$ with borohydride show a sharp extinction peak at 380 nm (yellow). After pyridine addition the color changes to red, then blue-grey. A shoulder develops at wavelengths higher than 380 nm, which almost grows into a second peak. The initial peak is indicative of the existence of single Ag spheres of size smaller than the wavelength of light. If the particles were elliposidal they would have had a double peak, one near 380 nm and a second, more intense one, at higher wavelength (see Section III.3.3). If the spheres had a large size they would have had a much broader extinction peak, extending to wavelengths higher than 380 nm. These considerations

rule out the presence of large numbers of ellipsoidal particles or of large spheres. Since one does not expect a change of particle size or shape in time, the change in extinction must come from aggregation.

Numerical calculations by Aravind, Nitzan and Metiu[122] show that the local field around two Rayleigh spheres has two peaks, one at the single sphere position and the other at higher wavelength. The observation that a high wavelength shoulder appears and grows in time is consistent with these calculation and the idea that as the size of the aggregate grows the extinction shifts to larger wavelengths. Recent work by Creighton[130,131] and Chang et. al.[127] confirm this inference by direct electron microscope observations.

§88. Having assigned these extinction peaks to aggregation, we can now consider Creighton's[124] results for the Raman excitation spectrum of the pyridine. The excitation spectrum varies in time and for each given time it peaks at the same wavelength at which the "aggregation" peaks appear in the extinction. The same phenomenon occurs in sols prepared by reducing $H[AuCl_4]$ with trisodium citrate. One is therefore forced to conclude that in these experiments[124] SERS is associated with colloid aggregation. Recently Creighton[130,131] obtained the SER signal for incident photons all the way down to 400 nm, where the single sphere ought to have a resonance (and where the extinction of aggregates also peaks). They did not detect the maximum predicted by the single sphere theory.

One would like to understand these observations in terms of the electromagnetic theory for single spheres and of the two sphere calculations of Aravind et.al.[122] Even though the experimental systems did not have pairs of spheres, but long strings of them, one might hope that the two sphere calculation may give some useful hints. The local field around the two spheres peaks at two frequencies. The peak positions depend on the parameter $\lambda = R_o/(2R_o+D)$

where R_o is the radius of the sphere (the spheres have equal radii) and D is the distance between them. One of the peaks is practically at the single sphere resonance position for all λ. The other occurs at higher wavelength and its wavelength gets higher as the spheres get closer (λ goes up). The computed high wavelength peak however is at a substantially smaller wavelength than the experimental one (experimental: [124] up to 600 nm at long times; computed: up to 450 nm for very close distances between spheres). This effect can be, however, understood qualitatively. It was pointed out by Aravind et.al. [122] that a system of two close spheres is similar in many ways to an ellipsoid. Now, adding a third etc., sphere to the chain, in the process of aggregation, corresponds crudely to a change of the aspect ratio (this is the ratio between semi-axes) of the "equivalent" ellipsoid, from two to three. This would change the extinction coefficient of an ellipsoid to a higher wavelength. The change could be substantial and it might explain why the extinction peak for strings of spheres is at 600 nm. Furthermore the calculations were done under the assumption that the two spheres were in vacuum. If they were immersed in water the second peak would be at higher wavelength. [132]

The two sphere calculations find that the local field between the spheres is very high. If the laser excites the short wavelength resonance the local field squared is ~790 times larger than that of the incident field. For the long wavelength resonance this quantity is ~2000, while for a single sphere it is 63 (at the same frequency as the short wavelength-two-sphere resonance, which does not correspond to a resonance of the single sphere). Using the reciprocity theorem [22] we infer that the same enhancement is obtained in emission, to give a total enhancement of 6.2×10^5, 4×10^6 and 4×10^3, for an excitation frequency corresponding to the low wavelength, the high wavelength and the single sphere resonances, respectively. On this basis one expects that the Raman signal is roughly 6.4 times higher when the laser excites the two sphere high wavelength resonance, than when it excites the low wavelength one, and it is a

thousand times smaller when the laser drives the single sphere resonance. The two sphere results[122] cannot be quantitatively applied to discuss beads of spheres, but they suggest that the experimental observations might be explained by the fact that most of the enhanced Raman signal comes from molecules located between the beads, when the laser drives the high wavelength resonance of that structure. We emphasize that this is not a firm conclusion and that a detailed analysis of unpublished data from R.L. Chang's laboratory,[133] in which the number of aggregated particles was counted suggests that this mechanism might not account for all the observed intensity.

§89. The interpretation of the results of Kerker et. al.[125] is even less clear since neither the extinction spectra at various times, nor electron microscope studies are available. The extinction spectrum is broader than Rayleigh predictions for single spheres (Fig. 12) and has a shoulder at high wavelength. If we assume that this is due to coagulation, the results can be "explained" in the same way as Creighton's. The measurements are compared to the single sphere calculations in Table 5. The observed enhancement is larger, by at least two orders of magnitude, than the computed one. The excitation spectrum predicted by the single sphere calculation peaks within the frequency range of the light sources used experimentally. However, no peak is detected experimentally. The intensity grows with the wavelength and if there is a peak at all (we expect one) it is at $\lambda \geq 647.1$ nm. Note that this would be a higher peak wavelength than those observed by Creighton.

§ 90. The most recent experiments are those of Chang et.al.[127,133] who studied the Raman spectrum of $Au(CN)_2^-$ adsorbed on Au particles,[127] and that of $Ag[CN]_2^-$ on Ag particles.[133] The Au colloids were prepared[134] by reduction of $KAuCl_4$ with cold $NaBH_4$ $(CN)_2$ with cold $NaBH_4$ (colloid A), by reduction of $KAuCl_4$ with cold $NaBH_4$ (colloid B) and by reduction of $KAu(CN)_2$ with room temperature $NaBH_4$ (colloid C). The preparation conditions are different and they yield colloids of different sizes and degrees of aggregation. The extinction spectra are consistent with the electron microscopy: the

higher the aggregation (C < B < A), the more pronounced is the high wavelength peak. Colloid C is almost aggregation free. The particle radii are small (Rayleigh regime).

The Raman excitation spectrum (for a 2138 cm^{-1} band corresponding to a mode of $Au(CN)_2^-$) for the colloids A and B (aggregated) follow the pattern observed in Creighton's work: the enhanced Raman intensity peaks at the wavelength at which the "aggregation" extinction peaks are formed.

The colloid C is however another matter. From electron microscopy we know that there are very few aggregates in the solution. One expects thus to see mostly Raman spectra enhanced by single spheres. The computed[113] excitation spectrum peak for this case is at 550 nm (see Fig. 11). No peak is experimentally seen in that region. The computation also shows that in the case of Au the enhancement produced by single spheres is rather small. It is possible therefore that the predicted peak is below the sensitivity of the detector. The observed Raman signal appears at wavelengths higher than 550 nm. This might mean that the signal is caused by the small number of aggregates present in solution or that a "molecular" mechanism is at work. It seems to us that the number of aggregates is too small to account for all the experimental intensity.

§91. Wetzel and Gerischer[126] are the only ones, so far, who seem to have detected signals resembling the theoretical predictions for the single sphere enhanced Raman spectrum. They worked with pyridine adsorbed on Ag sols prepared by reduction of a silver salt with ethylenediamine-tetraacetic disodium salt. No electron microscopy was carried out and the shape of the colloidal particles was not directly determined. The extinction spectrum peaks at 440 nm, and it is thus consistent with the presence of small (Rayleigh) radius spheres. The line shape is broader than that predicted by computation and this might indicate that some aggregation is present or that the imaginary part of the dielectric constant of the spheres is larger than that of the bulk silver (see §79). The Raman

excitation spectrum was measured for $\lambda > 480$ nm and unfortunately this range does not contain the wavelength where the peak predicted by the theory is located. However, for the existing wavelength points the Raman excitation spectrum does follow the extinction spectrum as the theory suggests.

§92. Work with matrix isolated spheres. A different system for surface enhanced spectroscopy with spheres can be prepared by evaporating metals in a gas stream whose pressure is adjusted to permit particle nucleation. The jet containing the metal particles and a second jet containing the molecules of interest can be frozen together on a cold surface. The spheres will be thus surrounded by an "ice" formed by the molecules whose spectroscopic properties are to be studied. Even though there is extensive experience in preparing such particles[135] it is not easy to prepare small spherical particles with the same radius. Claims that such a situation has been achieved ought to be carefully documented.

§93. The first to carry out such experiments were Abe, Manzel, Schulze, Moskovits and DiLella.[128] They prepared Ag spheres by a method described by Abe et.al.[135a] who established the fact (by electron microscopy) that the method produces spheres of 100 Å diameter. The spheres were imbedded in a CO matrix.

There are three Raman bands, at the vibrational frequencies 2113 cm^{-1}, 160 cm^{-1} and 64 cm^{-1}. They are assigned as CO stretch, C-Ag stretch and AgCO bend, respectively. Roughly the same lines are observed for CO on Ag films.[136]

The excitation wavelengths used experimentally[129] are to the right of the peak predicted by the theory. The excitation spectrum of the 2113 cm^{-1} line resembles the excitation spectrum predicted by the theory. However like in the Gerischer-Wetzel experiments, the experimental wavelength range does not cover the region where the theory predicts a peak. The excitation spectrum of the 160 cm^{-1} line does not follow the extinction curve and it slopes in the opposite direction. This is very unsettling as far as the purely electromagnetic theory is concerned, since the excitation spectra of two lines of the same molecule must have very similar shapes (see §84) and be almost parallel.

It seems therefore that, if the 160 cm^{-1} band is indeed the Ag-C stretch, we must accept the presence of a "molecular" effect which completely alters the frequency dependence predicted by the electromagnetic theory for the Raman intensity of that mode. The fact that only the C-Ag mode displays such an effect might be due to its closeness to the surface.

Some caution must however, be exercised in drawing any firm conclusion based on experiments with samples that were not characterized <u>in situ</u>. Other explanations can be produced if one suspects, for example, that sharp needle like features are present. The C-Agstretch signal comes only from molecules bound to the surface while the CO stretch signal comes from surface molecules as well as many molecules located far from the spheres (§85). The enhancement near a needle like structure is larger[114, 115] than that at other parts of the surface. Therefore the C-Ag Raman spectrum might be dominated by the electromagnetic properties of the needle while the CO spectrum is dominated by the sphere like enhancement. This, for example, might explain the difference between the excitation spectra of the two Raman lines.

§93. Conclusions. We feel that the small spherical systems offer an excellent opportunity for the study of the interplay between the molecular and the electromagnetic effects in SERS. Further experimental work must however, be done to overcome the uncertainties and the complications introduced by restricted frequency range, coagulation, uncertain particle shapes and modified dielectric properties.

III.3.2 Surface enhanced Raman spectroscopy with large spheres.

§94. The theory of SERS on large spheres has been developed by Kerker, Wang and Chew.[137] The computation of the primary field has been carried out by Mie and the results are discussed in standard textbooks.[8,11] The problem of dipole emission is the more difficult part of the calculation. A dipole perpendicular to the surface has been considered by people interested in radio wave propagation around earth. Nomura[138] seems to be the first to solve the problem for a horizontal dipole. Chew, Kerker and Cook[139] studied the problem in the context of molecular spectroscopy. Complete solutions, in terms of dyadic Green's functions, which include both the near field and the radiation field, can be found in Jones[140] and Tai.[14]

§95. Comparing to the case of small spheres the major difficulty comes from the fact that retardation cannot be neglected since the conditions discussed at §75 no longer apply. Therefore we must solve the full Maxwell equations. One technique of doing this[8, 11, 14, 140] expands the electric fields (incident dipole, reflected and radiated field) in vector spherical harmonics. The expansion coefficients for the incident and the dipole field are known. Those of the reflected and radiated field are determined from the boundary conditions. The resulting expressions are

rather complicated, but numerical values can be generated on a small computer, with no difficulty.

§ 96. The physical structure of the theory is the same as in the Rayleigh case. The sphere can resonate with the incident field and produce, as a result, enhanced fields outside. For a small sphere only one mode (dipole mode) can be excited by photons. Its frequency is given by $\mathrm{Re}\varepsilon_1(\omega) = -2\varepsilon_2$ ($\varepsilon_1(\omega)$ and ε_2 are the dielectric constants of the sphere and of the outside medium, respectively). For a large sphere many modes can be excited and their frequency is given by[8]

$$\mathrm{Re}\ \{h_\ell^{(1)}(k_2a)\ [k_1aj_\ell(k_1a)]' - j_\ell(k_1a)\ [k_2a\ h_\ell^{(1)}(k_2a)]'\ \} = 0 \qquad \text{(III.77)}$$

and

$$\mathrm{Re}\ \{h_\ell^{(1)}(k_2a)\ [k_1aj_\ell(k_1a)]' - (k_1/k_2)^2 j_\ell(k_1a)[k_2ah_\ell^{(1)}(k_2a)]'\ \}=0 \qquad \text{(III.78)}$$

The first condition gives resonances for the TE (transverse electric) modes and the second for the TM ones. Here $\ell = 1,2,\ldots \infty$, $k_i = \omega\sqrt{\varepsilon_i\mu_i}$, $i = 1,2$, where ε_i and μ_i are the dielectric constant and the magnetic permeability, respectively, for the medium i (2 is the sphere). j_ℓ is the spherical Bessel function and $h_\ell^{(1)}$ is the spherical Hankel function of the first kind. We also use the notation, $[xf(x)]' \equiv \frac{d}{dx}(xf(x))$.

The imaginary parts of the expressions appearing in Eqs. (77) and (78) are related to the strength of the respective resonance. The relative contribution of various resonances to the total intensity (laser + near field) around the sphere goes like one over that imaginary part squared.

The fields at the surface of the sphere have been computed by Messinger,

von Rabe, Chang and Barber.[113] Some illustrative results are displayed in Fig. 13. To give a feeling for the enhancement at the surface the quantity

$$Q_{NF} = (R^2/\pi a^2) \int_0^{2\pi} \int_0^{\pi} \vec{E}_r \cdot \vec{E}_r^* \sin\theta \, d\theta \, d\phi \Big|_{R = a}$$

is plotted, where $\vec{E}_r$ is the reflected (practically, the primary) field at the surface. This is compared to the scattering efficiency Q_{SCA}, extinction efficiency Q_E and absorption efficiency Q_{ABS}. Several qualitative features can be noted by comparing the Fig. 13 to Fig. 11. in which the same quantities were plotted for the small particle limit.

The local field is substantially smaller for larger spheres. The "excitation spectrum" is much broader. The extinction coefficient and Q_{NF} do not overlap. In other words the theory does not predict that the Raman excitation spectrum follows the extinction spectrum, nor that the excitation spectrum peaks at the frequency of maximum extinction. The results depend strongly on the radius but the above statements are qualitatively valid at all radii.

§97. A complete calculation of Raman scattering also requires the computation of the emission. As explained in Section II we expect the emission to have the same resonances as the reflected field. This is confirmed by the calculations of Kerker, Wang and Chew[137] who show that the emission resonances are given by Eqs. (77) and (78), with the incident frequency ω replaced by the emission frequency $\omega - \omega_v$.

Detailed calculations of the electromagnetic enhancement for various polarization schemes were computed by Kerker et al.[137] Some of their results are reproduced in Fig. 14.

In all these calculations the laser is incident along the z-axis and has the electric field along Oy (v-polarized). The detection plane is xOz, with the detector on the positive x axis. The detector accepts only photons with the electric field vector perpendicular to the detection plane (xOz) (v-polarized). The Raman dipole is located along the Oy axis and it is perpendicular to the surface. The Raman band has the frequency ω_v = 1010 cm^{-1} corresponding to a pyridine line and the material is Ag (Johnson and Christy[141] dielectric constant).

Figure 14(a) displays the dependence of the enhancement factor on the incident wavelength, for three radii. For a = 5 nm we are in Rayleigh regime while 50 nm and 500 nm are in the Mie regime. Obviously the enhancement goes up with the radius (in the Rayleigh regime see §84), and once the Mie regime is reached it goes down. Figure 14(b) shows the enhancement as a function of the ratio r'/a, where r' is the location of the dipole and a is the radius of the sphere. For a radius of 5 nm, the incident resonant wavelength is λ_o = 382 nm, for a 50 nm, λ_o = 511 nm and for a = 500 nm, λ_o = 528 nm. The enhancement is remarkably long ranged.

Figure 14(c) shows the dependence of the enhancement on the particle radius, for two incident wavelengths (382 nm and 514.5 nm). There are conspicuous oscillations which will probably be smeared out if the suspension prepared experimentally has spheres of various radii.

§98. We conclude this section with a technical comment concerning the apparent contradiction between the Efrima-Metiu theory for flat surfaces[2,21,23,24,142] and that of Kerker et.al,[137] for spheres. This has been discussed at length in Appendix B of Kerker et. al.[137] The multiple scattering effect introduced by Efrima and Metiu is the image field. The "multiple scattering" concept was introduced because the image field was computed by an "infinite order" perturbation theory. The n^{th} order term in the infinite perturbation series represents n successive scatterings between the dipole and the surface.

The same image effect must be present in the case of the sphere. For the case of a perfectly conducting sphere it is easy to prove (see, for example, Ref. 10, Ch. II, §3) that if the ratio $(d/a) << 1$ (d = molecule sphere distance, a = the radius of the sphere) the "image" field is identical to that at a flat surface. The same is true for a dielectric sphere, as discussed in §105-§111. We cannot concur with a statement[137] that such fields are much smaller for a sphere than for a flat surface,or that they are small near the surface.

Fortunately, the issue is irrelevant to normal Raman scattering, where the image field is unimportant (§20 and §21). The fact that Kerker et al.[137] leave out this field does not affect any of their conclusions, which were confined to normal Raman effect. The image field is very important however for electronic absorption, fluorescence life-time and intensity, and resonant Raman scattering. It was taken into account by Efrima and Metiu since they explored the possibility that SERS might be resonant Raman scattering disguised by surface effects.

Since the calculation of Kerker et al.[137] is rather tedious, we have not

gone through it in detail, to find why they arrived at the conclusion that the "multiple scattering" effects (i.e., the image field) is small for sphere. We venture to mention two possibilities: (a) Maybe they used an asymptotic formula for their dyadic Green function, since in many works on dipole radiation near a sphere only the radiative part is needed and the part giving the near field is eliminated. (b) Or their computer program failed in computing the image field at small molecule-sphere distances, for which the convergence of the multipole series is extremely poor. Again, we emphasize that the Raman enhancement factors computed by them are not affected by the image field and their results are correct. And so are the results of Efrima and Metiu.

§99. The fluorescence of molecules located near or inside a sphere. Fluorescence can be detected by two methods. The first keeps the laser intensity constant in time and monitors the emission intensity. This method is most convenient in those (frequent) cases in which the emission frequency differs from the excitation one. The second method turns the excitation source off (or on) suddenly and monitors the decay (or the rise) of the emission intensity.

The stationary experiments give easily the quantum yield (the number of emitted photons per incident photon). The relaxation measurements give easily the fluorescence lifetime. If the data is compared in detail to an adequate theory, the two methods provide the same information.

§100. When analysing fluorescence from the point of view of SES one must take into account two complementary effects. (a) There is an electromagnetic enhancement similar to that of Raman scattering. The reflected field can be enhanced and this yields an increase in the number of excited molecules, which in turn causes an increase in the emission intensity. A further increase can be achieved in emission, through a resonance in G_s (see §81). In this case the non-radiative near field

of the dipole excites radiative modes (i.e., electromagnetic resonances) of the solid, which emit brightly and add to the total radiation. (b) One must however also take into account a process which is important only for fluorescence, resonance Raman or absorption spectroscopy. The dipole excites non-radiative modes of the surface and these provide the molecule with a photon (i.e. energy) loss channel. The life-time is diminished and in some cases the fluorescence could be completely quenched.

The outcome of a given experiment depends on the interplay between these two effects. This interplay is made interesting by the fact that the efficiency of the two effects has a different distance and frequency dependence and one might influence the outcome of their competition by changing the material, the geometry, and the emission and excitation frequency.

For example, on a flat surface (see section III.1.3) the enhancement is minimal since neither the reflected field nor the emission process are resonantly enhanced (§27). The quench is very effective, at small molecule-surface distances, since the dipole couples either to electron-hole pairs or to the surface plasmon, which cannot radiate. Thus, the fluorescence from molecules located very close to the flat surface is severely quenched. On the other hand, if the surface is a sphere one expects both intensity enhancement and a decrease of the life-time. The experimental conditions determine which of these effects dominates the behavior of the observed intensity.

A qualitative demonstration of the difference between flat and particulate surfaces was provided by Ritchie, Chen and Burstein.[143] They have shown that the fluorescence of organic dyes (fluorescein, rhodamine 6G) is readily detectable when they are deposited on a glass surface. However, no fluorescence is detected if the molecules lie on a smooth Ag surface. The signal reappears if the molecules are deposited on small Ag islands.

§101. The steady state experiments have been examined by theorists[139,144-148] and performed in the laboratory[149], well before anyone was aware of their connection to surface enhanced spectroscopy, which at that time consisted of poorly understood SERS. The problem arises in biology and aerosol studies in which the fluorescence (or the Raman spectrum) of molecules imbedded inside spherical (or spheroidal) particles is measured. Furthermore, the fluorescence of dyes located on cylindrical surfaces (e.g., textile, plastic or glass fibers) can be used to determine very accurately[150] the radius of the cylinder.

The physics of the emission process when the dye is inside the sphere is very similar to the case when the molecule is located outside. The mathematical, and some minor physical details differ.

The theory was worked out by Kerker and his collaborators.[139,144-148] The electric fields of the dipole and laser, the field reflected by the surface and the field inside the particle are all expanded in vector spherical harmonics. The expansion coefficients are determined from the boundary conditions. The fact that the polarization of the sphere by the molecular dipole affects the molecular polarizability is ignored. Thus the change in fluorescence lifetime caused by the fact that the particle is inside the sphere does not appear in this calculation. It is possible that for the dielectric spheres considered in that work[144-148] the error caused by this omission is small.

The main physical result provided by the theory is the prediction that the near field of the emitting dipole drives the radiative resonances of the sphere and make them emit. As a result the emission intensity has peaks at the frequencies of these resonances. The resonance frequencies are the same as the ones given in §96. This statement has been tested experimentally

by Benner, Barber, Owen and Chang.[149] They used 9.92 μm polystyrene spheres containing a uniform concentration of dye. The sphere is driven by the 457.9 nm line of an Ar^+ laser and the fluorescence of the dye is monitored in the wavelength range 445-565 nm. The resonant peaks are clearly displayed in Fig. 15. Their position is so sensitive to the particle size that the dimension of the sphere can be obtained by this method with higher accuracy than the prescription of the manufacturer.

§ 102. Relaxation studies of fluorescence. It seems that in all but the simplest models, relaxation problems are more difficult to solve than steady state ones. A steady state experiment measures the Fourier transform (over time) of the field. The corresponding computation therefore, must Fourier transform Maxwell's equations and solve for the desired Fourier component of the field. The relaxation experiments follow the time evolution of the field, as it is decaying from a pre-set value. Thus, in computations we must Laplace transform the Maxwell equations (to introduce the initial condition in the problem), solve for the Laplace transform of the field and inverse Laplace transform it to get time evolution. It is this inverse Laplace transform that makes the relaxation problem more difficult than the steady state one.

One would like therefore to use models that can simplify the calculation and maybe make the physics more transparent, while still giving reliable results. An attempt in this direction was made by Gersten and Nitzan[151] and the resulting equations were applied by Nitzan and Brus.[152, 153] We present here a simpler treatment,[154] having roughly the same level of accuracy.

§103. One of the main reasons why the relaxation calculations are more difficult than those involving steady-state harmonic fields, can be seen by examining Maxwell's equations. The problem appears because the

electric displacement $\vec{D}(\vec{r};t)$ depends on the electric field through the equation

$$\vec{D}(\vec{r};t) = \int_{-\infty}^{t} \varepsilon(t-t')\vec{E}(\vec{r};t')dt'. \qquad \text{(III.79)}$$

Because of this the Ampère and Poisson equations are integro-differential equations:

$$\nabla \times \vec{H}(\vec{r};t) = c^{-1} \frac{\partial}{\partial t} \int_{-\infty}^{t} \varepsilon(t-t')\vec{E}(\vec{r};t')dt' \qquad \text{(III.80)}$$

and

$$\int_{-\infty}^{t} \varepsilon(t-t')\nabla\vec{E}(\vec{r};t')\,dt' = 0$$

For a steady state, harmonic field these equations become $\nabla \times \vec{H}(\vec{r};\omega) = -(i\omega/c)\varepsilon(\omega)\vec{E}(\omega)$ and $\varepsilon(\omega)\nabla\vec{E}(\vec{r};0) = 0$. The integral disappears and the resulting equations are much easier to solve than (80) and (81). For a relaxation problem no such simplification takes place.

Substantial progress however, can be made in solving (80) and (81) if the following simplifying assumption is accepted. We recognize that in most problems of interest here $\vec{E}(t)$ can be written as $\vec{E}(t) = \vec{E}_o(t)e^{-i\omega_o t}$ where $\vec{E}_o(t)$ is a slowly varying function of time. Since we are looking at relaxation problems $\vec{E}_o(t)$ must decay to zero and we assume that it does this in an enormous number of periods $2\pi/\omega_o$. We then make the key assumption which consists in replacing Eq. (79) with

$$\vec{D}(\vec{r};t) \simeq \vec{E}_o(\vec{r},t)e^{-i\omega_o t}\,\varepsilon(\omega_o) \qquad \text{(III.81)}$$

This essentially states that the dielectric responds to the fast, harmonic part of the field only. On physical grounds we feel that this assumption is reasonable as long as the relaxation time is much larger than $2\pi/\omega_o$. We have however no numerical analysis to back this up.

Obviously, the use of Eq. (82) turns the integro-differential Maxwell equations into the differential equations (local in time), $\nabla \times \vec{H}(t) = \frac{1}{c}\,\varepsilon(\omega_o)\,\frac{\partial \vec{E}(t)}{\partial t}$, and $\varepsilon(\omega_o)\nabla E(\vec{r};t) = 0$.

§104. Once we put Maxwell's equations in this tractable form we turn to the Drude-Lorentz model for the molecular oscillator. To eliminate all directional complications and concentrate on conceptual aspects only, we consider a dipole directed along the Oz axis (perpendicular to the surface of the sphere), and an incident laser beam coming along the Oy axis with the electric field vector polarized along Oz. The molecule is considered to have the oscillator strength tensor $\overleftrightarrow{f} = f\hat{z}\hat{z}$ so that a field directed along Oz induces a dipole along the same direction. We can therefore write for the induced molecular dipole (this is the "oversimplified model" of §18):

$$\ddot{\mu} + \omega_o^2\mu + \Gamma_o\dot{\mu} = (e^2/m)f[E_i(t) + E_r(t) + E_{im}(t)]. \qquad \text{(III.82)}$$

Here E_i, E_r, and E_{im} are the incident, reflected and image fields, respectively (§4).

§105. Following the simplifications introduced in Maxwell's equations at §103, we can now compute the reflected field from Eqs. (56-58) of §76. The result is:

$$E_r(t) = \frac{2p(t)}{(a+d)^3} = \frac{2\beta(\omega)}{(a+d)^3} E_i(t) \equiv B\, E_i(t) \qquad \text{(III.83)}$$

The image field can be computed using the methods outlined by Stratton[8] (Chapter 3.23, p. 204) which give

$$E_{im} \approx \mu(t) \sum_{n=1}^{\infty} (n+1)^2 (\varepsilon_1(\omega) - \varepsilon_2)(\varepsilon_1(\omega) + \frac{(n+1)}{n}\varepsilon_2)^{-1} \cdot \qquad \text{(III.84)}$$

$$[a/(a+d)]^{2n+1} (a+d)^{-3} \equiv \gamma(\omega,a,d)\mu(t) \equiv \gamma\mu(t)$$

In these equations $\varepsilon_1(\omega)$ is the dielectric constant of the sphere at the frequency of the outside field and ε_2 is the dielectric constant of the medium in which the molecule and the sphere are imbedded. d is the distance from the molecule to the surface of the sphere and $\vec{r}$ is the distance of the molecule to center of the sphere. We have $\hat{r} \equiv \vec{r}/r$ and $|\vec{r}| = (a+d)$ where a is the radius of the sphere.

Introducing Eqs. (83) and (84) in Eq. (82) yields

$$\ddot{\mu}(t) + \omega_o^2 \mu(t) + \Gamma_o \dot{\mu}(t) = (e^2/m) f \tilde{E}_i(t) + (e^2/m) f \gamma \mu(t) \qquad \text{(III.85)}$$

with the effective oscillator strength given by

$$\tilde{f} = f(1 + B(\omega)) = \left(1 + \frac{2(\varepsilon_1(\omega) - \varepsilon_2)}{(\varepsilon_1(\omega) + 2\varepsilon_2)} \left(\frac{a}{a+d}\right)^3\right) f \qquad \text{(III.86)}$$

The dipole induced at the center of the sphere is

$$p(t) = \frac{2\beta}{(a+d)^3}\mu(t) + \beta E_i. \qquad \text{(III.87)}$$

The emitting dipole is the sum $\mu(t) + p(t)$. To compute the emission intensity as a function of time we must solve the differential equation (85) and then compute $p(t)$ from (87). One can do this numerically or by using Laplace transforms.

§ 106. A lot of insight into the physical role of various terms appearing in (85) can be gained by following the procedure used in §25 (see also §20). For this we consider a harmonic field $E_i(\omega)e^{-i\omega t}$ and solve Eq. (85) for $\mu(\omega)$ (defined by $\mu(t) = \mu(\omega)e^{-i\omega t}$). We obtain

$$\mu(\omega) = (\tilde{\omega}_o^2 - \omega^2 - i\omega\tilde{\Gamma}_o)^{-1}(e^2/m)\tilde{f} \cdot E_i(\omega) \equiv \alpha_{eff}(\omega)E_i(\omega) \qquad \text{(III.88)}$$

with

$$\tilde{\omega}_o^2 = \omega_o^2 - (e^2/m)\, f\, \mathrm{Re}\,\gamma(a,d,\omega) \qquad \text{(III.89)}$$

and

$$\tilde{\Gamma}_o = \Gamma_o + (e^2/m\omega) f\, \mathrm{Im}\,\gamma(a,d,\omega). \qquad \text{(III.90)}$$

We see that the presence of the sphere shifts the frequency and the width

of the oscillator by quantities that are proportional to the real and the imaginary part of the image field, respectively. The structure of the theory is identical to the general theory of §20 and §25. However, the width has specific properties caused by the fact that the surface is spherical and the radius is small.

§ 107. We analyse now the contribution of the sphere to the width (Eq. (19)). Using (90) and (84) we obtain

$$\tilde{\Gamma}_o = \Gamma_o + (e^2/m\omega) f \sum_{n=1}^{\infty} (n+1)^2 \, \mathrm{Im} \left[\frac{(\varepsilon_1(\omega) - \varepsilon_2)}{\varepsilon_1(\omega) + \varepsilon_2 \left(\frac{n+1}{n} \right)} \right] \qquad \text{(III.91)}$$

$$[a/(a+d)]^{2n+1} (a+d)^{-3} \equiv \Gamma_o + \Gamma_s$$

The second term is the rate of energy flow from the molecular oscillator into the sphere.

The term corresponding to n = 1 is easy to interpret. We write it as

$$(e^2/m\omega) f \frac{2}{(a+d)^3} \, \mathrm{Im} \left[\frac{(\varepsilon_1 - \varepsilon_2)}{(\varepsilon_1 + 2\varepsilon_2)} \right] a^3 \frac{2}{(a+d)^3} = (e^2/m\omega) f \frac{2}{(a+d)^3} \mathrm{Im}\beta(\omega) \frac{2}{(a+d)^3},$$

with the polarization of the sphere $\beta(\omega)$ given by Eq. (58) §76. This represents a process started by the dipole μ, which exerts on the sphere the field $2\mu/(a+d)^3$; this induces the dipole $\frac{\beta(\omega) 2\mu}{(a+d)^3}$ at the center of the sphere, which in turn exerts on the molecular dipole the field $[2/(a+d)^3]\beta(\omega)[2/(a+d)^3]$. Therefore this part (n = 1) of the rate of energy transfer Γ_s corresponds to the molecular dipole inducing a dipole in the sphere and interacting with it.

A portion of the energy transferred from the molecular dipole to polarize the sphere is radiated by the dipole induced in the sphere; another portion is lost irreversibly to heat up the sphere; the remainder may be temporarily (reversibly) stored into the sphere.

The terms corresponding to n = 2,3...etc. represent the processes by which the molecular dipole induces a quadrupole, etc... in the sphere and interacts with it. The energy stored in these multipoles (other than the dipole) cannot be radiated. Part of it is irreversibly lost to heat up the sphere and the remainder is stored reversibly.

§107. The width Γ_s in Eq. (91) has a very interesting resonant behavior and distance dependence, which is analyzed here. Let us assume that we look at the emission of a molecule at the frequency $\tilde{\omega}_o$. The emission lifetime is $\tilde{\Gamma}_o^{-1}$ and it is diminished whenever Γ_s goes up. An increase in Γ_s must occur whenever

$$\mathrm{Re}\varepsilon_1(\tilde{\omega}_o) + \frac{(n+1)}{n}\varepsilon_2 = 0, \qquad n = 1,2..., \tag{III.92}$$

since one of the denominators in Γ_s (see Eq. (91)) is minimized. This is not however sufficient for a large effect. Additional conditions are examined below. Since $\mathrm{Im}\left[\frac{\varepsilon_1(\omega) - \varepsilon_2}{\varepsilon_1(\omega) + (n+1)\varepsilon_2/n}\right] = ((2n+1)/n)\varepsilon_2 \mathrm{Im}\varepsilon_1(\omega)\left[(\mathrm{Re}\varepsilon_1(\omega) + ((n+1)/n)\varepsilon_2)^2 + (\mathrm{Im}\varepsilon_1(\omega))^2\right]^{-1}$, we have, for $\tilde{\omega}_o$ satisfying the resonance condition (92) $\mathrm{Im}\frac{(\varepsilon_1 - \varepsilon_2)}{\varepsilon_1 + (n+1)\varepsilon_2/n} = \frac{(2n+1)\varepsilon_2}{n\ \mathrm{Im}\ \varepsilon_1(\omega)}$. Inserting that in Eq. (91) we find that the resonance condition (92) will result in an enhancement of Γ_s if

$$\mathrm{Im}\ \varepsilon_1(\tilde{\omega}_o) \text{ is small,} \tag{III.93}$$

(for $\tilde{\omega}_o$ satisfying Eq. (92)), and if

$$I_n \equiv (n+1)^2[(2n+1)/n] \quad (a/a+d)^{2n+1}(a+d)^{-3}, \qquad \text{(III.94)}$$

at the value of n entering in Eq. (92) is larger or comparable to the values it takes for other n.

Whether or not the condition (94) is fulfilled depends on the radius of the sphere and the molecule-sphere distance d. This is shown by Table 6 which gives the values of I_n for a variety of n values and distances. In Table 3 we show the resonance frequencies ω_n for Ag and Au and the value of Im $\varepsilon(\omega_n)^{-1}$.

These two tables allow us to understand how the resonances of the sphere participate in modifying the lifetime of the molecule.

§108. If one were to make a guess concerning Γ_s one would suggest that it is largest for molecules located very close to the surface and that at small distances d its value is identical to that obtained for a molecule that is located at the same distance d from a flat surface. We know that this is true in the case of a perfectly conducting sphere,[10] when the image field is equal to that at a perfectly conducting flat surface, if $d/a \ll 1$. However, a perfectly conducting sphere does not have resonances. When we consider a dielectric sphere its resonances play a fundamental role in taking the energy from the molecule. On a flat surface a dipole excites only one non-radiative resonance, the unretarded plasmon (resonance condition: $\varepsilon_1(\omega) = -\varepsilon_2$), and the fluorescence is thus quenched very effectively.[36] The sphere has quite different resonances (resonance condition $\varepsilon_1(\omega) = -[(n+1)/n]\varepsilon_2$) and we need to understand why, in spite of that, if $d/a \ll 1$ they will quench fluorescence like the flat surface resonance.

The answer is provided by Table 6. If (d/a) is small, the terms corresponding to small n in the series appearing in Eq. (91) are unimportant (see Table 6). So we can modify these terms slightly without dire consequences as far as Γ_s is concerned. We can therefore, for small n, replace (n+1)/n, under the Im sign in Eq. (91) with 1. For large n the replacement of (n+1)/n with 1 is accurate. Hence, if (d/a) is small we can take $\mathrm{Im}\,\frac{(\epsilon_1 - \epsilon_2)}{\epsilon_1+(n+1)\epsilon_2/n} \simeq \mathrm{Im}\left\{\frac{(\epsilon_1-\epsilon_2)}{\epsilon_1+\epsilon_2}\right\}$ for all n, without causing serious errors in Γ_s. The series obtained in this way can be summed up to give (in the limit d/a << 1) the flat surface image formula.

§109 On the basis of the information developed so far we have the following expectations for Γ_s. For small distances the lifetime is exactly equal to that of a molecule located near a flat surface. From Table 6 we infer that small deviation from this rule might appear only at d/a = 50/300 = 0.16. Experiments with flat surfaces[40,43] (§33) show that fluorescence can be detected even for molecules as close to the surface as 10Å. Therefore, a molecule located at 10Å from the surface of a sphere will also fluoresce.

Consider now what happens at larger distances. From Table 6 we see that the resonances with n=1,..., 5 contribute most to Γ_s. These are different from the flat surface ones. If, for example, the sphere is made of Ag, and if a=300Å and d=150Å, a molecule emitting at the frequency 3.48 eV excites the resonance n = 1. The first term will contribute to the sum in Eq. (91) the quantity $I_1[\mathrm{Im}\epsilon(\omega_1)]^{-1} = 0.39\times10^{-7} \times 1.61 = 0.63\times10^{-7}$ (see Tables 3 and 6). This will make the n=1 term somewhat larger than the others, for which ω = 3.48 eV is an off-resonance frequency. A molecule emitting at 3.56 eV will enhance somewhat the term n=2, etc...

Since the molecular emission has a broad band it is possible to study the

emission and measure the life-time at various emission frequencies. According to the above analysis one can get different values for the lifetime at different frequencies even though the photons come from the same molecule and the same electronic state. The fact that the emission from molecules located at all distances to the sphere is simultaneously detected, makes however the analysis very complicated.

§110. So far we have discussed the modifications of the life-time, introduced by the presence of the sphere. The Eq.(88) shows however that the presence of the sphere also modifies the oscillator strength. The effective oscillator strength $\tilde{f}$ given by Eq. (86) reflects the presence of enhanced emission, as discussed generally at §11 and specifically for sphere, at §82.

The effective oscillator strength is enhanced if the molecule emits at the frequency ω_o of the dipolar resonance of the sphere. Since $\tilde{f}$ appears in the emission intensity squared, the enhancement by different materials is proportional to $[\mathrm{Im}\varepsilon(\omega_1)]^{-2}$. The distance dependence of $\tilde{f}^2$ is $[a/(a+d)]^6$ and therefore the enhancement effect is long ranged.

Note that the lifetime and the effective oscillator strength have different dependence on d. The lifetime varies faster, at small d, where a d^{-3} dependence (like for a flat surface) is valid. It is conceivable that in some cases for small d the oscillator strength is very large but the lifetime is so short that the emission is not detectable. Therefore, the molecules located at moderate distances emit most effectively.

Note that the analysis pursued here is relevant to the question whether one can carry out surface enhanced photo-chemistry. Bringing the molecule close to a sphere will result in an enhanced oscillator strength and therefore in an increased population of the photo-active state. However, the life-time becomes very small and the molecule will transfer the photo-excitation energy to the sphere before a photo-decomposition or rearrangement can

take place. Therefore, in spite of the increased local laser intensity, the rate of the photochemical processes is diminished if the molecule is too close to the surface. At distances of roughly 20-30Å the situation is changed. The oscillator strength is still enhanced but the life-time is considerably increased, so that a rate enhancement becomes possible.

III. 3.3 Surface Enhanced Spectroscopy on Small Ellipsoids.

§111. An ellipsoid is a reasonable model for the elongated or flattened particles formed in the course of metal vapor deposition on glass slides. Such particles have some advantages over spheres.

(a) For a small sphere there is only one dipole resonance frequency for a given material. For a small ellipsoid, the dipole resonance frequency can be continuously changed by varying the aspect ratio (i.e. the ratio between the semi-axes). This is important since it provides a possibility of matching the particle resonance with a molecular resonance of interest, by changing the shape of the particle.

(b) Calculations[115] with prolate spheroids with high aspect ratio show that the reflected field is substantially enhanced in regions located near high surface curvature. This effect is present at all frequencies and therefore permits large resonance enhancements.

(c) Small ellipsoids are better enhancers than spheres. A Ag ellipsoid of very high aspect ratio can provide[115] a Raman enhancement factor of 10^{11}, for a molecule located at the tip. Even if the molecules are spread around the ellipsoid, and the ellipsoid position with respect to the incident field is random, poor enhancers like Au and Cu can provide[115] a Raman enhancement factor of $10^6 - 10^7$, if the aspect ratio is 3.

The drawback of such systems is that we cannot yet prepare them so that the values of the semi-axes have a known, narrow distribution. This makes it difficult to test the theory in detail.

§112. Several groups[115, 116, 155 - 157] have discussed the electrodynamic theory of SES on ellipsoids. We review here some of the results of Gersten and Nitzan[115] since they used the simplest model, which displays some of the

important physical effects. We quote then selected results from the work of Wang and Kerker[115] since they computed observable quantities, by using the most realistic model to date.

§113. In solving the electromagnetic problems appearing in surface enhanced spectroscopy on small ellipsoids, we follow the pattern established in describing the work on small spheres. We need the reflected field, and the reflection tensor, which multiplies the oscillator strength. For resonant Raman, fluorescence and absorption studies, we need the change in lifetime, given by the "image field." In order to understand the emission by the ellipsoid-molecule system, we need to know the dipole induced in the particle by the molecular dipole. Since the ellipsoid is small compared to the wave length, we can obtain all this information by solving Laplace equation (§75).

§114. In order to obtain the simplest possible results, we consider[115] a prolate spheroid *with the semi-major axis a and the semi-minor axis* b. The coordinate system has the oz axis oriented along a and the origin at the center of the ellipsoid. The molecule is placed on the oz axis at a distance H from the surface. The incident field and the induced molecular dipole are taken parallel to oz.

The problems stated at §113 are solved by seeking a solution of Laplace equation in a system of prolate spheroidal coordinates (ξ, η, ϕ). The equation ξ = constant generates a family of prolate spheroids. The surface of the metal is given by $\xi = a/\mathcal{F} \equiv \xi_0$ and the position of the dipole by $\xi = (a + H)/\mathcal{F} \equiv \xi_1$ and $\eta = 1$. Here $\mathcal{F} = (a^2 - b^2)^{1/2}$.

The potential outside the sphere has the form:[9]

$$\Phi_{out}(\eta,\xi) = -E_i f\xi\eta + (\mu/f^2) \sum_n (2n+1)P_n(\xi)Q'_n(\xi_1)P_n(\eta)P_n(\eta_1) + \sum_n c_n P_n(\eta)Q_n(\xi) \qquad \text{(III.95)}$$

The first term is a "spatially homogeneous" incident field, written in ellipsoidal coordinates. The second is the field exerted by the molecular dipole μ at the point (ξ, η) for $\xi_0 < \xi < \xi_1$. The third is the field caused by the polarization of the ellipsoid. There is no ϕ dependence because a highly symmetrical arrangement is considered.[115]

The symbols P_n and Q_n denote the n-th order legendre polynomials of first and second kind,[158] respectively. The potential inside the ellipsoid is written as

$$\Phi_{in}(\eta,\xi) = \sum_n b_n P_n(\eta) P_n(\xi). \qquad \text{(III.96)}$$

The constants b_n and c_n are unknown.

The expressions (95) and (96) are solutions of Laplace's equation, chosen to give a finite potential at the center of the ellipsoid and a zero potential at infinity.

The values of b_n and c_n are obtained by requiring Φ_{out} and Φ_{in} to satisfy the boundary conditions for $\xi = \xi_0$ and arbitrary values of η. This yields

$$c_n = \frac{(\varepsilon - 1)f\xi_0 \, \delta_{n,1}}{[\varepsilon Q_1(\xi_0) - \xi_0 Q'_1(\xi_0)} E_i + \frac{(2n+1)(1-\varepsilon) P'_n(\xi_0)Q'_n(\xi_1)P_n(\xi_0)}{f^2[\varepsilon Q_n(\xi_0)P'_n(\xi_0) - Q'_n(\xi_0)P_n(\xi_0)]} \mu \qquad \text{(III.97)}$$

Inserting this into the third term of Eq. (95), we obtain the potential caused in the vacuum by the polarization of the ellipsoid. The term proportional to E_i gives the polarization caused by laser and the one proportional to μ gives the "image effect". The electric field along the

z-direction, at the dipole position ($x = 0$, $y = 0$, $z = a + H$) $\equiv$ ($\xi = \xi_1$, $\eta = 1$, $\phi = 0$) is

$$E = -\frac{\partial}{\partial z}\Phi_{out} = -f^{-1}\sum_n c_n Q'_n(\xi_1) + E_i \qquad \text{(III.98)}$$

Inserting the expression (97) for c_n into (98) we obtain for the z-component of the reflected field

$$E_{z,r} = \frac{(1-\epsilon)\xi_0 Q'_1(\xi_1)}{[\epsilon Q_1(\xi_0) - \xi_0 Q'_1(\xi_0)]} E_i \equiv B(\omega)E_i \qquad \text{(III.99)}$$

and for the z-component of the image field

$$E_{z,im} = \left(\sum_n \frac{(2n+1)(\epsilon-1)\ P'_n(\xi_0)\ (Q'_n(\xi_1))^2 P_n(\xi_0)}{f^3[\epsilon Q_n(\xi_0)P'_n(\xi_0) - Q'_n(\xi_0)P_n(\xi_0)]}\right)\mu \equiv \gamma(\omega)\mu \qquad \text{(III.100)}$$

§115. The reflected field has a resonant behavior if the frequency of the incident beam is chosen so that

$$\text{Re}\ \epsilon(\omega)\ Q_1(\xi_0) = \xi_0 Q'_1(\xi_0). \qquad \text{(III.101)}$$

The resonance frequency can be easily computed since[158] $Q_1(\xi_0) = (\xi_0/2)\ \ln\left[\frac{(\xi_0+1)}{(\xi_0-1)}\right] - 1$. The equation (101) is the analog of Eq. (60) §77 which gives the resonant frequency for a sphere. In fact, as $a \to b$, Eq. (101) reduces to Eq. (60) §77. While a Rayleigh sphere has only one resonance frequency per material, the resonance frequency of a small spheroid depends on the aspect ratio (a/b). A plot of this dependence is given in Fig. 16. The resonance of a Ag spheroid can vary from near infrared to blue.

The ability of various materials to enhance resonantly the reflected field depends on the magnitude of $\text{Im}\ \epsilon(\omega_{res})$, since at resonance the reflected field becomes

$$(E_{z,r})_{res} = [1 - \epsilon(\omega_{res})]\xi_0 Q'_1(\xi_0)\ (\text{Im}\ \epsilon(\omega_{res})Q_1(\xi_0))^{-1}. \qquad \text{(III.102)}$$

§116. It is now easy to compute the effective polarizability, by following the derivation outlined in §104-106. Since we used here the same notation as in §104-106, we obtain

$$\mu(\omega) = (\tilde{\omega}_o^2 - \omega^2 - i\omega\tilde{\Gamma}_o)^{-1}(e^2/m)\tilde{f} \cdot E_i \qquad \text{(III.103a)}$$

$$\tilde{f} = f(1 + B), \qquad \text{(III.103b)}$$

$$\tilde{\omega}_o^2 = \omega_o^2 - (e^2/m)f \operatorname{Re} \chi(\omega) \qquad \text{(III.103c)}$$

and

$$\tilde{\Gamma}_o = \Gamma_o + (e^2/m\omega)f \operatorname{Im} \chi(\omega). \qquad \text{(III.103c)}$$

The quantities B and χ are defined by Eqs. (99) and (100), respectively.

The results follow the pattern established by the general theory (§20) and the work on spheres (§104-106). The effect of the spheroid on the molecule is to increase the oscillator strength from f to $\tilde{f}$, to shift the resonance frequency from ω_o to $\tilde{\omega}_o$ and the width from Γ_o to $\tilde{\Gamma}_o$. The change in oscillator strength is due to the reflected field and the shifts in ω_o and Γ_o to the "image field".

For normal Raman scattering the laser is operated so that $\omega_o >> \omega$ and $\omega_o >> \omega\tilde{\Gamma}$, therefore μ becomes $\mu_o = (e^2/m\omega_o^2)\tilde{f} \cdot E_i = \alpha_o(1 + B)E_i$, where $\alpha_o = (e^2/m\omega_o^2)f$ is the static polarizability $\alpha(\omega = o)$ of the free molecule. Thus, the image field and the corresponding changes in the polarizability are irrelevant. Only the change in the oscillator strength matters. In the case of resonance Raman we operate the laser at $\omega \sim \omega_o$ and the theory ought to be done carefully.[21] In the case of fluorescence decay experiments, the intensity depends on both the lifetime $\tilde{\Gamma}^{-1}$ and the absorption oscillator strength.

§117. Surface enhanced Raman scattering near ellipsoids. According to the discussion in §116, the Raman dipole is given by

$$\mu_{RS}\ (\omega - \omega_v) = \left(\frac{\partial \mu_o}{\partial Q} \right) \delta Q = \left(\frac{\partial \alpha_o}{\partial Q} \right) \delta Q\ (1 + B)\ E_i \qquad \text{(III.104)}$$

where δQ is the normal mode of interest. This dipole radiates photons of frequency $\omega - \omega_v$ directly to the detector, and also drives the ellipsoid, polarizes it, and makes it radiate at the frequency $\omega - \omega_v$. We detect the radiation produced by both these processes and therefore to obtain the total Raman intensity we need to establish what is the dipole of an ellipsoid driven by μ_{RS}. The answer is given by the asymptotic form (for $\xi \to \infty$) of

$$\Phi_{out}\ (\eta,\varepsilon) = \sum_n c_n p_n(\eta) Q_n(\xi), \qquad \text{(III.105)}$$

with c_n given by Eq. (97). We can identify the dipole corresponding to the polarized ellipsoid because we know that for large ξ the potential caused by a dipole p located at the center of the ellipsoid and oriented along oz is of the form $\frac{p\,\eta}{(f\xi)^2}$. Comparing the asymptotic form (large ξ) of Eq.(105) to $p\eta(f\xi)^{-2}$ gives

$$p = \frac{(1 - \varepsilon)\xi_o Q'_1(\xi_1)}{\varepsilon Q_1(\xi_o) - \xi_o Q'_1(\xi_o)}\ \mu \equiv B(\omega - \omega_v)\mu \qquad \text{(III.106)}$$

Note that in the case of SERS the dipole of interest in Eq. (106) is given by the μ_{RS} of Eq.(104) and the frequency (at which the dielectric constant ε of the metal must be taken) is $\omega - \omega_v$.

The total emission arriving at the detector is due to the coherent sum of p and μ_{RS}, exactly as in the case of the sphere (§83,84).

The field reaching the detector is

$$\vec{E}(\vec{R}_d;\ \omega - \omega_v) = \overleftrightarrow{G}_o(\vec{R}_d,\ \omega - \omega_v)\cdot z\ (\mu_{RS} + p), \qquad \text{(III.107)}$$

where $\overleftrightarrow{G}_o$ is defined by Eq. (63) §81. Using Eqs. (104) and (106), we find that the intensity is proportional to

$$I_{RS} \alpha \left| \overleftrightarrow{G}_o(\vec{R}_d;\omega - \omega_v) \cdot \hat{z} \right|^2 \left| (1 + B(\omega - \omega_v)) \frac{\delta\alpha_o}{\delta Q} \delta Q\ (1 + B(\omega)) \right|^2. \qquad \text{(III.1}$$

Comparing to the case of the sphere we find that $B(\omega)$ replaces the expression $\beta \overleftrightarrow{T}$ appearing in Eq. (74), §84.

Maximum enhancement comes from the term containing $|B(\omega - \omega_v)|^2 |B(\omega)|^2$ since B is generally larger than 1 and can become rather large if either $\omega = \omega_{res}$ or $\omega - \omega_v = \omega_{res}$; the resonance frequency ω_{res} is discussed in §115 and is given by Eq. (101).

§118. To illustrate the properties of the enhancement caused by the ellipsoid we reproduce some of the numerical results of Gersten and Nitzan.[115] These were obtained for a half-ellipsoid imbedded in a perfectly conducting half-space. As we explain in Section III 5, this is equivalent to having a full ellipsoid and two dipoles placed on the oz axis so that one is the mirror image of the other with respect to the mid-plane of the ellipsoid. Therefore the plots in their paper are relevant to the present section. While the numbers are not the same for a full ellipsoid and one dipole, the order of magnitude and the trends are very similar.

In Fig. 17 ' we present the enhancement factor for Raman intensity as a function of photon energy. Note the enormous enhancement of 10^{11} for Ag at the resonance frequency. The peak value for Cu and Au is smaller (since Im $\varepsilon(\omega)$ for them is larger than for Ag), but it is still substantial.

Note that in Eq. (108) the factors B that contain the resonant denominator appear at two frequencies, contributing to the enhancement factor through $|B(\omega - \omega_v)|^2 |B(\omega)|^2$. However, Gersten and Nitzan[115] took both frequencies equal and this increases to some extent the enhancement factor at resonance frequency, since the approximate factor $|B(\omega)|^4$ used by them has a sharper resonance than the correct expression $|B(\omega - \omega_v)|^2 |B(\omega)|^2$. For Ag, whose resonance is very narrow, $|B(\omega - \omega_v)|^2 |B(\omega)|^2$ may give a double peak if ω_v is larger than or comparable to the width of the resonance. This seems to be the case for pyridine where ω_v is of order 1000 cm^{-1} and the width of the electromagnetic resonance is roughly 40 cm^{-1}. Such a peak does not appear in the GN calculations but it is present in those of Wang and Kerker.[155]

As we discussed in § 79, the dielectric constant of a particle whose size is smaller than the mean free path of the electron (200 - 300 Å) is expected to be lossier than that of the bulk material. The resonant enhancement is therefore expected to be smaller than the computed one, and the resonance broader. The two peaks mentioned above may be washed out by such effects. Furthermore, unavoidable statistical dispersion in a and b will cause different ellipsoids in the sample to have different resonance frequency, causing a further smear of the sharp resonance predicted by Fig. 17.

The dependence of the enhancement factor on the molecule-ellipsoid distance is displayed in Fig. 18. In all cases the enhancement is long ranged and its rate of decay with H depends on the aspect ratio. The decay is faster for more elongated ellipsoids. The shape of these curves seems to be independent on frequency, (Fig. 19). Note that the enhancement factor is fairly large even for off-resonance frequency. This is due to the high curvature of the tip of the ellipsoid.

One should keep in mind that the geometry discussed here[115] is very peculiar. The field and the dipole are along the semi-major axis and they couple only to modes in which the plasma oscillate in that direction. Other modes can be excited if the driving field has a component along the semi-minor axis b. These modes have different resonance frequencies and properties from the ones discussed here. Furthermore, the molecule is placed near the tip, where the enhancement is likely to be largest.

§119. Very recently Wokaun, Gordon and Liao[159] pointed out that since the dipole induced in the ellipsoid by the external field is very large, it might be necessary to take into account the radiation reaction field. This is given[160] by $E = (2/3c^3)\dddot{\vec{p}}$, where $\vec{p}$ is the dipole of the system. Applying this to the polarization of the ellipsoid gives (we assume a diagonal polarization tensor for ellipsoid)

$$p_i(\omega) = \alpha_{ii}(E_i^{ext} + i\,(2\omega^3/3c^3)p_i),\ i = x,\ y \text{ or } z \qquad \text{(III.109)}$$

which leads to

$$p_i(\omega) = \frac{\alpha_{ii}(\omega)E_i^{ext}(\omega)}{1 - i(2/3)(\omega/c)^3\alpha_{ii}(\omega)} \equiv \alpha_{ii}^{eff} \cdot E_i^{ext} \qquad \text{(III.110)}$$

The reaction force changes the polarizability of the ellipsoid making it smaller and "skewing" its frequency dependence. This lowers both the reflected field and the emission enhancement (which are each proportional to p^2) diminishing substantially the enhancement factor. There seems to be some experimental support[159] for this idea.

The reaction field should not be introduced in the Drude equation describing the molecular dipole, since it is taken into account through use of the experimental natural linewidth.[15]

§120. Recently Wang and Kerker[155] have removed the geometrical restrictions imposed by GN.[115] They considered an ensemble of randomly oriented, non-interacting spheroids covered with a molecular monolayer, with the molecular dipoles perpendicular to the surface. The Raman intensity is averaged over the orientations of the spheroid. The enhancement factors for the 1010 cm^{-1} Raman line of the pyridine, for prolate Ag, Cu and Au spheroids in water, for various aspect ratios are plotted in Figs. 20, 21 and 22 as a function of wavelength. The enhancement for a Ag oblate spheroid is plotted in Fig. 23.

The double peak mentioned at §118 is present for Ag at all aspect ratios. For Cu and Au, it is only visible at the highest aspect ratio. The peak enhancement grows with a/b, while the resonance position shifts to higher wavelength. For Ag, a change of a/b from 1 to 3 changes the resonance frequency from blue to green. The enhancement is much lower than the one predicted by Gersten and Nitzan.[1] This happens because GN have placed the molecule near the tip of the ellipsoid and the incident field was taken along the major axis of the ellipsoid, and these conditions yield very large enhancements.

The resonant enhancement for Cu and Au is less than that for Ag since $Im\epsilon$ for these metals is smaller. It is, however, substantially increased by going to larger aspect ratios, probably due to an increase in the curvature effect, which is roughly equally strong for Cu, Ag and Au. The oblate spheroids (Fig. 23) give an enhancement comparable to the prolate ones but the resonance frequency and the enhancement are less sensitive to the aspect ratio.

§121. Recent work by Liao et. al.[161] has tested some of the qualitative features predicted by the theory. They used a holographic method to produce a regular array of conical SiO_2 posts, 500 nm high and 100 nm in diameter, and separated by 300 nm. On top of them they deposited, by vapor condensation, Ag particles of regular and resonably uniform ellipsoidal shape, with aspect ratio of roughly 3:1 and a dimension of about 100 nm. They studied the SER spectrum of the AgCN formed on the Ag particles. The excitation spectrum (Fig. 24) is in general agreement with the Gersten-Nitzan[115] calculations (Fig. 17). Changing the aspect ratio or dipping the structure in water or cyclohexane (to change ε_2) modifies the excitation spectrum in the direction predicted by the theory. At first it may seem surprising that the GN theory which makes some drastic simplifications (the incident field is parallel to the semi-major axis and the molecules are all located at the tip of the ellipsoid) would fit the data so well. This happens because only the shape of the excitation spectrum is measured. This quantity is least dependent on the position of the molecule. The measured enhancement factor is $\sim 10^7$ which is comparable to the predictions made by Wang and Kerker.[155]

Experimental work[162] with islands formed by vapor deposition is also in general agreement with the theory.

§122. <u>Absorption and fluorescence by molecules located near an ellipsoid.</u> In most cases the fluorescence process is a sequence of events. First the photon is absorbed to excite the molecule to an electronic state A. This is followed by a relaxation process which can be (1) a radiationless transition to an electronic state B or (2) vibrational relaxation to lower vibrational states of A. After that, either A or B emits a photon and the molecule ends in the ground electronic state.

The equation (II.46) §18 gives a rate of absorption proportional to

$$P = \frac{\tilde{\Gamma}(\omega_i)\,|E_p^2|}{(\omega_o^2 - \omega^2)^2 + \omega^2\tilde{\Gamma}^2} \simeq \frac{\tilde{\Gamma}(\omega_i)\,|1 + B(\omega_i)|^2\,|E_i|^2}{\omega_o^2[(\omega_o - \omega)^2 + \tilde{\Gamma}^2]} \qquad \text{(III.111)}$$

To go from the second to the third term we have used Eq.(99) for the primary field, as well as the conditions ω close to ω_o and $\tilde{\omega}_o >> \Gamma$. Assuming that the probability of the radiationless transition or vibrational relaxation is the same as in the gas phase we can consider that the population of the emitting state C (which is either A or B) is proportional to P given by Eq. 111).

The dipole μ' corresponding to the excitation of C induces a dipole $p = B(\omega_s)\mu'$ in the ellipsoid and the two of them emit coherently. In a relaxation experiment the emission intensity at the frequency ω_s is proportional to $e^{-\tilde{\Gamma}(\omega_s)t}\,|p + \mu'|^2\,P$, which gives

$$I \propto |(1 + B(\omega_s)|^2\,|\mu'(\omega)|^2\,\frac{\tilde{\Gamma}(\omega_i)\,|1 + B(\omega_i)|^2}{[(\tilde{\omega}_o - \omega_i)^2 + \tilde{\Gamma}(\omega_i)^2]}\,\exp(-\tilde{\Gamma}^1(\omega_s)t) \qquad \text{(III. 112)}$$

We have used here the probability of exciting the state C given by Eq. (111). The dipole $\mu'(\omega_s)$ corresponding to the excited state C is $(e^2/m)f'\{(\omega'_o)^2 - \omega^2 - i\omega\Gamma'\}^{-1}$, where the parameters ω'_o, Γ'_o and f' corresponding to the state C are used. Note that μ' is proportional to the free molecule oscillator strength f'; the "renormalization" of f' to $\tilde{f}$ (given by Eq. 103b) does not appear since C is not populated through an optical process (which would enhance f' through the reflected field) but through relaxation. The width $\tilde{\Gamma}$ is renormalized because the image field is present during the emission process.

Assuming now that the frequency ω_s of the detected fluorescence equals $\tilde{\omega}'_o$ we have $|\mu'(\omega_s)|^2 = (\alpha'_o)^2\,|\tilde{\Gamma}(\omega_s)|^{-2}$; here α'_o is the free molecule static polarizability $\alpha'_o \equiv (e^2 f'/m\omega'^2_o)$. Using this result we can write Eq.(112) in the form (we retain only the terms that differ from the free

molecule case):

$$I \propto |(1 + B(\omega_s)|^2 (\tilde{\Gamma}(\omega_s))^{-1} \frac{\tilde{\Gamma}(\omega_i)\,|(1 + B(\omega_i)|^2}{[(\tilde{\omega}_o - \omega_i)^2 + \tilde{\Gamma}(\omega_i)^2]} e^{-\tilde{\Gamma}(\omega_s)t} \qquad \text{(III.113)}$$

For a steady state experiment one should suppress the exponential.

§123. Since there are no detailed numerical studies of these quantities we can only give a general outline of what one should expect. The widths $\tilde{\Gamma}(\omega_i) = \Gamma_o + \Gamma_s(\omega_i)$ and $\tilde{\Gamma}'(\omega_f) = \Gamma_o' + \Gamma_s'(\omega_s)$ have the general properties discussed at §107-110 for spheres. At small molecule surface distances H the value of $\tilde{\Gamma}(\omega)$ is practically equal to that at a flat surface. This happens because in Eq.(100) giving the image field (hence Γ_s) the sum is dominated by the high n terms. This parallels the behavior discussed at §108 for spheres. The distance dependence of Γ_s for small H is H^{-3}. For this reason as H is increased Γ_s is rapidly diminished. As we know from experiments with flat surfaces (Section III.1) the fluorescence by a molecule located at the surface is very effectively quenched. This happens because the factors $\tilde{\Gamma}'$ and $\tilde{\Gamma}$ appearing in Eq.(113) become very large. The exponential $e^{-\tilde{\Gamma}'t}$ decays very fast, overlapping in time with the excitation pulse. The detection of fluorescence is then more difficult. Furthermore, the absorption line is very broad and the absorption is inefficient. If the excitation frequency $\omega_i = \omega_o$ then the "absorption part" of Eq.(113) is $|1 + B(\omega_i)|^2/\Gamma(\omega_i)$. If ω_i is chosen so that $B(\omega_i)$ has a resonance (see Eq.(101) $\tilde{\Gamma}(\omega_i)$ will also resonate (through its dipole term n = 1 in Eq. 100). This will diminish the enhancement brought about by $|B(\omega_i)|^2$. Furthermore, if we make the incident frequency resonate with the ellipsoid the emission frequency might be off-resonance. Hence, $|(1 + B(\omega_s)|^2/\Gamma(\omega_s)$ is small. Therefore, the intuitive feeling that the fluorescence from a molecule located at the surface of an ellipsoid is quenched is justified qualitatively by Eq. (113).

The situation changes as H is increased since $\tilde{\Gamma}$ decays with H faster than B does. Therefore the exponent is diminished and the pre-exponential grows. Under these conditions enhanced fluorescence can be observed. Equation (113) indicate that the enhancement may come from two sources: absorption or emission; in other words either ω_i or ω_s could be on resonance with the ellipsoid, with the enhancement of $|B(\omega_i)|^2$ or $|B(\omega_s)|^2$, respectively. Since the resonance frequency of the ellipsoid varies with the aspect ratio, we can change the shape and "tune" the resonance with ω_i or ω_s. Two intensity maxima can thus be achieved when either absorption or emission are enhanced.

The excitation spectrum of fluorescence (i.e. the fluorescence intensity as a function of the incident frequency) follows the absorption spectrum of the molecule (as modified by the presence of the ellipsoid) if ω_s is independent on ω_i (which is often true).

It is interesting to compare the pre-exponential appearing in Eq.(113) to the enhancement factor in SERS, which is $|(1 + B(\omega_i - \omega_v))|^2 |(1 + B(\omega_i))|^2$. The pre-exponential differs from this expression in two respects. The frequency difference $\omega_i - \omega_s$ could be larger than ω_v. Therefore, while in a Raman experiment both ω_i and $\omega_i - \omega_v$ could be in resonance with the ellipsoid, this might not be the case if $|\omega_s - \omega_i|$ is large. Furthermore, in fluorescence the pre-exponential is divided by $\tilde{\Gamma}(\omega_s)\tilde{\Gamma}(\omega_i)$ and this diminishes the fluorescence enhancement as compared to the Raman enhancement factor. It also affects the distance dependence since the pre-exponential is low at small H, reaches a maximum at moderate H and then it goes down. For these reasons the enhancement of fluorescence though related to that of SERS, is smaller and has a different distance dependence.

Note that the discussion of fluorescence can be applied to develop a simplified theory of Resonance Raman scattering, with very minor and obvious modifications

§ 12.4. The experimental work on fluorescence[164-169] has been carried out by using islands formed[170-171] when metal vapors are condensed on a glass substrate. The size of the islands depends on the amount of metal deposited or, equivalently, on the film thickness defined as the volume deposited per unit area. By varying the thickness from zero to 80 Å one obtains particles ranging from 40 Å to 1000 Å. For a given thickness the particle sizes vary by a factor of 2 from the mean value. When the film thickness is about 80 Å the particles begin to touch each other and continuous film is formed.

Glass, Liao, Bergman and Olson[166] have prepared a metal wedge on top of a glass slide, of thickness varying from zero to about 200 Å. They spun Rhodamine B or nile blue on the wedge and measured the absorption and the fluorescence spectrum of the dye-metal system, at different places (i.e. different sizes metal islands) on the wedge. Rhodamine on glass absorbs at ~580 nm while the Ag islands have broad absorption bands with peak frequencies between ~460 nm (smaller islands) and ~600 nm (larger islands). The absorption band of the combined island-dye system differs from a superposition of the bands of the isolated components. The islands influence the dye absorption by increasing the effective oscillator strength f (through the reflected field) (Eq. 111)). The general form of the curves is similar to the one computed by Nitzan and Brus[152-153] for a molecule near a sphere.

The fluorescence intensity has a peak as a function of film thickness and it is completely quenched when a continuous film is formed. The two dyes used have well separated maximum excitation and emission frequencies. For Rhodamine B, the excitation takes place at 514.5 nm and the emission maximum is at 600 nm. For nile blue the excitation is at 632.8 nm and the emission is at 700 nm. Roughly, the data indicates that the maximum in fluorescence intensity is reached when the particle sizes are such that

the excitation frequency overlaps with the resonance frequency of the particles. Thus, the enhancement of the intensity occurs through enhanced absorption, that is, through the factor $\frac{|(1+B(\omega))|^2}{\tilde{\Gamma}(\omega)}$ in Eq. (113). The emission wavelength is too large to resonate with the particles.

A study of the fluorescence excitation spectrum shows that it does not replicate the absorption spectrum of the dye-island assembly. This is expected since in fluorescence spectroscopy we do not detect the energy absorbed into the particle but only that going into the molecule. The absorption spectrum does not distinguish between the two. A comparison of the excitation spectrum of Rhodamine B on glass and on islands shows that the latter is substantially broadened, as expected from the theory (§123).

If a layer of polymethyl metacrylate (PMMA) is spun on the islands and the dye is placed on top of it, the intensity of fluorescence is diminished but the dependence of the fluorescence intensity on island size is not altered. It is believed that the PMMA film has a thickness of 30 Å and therefore the experiment indicates that the long range effect predicted by the electromagnetic theory is present.

§125. The relaxation experiments of Weitz, Garoff. Hanson, Gramilla and Gersten[169] complement the study of Glass et.al.[166] They[169] worked with islands having a circular cross section and a diameter of approximately 200 Å. The dye used was Europium III thenoyltrifluoroacetonate (ETA) which is excited at 390 nm and emits at 613 nm. When ETA is deposited on silica, its fluorescence decays exponentially with a lifetime of 280 μsec and a quantum yield of 0.4.

When the dye is spun on the silica-island system, the life-time is not exponential. Preparing the islands on an oxydized Aluminum surface eliminates the long time part of the fluorescence. This happens because the fluorescence on the flat Al surface is quenched very effectively, while on the flat silica surface it is not. Therefore the long time

emission must come from ETA located on the flat silica surface between the islands. These molecules interact with the islands, but their distance to the island is variable and fairly large compared to the molecules located on the island. The theory shows (§123) that the life-time depends on the molecule-island distance and goes up with it. This is in agreement with the observations that the molecules located on silica have longer life-times and with the fact that the decay is not exponential.

To decice whether the increased fluorescence signal is caused by enhanced absorption or emission Weitz et. al.[169] have looked for SER spectrum of ETA. They could not detect the SER intensity and this indicates that the reflected field, at the excitation frequency, is small. Furthermore, a semi-quantitative analysis is consistent with the assumption that the molecular emission is enhanced by the polarization of the ellipsoids.

III.4. The Electrodynamic interaction between particles and its possible role in SES.

§126. All the calculations presented so far have considered isolated particles surrounded by an optically "indifferent" medium containing the molecules of interest. In many experimental situations it is not however possible to create the desired particle isolation. The local field energy is proportional to $\vec{E} \cdot \vec{E}^*$ and since E is the sum of the electric fields $\vec{E}_1$ and $\vec{E}_2$ produced by the polarization of the particle 1 and 2, the Hamiltonian contains the terms $\vec{E}_1 \cdot \vec{E}_2^* + \vec{E}_2 \cdot \vec{E}_1^*$ through which the two particles interact electromagnetically. Since both $\vec{E}_1$ and $\vec{E}_2$ extend at hundreds of Å into the vacuum the interaction Hamiltonian is sizable even if the surfaces of the two particles are hundreds of Å apart.

This interaction can have a variety of effects. (a) If the two particles are identical their electromagnetic resonances are degenerate. The interaction between them shifts their frequencies creating two or more resonances, changing thus the excitation spectrum of the system. The new resonance frequencies depend on the interparticle distance. This happens, for example, when colloidal solutions are too concentrated or when they start to aggregate. (b) From the existing calculations[31, 106, 107, 122] it appears that the primary field between two interacting particles is enhanced well above the sum of the fields generated by the non-interacting objects. This effect is caused by the mutual polarization between the particles. As a result, the resonances of the interacting objects have most of the electromagnetic energy (hence the electric field intensity) packed in the space between them. This is apparently the reason why the SERS signal in aggregated colloids is higher than that in solutions with isolated particles. (c) The above features are likely to be present whenever two particles interact electromagnetically. What happens if a large number of such particles are crowded together is not yet clear. The electric field enhancement produced by the localized electromagnetic resonances sustained

by small particles can be qualitatively viewed as the result of packing the absorbed photon energy in a small space around the particle. If two resonances have the same oscillator strength, the more localized one should produce a higher electric field in the localization region. If such resonating objects are crowded together the resonance might be delocalized and this may result in a reduction of the local field intensity. One extreme example of such an occurrence is provided by the case of a surface having isolated parallelpipeds on a flat surface. Their electromagnetic resonances can be excited optically to produce large electric field enhancements. If we increase the number of parallelpipeds on the surface and pack them so tightly that their tops form a flat surface, their resonances combine to form the surface plasmon of the flat surface. This can no longer be excited optically and a very minimal field enhancement is possible. Even if we excite the surface plasmon by ATR the corresponding field enhancement is low compared to that generated by isolated parallelpipeds. In the same spirit, by crowding hemisphere on a flat surface we can make a crossed grating. The enhancement of the field is then possible only at a well defined angle and it is smaller than in the case of the isolated hemispheres.

These extreme examples of the effect of overcrowding should induce us to use isolated particle models with extreme caution if the required isolation is not experimentally realized. The problem of delocalization by overcrowding has not yet been addressed in the context of surface enhanced spectroscopy. A preliminary study by Laor and Schatz[172] indicates that the local field is lowered by the delocalization caused by resonance interactions. A large body of work exists[173] concerning the dielectric properties of composite materials, which can be adapted to study the same problem for SES. The analogy to Anderson localization[174] should make this problem appealing to theorists.

III.4.1. Two interacting spheres.

§127. The simplest system on which we can study the effect of the electromagnetic interaction between two particles on SES consists of two small spheres of equal radius. The smallness of the spheres allows us to obtain the fields by solving Laplace's equation. The geometry permits the separation of variables if bispherical coordinates[ ] are used; this simplifies the problem enormously.

Aravind, Nitzan and Metiu[ ] have obtained numerically the properties of the quantity $\tilde{I}$ defined in § 71, Eq. (53). This is the ratio of the "local laser intensity" versus the intensity of the incident beam. We chose this quantity since it is a scalar which gives a feeling for the primary field enhancement. It depends on the point of "observation," the geometric parameter $\lambda=(2R_o+D)^{-1}R_o$ (see Fig. 25), the direction of the electric vector of the incident field, and the dielectric constants of the spheres and of the material surrounding them.
(a) In order to display the excitation spectrum we plot $\tilde{I}$ as a function of the incident frequency (Fig. 26) for various values of the geometrical parameter λ. The plotted values of $\tilde{I}$ are computed at the "observation point" indicated in Fig. 25. The curve $\lambda=0$ represents the case of an isolated sphere. It is clear that the presence of the second sphere causes the appearance of a second resonance, at a frequency below the single sphere resonance. The value of the resonance frequency is independent of the observation point. The relative peak intensities are very sensitive to the value of λ, the angle of incidence and the position of the observation point.

The magnitude of $\tilde{I}$ in the region between the spheres is illustrated by Fig. 27. Here we plot $\log_{10}\tilde{I}$ as a function of the position on the line between the spheres as given by d/D. Fig. 27 (a) corresponds to the higher resonance frequency (ω=3.48eV) and Fig. 27 (b) for the lower one (ω=3.21eV). The value of $\tilde{I}$ between spheres is at least an order of magnitude

larger than for the single sphere. The enhancement is larger at the frequency of the "new" resonance, created by the interaction between the spheres. The relevance of these findings to the experiments in colloidal systems has been discussed at § 88. Using the reciprocity theorem[22] we infer that the SERS enhancement for molecules located between spheres at $\omega = 3.2$ leV is $4 \times 10^6 = (2 \times 10^3)^2$ while for a single sphere is 400. However, one should keep in mind that these numbers are valid for molecules located between the spheres where the amplifying ability is largest.

§128. It is interesting to note that these calculations have a bearing on the study of the effect of interparticle interaction on the Brownian motion in quasi-dilute colloidal solution. This is an interesting problem in its own right. The interest in the problem is further enhanced by the fact that if we could control coagulation such systems could provide a useful simplified model for micellar solutions. The manner in which micelle interactions affect the properties of the light scattering is a matter of current debate. Some insight might be gained by studying the problem on a simpler model system such as a colloidal solution.

The electromagnetic interaction between two spheres has detectable effects which are sensitive functions of the instantaneous distance between spheres. The polarization of an isolated sphere is isotropic and the induced dipole has the direction of the incident electric field. As a result, if multiple scattering is prevented, the scattered light is not depolarized; in other words, if we send light in with a vertically polarized electric vector and count photons scattered at 90° with a horizontally polarized electric vector, we should get no signal. The pairwise electromagnetic interaction changes this situation, essentially because the problem has now two important directions: that of the

incident electric field and that joining the centers of the two spheres. One sphere is polarized like an atom, while two interacting spheres are polarized like a diatomic molecule. The pair depolarizes the light while the single sphere does not. The depolarized light scattering in this situation is similar to the collision induced depolarization in noble gas liquids.[176]

Therefore, the depolarized scattering is all caused by the interacting spheres (this of course assumes that no depolarization is caused by the solvent; if this is not the case the solvent depolarization acts as background). Its intensity depends on the number of interacting pairs in the scattering volume, the distance between them and their orientation. These change in time with the Brownian motion of the particles and as a result the intensity of the depolarized light fluctuates. This fluctuation can in principle be measured to provide information on the stochastic dynamics of Brownian motion.

III.4.2. The interaction between a sphere and a plane.

§129. We have already considered a sphere-flat surface system in Section III.2.5. There we have used a perfectly conducting sphere which cannot sustain an electromagnetic resonance. Its role was to break the translational symmetry parallel to the surface, modify the plasmon of the flat surface and allow its optical excitation. In the present section we consider the case when both the sphere and the plane can support resonances. The joint system has two resonances, one at low frequency, originating from the resonance of the isolated sphere and one at higher frequency, originating from the plasmon.

§130. (1) In Fig. 28 (a) and (b) we plot $\tilde{I}$ as a function of frequency, for various ratios $\lambda = D/R_o$ (D is the sphere-plane separation and R_o is the radius of the sphere. The dotted curve in Fig. 28 (a) corresponds to an s-polarized source. All others are for p-polarization. The angle of incidence is 45^o. The sphere and the plane are made of silver. The point at which $\tilde{I}$ is measured is

located on the rotational symmetry axis at 1Å above the plane surface. The resonance frequency does not depend on the position of the observation point.

The shape of $\tilde{I}(\omega)$ is roughly the same for all values of λ, for p-polarized light. The resonance for the isolated sphere is at 3.49eV while the resonance frequency for the plane-sphere system is well below this value. The presence of the flat surface pushes the resonance downwards.

The curve $\tilde{I}(\omega)$ for a Au sphere on a gold surface looks, at λ=0.05, somewhat different. It has one peak with no shoulder at high frequency. For a SiC sphere and a SiC plane the $\tilde{I}(\omega)$ curve has two pronounced peaks and a shoulder. Therefore the shape of the $\tilde{I}(\omega)$ curves changes from material to material. This is mainly due to the fact that each curve consists of a number of overlapping resonances. For some materials the width of these resonances is small and they can be partly resolved in the excitation spectrum, producing peaks and/or shoulders. For other materials the widths are large and a single, broad feature is present.

(2) The magnitude of $\tilde{I}$ at resonance is extremely large, as seen in Table 2 (for λ=0.05). In Table 7 we give the resonance frequencies and the peak values of $\tilde{I}$ for the Ag-Ag system at various values of λ, for p-polarized light. Note the enormous enhancement of $\tilde{I}$ at small values of λ. The reciprocity theorem[22] implies a Raman enhancement factor of $2 \cdot 10^{10}$, for λ=0.03, for molecules placed between the sphere and the plane. Another interesting feature is the fact that the resonance is not very sharp. For example, for λ=0.03 $\tilde{I} > 2 \times 10^3$ for all frequencies between 2.3eV and 3.2eV. This assures a Raman enhancement factor larger than 4×10^6 in a fairly large range of incident frequencies. It is also interesting to note that even though Au is a rather ineffective enhancer in other configurations, it has a large enhancement in the sphere-plane arrangement. For λ=0.05 and p-polarized light $\tilde{I}$ is

1.4×10^4. Finally, note that the SiC-SiC system has the largest enhancement.

(3) The resonance is localized between the sphere and the plane, in the sense that $\tilde{I}$ has the largest value in that region. We find that the value of $\tilde{I}$ is practically constant along the symmetry axis of the system. When we compute the value of $\tilde{I}$ in the plane of incidence, along the flat surface, we find that it decays very rapidly. Crudely, at 100 Å away from the rotational symmetry axis $\tilde{I}$ is five times smaller than on the axis. If we compute $\tilde{I}$ along the circle formed by the plane of incidence and the sphere we find variations of several orders of magnitude. We exemplify this, by quoting some results for the Ag-Ag system with $\lambda=0.05$, p-polarized light and a beam coming at 45^o from the right. Between the sphere and the plane $\tilde{I}$ is roughly 4×10^4 (Table 2). At 90^o from the normal at the "sunny" side of the sphere $\tilde{I}$ is about 20. At 90^o from the normal in the "shaded" side of the sphere, $\tilde{I}$ is almost zero. The other systems studied have very similar features.

(4) The polarization of light and the direction of incidence are very important. In all our calculations we find a useful prospensity rule: the largest enhancement is obtained if the electric vector of the incident field oscillates in a direction in which the electrons in the material encounter most obstacles. Furthermore, the enhancement is largest between these obstacles. For the sphere-plane case the rule says that the largest enhancement is obtained if the electric field is directed along the rotational symmetry axis of the system. In fact we find numerically that at any given incidence in the p-polarized case, more than 95% of the field is induced by the component of the incident field along this symmetry axis. For gratings the rule says that an incident field perpendicular to the grooves is most effective. Hence, normal incidence with $\vec{E}_i$ perpendicular to the grooves is best, while s-polarized with $\vec{E}$ along the grooves is least effective. This again is confirmed by our calculations.

§130. The overall conclusion provided by these examples is that the interaction between resonances affects strongly all aspects of the primary field enhancement and of the enhanced emission. The excitation spectrum, the magnitude of the enhancement, the spatial distribution of the field, the dependence on polarization, angle of incidence and angle of detection, are all changed. Of course this suggests that there are difficulties when using isolated particle theories to interpret the data on samples with crowded particles.

The interaction between resonances has a number of good features which could be exploited if such systems can be prepared under controlled conditions. The frequency range in which one can obtain a large enhancement is extended by the fact that we can combine pairs of different materials and have different interparticle distances. The enhancement is also larger. Furthermore, it becomes possible to do surface enhanced scattering with materials that are poor enhancers. For example one could trap in a matrix made of molecules A a mixture of Ag spheres and spheres made of another metal M. The interaction between the Ag spheres and the spheres made of M permits us to obtain enhanced spectra of the molecules A adsorbed on M. One can also deposit a matrix of A containing Ag spheres on a flat surface of M. Or even better preadsorb A on a flat surface of M and then trap Ag spheres in a noble gas matrix frozen on the A-M surface.

III.5. Coarse surfaces.

§131. We use the name coarse surface or coarse roughness in those cases when large size (500 – 2000 Å) boulders protrude from or lie on a flat surface. A coarse surface differs from a system of "islands" since the boulders and the flat surface are made of the same materials, while the islands are placed on glass or other similar substrate. It differs from small random roughness because the boulders are fairly isolated and their height is large. It is to some extent similar to a collection of spheres or irregular particles deposited on a flat surface. Clearly the concept of coarse surface is not sharply defined, but we find it useful.

Such surfaces can be prepared electrochemically by anodization, or photochemically[33] by the decomposition of a AgI film located on top of a Ag surface (or by exposure of a Ag surface to laser radiation and I_2 vapors). Condensation of Ag vapors, at room temperature, on an ion-milled silicon substrate achieves the same result.[34]

The theory of SES on realistic coarse surfaces has not yet been developed, but few model calculations aimed at predicting the qualitative behaviour of such systems are available.[31, 106, 107, 115, 157]

§132. Gersten and Nitzan[115] have computed the properties of a prolate half-ellipsoid imbedded in a perfectly conducting semi-infinite, flat material. In their calculation the molecule is located on a line containing the semi-major axis of the half-ellipsoid. The electric field of the incident radiation is parallel to the same line.

The electromagnetic properties of this system resemble closely those of an isolated ellipsoid. (§114-116), for the reasons outlined below. The presence of the perfectly conducting flat surface requires the use of an eigenfunction expansion giving a null potential on the surface. This is guaranteed if we use the expression for the

potential of an isolated ellipsoid (Eqs. (95) and (96), §114) but keep only the terms corresponding to odd values of n. The presence of the perfectly conducting surface has an additional effect: we must consider both the molecular dipole and its image with respect to the perfectly conducting plane. The calculations are substantially simplified by the fact that in SERS we only need the term n=1 in the potential expansion, since we are only interested in the dipole of the system. For this reason the half-ellipsoid calculation gives the same result as that for isolated ellipsoid driven by the molecular dipole and its image with respect to the mid-plane. This happens because the two systems differ mathematically only through the terms n=2, 4, etc., which are negligible in SERS calculations.

We can use, therefore, the isolated ellipsoid results of §114-116 for the present case, if we replace the dipole μ by 2μ.

§133. Aravind and Metiu[31,106,107] have modeled coarse surfaces by using a sphere placed near a semi-infinite plane. This has its own obvious limitations as far as realism is concerned. It does however complement the existing work since it does not assume a perfectly conducting plane surface. Such an assumption might alter the way the existence of the flat surface affects the properties of the sphere. The results obtained with this model are reviewed at III.4.2.

§134. Since both models have been reviewed elsewhere in this article we summarize here the qualitative conclusions supported by both calculations which are, therefore, likely to also characterize a real coarse surface. (1) The enhancement has two sources: the surface curvature and the electromagnetic resonances localized around the "boulder." Since the curvature also affects the properties of the resonance the two effects cannot be strictly separated. However, it is clear that at off resonance frequency an increase in curvature (e.g., an increase in the aspect ratio of the half ellipsoid) increases the enhancement. (2) Different

proturberances have different resonance energies. When we choose an incident frequency ω_i we enhance the field around a few protuberances whose resonance frequency equals ω_i. If we change ω_i we change the protuberances that are resonantly excited. If ω_i exceeds a certain limit no resonant enhancement is possible. As a result of all these the excitation spectrum is broad, unstructured, and has a cut-off at high frequency. The Raman excitation spectrum of the molecules lying on such a surface follows the excitation spectrum of the surface and it must be the same for all molecules, in the frequency range in which normal Raman scattering takes place. (3) Both calculations[106,107,115] indicate that the electromagnetic enhancement has a long spatial range, which is shortened as the size of the "boulders" gets smaller. One might be concerned that the Gersten-Nitzan[115] calculation exaggerates this trend since the presence of the perfectly conducting half space might "push the resonance" and localize it towards the tip of the ellipsoid, forcing the field to extend further in the vacuum than it would in the realistic case when the half space has the same dielectric constant as the boulder. The Aravind-Metiu calculation[106, 107] does not have this difficulty and indeed the presence of the dielectric plane moves the sphere resonance towards it; however, this does not cause a significant decrease of the spatial range of the resonance. This can be seen in Table 8 where we plotted the intensity $\tilde{I} = \vec{E} \cdot \vec{E}^* / \vec{E}_o \cdot \vec{E}_o^*$ as a function of distance from an isolated sphere and from the sphere-plane system. (4) The calculations of Aravind and Metiu[106, 107] indicate that the enhancement is much larger for molecules located between the plane and the sphere. The two sphere calculation of Aravind, Nitzan and Metiu[122] shows that the same is true for the space between two spheres. This suggests that on real coarse surfaces it is likely that the signals from molecules adsorbed in the cracks between boulders, or trapped on the flat surface under boulders, will give higher Raman signals. This might cause some confusion when the data is interpreted since one expects that the first

molecules to be adsorbed might go into these positions and their spectroscopic signals are larger than those of the molecules deposited subsequently. This might lead one to believe that there is some "chemical" mechanism increasing the enhancement for molecules located in the "first monolayer" or on some postulated "active sites."

§135 Since in what follows, we concentrate on UHV experiments and thus ignore a large body of electrochemical work, it is necessary to make few historical remarks to restore balance and a proper perspective. The SERS effect was discovered[177-179] by electrochemists who managed to do almost all the early, ground breaking work. They established that Ag, Cu and Au are good enhancers, that the phenomenon is displayed by a very large number of molecules, that the excitation spectrum and the depolarization ratio are unusual and that roughness plays an important role. In act the electrochemical data motivated Moskovits[157] to propose the first theory of SERS in which the electromagnetic resonances of the rough surface played a crucial role. Finally, it is likely that the most exciting applications of SES might come in electrochemistry for lack of competing probes (EELS and IR reflectance are not possible in a liquid environment) and because electrochemists are not as reticent in using polycrystalline or rough surfaces as their colleagues in surface science.

The early electrochemical work has caused some confusion regarding the role of roughness. The required anodization was very mild and there was the possibility that following it the surface was still flat.[28] No electron microscopy was done and the optical probes used to find whether the surface was flat might be inconclusive. The availability of in situ methods for surface characterization (AES, work functions, UPS, XPS, etc.), clearly give the UHV systems an edge in carrying out experiments designed to test mechanistic assumptions. The recent development of laboratories which can do both (e.g., Van Duyne's at Northwestern) types of work will certainly return electrochemistry to prominence among people interested in the mechanism of SES.

§136. Having now paid a necessary tribute to electrochemistry we can proceed to ignore it in this section and concentrate on the UHV experiments, without excessive feelings of guilt. A paper by Rowe, Shank, Zwemer and Murray[33] opened the current controversy concerning the properties of SERS on coarse surfaces. (a) They found that the enhancement of the Raman intensity for Py on Ag (111), Ag (110), stepped Ag (100) or selectively etched Ag (100) with 2-5 μm facets, must be less than 10^2 (which is the detection limit of their instrument). Scanning electron microscopy shows that these surfaces have shallow ripples of about 150 Å height. (b) A coarse surface was then produced,[34] by exposing a clean Ag (100) face, in UHV, to I_2 vapor and 4880 Å laser radiation. The surface roughness, determined by SEM, consists of particles of spherical shape, of ~500 Å radius, separated by an average distance of 1500—3000 Å. Pyridine was deposited on this surface and the coverage was monitored by AES. The first molecular layer had two Raman modes ω_v=1003 cm^{-1} and ω_v= 1032. The second and succeeding layers had a smaller sticking coefficient (a change from ~0.65 to 0.35) and vibrational frequencies of ω_v= 991 cm^{-1} and 1032 cm^{-1}. This corresponds to the formation of solid pyridine.[33]

If this assignment is accepted the intensity of the 991 cm^{-1} mode gives the enhancement (if any) of the signal from second, third, etc., molecular layers. The data of Rowe et. al.[33] would then indicate that the enhancement extends as far as 50-100 Å from the surface. This discovery came at a time when it was widely believed that only the Raman signals coming from the adsorbed layer were enhanced.[28,180] Since only an electromagnetic mechanism can explain the long range enhancement, the paper[33] caused a large number of people to consider seriously developing the idea that the roughness plays a role through its electromagnetic properties.

§137 The above conclusions were challenged by subsequent work. Van Duyne et.al.[26] have observed large (10^4) enhancements on flat surfaces in an electrochemical environment without anodization. Their work is discussed at §31 . and as explained there, its conclusion is weakened by the fact that the resolution of the SEM photographs is less than 250 Å. It is however strengthened by the fact that the method of preparation of their "flat," single crystal surface is the same as that used by the Bell group[33] to produce surfaces with an enhancement factor of less than one hundred. The work of Hemminger, Ushioda et.al.[32] (See §32) is in general agreement with the conclusion[33] that the enhancement on flat surfaces is about two orders of magnitude. One should keep in mind that absolute intensity calibration is difficult and that in many cases the numbers must be considered as order of magnitude estimates.

§138 The observation that the enhancement is long ranged came also soon under fire.[181, 182] Eesley[181] repeated the experiments of Rowe et. al.[33] but used a polished polycrystalline Ag surface sputtered with Ar^+ in the UHV chamber. SEM photographs show that the surface consists of plateaus of 1000-3000 Å diameter separated by 1-3 μm. The area between plateaus is a flat surface covered with either ~200 Å diameter Ag balls separated by 200-400 Å (between centers) or with ~400 Å balls with a separation of 1000-5000 Å. This is similar to the coarse surface used at Bell.[33] Eesley assumes that the Auger electron spectroscopy used by Rowe et. al.[33] to monitor the coverage is too destructive a probe for a system as weakly bound as pyridine. He prefers to use work function and, in later work[181b] UPS and XPS. He observes essentially the same frequencies as Rowe et.al.[33] The 1032 cm^{-1} lines appear at the lowest dosages while the 990 cm^{-1} appears only at higher dosages. Eesley's interpretation is that <u>all</u> these Raman lines are due to molecules located in the first monolayer and that the 1002 cm^{-1} and 990 cm^{-1} lines correspond to the same mode but for molecules adsorbed at two different sites. The

interpretation is based on the fact that his Raman signal saturates as the work function does, therefore there is only a very weak signal from Py molecules located on top of the first Py layer. The UPS and XPS data[181b] seems to confirm this. Rowe et. al.[34] observe that the 1002 cm^{-1} line saturates when the AES signal indicates the completion of a monolayer and the 991 cm^{-1} appears as the second, third, etc., layer is formed and it does not saturate until many layers are completed. The 1032 cm^{-1} line is present in both experiments from the beginning but its intensity saturates when the work function does (hence when one monolayer is completed) in one experiment[181b] and continues to grow in the other.[33] Unfortunately the surface structures of the two studies are fairly different and this might cause problems in comparing the two experiments. Ideally, all these measurements (i.e., AES, UPS, XPS and Raman) should be done on the same sample.

§139. It is difficult to believe that one can blame the discrepancy between the two experiments on the use of AES for coverage measurements.[33] The measurements of Murray, Allara and Rhinewine[183] give support to the interpretation of Rowe et. al.[34] Using a tunneling junction geometry[60] they[183] put polymeric spacers between the molecules and the rough Ag layer. ASE micrograph indicate that the coarse Ag surface is similar to that of Rowe et. al.[33] and the boulders are of comparable size. Care was taken to make sure that there are no holes in the polymer films that would permit the molecules to reach the Ag surface and that the measurements were finished before the molecules could diffuse through the film to the Ag surface. The conclusion is that the Raman enhancement is long ranged. A possible reconciliation between these opposite conclusions was suggested by Wood et. al.[34] who studied SERS on two surfaces prepared

in the same UHV system. The surface one is prepared either by exposure of the Ag surface to I_2 and laser radiation or by Ag deposition on a ion-milled Si surface. The boulders have dimensions of 100-1000 Å and annealing at room temperature does not change the enhancing properties. Surface two is prepared[184-185] by deposition of Ag vapors on a polished Cu substrate held at 100°K. This surface loses its enhancing properties at room temperature and for this reason SEM cannot be used to establish the magnitude of the boulders. However, the fact that the enhancement properties disappear at room temperature is considered[34] to indicate that the boulders are mobile, hence small, and coalesce at room temperature to form a flat surface.

The Raman enhancement is higher on surface two and has a very short range (~1 monolayer); on surface one the enhancement is long ranged. The coverage is determined in both cases, by AES. These results are consistent with the electromagnetic theory which predicts that small boulders have larger enhancements and much shorter range. It appears that the discrepancy between Easley's results and those obtained at Bell laboratories might be caused by a difference in the size of roughness and that all the results are in qualitative agreement with the electromagnetic theory.

§ 140. Since the situation is still rather confusing it is useful to consider other possible surface roughness probes which can supplement the information obtained through SEM and SERS. One possibility[186, 187] is to use electron beams to excite the electromagnetic resonances of the rough surface and monitor their emission and the electron energy loss. The emission intensity must correlate with the intensity of the enhanced Raman spectrum of molecules deposited on the same surface.

The electron can excite the electromagnetic resonances of any surface, including a flat one. The classical theory is easy to construct.[7, 50] It consists of inserting the current density $\vec{j}(\vec{r}, t) = e\vec{v}\,\delta(\vec{r} - \vec{v}t)$ (here $\vec{v}$ is the velocity of the electron) into Maxwell's equations and solving to compute the electromagnetic polarization fields, in the presence of the surface (e.g., a sphere, an ellipsoid, a grating, small roughness, or flat). One can then compute the energy lost by the electron while interacting with the polarization field. This peaks at frequencies corresponding to the electromagnetic resonance. Since there are no "selection rules" the electron can excite even the surface plasmon of the flat surface and the presence of the excitation can be detected by measuring electron energy loss.[50] In all cases in which the resonance can radiate the excitation is accompanied by photon emission.

Obviously the characteristics of both resonance excitation and photon emission depend critically on the shape of the surface. Some predictions can, however, be made without detailed calculations. For flat surfaces the surface plasmon is excited but it cannot emit. For surfaces with small roughness both excitation and emission are possible. Assuming that the perturbation theory described at §64-66 holds, the electron induced emission intensity $I_e(\delta)$ is proportional to the square of the roughness height δ and the amount of energy transferred from the electrons to the plasmon. The latter is, in first order, independent on the roughness height, therefore the emission intensity $I_e(\delta)$ is quadratic in δ.

If we deposit molecules on such a surface and perform Raman scattering both the emission[34] and the excitation[22] process are proportional to δ^2. The Raman intensity $I_R(\delta)$ is therefore proportional to δ^4. Since δ can be varied experimentally (e.g., by using CaF_2 films and varying their thickness or by increasing the duration of the anodization-reduction cycle) we can monitor whether the ratio $I_R(\delta) / I_e(\delta)$ is linear in δ^2. One should keep in mind that as δ is increased, $I_R(\delta)$ varies like $\delta^4(a^2 + \delta^2)^{-2}$ while $I_e(\delta) \sim \delta^2(a^2 + \delta^2)^{-2}$. The additional factor $(a^2 + \delta^2)^{-1}$ is due to the interaction of the plasmon with the roughness.[67]

The straight line dependence mentioned above is expected only[67] when $\delta << a$. Also, as δ becomes comparable to wavelength the perturbation theory breaks down and the dependence on δ is unknown.

For gratings[57,58] the situation is more interesting, since both the resonance emission and the excitation process take place only at well defined detection and incidence angles, respectively. If both angles are on resonance $I_R(\delta) \sim \delta^4$ and if both are off resonance $I_R(\delta)$ it is independent on δ. The same argument applies to $I_e(\delta)$.

For other geometries (e.g., spheres, sphere-plane system, ellipsoids, large coarse roughness) the dependence on the "roughness size" depends on the type of roughness. In the case of Rayleigh spheres the excitation probability is known[188] and depends on the radius in a complicated manner.

A further qualitative prediction of the electromagnetic theory is that the angular distribution of electron induced surface fluorescence must be similar to that of the Raman intensity, at the same frequencies. The reason for this is that the enhanced emission of Raman photons is mostly performed by electromagnetic resonance driven by the Raman dipole.

§ 141 Recently Eesley[187] carried out such experiments. He worked with an anodized Ag surface. The electron induced emission intensity is corrected for background transition radiation and/or roughness aided bulk plasmon radiation, so that only the surface plasmon emission is retained. Only this is related to the Raman intensity. The analysis of the data, based on perturbation theory,[189] yields a roughness correlation length of 346 Å. Since no SEM measurements were made the type of roughness is not known. The analysis is based on small roughness equations and suggests surface "features" of ~300 Å magnitude. Then molecules were deposited on the surface and their Raman spectrum was taken. The roughness of the surface was varied by increasing the duration of the oxydation-reduction cycle. Plotting $\ln[I_R(\delta)/I_e(\delta)$ for different degrees of anodization Eesley obtained a straight line with a slope equal to 2. Hence the ratio $I_R(\delta)/I_e(\delta)$ is

proportional to δ^2, as predicted by the electromagnetic theory. Note however that the value of the exponent is sensitive to the intensity corrections made to obtain the surface plasmon emission. While there are uncertainties in the interpretation of such measurements, they can provide worthwhile information, if performed in situ to accompany the enhanced Raman experiments.

§142. Another qualitative way of testing the electromagnetic theory is to compare either the excitation spectra of the Raman lines of two co-adsorbed molecules or the excitation spectra of different lines of the same molecule. The enhancement factor is proportional to $|G_s(\omega-\omega_v)|^2 \left|\frac{\partial\alpha}{\delta Q}\right|^2 |R(\omega)|^2$. If there are no "molecular" effects which can make $|\partial\alpha/\partial Q)\delta Q|^2$ frequency dependent, the excitation spectrum depends only on electrodynamic effects through G_s and R. Assume now that we have two molecules on the same surface, and that for both $|\partial\alpha/\partial Q)\,\delta Q|^2$ is frequency independent. The excitation spectra of the Raman signals for the two molecules must therefore have almost the same shape; the only difference comes from the fact that the vibrational frequency ω_v is slightly different for the two molecules. In most cases this difference is too small to matter.

This test cannot be used to rule out molecular effects, but only to demonstrate that chemisorption does not make the polarizability of the molecule frequency dependent, in a frequency range in which the polarizability of the same molecule in liquid or gas phase is known to be frequency independent. The test may give confusing results if the two molecules have a tendency to segregate on the surface and stick to places having different electromagnetic properties.

§143. Such a test has been conducted by Blatchford, Campbell and Creighton.[190] They coadsorbed deuterated pyridine and triphenylphosphine on an anodized Ag surface. This was done by immersing a Ag electrode in a deoxygenated

aqueous solution containing 0.1 M KCl, 0.01 M Py-5D and 2.10^{-5} M triphenylphosphine. The anodization was carried out by varyihg the potential from -100 mV to 200 mV in 30 seconds and then going back to -100 mV. The total charge passes was 300 mC/cu^2. Then the voltage was held at -950 mV and the Raman spectrum was taken. The excitation spectra are consistent with those of earlier work.[1, 2, 191, 192] It is clear that the shape of the excitation spectra are very similar and that, as expected, they can be shifted by changing the anodization conditions (i.e. surface roughness).

§144. In closing this section we mention that we have left out a number of very interesting papers, especially those of Seki et. al.[193] and Pockrand, Otto et. al.[194] This was done due to lack of space, and to our policy of not reviewing the experiments exhaustively but to the minimum extent required by the theoretical discussion.

IV. Is phenomenological electrodynamics valid near the surface?

IV.1 Introductory remarks.

§145. The electromagnetic theory of surface enhanced spectroscopy is based on phenomenological electrodynamics. This is a model which contains certain assumptions whose validity must be re-examined when we are interested in computing electric fields near the surface (e.g., 5-10 Å of each side of the interface) or when the field source (e.g., oscillating dipole) is located in the interface region. The model assumes that (a) the dielectric constant of the solid is constant all the way up to the interface, where it changes discontinuously to take its vacuum value. This assumption implies (through Gauss theorem[11]) that the electric fields at the two sides of the interface must satisfy certain boundary conditions. If we define the interface as the surface region in which the electron density is different from both that of the vacuum and that of the bulk solid, then the thickness of the interface region is of roughly 10 Å and the major variation of the charge density occurs over roughly 3 or 4 Å. If we are concerned with fields or sources at points 20-30 Å away from the interface we should not expect that we will perceive a substantial difference between the sharp interface model and the real situation. If we get closer the situation may change dramatically and we might have to consider a continuous interface model and abandon the boundary conditions.

(b) A second assumption is that the value of the dielectric constant is independent of the type of electromagnetic probe used to measure it. In a sense, to be explained below, this is not true. In the phenomenological model it is postulated that the displacement vector is related to the electric field through the relationship

$$\vec{D}(\vec{r}, t) = \int_{-\infty}^{t} dt' \overleftrightarrow{\epsilon}(t-t') \cdot \vec{E}(\vec{r}, t'). \qquad \text{(IV.1)}$$

The important point is that the displacement at $\vec{r}$ depends only on the field value at $\vec{r}$. For this reason Eq. (1) is sometimes called the "local approximation." Fourier transforming Eq. (1) yields

$$\vec{D}(\vec{k}, \omega) = \overleftrightarrow{\epsilon}(\omega) \cdot \vec{E}(\vec{k}; \omega). \tag{IV.2}$$

The local approximation is equivalent to the statement that the solid responds to all planar waves in the same way as long as they have the same frequency. That is, $\overleftrightarrow{\epsilon}(\omega)$ does not depend on the wave vector. When this is true it is said that the medium does not have spatial dispersion. The words local approximation and lack of spatial dispersion are each other's Fourier transforms.

§146. The microscopic theory[1] indicates† that Eq. (1) is at best an approximation to real situation given by

$$\vec{D}(\vec{r}, t) = \int dt' \int d\vec{r}\,' \overleftrightarrow{\epsilon}(\vec{r} - \vec{r}'; t-t') \cdot \vec{E}(\vec{r}', t') \tag{IV.3}$$

or equivalently

$$\vec{D}(\vec{k}, \omega) = \overleftrightarrow{\epsilon}(\vec{k}, \omega) \cdot \vec{E}(\vec{k}, \omega) \tag{V.4}$$

Thus we would expect the response to be non-local, or equivalently, to have spatial dispersion. If we measure the dielectric response with light, the wave vector is so small compared to the increments of $\vec{k}$ that would cause a change in $\overleftrightarrow{\epsilon}(\vec{k}, \omega)$, that we are practically measuring $\epsilon(\vec{k} = 0, \omega)$. The phenomenological theory uses this measured $\vec{k}=0$ value for all $\vec{k}$-s. The question is if and when this might cause errors.

† To keep things simple in this qualitative discussion we do not distinguish here between longitudinal and transverse response, nor do we take into account the symmetry breaking role of the surface. The calculations, mentioned later, do take these effects into account.

§147. Before proceeding to discuss the impact of non-locality on surface electrodynamics we give some simple examples in which non-locality is crucially important and leads to qualitative physical effects that cannot be explained if the medium is assumed to be local. One example is the scattering of fast electrons passing through a solid film. The probability per unit time that the electron loses the energy $\hbar\omega$ and changes its momentum from $\hbar\vec{k}_i$ to $\hbar\vec{k}_f$ is [1b]

$$P(\vec{q}, \omega) = 8\pi e^2 q^{-2} \operatorname{Im}(\epsilon(\vec{q}, \omega)^{-1}). \tag{IV.5}$$

Here $\hbar\vec{q} = (\vec{k}_f - \vec{k}_i)\hbar$ is the momentum transferred to the sample. If $\epsilon(\vec{q}; \omega)$ is independent of the wave vector, as assumed by the phenomenological theory, the probability of momentum change is proportional to q^{-2}. If all materials were non-local the elastically scattered electrons will have exactly the same angular distribution for all of them. This does not happen and the experiments force us to accept the fact that ϵ does depend on $\vec{k}$.

Another example that illuminates the role of spatial dispersion is the screening of the Coulomb potential in a polarizable medium. Consider a charge e in such a medium, located at $\vec{r} = 0$. Poisson equation gives $\nabla \cdot \vec{D}(\vec{r}, t) = 4\pi r\, \delta(\vec{r})$, where $e\delta(\vec{r})$ is the "free charge" density corresponding to the single change. Using $\vec{E}(\vec{r}) = -\nabla\Phi(\vec{r})$ and Eq. (3) in the Poisson equation, and then Fourier transforming gives

$$k^2 \epsilon(\vec{k}) \Phi(\vec{k}) = 4\pi e. \tag{IV.6}$$

If the medium does not have spatial dispersion, $\epsilon(\vec{k}) = \epsilon_0$ and the Fourier transform of Eq. (6) is $\Phi(\vec{r}) = \dfrac{e}{\epsilon_0 |\vec{r}|}$, which is the Coulomb potential. Assuming now a medium with spatial dispersion and the specific form of the dielectric

constant $\epsilon(\vec{k}) = \epsilon_o(1\pi k_s^2/k^2)$ (Thomas-Fermi) we find that the Fourier transform of Eq. (6) gives

$$\Phi(\vec{r}) = \frac{e}{\epsilon_o|\vec{r}|} e^{-k_s|\vec{r}|} .$$

If $k_s r << 1$ (a distance close to the charge) the potential is $e/(\epsilon_o|\vec{r}|)$, which is the same as in the case of a local medium. If $k_s|\vec{r}|$ is large, the potential in the non-local medium goes to zero rapidly, while in the local medium it goes like $|\vec{r}|^{-1}$. This long distance screening is exclusively caused by the non-locality. The fact that the potential is screened only at distances $|\vec{r}| > k_s^{-1}$ (k_s^{-1} is of order 0.5 Å) is caused by the use of the Thomas-Fermi expression for $\epsilon(\vec{k})$, which is valid for small k only. The high k part of $\epsilon(k)$, where present, screens the potential at smaller distances.

§148. We can now begin to understand why spatial dispersion might be important in surface spectroscopy.[196,197] Consider a dipole oscillating near the surface. The electric field generated by it, and acting on the interface, varies in space much faster than the field of light. In other words, if we represent the dipole field $\vec{E}_{dip}$ as a superposition of planar waves

$$\vec{E}_{dip}(\vec{r}, \omega) = \int \frac{d\vec{k}}{(2\pi)^3} \vec{E}_{dip}(\vec{k}, \omega) e^{i\vec{k}\cdot\vec{r}},$$

then the superposition must contain fields $\vec{E}_{dip}(\vec{k}, \omega)$ with high $\vec{k}$. Otherwise $\vec{E}(\vec{r}, \omega)$ could not vary rapidly with $\vec{r}$. Now, as we have exemplified in §147, the non-local solid responds to each planar wave of given $\vec{k}$ with the dielectric constant $\epsilon(\vec{k}; \omega)$ corresponding to that value of $\vec{k}$. The phenomenological theory uses the same value, namely $\epsilon(\vec{k} \equiv 0; \omega)$, for all values of $\vec{k}$. This, of course, may cause errors. The errors are not expected to be substantial when the dipole is far from the surface and the field acting on the surface is smooth.

Another way of understanding why errors must appear, is to remember that the interaction between the dipole and the metal is given by the Coulomb interaction between the two charges forming the dipole and the electrons in the metal. If spatial dispersion is taken into account this interaction is screened, by the mechanism discussed at §147, and becomes short ranged. This lowers the coupling of the dipole to the metal, thus lowering the ability of the dipole to polarize the latter.

IV.2. Model calculations which consider spatial dispersion and interface continuity.

§148. The discussion in the introductory Section IV.1 was meant to state possible difficulties of the phenomenological model and some reasons for expecting them to be potentially important. To understand how large the errors are one must carry out model calculations which permit the evaluation of the electric fields when the interface is continuous and the medium is non-local as well as when the medium is local and discontinuous. The point is, that the local and non-local dielectric response should be computed by the same model for electronic properties of the material, at the same level of sophistication. The errors made by the local-discontinuous theory can be established by comparing the two sets of numerical results obtained for the fields.

Such a program has been carried out by Maniv, Korzeniewski and Metiu,[45, 46, 196-199] who used a jellium model and computed the response of the electrons to an arbitrary time-dependent electric field by using the Random Phase Approximation.[200-202] A very useful model which ignores the continuity of the interface, but takes into account the non-locality of the dielectric response, (developed by Kliewer and Fuchs) has been recently applied to surface spectroscopy.[47, 48]

The results obtained by the numerical calculations[45,46,196-199] indicate that if the "metal" is driven by a laser and one is interested in the field outside the metal, the Fresnel formulae are resonably accurate. This is not the

case for the fields inside the interface, but these do not concern us in the present article. The phenomenological theory is in error when used for the computation of the field generated by an oscillating dipole located near a metal, if the metal-dipole distance is small.[45-48] The phenomenological theory yields for this problem the image formula, in which the molecule-surface distance dependence is d^{-3} and leads to a divergence when $d \to 0$. In the microscopic calculation[45] this divergence is removed. Furthermore the fields generated by the dipole along the surface can also be radically modified especially when[46] the dipole frequency is above and close to the unretarded surface plasmon frequency (which in the phenomenological theory is given by $\epsilon(\omega) = -1$).

The rate of energy transfer from the dipole to the metal is very much affected by non-locality. At large dipole-metal distances (larger than roughly 10 Å) the local theory works reasonably well. At a diminished distance the rate may become larger than that given by the local theory, because the number of theory considers only the electron-hole pairs having low wave vector while the non-local one considers in addition, those with high $\vec{k}$. Finally when the molecule-surface distance is very small, the rate given by the local theory diverges (like d^{-3}) while the non-local result levels off.[45]

One should keep in mind that these results are themselves approximate. Ag, Cu and Au are not "free electron" metals. Furthermore the RPA method has its own limitations.[195] The model calculations are meant to give a feeling for the trends expected when non-local effects and surface continuity are taken into account.

V. Summary, problems and perspectives.

V.1. Introductory remarks

§149. We have presented in this article a combined body of theoretical and experimental work centered around the idea that non-flat surfaces of certain materials have electromagnetic properties that can alter radically the spectroscopic properties of molecules located nearby. A major question in the field is whether this idea alone is sufficient to explain all the data accumulated so far in surface enhanced spectroscopy. In what follows we attempt to summarize the theories and the facts most pertinent to this question.

§150. For better focus we are going to use SERS as our main example. The enhancement factor is given by (we ignore here all tensor indeces):

$$|G_s(\omega - \omega_v)|^2 \left| \frac{\partial \alpha}{\partial Q} \right|^2 |R(\omega)|^2 \qquad (V.1)$$

This formula has two electromagnetic factors describing the enhancement of the primary field (through R) and that of the emission (through G_s). A third electromagnetic factor, the image field, affects the excited state life-time which does not appear in the Raman enhancement given by Eq. (1), but it is important in other spectroscopic measurements. The molecular effects can appear in Eq. (1) through surface induced changes in the derivative of the polarizability tensor with the normal coordinate amplitude Q. This division into electromagnetic and molecular effects can be carried out, in a similar fashion, for each surface enhanced spectroscopic process, by using the equations presented in Section II.

In examining the adequacy of the electromagnetic theory we must address the following questions:

Q1a. Can we compute the electromagnetic effects accurately for the simplest system that we can hope to prepare in the laboratory?

Q1b. Are the electromagnetic effects computed accurately for the systems currently used in the experimental work?

Q2. Can we compute how large are the molecular effects? Specifically, for Raman scattering, is the value of $\frac{\partial \alpha}{\partial Q}$ for a chemisorbed molecule, altered by chemisorption?

Q3. Is the enhancement mostly electromagnetic, mostly molecular or is it caused jointly by both effects?

Note that according to Eq. (1) the molecular and the electromagnetic effects multiply each other to give the total enhancement. For this reason it is difficult to separate them by examining the data. Furthermore, the detectors commonly used in SERS can measure only those Raman signals from the surface molecules having an enhancement factor between 200 and 1000. We are in the peculiar position of a geographer who lacks underwater equipment but wants to study the mountains on the ocean floor when the depth of water is 1000 meters. This situation can cause confusion, as illustrated below. Assume that we have a surface for which the electromagnetic enhancement is 200 and the detector can pick up the Raman signal from adsorbed molecules if the enhancement is 300. Now assume that the value of $\partial\alpha/\partial Q$ for the molecule bound to the surface equals the gas phase value. For such molecules the enhancement factor is purely electromagnetic, equals 200, and as a consequence the Raman signal of these molecules is not seen. Now let us further assume that we treat the surface in some way (i.e., electrochemically, sputtering, etc.) which creates new "binding sites" on which the value of $\partial\alpha/\partial Q$ is 1.3 times that of the gase phase molecule. The total enhancement jumps to $200 \times (1.3)^2 = 338$ and the Raman signal of the peculiarly bound molecule is detectable. It would be tempting, but misleading, to conclude that chemical effects (i.e., the peculiar binding) are

AD-A114 274 CALIFORNIA UNIV SANTA BARBARA DEPT OF CHEMISTRY F/G 7/4
SURFACE ENHANCED SPECTROSCOPY.(U)
JAN 82 H METIU N00014-81-K-0598
UNCLASSIFIED TR-2 NL

3 OF 3
AD
A114274

END
DATE FILMED
5-82
DTIC

responsible for the enhancement. They represent a factor of 1.69 out of a total of 338 but the molecular effect is, so to speak, the part that gets the mountain "above the water."

V.2 A theoretical discussion of the key questions.

§150. Question Q1a. The accuracy of the electromagnetic calculation is doubtful for several reasons. (1) If the metalic objects (e.g., colloids, bumps on a surface, islands) have sizes comparable to mean free path of the electrons, the imaginary part of the dielectric constant will be increased by electron scattering from surface. This affects the resonant enhancement of both the reflected field and emission, which are each proportional to $(\mathrm{Im}\,\epsilon(\omega))^{-2}$. An increase in the particle size diminishes the relative importance of this effect. (2) If the molecule is within 2-3 Å from the surface the models used here tend to break down. The local dielectric constant, the assumption of sharp boundaries and the use of a Drude-Lorentz model for the molecular response, become questionable (see Section V). While we expect that the reflected field is not strongly affected,[198] the image field will be considerably altered both because of non-local effects[45-48] and the break down of the point dipole approximation.[204-206] This affects those spectroscopic measurements in which the molecular life-time (or level width) is important such as fluorescence, absorption and resonant Raman.

§151. Question Q1b: It is very difficult to prepare in the laboratory those surfaces for which the electromagnetic effects can be accurately (within the limitations discussed at §150) computed. The gratings and the flat surfaces used experimentally might have some small roughness or small "boulders," which may contribute to enhancement as much as or more than the rest of the surface. The colloids coagulate thus making the interpretation of the data questionable. The islands have poorly defined shapes and the surfaces

covered by coarse roughness are plagued by the effects of the interaction between resonances. For these reasons the properties of the electromagnetic fields in the real systems could be rather different than those computed on simple models. In such situations the theory gives, at best, guidance concerning expected qualitative features.

§152. Question Q2: The current status of the quantum theory of chemisorption is such that we do not expect to have reliable calculations giving the change of the optical constants (e.g., frequency dependent polarizability and its derivative with the normal coordinates) caused by chemisorption. Using simple models, with moderate quantitative predictive power, the theorists have proposed a variety of interesting and imaginative mechanisms[142, 207-214] by which the metal can enhance the polarizability of the adsorbed molecule. These are surveyed below.

(1) It has been suggested[142] that chemisorption might create new excited states or shift the existing ones into the frequency region where surface spectroscopy is done. In such cases the experimentalist will observe, unknowingly, a resonant Raman signal and confuse it with a surface enhanced signal. Such confusion is likely since the usual features of the resonant Raman spectrum are altered by the presence of the surface.[142]

(2) It is conceivable that[209, 210] the incident photons might excite the electrons of the metal into a joint molecule-metal state, formed by the interaction between an empty metal state and an empty molecular state. Then, they might emit a photon by going into a vibrationally excited electronic ground state. This is a resonant Raman process which takes place by exciting a ground state band into a discrete excited state. The width of the excited state is large due to the coupling of the molecular state to the continuum formed by the empty states of the solid,[215] and to the image field effects.[142] This

diminishes the resonant enhancement. Furthermore, it is not known whether such transitions have appreciable oscillator strength to give a sizable resonant Raman signal.

Recent detection, by electron loss spectroscopy, of new electronic excitations for benzene, pyridine and pyrazine on Ag[216] suggests that the possibilities outlined at (1) and (2) might be important for such systems.

(3) The process of polarization of the molecule consists of charge displacements caused by the molecular electrons following the oscillating electric field of light. For chemisorbed molecules it is possible that, as the molecular electrons follow the laser, some electronic charge is transferred back and forth between the metal and the molecule.[208] This charge transfer contributes to the polarizability of the chemisorbed molecule,[208] and therefore affects the Raman cross section.

(4) Raman scattering is an electronic process in the sense that the light drives the electrons which absorb a photon and then emit it with simultaneous excitation of a molecular vibration. Therefore, any electron which is capable of interacting with the light and the molecular nuclei can participate in the Raman process. Of particular interest in this respect are the electrons of the metal located near the molecule.[207] An equivalent way of describing this process, which can be turned into a computational method,[207] is that a photon of energy $\hbar\omega$ excites an electron-hole pair in the metal, then the electron (or the hole) "collides" with and excites the molecular nuclei (transferring to them the energy $\hbar\omega_v$) and then recombines with the hole (or the electron) by emitting a photon of frequency $\omega - \omega_v$. This participation of the metal electrons to the Raman scattering process increases the Raman cross section.

The computational methods available for the study of the processes described above are not very accurate. Nor do the qualitative results

contain striking features that can be searched for in experiments. For these reasons, in spite of rather imaginative arguments, the question of the magnitude of the molecular effects in surface enhanced spectroscopy has not been settled theoretically.

§153. Question Q3: The answers provided to the questions raised above indicate why the issue of molecular versus electromagnetic enhancement is so complicated. Since we cannot compute the molecular effects directly, we need to find their magnitude by combined use of experiment and theory. We must fit the experimental measurements to a theoretical model in which the electromagnetic factors are computed exactly and the molecular factors are taken as variable parameters. We can find then, in principle, whether the value of the molecular factors which fits the experiment is substantially different from the gas phase values.

Unfortunately, as we have already stated, the electromagnetic calculations are not yet able to achieve the required accuracy, for the systems on which experiments are currently being carried out. As a result, we have to sort things out by a qualitative analysis of a large number of "imperfect" experiments based on a large number of "imperfect" theories. This process resembles a trial by jury in which the decision is not reached by absolute proof but by sifting through a large mass of circumstantial evidence; no item is sufficient by itself, but it may be an important part of the whole story.

V.3 Experiments which are hard to reconcile with a purely electromagnetic theory

§154. We have collected in this section several experiments which are difficult to understand, even qualitatively, in terms of the electromagnetic theory. Our selection is somewhat arbitrary. In choosing the examples we have kept in mind that many measurements that have not been reproduced by others might be experimental artifacts. Furthermore, effects that have not been broadly tested, might appear only for certain molecules on certain systems under certain surface preparation and conditions. As such, they lack a broad mechanistic significance. Even under these circumstances there are some arresting facts which are presented below.

SERS on mercury: Naaman, Buelow, Chesnowsky and Herschbach[217] have observed the surface enhanced Raman spectrum of Pyridine, Benzene, Cyclohexane, CCl_4 and CH_3OH adsorbed on a mercury droplet. An enhancement of 10^4- 10^6 was obtained whether the droplet was in contact with the gas phase molecules ($p = 10^{-3}$ torr) or immersed in neat liquid. The droplet size is too large to give a substantial enhancement by the electromagnetic mechanism discussed in Section III.3.2. Furthermore, it is difficult to conjure up some other form of roughness that can cause electromagnetic effects. The obvious candidate would be thermally excited Rayleigh waves which would cause a small roughness on the surface. However, the enhancement of the local field (through R) and emission (through G_s) are each proportional to the mean amplitude, δ, squared.[94] The enhancement is then proportional to δ^4, and because the amplitude of the Rayleigh waves that can be excited at room temperature is very small ($\delta \sim 10$-30 Å), the electromagnetic enhancement from these waves must be very small; smaller, in fact, than that for a Ag grating of the same amplitude. Detailed calculations[218] confirm this prediction. Therefore, this experiment seems to provide a clear example of a sizable non-electromagnetic enhancement.

Unfortunately the evidence that the measured signal is caused by the surface molecules is not very strong. The Raman signal is proportional to the surface area but so is the amount of light reflected by droplet, which then passes through the gaseous molecules contributing to the observed Raman signal. In view of its singular importance, this experiment should be carefully repeated. This is done now at Exxon research laboratory.[219] Early attempts have failed to detect the enhancement but this is not considered a definitive result.[219]

Developments subsequent to Naaman et.al.[217] experiment are instructive. Sanchez, Birke and Lombardi[220] have communicated that the SERS spectrum of pyridine on a mercury film deposited on a Pt electrode is substantially enhanced. They carried out the customary test of deciding whether the Raman signal obtained from an electrochemical cell is due to SERS or to bulk scattering: they varied the potential and noticed that the intensity of the pyridine Raman line varied. Normally the change of intensity with the potential is caused by the change in Py concentration near the electrode and it does affect the Raman scattering by surface molecules and not that from the bulk ones.

Subsequently it was discovered[221,222] that the presumed pyridine Raman lines were in fact plasma emission lines from the laser, which somehow were not eliminated by the filter placed between the laser and the cell and were scattered by the Hg electrode into the detector. Their intensity varied with the electrod potential because of changes in surface reflectance, caused by formation of mercurous cloride. It is not known whether the experiment of Naaman et. al.[217] has been affected by similar artifacts, nor is it widely accepted that surface rather than gulk signals were detected. If the results[217] are confirmed, there is not electromagnetic explanation for them and molecular effects ought to be invoked as the cause of a very large enhancement.

§155. The mysterious behavior of water: The fact that the Raman spectrum of water has never been observed in early electrochemical experiments is rather puzzling. Even though water is a poorer Raman scatterer than pyridine, it is much more abundant near the electrode. If the enhancement mechanism is purely electromagnetic, then water would be exposed to the same local field as pyridine and its emission will be enhanced like that of pyridine. The fact that the gas phase value of $\partial\alpha/\partial Q$ is much smaller for water than for pyridine, is partly compensated by higher water concentration at the surface. So, when the enhancement factor for pyridine is 10^6 that of water must be well above the detection limit if the enhancement is entirely due to electromagnetic effects. Since no water signal was observed one can infer that there are substantial molecular effects in the enhancement factor for pyridine. Let us denote by A_s the value of $(\partial\alpha/\partial Q)\,\delta Q$ for pyridine at the surface, and by A_g the same quantity for liquid pyridine. The equation $A_s = R_p A_g$ defines a molecular enhancement factor R_p for pyridine. Furthermore, we denote the corresponding quantities for water by B_s, B_g and R_w, respectively. The enhancement factors for the two molecules are proportional to $E_p \equiv |G_s(\omega - \omega_v^p)|^2\ |R_p|^2\ |R(\omega)|^2$, for pyridine, and to $E_w \equiv |G_s(\omega-\omega_v^w)|^2\ |R_w|^2\ |R(\omega)|^2$ for water. Here ω_v^p and ω_v^w are the ring breathing vibrational frequency of Py ($\sim$1000 cm^{-1}) and the symmetric OH stretch ν_1 for water ($\sim$3200 cm^{-1}), respectively. If we assume that the pyridine spectrum for a monolayer is observable only if the enhancement factor is 200 (this is a fairly representative figure for many experiments) then the spectrum of a monolayer of water becomes observable if the enhancement factor is 2000. We arrived at this figure by using the fact[223] that the ratio $|A_g^p|/A_g^w|^2$ for the ring breathing mode of pyridine and the symmetric stretch of water is about 10. Since no water has been observed we must conclude that $E_w \leq 10^3$.

If we take[26] for the enhancement factor of the pyridine a value of 10^6, we must have

$$(E_p/E_w) = \frac{|G_s(\omega - \omega_v^p)|^2 \; {}^2R_p^2}{|G_s(\omega - \omega_v^w|^2 \; R_w^2} \leq 10^3 .$$

The emission enhancements G_s for the two molecules differ because they have different emission frequencies (corresponding to different vibrational frequencies). Because of this, the factors $(\omega - \omega_v)^4$ and the electromagnetic response of the surface, both present in G_s, differ. Since the experiments did not vary the incident frequency and the surface i; very coarse and poorly defined, we do not know $|G_s(\omega - \omega_v^p)|^2 \; |G_s(\omega - \omega_v^w)|^2$, but we take it to be 10. This gives $|R_p| / |R_w| = 10$. Assuming that the Raman polarizability of the water is not affected by the presecne of the surface we get a molecular enhancement factor R_p for pyridine equal to 10. This is quite a large molecular enhancement, and we obtained it by using assumptions which tend to give a low value.

One way of rationalizing the data in terms of an electromagnetic model is to postulate that (1) the surface roughness consists of small boulders (~200 Å) which give a short range electromagnetic enhancement and that (2) somehow the water is prevented by the pyridine and the ions from coming in contact with the surface. A simpler explanation may be that in most cases the surface enhanced Raman spectrum of water is obscured by the presence of a large bulk water signal.

§156. Very recently Fleischmann et. al.[224] and Pettinger, Philpott and Gordon[223, 225] have shown that the surface enhanced spectrum of water can be observed from an aqueous solution having a high electrolyte concentration (10M NaBr). The surface is anodised and the voltage is maintained[223, 225] at -0.3V with respect to Ag/AgCl. A Raman signal is observed at 3520 cm^{-1}

and this has been assigned to the symmetric stretch of water. This is considerably shifted with respect to the ν_1 mode of water in electrolyte solution, which appears at 3222 cm^{-1}. There seems to be a correlation between the 3520 cm^{-1} and that corresponding to Ag-Cl vibrations: they disappear together when the voltage is changed. Unfortunately these experiments did not have any pyridine in solution and the kind of discussion made earlier, which calibrates the enhancement of water with respect to that of the pyridine, cannot be made. It is difficult to understand the apparent need for the high electrolyte concentration in terms of a purely electromagnetic theory. One might state that perhaps under these conditions some peculiar surface shape and perhaps dielectric property is achieved.

§157. Unpublished work from Richard Chang laboratory[226] added some new information to the puzzle. He has the advantage of using an optical multichannel analyzer[219,220] which is capable of taking a Raman spectrum (over a 400 cm^{-1} range) in 25 msec. This is an excellent system for electrochemical studies since it permits the study of the change in Raman spectrum in time, as the oxydation-reduction cycle takes place. Such spectra are displayed in Figure 30b together with the voltamogram (Fig. 30a). The oxydation-reduction cycle starts at -0.76V and the voltage is varied towards positive values. When the voltage becomes zero a negative current appears, signaling the transformation of the Ag surface into AgCl. At negative voltages the Raman spectrum shows a very broad peak which corresponds to the symmetric stretch of water in the 1M KCl electrolyte solution. This happens because the Ag electrode is located at 5 mm from the optical window through which the spectrum is taken. At 0.18V the bulk water spectrum disappears, presumably because the reflectance of the surface is very small and its mirror effect is removed. As the voltage changes back towards zero, positive current flows and at V = -0.2 all the AgCl is reduced

to Ag. At V = -0.16 the bulk water spectrum reappears and at slightly higher voltage a peak, attributed to surface enhanced Raman signal from the ν_1 symmetric stretch of water, appears. As the voltage is changed to more negative values the peak disappears. This is quite strange since the voltamogram shows no discernible physical or chemical surface change.

Existing UHV experiments[210] indicate that oxydised Ag reacts with H_2O forming OH groups on the surface. The spectrum presented in Fig. 30(c) shows the bending modes of the water, which indicates that at least some of the water molecules are intact.

The SER spectrum of a mixture of 50% H_2O and 50% D_2O in 1M electrolyte solution is shown in Fig. 31. This shows the ν_1 stretch in D_2O (Fig. 31(b)) and the bending modes (Fig. 31(c)). It is not clear why the ν_1 stretch is doubled in the isotopic mixture and it is absent in the electrolyte-water system shown in Fig. (30)

Chang[226] has also informed us that the water spectrum does not appear if the electrolyte is 1M KF, but it does appear for 1M solutions of KCl, KBr and KI. Furthermore if the concentration of electrolyte is 0.5M the H_2O SER lines are not detectable.

It is rather difficult to interpret these results (i.e., disappearance of the spectrum at negative voltages, the special properties of KF and the need for high electrolyte concentration) in terms of an electromagnetic theory. Our understanding of this system will be very much aided by addition of pyridine to the system and by a comparison of the pyridine and water spectra as explained in §155. R. Chang is in process of carrying out such experiments. It will also be extremely useful to have electron microscope studies of the surface shape at various voltages. Finally, one would like to transfer, without contamination,[230-232] the electrochemical surfaces in a UHV

instrument and study their surface composition (by standard UHV methods) and their SERS properties. One would like to know whether the liquid-solid interface at specified voltages is optically different from the surfaces commonly used in UHV systems.

In the absence of such information one could only speculate whether an electromagnetic explanation for the facts mentioned above might be found. One possibility is to invoke orientational effects and spatial competition. As is well known[23, 24] there is a propensity, even at optical frequencies, for the electric field vector to be perpendicular to the solid surface. Imagine now a molecule like pyridine which can bind to the metal through the nitrogen, or edgewise, or lie flat[225] according to the bulk concentration[225] and perhaps voltage. Since the Raman signal depends on the dot product between the polarizability of the molecule and the local field (through $\delta Q \frac{\partial}{\partial Q} (\vec{\alpha} \cdot \vec{E})$), the orientation of the molecule is important especially for molecules like pyridine for which the polarizability tensor is very anisotropic. If the cycle is perpendicular to the surface, the signal is much larger than if the molecules lie flat on it. Change in voltage may cause change in orientation, which in turn cause "strange" intensity evolution. Note that in systems with low enhancement (10^3 - 10^4) and poor detector sensitivity, the signal may disappear if the orientational effects lower the cross-section by an order of magnitude. Furthermore on surfaces whose roughness consists of small boulders the spatial range of the enhancement is short and voltage changes can cause changes in the composition of the one or two layers near the surface, which result in large Raman intensity changes. This might explain why the ion concentration and the size of the ion might play a role within the framework of an electromagnetic theory. Note that orientational effects differ for different modes and this might explain unusual relative mode intensities.

§158. Other potentially disturbing facts. (a) Chang, et.al.[227,228] have noticed (for pyridine on Ag) that in the process of anodization, the SERS signal for the 1008 cm^{-1} and 1036 cm^{-1} modes appear much earlier than the 1214 cm^{-1} and the 1595 cm^{-1} ones. The electromagnetic theory requires that (in the absence of very peculiar orientational effects) all modes should be enhanced at the same time (i.e., at the same potential or the same surface structure). It may be that the missing modes are enhanced but their intensity is lower than the detection limit and they appear only upon the completion of the anodization. (b) We have already discussed (Section III.1) in detail the controversy over the ability of flat silver surface to produce large enhancement. If the statement[26] that flat Ag surfaces produce a 10^4 enhancement of the pyridine Raman spectrum is confirmed (doubts are caused by the possibility[26] that surface features of less than 250 Å might be present and cause the enhancement) this will clearly prove that the electromagnetic enhancement provides only a factor of 100. (c) Finally, there is a great body of work which has gathered arguments in favor of the hypothesis that single Ag atoms protruding from the flat surface, or some other "active sites," are essential to SERS. Since this area has been reviewed by Otto,[5,6] who is the proponent of the theory and the leader of the movement, we do not review it here. The idea is interesting, but still controversial and we are not yet in a position to accept or reject it.

V.4. Concluding impressions.

§159. In spite of all the difficulties mentioned throughout this section, there is no doubt that the electromagnetic effects play an important role. If one avoids getting too engulfed in details and one tries to take a broad view of the field, then the mass of circumstantial evidence provided by the experimental confirmation of many of the qualitative predictions of the theory, for

a great variety of surface shapes and spectroscopic techniques, is very impressive. What is not yet clear is whether the electromagnetic effects provide most of the enhancement. Furthermore, as so often happens in chemistry, one is never secure in making broad, general statements. It is quite conceivable that certain types of molecules have their polarizability radically altered by peculiar modes of binding to specific metals, while others could care less that the metal is present. For this reason the theoretical ideas must be tested against a rich data base, in which such peculiar behavior would stand out isolated, and be identifiable. Such a data base is not yet available.

Acknowledgement: I am very grateful to the National Science Foundation and the Office of Naval Research for support. I have had numerous and useful discussions and/or correspondence on the topics described here with Richard Chang, Richard Van Duyne, Bruno Pettinger, Andreas Otto, Alan Compion, Bill Webber, John Kirtley, Mike Philpott, Joe Demuch, Phaedon Avouris, Martin Moskovits, Jack Rowe, Cherry Murray, Abe Nitzan, Alan Creighton, David Weitz, Azi Genack, Ron Birke, Milton Kerker, Ivan Pockrand, Phil Platzman, Eli Burstein, Paul Liao and many others. I am grateful for their patience, friendliness and willingness to instruct me. I have benefitted enormously from working, for two summers, in the Surface Science Division of the National Bureau of Standards. The competence and the hospitality of my NBS colleagues affected me deeply. Finally, at Santa Barbara, I benefitted from interesting discussions and the stimulating atmosphere created by my colleagues P.K. Hansma, A. Adams, R. Schrieffer, R. Kohn, D. Scalapino, A. Hubbard, R. Martin, S. Efrima, T. Maniv, P.K. Aravind and R. Petschek.

Table 1. The dependence of the resonance frequency ω_{res}, amplification factor $\tilde{I}$ and spatial extent factors ξ_1 and ξ_2 on the geometric parameter $\lambda = D/R_o$. The system studied in the table is a perfectly conducting sphere on a SiC plane surface. The incident laser beam is p-polarized. Reproduced from Ref. [31].

λ	ω_{res}	$\tilde{I}_{res}$	$\xi_2 x10^{-2}$ Å	$\xi_1 x10^{-2}$ Å
.5	944	$5.1x10$	4.80	1.53
.3	941	$2.4x10^2$	3.80	1.55
.2	937	$8.83x10^2$	3.30	1.50
.1	928	$7.37x10^3$	3.08	1.46
.05	916	$5.00x10^4$	3.25	1.45
	935	$1.1x10^4$		
.03	905	$1.8x10^5$	3.20	1.44
	930	$5.2x10^4$		
.01	878	$1.8x10^6$	2.41	1.35
	911	$1.13x10^6$		
	925	$4.4x10^5$		

Table 2. Few representative values of resonance frequencies ω_{res}, amplification factor $\tilde{I}_{res}$ and spatial extent of the resonance characterized by ξ_1 and ξ_2. The geometrical parameter $\lambda = D/R_o$ is fixed at a value of .05. The method of calculation of these quantities and their precise definition is discussed in the text. Reproduced from Ref. [31].

Plane	Sphere	Polarization	ω_{res}	$\tilde{I}_{res}$	$\xi_2 \times 10^{-2}$ Å	$\xi_1 \times 10^{-2}$ Å
Ag	p.c.(1)	p	3.27 eV	8.6×10^3	2.47	1.20
"	"	s	3.50 eV	8.2×10	≥5.00	0.59
SiC(2)	p.c.	p	916 cm^{-1} 935 cm^{-1}	5.0×10^4 1.1×10^4	3.25	1.45
"	"	s	930 cm^{-1} 939 cm^{-1}	6.0×10^2 6.8×10^2	≥5.00	0.79
InSb(3)	p.c.	p	931 cm^{-1}	1.76×10^4	2.51	1.24
"	"	s	962 cm^{-1}	1.16×10^2	≥5.00	0.67
Org. film	p.c.	p	2.27 eV	2.6×10^2	2.50	0.94
"	"	s	2.28 eV	1		
Ag	Ag	p	2.73 eV 3.17 eV	4.2×10^4 1.3×10^4	5.12	1.53
"	"	s	3.33 eV	1.35×10^2	1.40	0.35
SiC	SiC	p	882 cm^{-1} 913 cm^{-1} 925 cm^{-1}	1.41×10^5 9.56×10^4 4.08×10^4	4.21	1.73
"	"	s	902 cm^{-1} 920 cm^{-1} 928 cm^{-1}	3.4×10^2 1.86×10^3 2.01×10^3	1.01	0.64
Au	Au	p	2.2 eV 3.1 eV	1.4×10^4 5.6×10	3.40	1.33
"	"	s	2.2 eV	3		

(1) p.c. = perfect conductor, characterized by $|\varepsilon(\omega)| \to \infty$

(2) If more than one entry is shown for ω_{res} (as for SiC), each corresponds to a local maximum of $\tilde{I}_{res}$. Thus, multiple entries are indicative of structure in the resonance spectrum.

(3) InSb is doped to have the electron concentration corresponding to the bulk plasma frequency $\omega_p = 1023\ cm^{-1}$.

Table 3. Resonance frequencies ω_n (from Eq. (92)) and $[\mathrm{Im}\epsilon_1(\omega_n)]^{-1}$ for Ag and Au. Dielectric constants from H. J. Haggmann, W. Gudat and C. Kunz, DESY SR-7417.

	Silver				Gold			
	$\xi_2 = 1$		$\xi_2 = 1.5$		$\xi_2 = 1$		$\xi_2 = 1.5$	
n	ω_n(eV)	$[\mathrm{Im}\epsilon(\omega_n)]^{-1}$	ω_n(eV)	$[\mathrm{Im}\epsilon(\omega_n)]^{-1}$	ω_n(eV)	$[\mathrm{Im}\epsilon(\omega_n)]^{-1}$	ω_n(eV)	$[\mathrm{Im}\epsilon(\omega_n)]^{-1}$
1	3.48	1.61	3.3	1.25	2.51	.26	2.41	0.36
2	3.56	1.82	3.45	1.53	2.56	.23	2.49	0.27
3	3.58	1.85	3.48	1.61	2.58	.22	2.51	0.25
4	3.60	1.92	3.51	1.69	2.585	.22	2.53	0.24
5	3.605	1.92	3.52	1.69				
6	3.61	1.92	3.53	1.72				
n=	3.61	1.92	3.54	1.75	2.585	.22	2.53	0.24

Table 4. Dependence of SERS intensity on molecule-sphere distance d. The radius of the sphere is a.

a = 300 Å		a = 400 Å	
d(Å)	$(a/(a+d)^{12}$	d(Å)	$(a/(a+d)^{12}$
10	0.67	10	.74
20	0.46	20	.56
30	0.32	30	.42

Table 5. A comparison between the measured Raman intensity for a citrate ion adsorbed on silver sols and the results of an isolated Rayleigh sphere computation. From Ref. [125].

Wavelength (nm)	Measured enhancement	Calculated enhancement for various radii (nm)				
		20	30	40	50	60
350.7	3.1×10^{3}	3.5×10^{2}	2.1×10^{2}	7.6×10^{1}	5.4×10^{1}	4.7×10^{1}
406.7	3.1×10^{4}	5.2×10^{4}	2.4×10^{4}	1.9×10^{3}	5.6×10^{2}	8.8×10^{2}
457.9	3.2×10^{5}	1.7×10^{3}	4.2×10^{3}	4.8×10^{3}	1.2×10^{3}	$2/8 \times 10^{2}$
514.5	3.6×10^{5}	5.6×10^{2}	1.0×10^{3}	1.8×10^{3}	1.7×10^{3}	6.1×10^{2}
647.1	6.0×10^{5}	2.1×10^{2}	2.8×10^{2}	4.1×10^{2}	6.0×10^{2}	7.4×10^{2}

Table 6. The contribution of various multipoles to the molecular lifetime. The radius is a = 300 Å. The molecule surface d is varied. n is the order of the resonance. $I_n = (n+1)\ (2n+1)n^{-1}[a/(a+d)]^{2n+1}(a+d)^{-3}$.

	d = 1Å	d = 10Å	d = 50Å	d = 100Å	d = 150Å
n	$I_n x10^7$	$I_n x10^7$	$I_n 10^7$	$I_n x10^7$	$I_n x10^7$
1	4.35	4.	1.76	0.79	0.39
2	8.	6.	2.42	0.83	0.32
3	13.	10.	2.96	0.78	0.24
4	20.	14.	3.27	0.66	0.16
5	28.	19.	3.38	0.52	0.1
10	87.	42.8	2.32	$0.94x10^{-1}$	$0.59x10^{-1}$
50	$13.x10^{+2}$	64.2	$2.12x10^{-4}$		
100	--	9.44			
200		$5.32x10^{-2}$			
1000	$9.4x10^{+2}$				
2000	5.				
5000	$6.4x10^{-8}$				

Table 7. The two resonance frequencies and the corresponding local intensities in the region between a Ag sphere and a Ag half-plane, as a function of $\lambda = D/R_o$. p-polarized light, $\theta = 45^o$.

λ	ω_1(eV)	$\tilde{I}_1$	ω_2 (eV)	$\tilde{I}_2$
0.03	2.5	1.4×10^5	3.05	5.0×10^4
0.05	2.73	4.2×10^4	3.17	1.3×10^4
0.10	3.0	7.9×10^3	-	
0.20	3.2	1.3×10^3	-	

Table 8. Distance dependence of the enhancement factor of the local laser intensity ($\vec{E} \cdot \vec{E}^* / \vec{E}_o^* \vec{E}_o^*$) for an isolated sphere and a sphere-plane system. The incident laser electric field is at 45° with respect to the normal to the flat surface. The distance is measured along the normal, away from the surface of the sphere and the plane. The isolated sphere calculation is done with the same program by taking the dielectric constant of the half-space to be equal to that of the vacuum.

Distance Å	1.	20.	40.	60.	80.	100.	120.
Sphere	66.	23.	10.	5.	3.	2.	1.7
Sphere-Plane	50.	23.	12.	8.	5.6	4.3	3.5

Figure Captions:

Fig. 1. Geometric characteristics of a grating and the choice of the coordinate system. The grating wave-length L is the distance between two consecutive maxima. ϕ (not shown) is the azimuthal angle.

Fig. 2. The reflectivity of p and s-polarized light scattered from a grating (full lines) and the Raman intensity (dotted lines) of the 1000 cm^{-1} line of a polystyrene film deposited on the grating, as a function of the polar angle of incidence. The azimuthal angle $\phi=0$. The reflectivity and the Raman intensity for s-polarized incident light does not depend on the polar angle. Reproduced from Ref. 61.

Fig. 3. The emission intensity from a dipole located above a Ag grating. The azimuthal angle of detection is fixed at $\phi=10^{o}$ and the polar angle of detection is varied. Various curves correspond to different emission frequencies. Note the existence of double peaks for the lower frequencies. Reproduced from Ref. [50].

Fig. 4. The emission intensity for a dipole located near a silver grating. The emission frequency is held at 2.4 eV and the polar angle of detection is varied. Different curves correspond to different azimuthal angles of detection. When $\phi=90^{o}$ the detection plane is perpendicular to the troughs of the grating. Reproduced from Ref. [50].

Fig. 5. Various detection-excitation schemes for studying fluorescence with the aid of an ATR prism, or a grating or both. Various possibilities are discussed in the text.

Fig. 6. Surface plasmon emission produced by exciting the molecules in the configuration (5a) and detecting plasmon emission in direction 6 (Fig. 5a). The plot gives the intensity as a function of the molecule-surface distance d (see Fig. (5a) for definition). The intensity is different if the dipole is perpendicular or parallel to the surface. The dotted line is an average emission for random orientation. Reproduced from Ref. [75].

Fig. 7. Fluorescence intensity (the area under the fluorescence peak) for various molecule-metal distances. (a) Ag with the excitation-detection scheme I (see text). (b) Ag with the excitation-detection scheme II (see text). (c) Au with the excitation detection scheme I. The excitation frequency $\lambda_o = 457.9\,\text{nm}$. The points are experimental data from Ref. 78. The full line is the theory of Ref. 75 as applied by Dr. Ivar Pockrand (private communication).

Fig. 8. A surface with small random roughness. The figure defines the mean surface plane (full, horizontal line) and the choice of coordinate system.

Fig. 9. $I_{flat} \equiv I_o$ is the intensity radiated by the dipole in the presence of the flat surface. I_{rough} is the difference between the emission for rough and that for a flat surface. The parameters are: the mean amplitude $\delta = 30\,\text{Å}$, the angle of detection from normal is $\theta = 45^o$; the metal is silver. The curves correspond to three different correlation lengths a. The arrow indicates the position of the unretarded plasmon frequency. Reproduced from Ref. [94].

Fig. 10. The quantities b and b_F are the rates of energy transfer from a dipole to a surface with small roughness and a flat surface, respectively. The mean height of the roughness is $\delta = 20$ Å and the correlation length is $a = 60$ Å. The metal is Ag, and the surface plasmon frequency is 3.63 eV. The distance to the mean surface is d. Reproduced from Ref. [49].

Fig. 11. Extinction, far-field scattering, absorption efficiency and near field intensity for spheres of 22 nm radius, immersed in water. (a) Ag; (b) Cu; (c) Au. From Ref. [113].

Fig. 12. Absorption spectrum of 500:1 diluted silver sol with adsorbed citrate (full line). The best theoretical extinction ht, normalized to give a peak intensity equal to the measured one (dotted line). From Ref. [125].

Fig. 13. Extinction, far-field scattering, absorption efficiency and the near field intensity, for spheres of 100 nm radius, immersed in water. (a) Ag; (b) Cu; (c) Au. From Ref. [113].

Fig. 14. The enhancement factor for the dipole-sphere-laser configuration described in the text. The Raman band is at 1010 cm^{-1} and the material is Ag. (a) The dependence on the incident wavelength (for fixed radii). (b) The dependence on the dipole-sphere distance (for fixed radii). (c) The dependence on the radius (for fixed incident wavelengths). Reproduced from Ref. [137].

Fig. 15. Fluorescence spectra of three different micro-spheres of 9.92 μm diameter, suspended in water. The incident wavelength is 457.9 nm. The emission spectrum in the range from 454 nm to 565 nm shows spikes due to the electromagnetic resonances of the sphere. From Ref. [149].

Fig. 16. The energy of the electromagnetic resonance of Ag, Cu, and Au as a function of the aspect ratio a/b of the spheroid. From Ref. [115].

Fig. 17 (a). Enhancement ratio for a molecule adsorbed on Ag versus photon energy in the neighborhood of the surface plasmon resonance. Here a = 500 Å, b = 100 Å, H = 5 Å, and $\alpha = 10\,\text{Å}^3$. (b) Same, for Au and Cu. From Ref. [115].

Fig. 18. Enhancement factor, R, as a function of molecule-surface distance H for three sets of (a, b) values: 1: (500, 250) Å; 2: (500, 100) Å; 3: (500, 50) Å; 4: (500, 500) Å. Here $\hbar\omega = 2.50$ eV and $\alpha = 10\,\text{Å}^3$. From Ref. [115].

Fig. 19. Enhancement ratio of Ag versus distance from surface for several photon energies. Here a = 500 Å and b = 250 Å; and $\alpha = 10\,\text{Å}^3$. Note the fairly slow fall off with distance. The labels a-f refer to photon energies of 2.01, 2.26, 2.50, 2.75, 3.00, and 3.25 eV respectively. From Ref. [108].

Fig. 20. Enhancement of 1010 cm^{-1} Raman line vs. excitation wavelength (in vacuum) for a monolayer adsorbed on randomly oriented silver prolate spheroids in water for various axial ratios (a/b). From Ref. [155].

Fig. 21. Same as Fig. 20 for gold. From Ref. [155].

Fig. 22. Same as Fig. 20 for copper. From Ref. [155].

Fig. 23. Same as Fib. 20, for oblate spheroids. From Ref. [155].

Fig. 24. Dependence of the Raman signal on the aspect ratio of the silver ellipsoids. The normalized Raman intensity of the CN (2144 cm^{-1}) vibration in nitrogen is shown as a function of incident photon energy. (a) 3:1 aspect ratio ellipsoids (Fig. 1). (b) 2:1 aspect ratio ellipsoids. From Ref. [162].

Fig. 25. The 2-sphere system. Shown here are the relative dispositions of the two spheres, the orientation of the external field $\vec{E}_o$ and the observation point at which the field enhancement is calculated.

Fig. 26. Resonance of the 2-sphere system for different scale factors λ. For each λ, the intensity enhancement $\tilde{I}$ at the observation point is plotted as a function of laser frequency.

Fig. 27(a). The upper curve ($\lambda = .4545$) is a plot of $\tilde{I}$ (on a log scale) versus distance d/D as one proceeds from the surface of one sphere to the other, along their common axis. The lower curve is for the isolated sphere $\lambda = 0$ and the abcissa for this case should be read $\frac{5d}{R_o}$ rather than d/D as shown. The external frequency $\omega = 3.48$ eV is the resonance of the isolated sphere.

Fig. 27(b). Same as Figure 27(a) but for $\omega = 3.21$ eV, the lower resonance frequency of the 2-sphere system, with $\lambda = .4545$ and $\lambda = 0$.

Figure 28(a). The enhanced laser intensity between a Ag sphere and a Ag plane at 1Å from the plane surface, as a function of laser frequency. (a) The full line is for p-polarized light and the dotted line is for s-polarization. $\lambda = D/R_o = 0.05$. (b) The same for various values of λ and p-polarization. The full line corresponds to $\lambda = 0.05$ and a scale factor FAC = .001; the dash-dotted line to $\lambda = 0.03$ and FAC = 0.0005; the dashed line to $\lambda = 0.1$ and FAC = .01. In all cases the angle of incidence (with the normal to the flat surface) is $\theta = 45^o$.

Fig. 29. Raman excitation profiles for adsorbates at electrochemically roughened silver electrodes: (----) $[CN]^-$ (2114 cm^{-1}); (----) triphenylphosphine (997 cm^{-1}); (——) pyridine-d_5 (969 cm^{-1}, corresponding to the 1008 cm^{-1} mode of normal pyridine). x and • indicate coadsorbed triphenylphosphine and pyridine-d_5. Potential limits for the anodization cycle: (□) - 150 → 250 mV (130 mC/cm^2); (o) - 150 → 250 mV (280 mC/cm^{-2}); (x), (•) - 100 → 200 mV (300 mC/cm^2); (Δ) - 800 → 500 mV (25 mC/cm^2). Reproduced from Ref. [190].

Fig. 30. (a) Anodization voltamogram. (b) Successive Raman spectra, for various electrode potentials, displaying the bulk and surface ν_1 line (symmetric stretch) of H_2O. (c) Same as (b) for the bending mode of water. From unpublished work done in Prof. R.K. Chang's laboratory at Yale.

Fig. 31. Isotope effects on Raman frequencies of H_2O and D_2O. The meaning of the successive graphs is the same as in Fig. 30(b). (a) The ν_1 mode of H_2O. (b) The ν_1 mode of D_2O. (c) The bending modes. Unpublished work done in Prof. R.K. Chang's laboratory at Yale.

Fig. 1

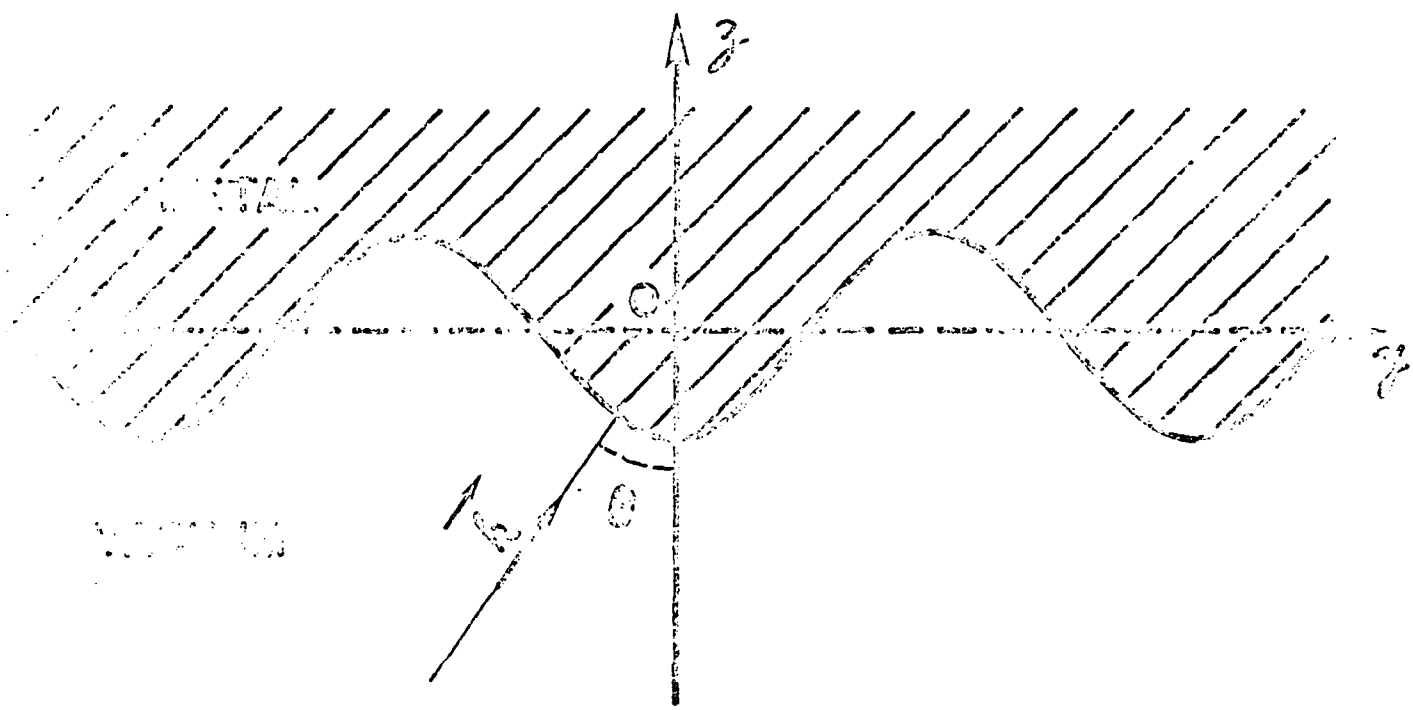

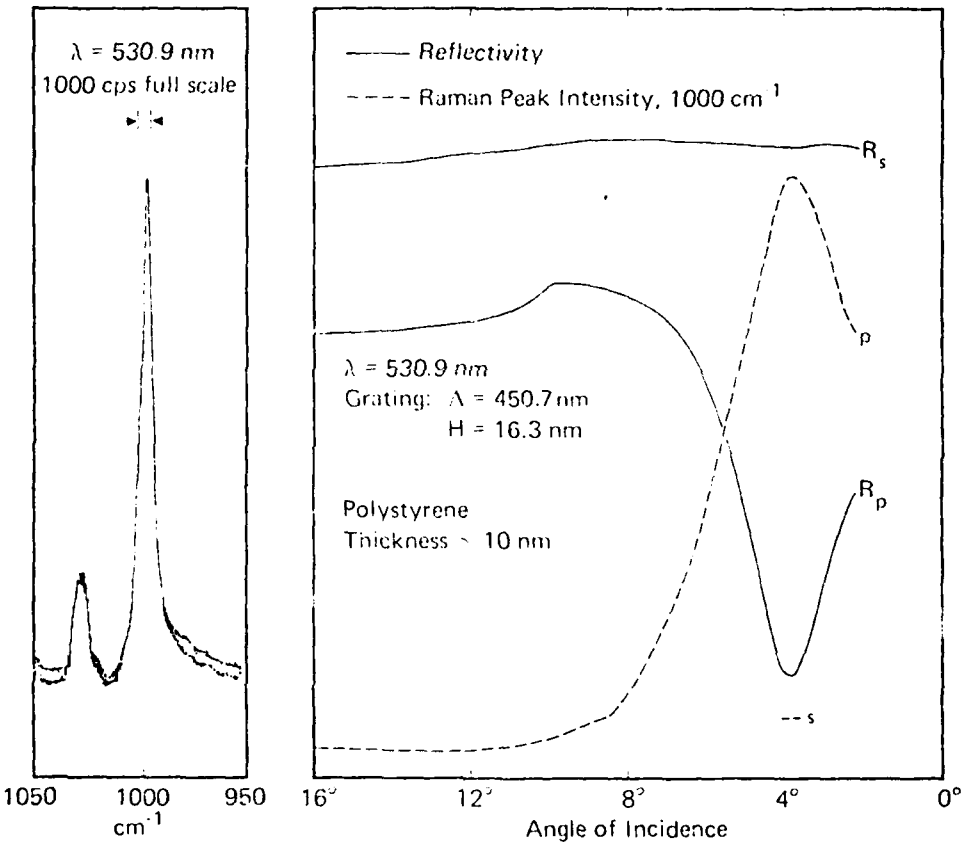

JCP-1MAY-BA9-FIG.4-f80

Fig. 2

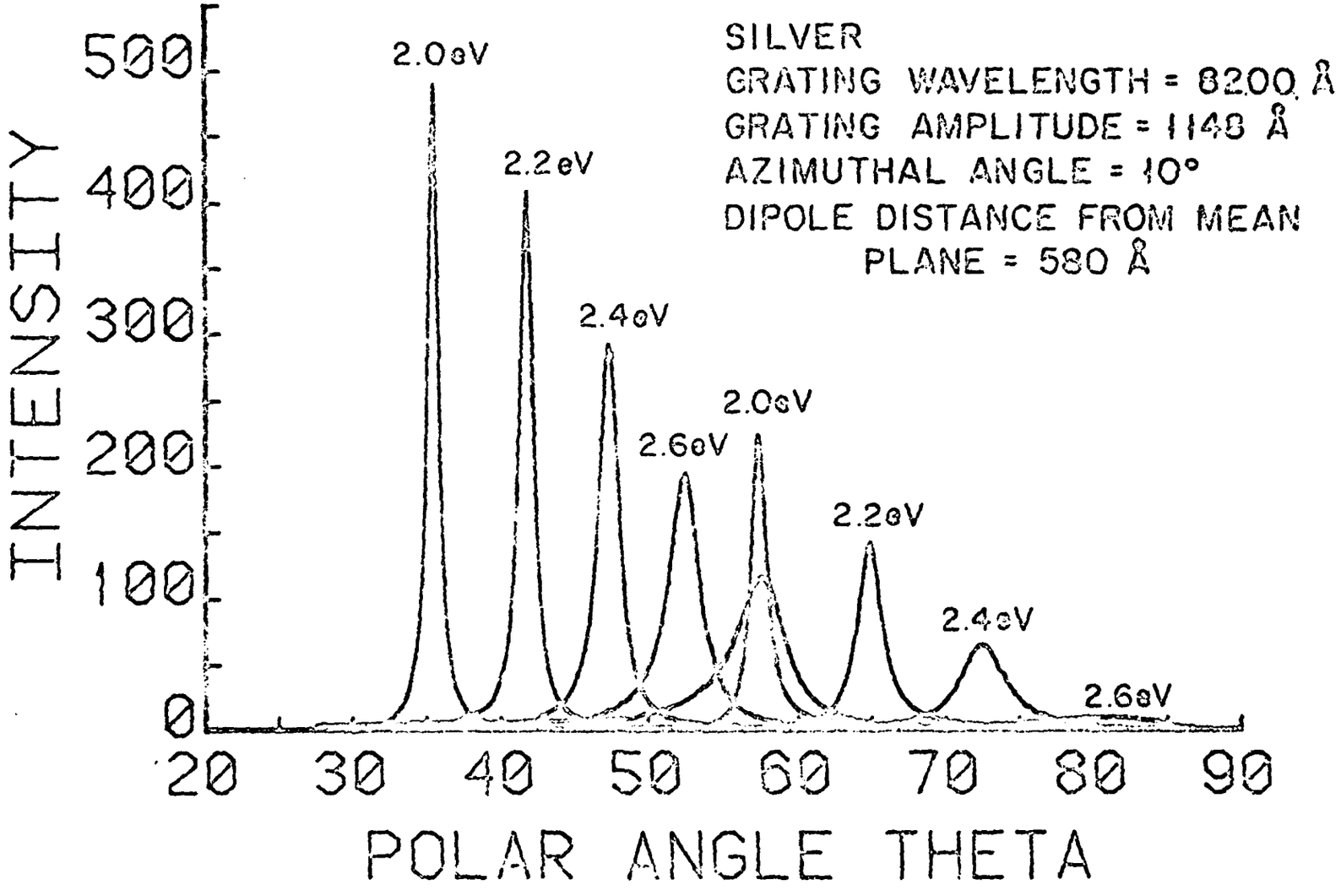
SILVER
GRATING WAVELENGTH = 6200 Å
GRATING AMPLITUDE = 1148 Å
AZIMUTHAL ANGLE = 10°
DIPOLE DISTANCE FROM MEAN PLANE = 580 Å
2.0eV
2.2eV
2.4eV
2.0eV
2.6eV
2.2eV
2.4eV
2.6eV
INTENSITY
500
400
300
200
100
0
20
30
40
50
60
70
80
90
POLAR ANGLE THETA

Fig. 3

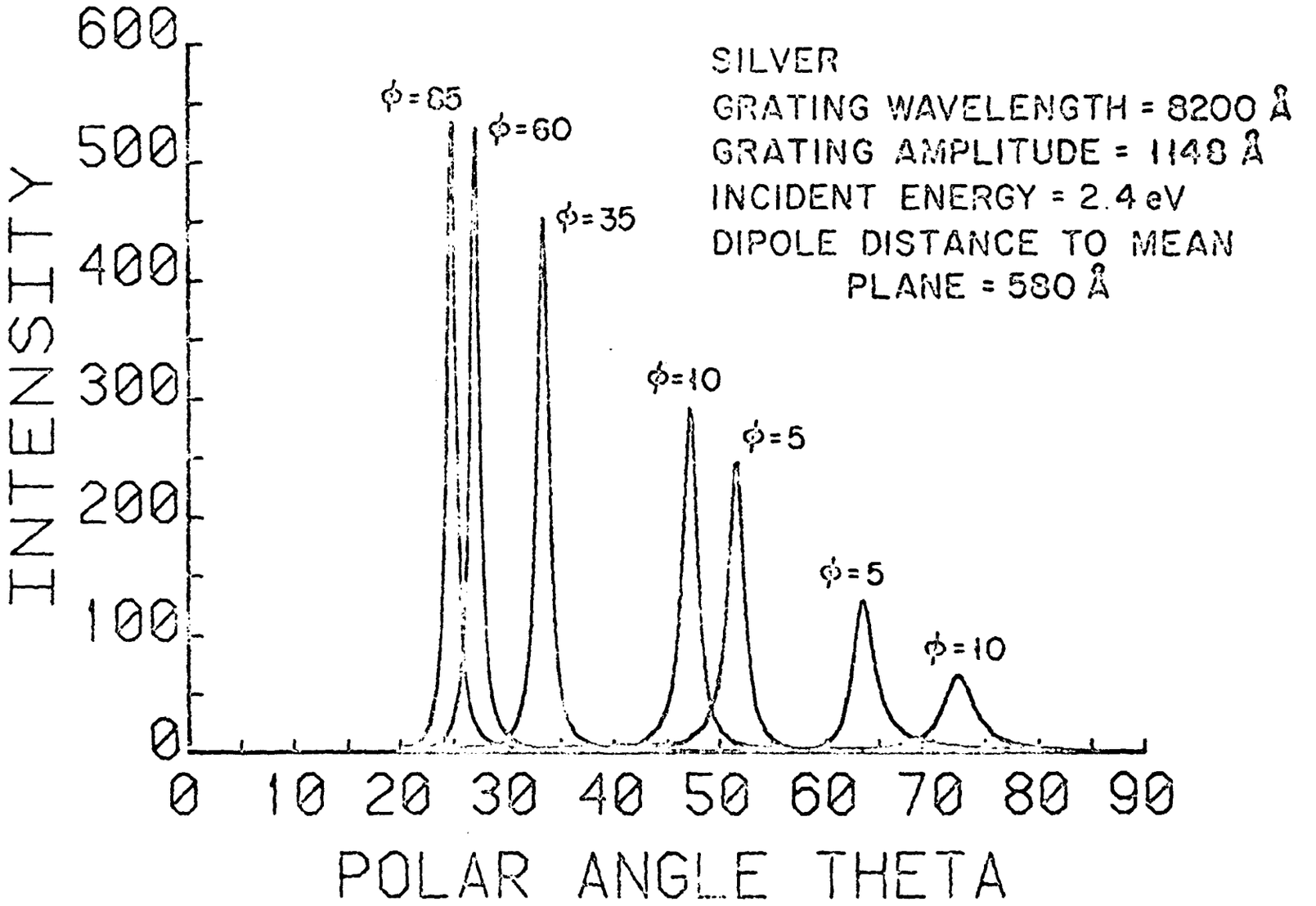
SILVER
GRATING WAVELENGTH = 8200 Å
GRATING AMPLITUDE = 1148 Å
INCIDENT ENERGY = 2.4 eV
DIPOLE DISTANCE TO MEAN PLANE = 580 Å
φ = 65
φ = 60
φ = 35
φ = 10
φ = 5
φ = 5
φ = 10
INTENSITY
600
500
400
300
200
100
0
0 10 20 30 40 50 60 70 80 90
POLAR ANGLE THETA

Fig. 4

Fig. 5

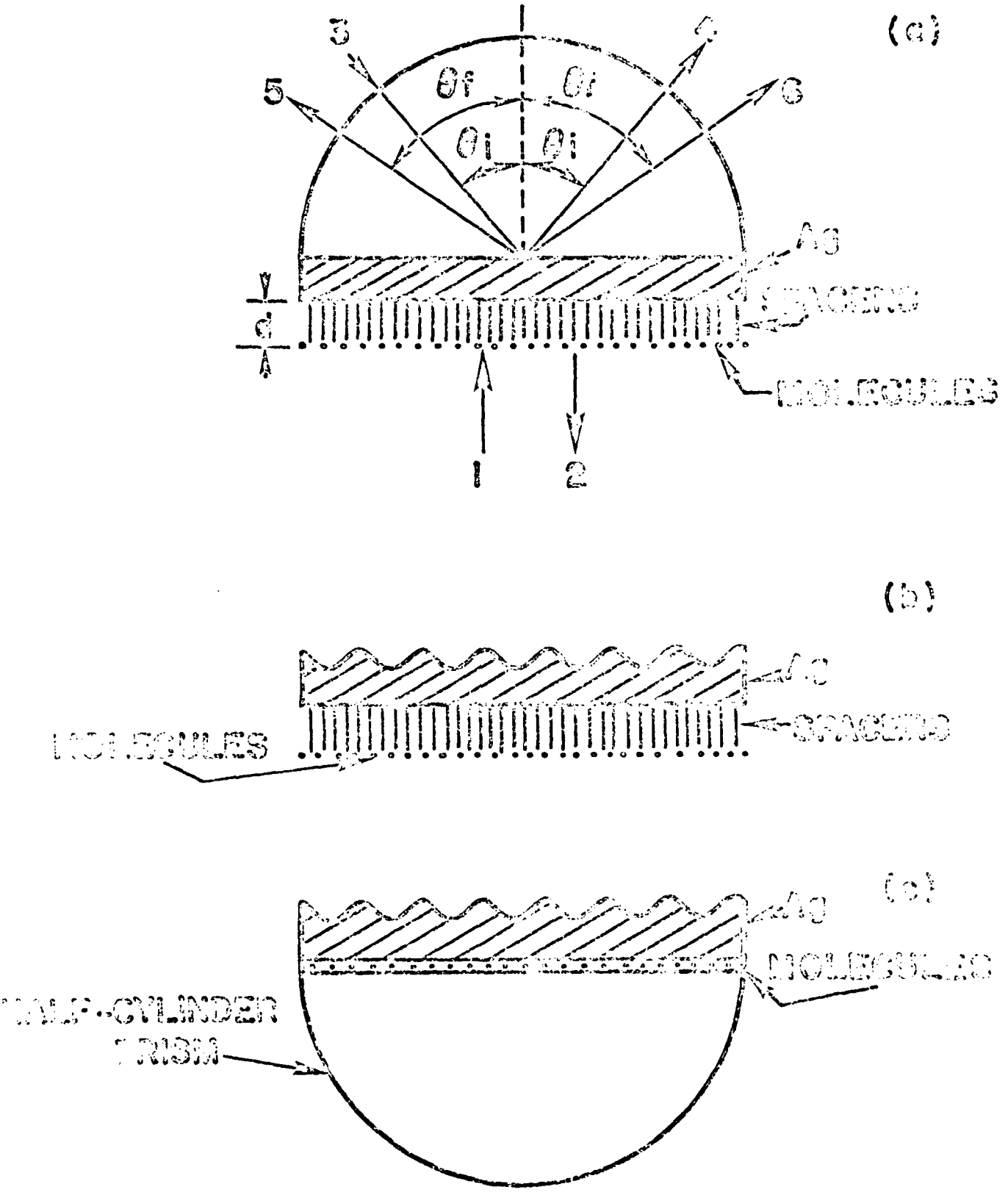
(a)
3
4
5
6
θf
θi
θi
θi
θi
Ag
SPACERS
y
d
MOLECULES
1
2
(b)
Ag
SPACERS
MOLECULES
(c)
Ag
MOLECULES
HALF-CYLINDER
PRISM

Fig. 6

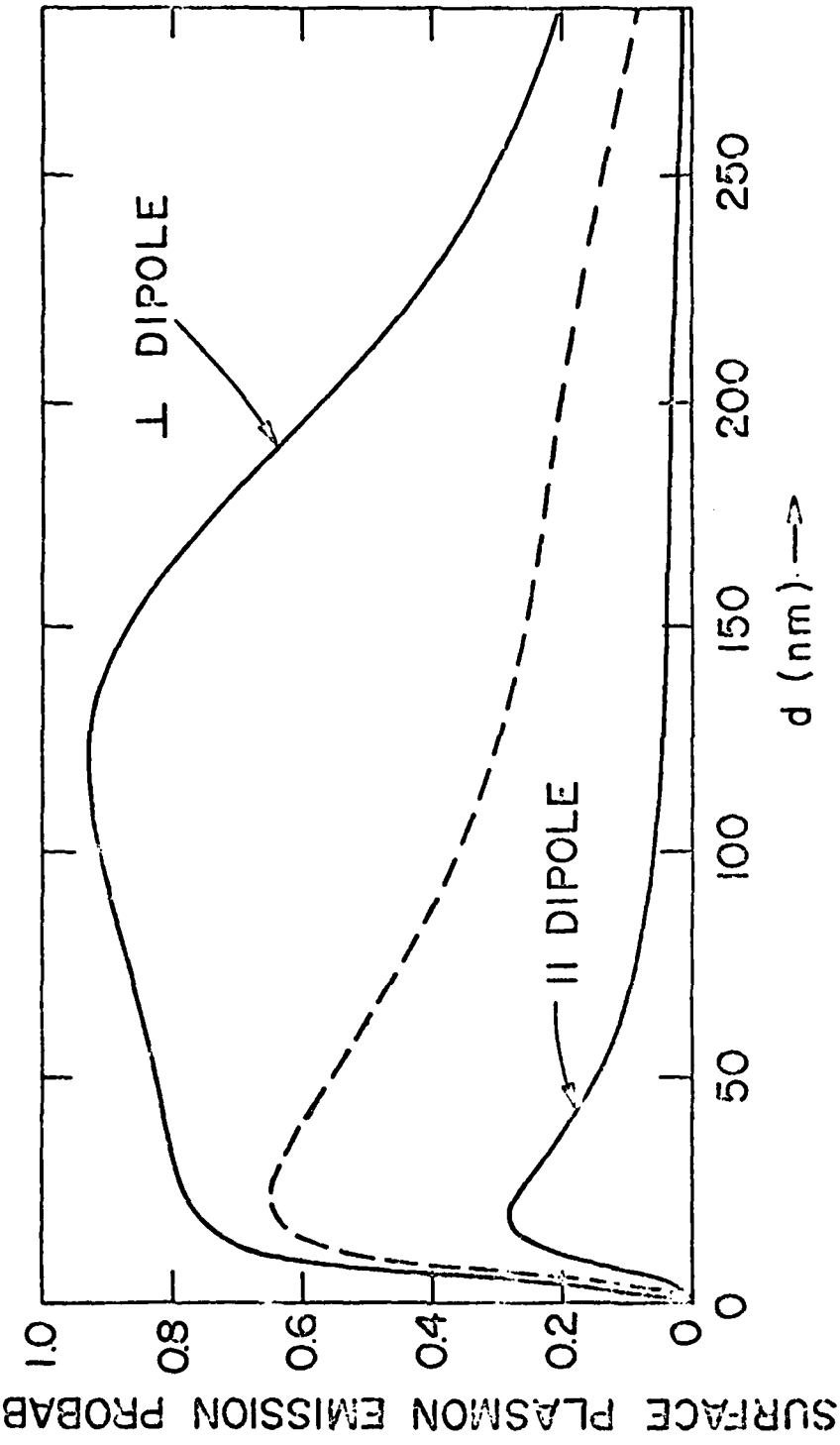

JRL ISSUE KB FIG
% OF ORIG DENSITOMETER

Fig. 7

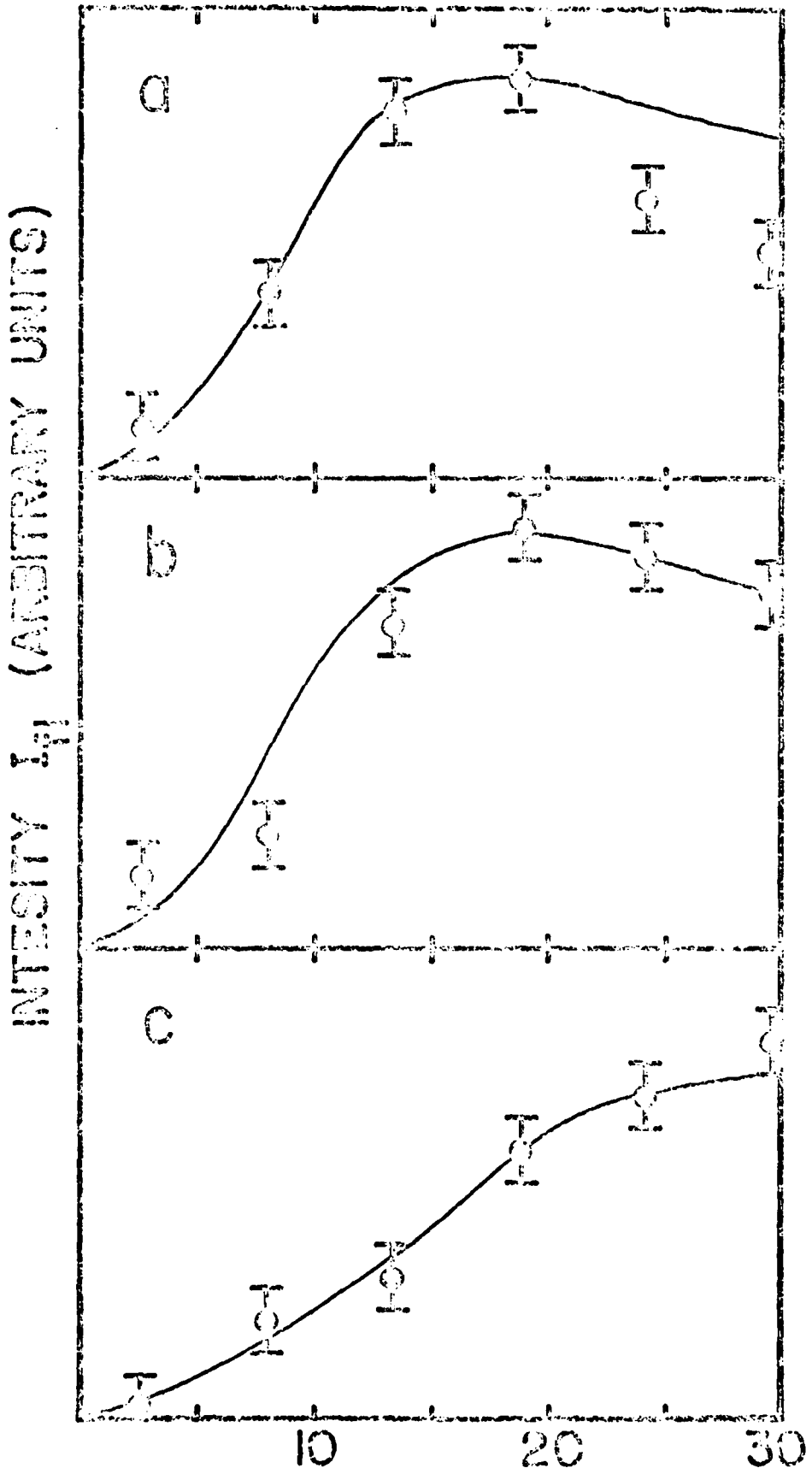

Fig. 8

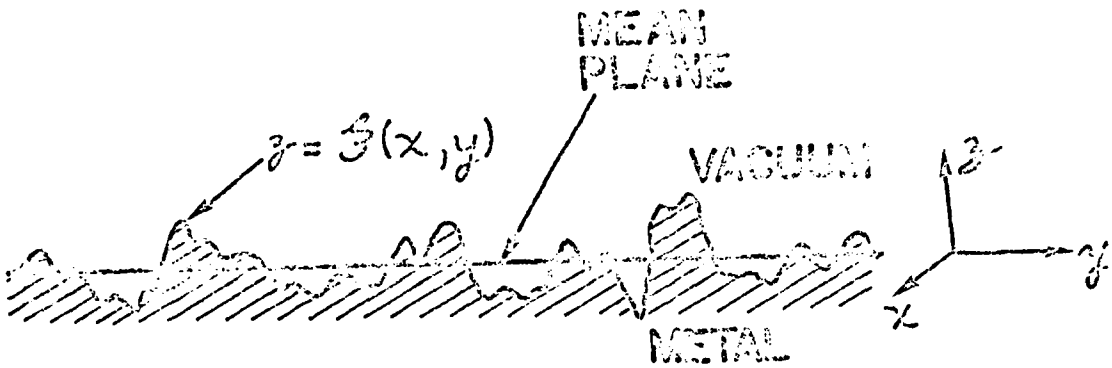

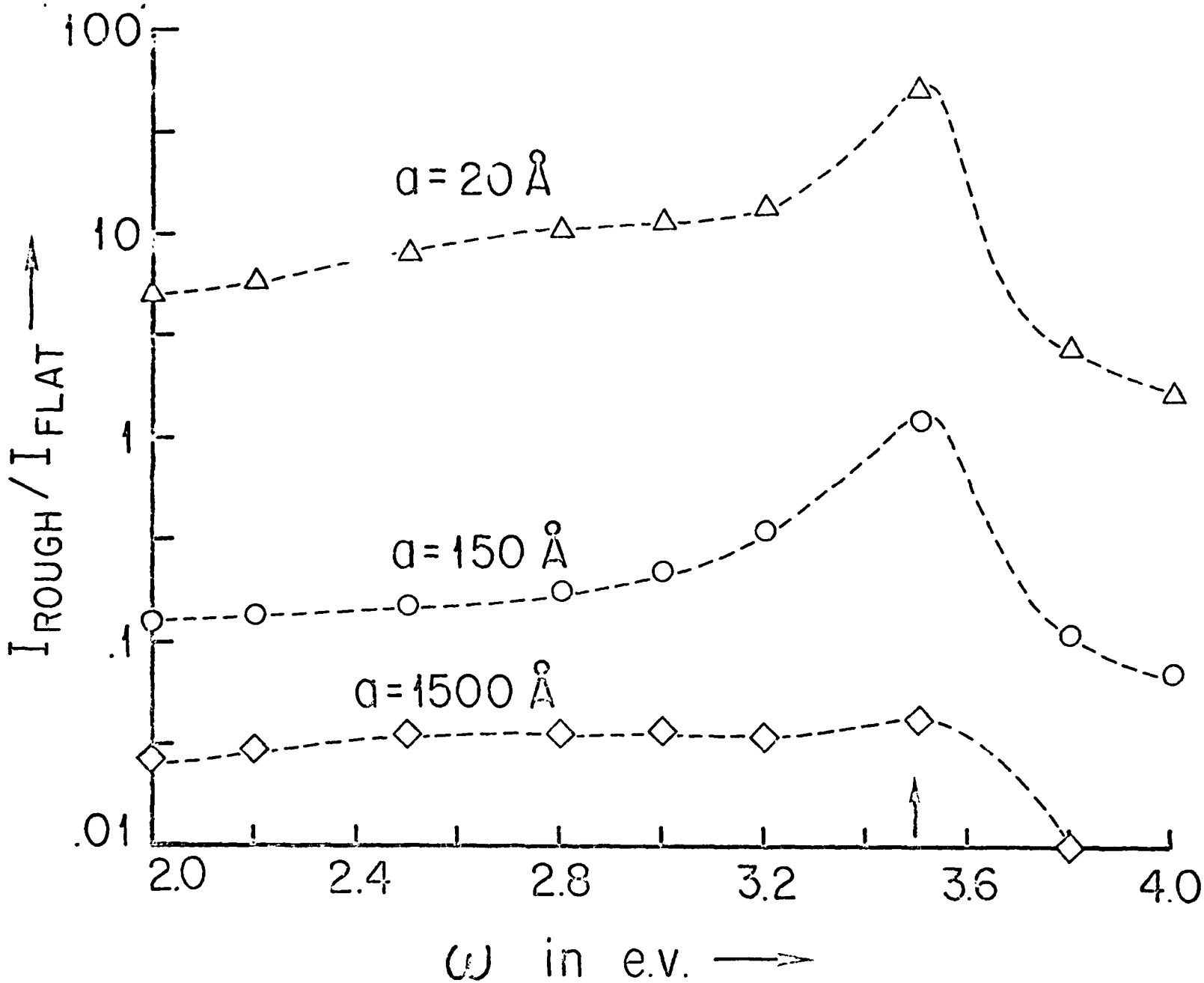
100
10
1
.1
.01
I_{ROUGH}/I_{FLAT} ⟶
a = 20 Å
a = 150 Å
a = 1500 Å
2.0
2.4
2.8
3.2
3.6
4.0
ω in e.v. ⟶

Fig. 9

Fig. 13

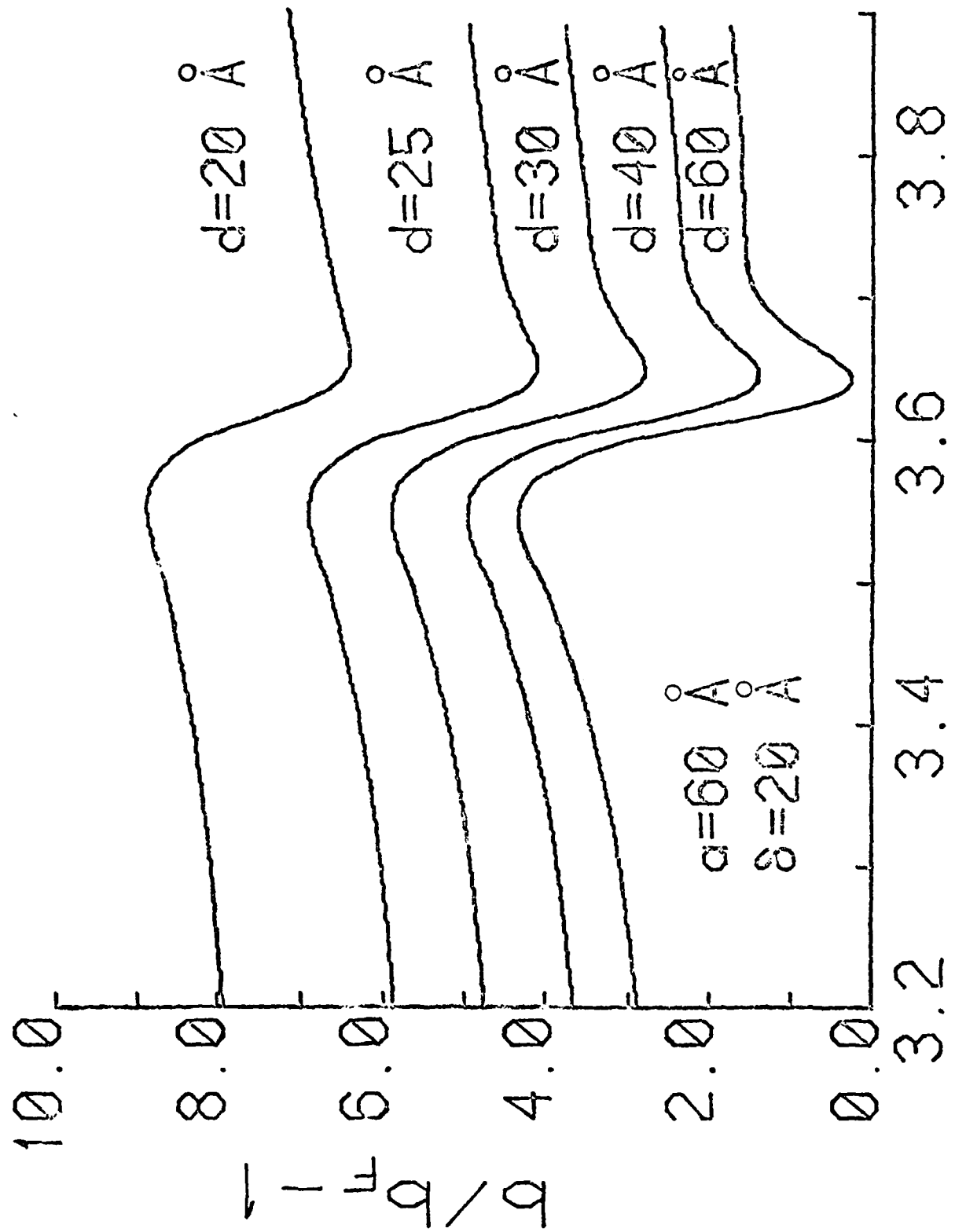
d=20 Å
d=25 Å
d=30 Å
d=40 Å
d=60 Å
d=60 Å
s=20 Å
10.0
8.0
6.0
4.0
2.0
0.0
3.2
3.4
3.6
3.8
ω (eV)
b/b_F − 1

Fig. 11a

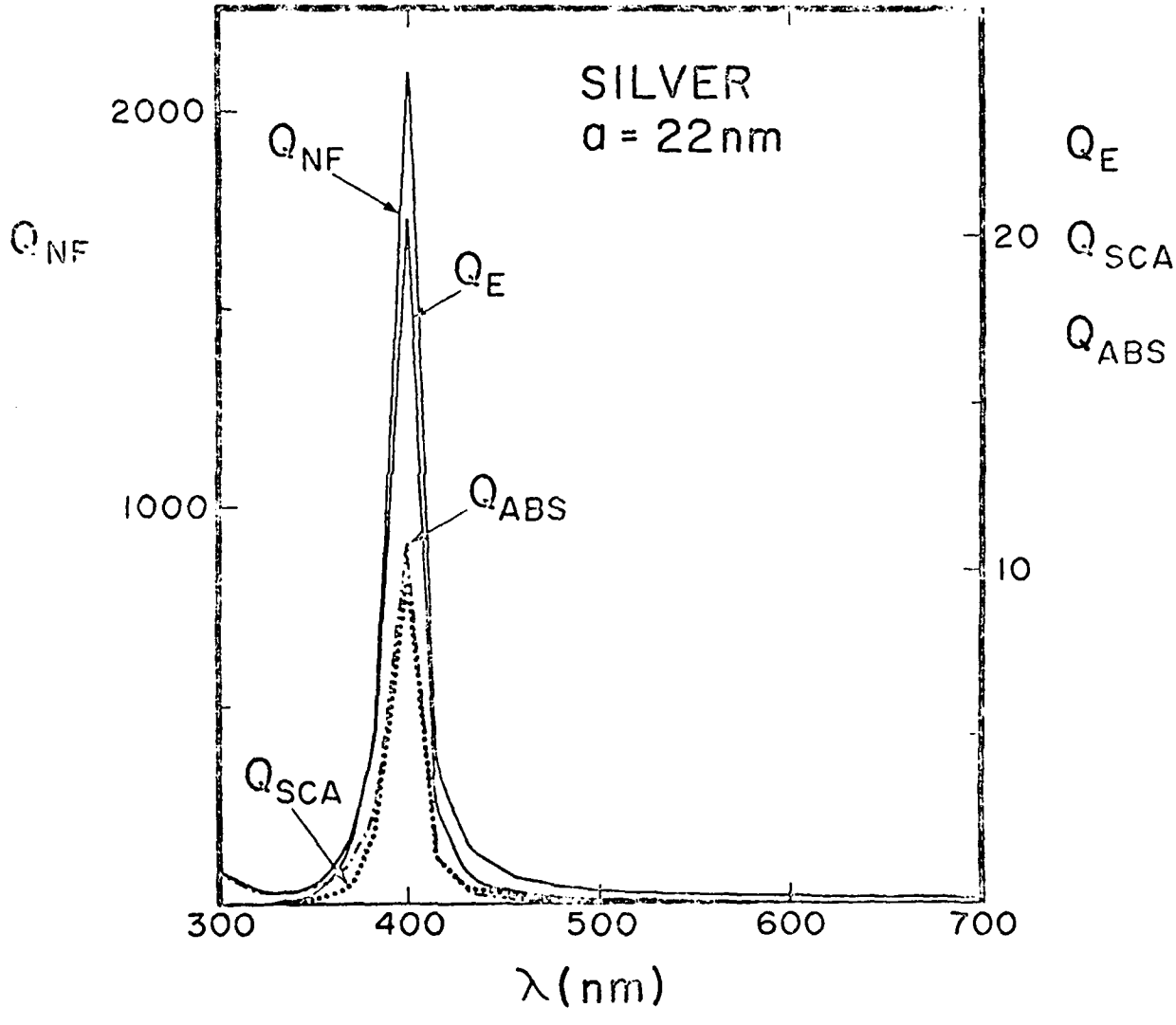
SILVER
a = 22nm
Q_{NF}
Q_E
Q_{ABS}
Q_{SCA}
2000
1000
20
10
300
400
500
600
700
λ(nm)

Fig. 11b

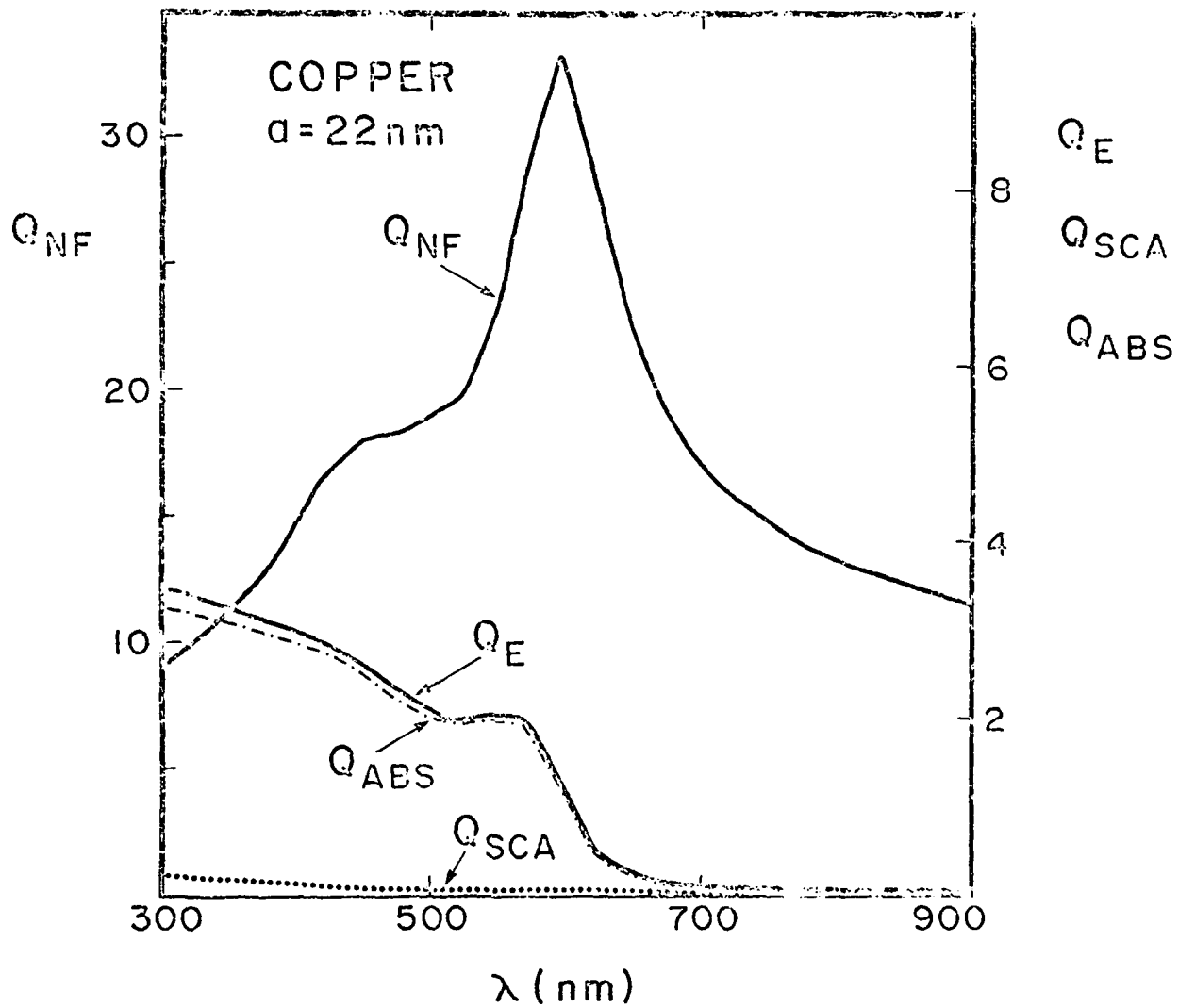

Fig. 11c

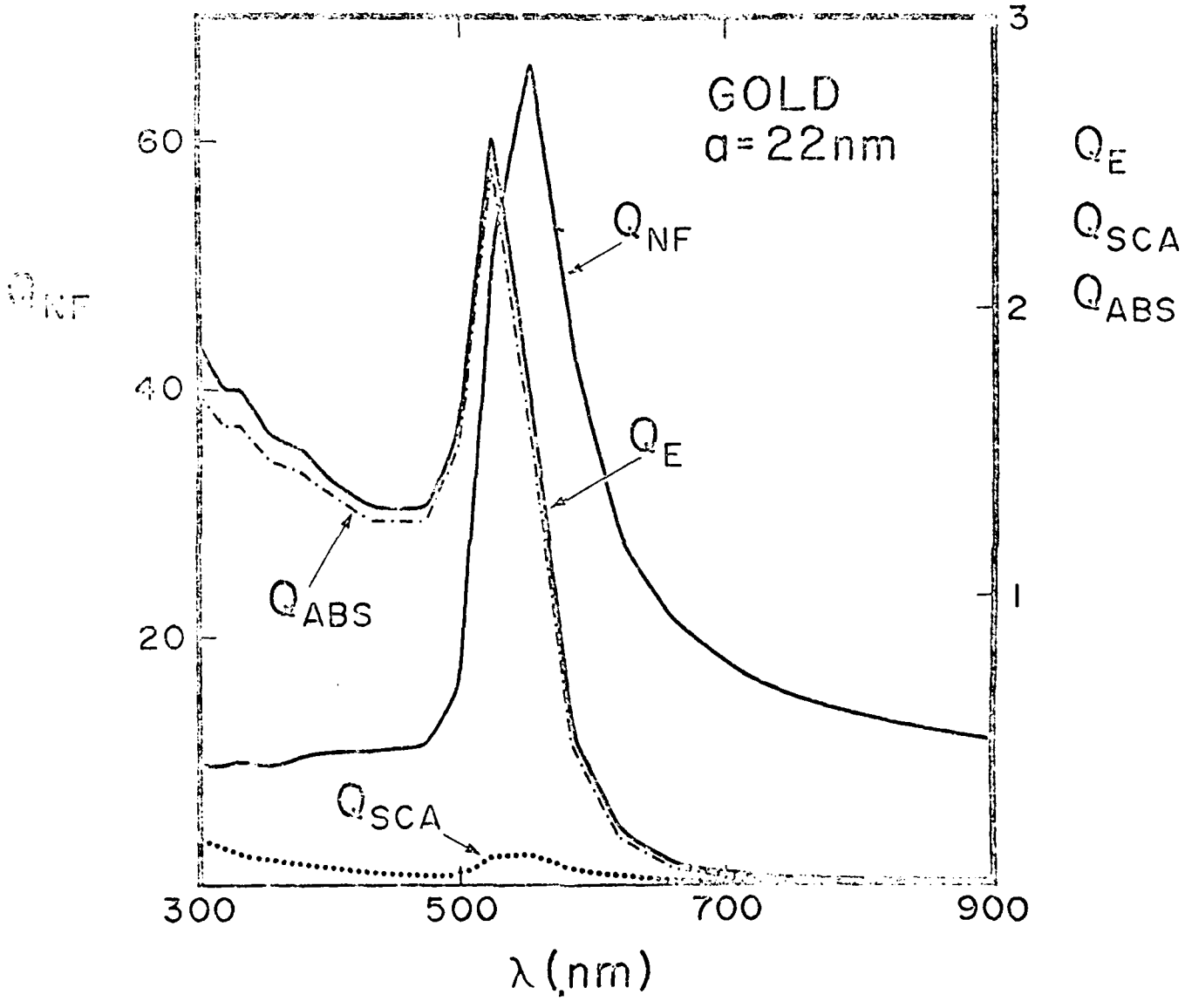

Fig. 12

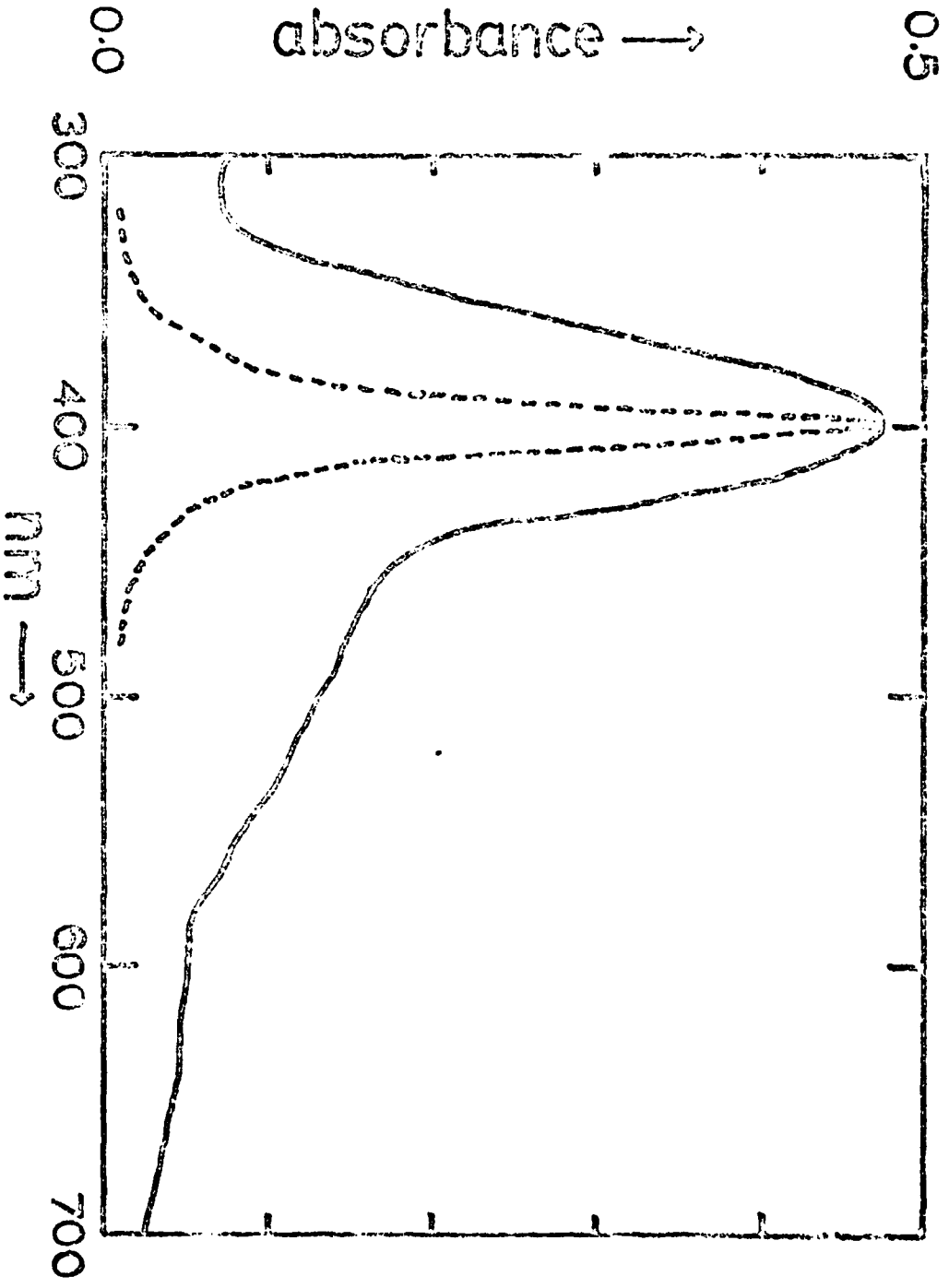

Fig. 13a

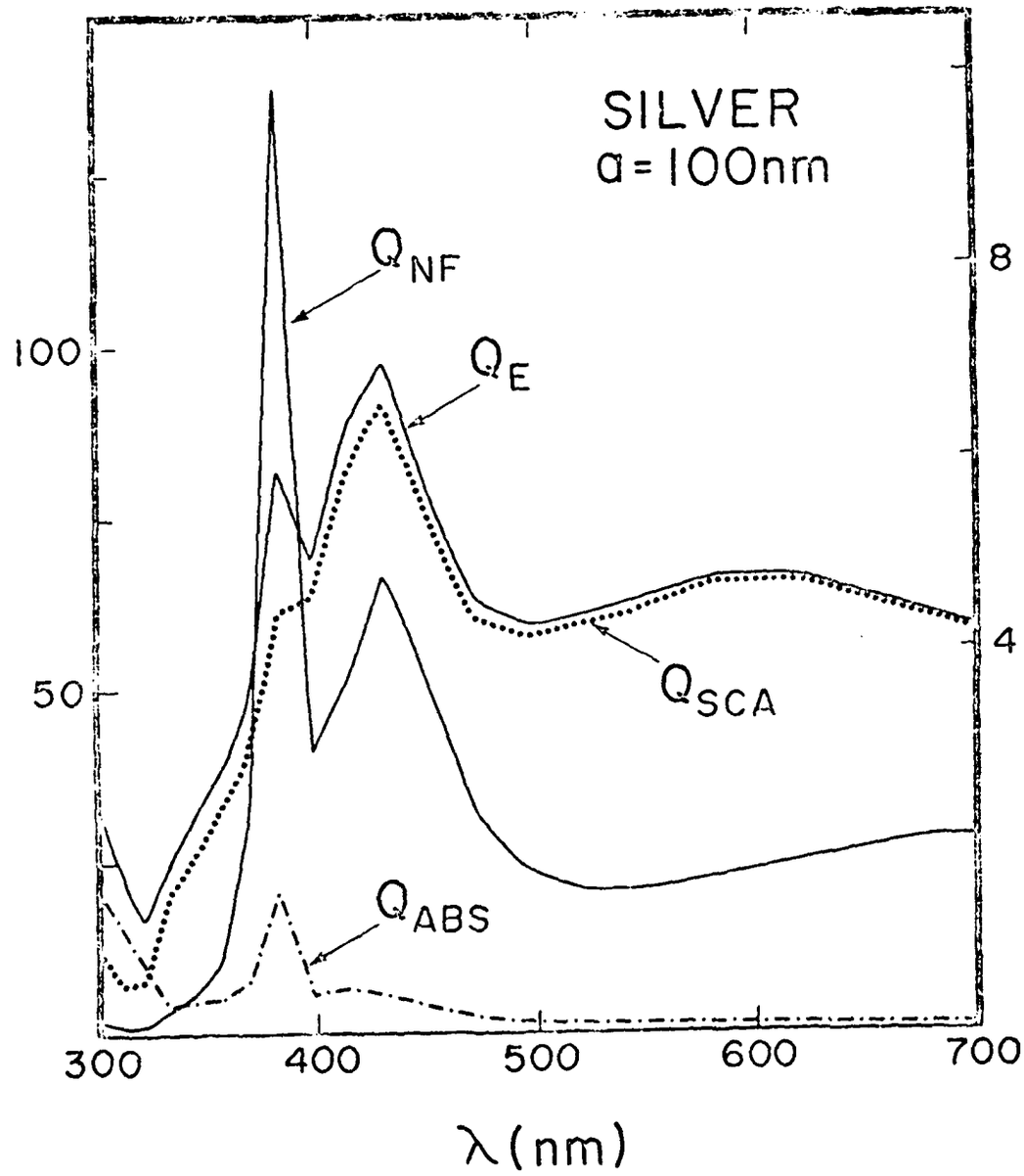
SILVER
a = 100nm
Q_{NF}
Q_E
Q_{SCA}
Q_{ABS}
100
50
8
4
300
400
500
600
700
λ(nm)

Fig. 13b

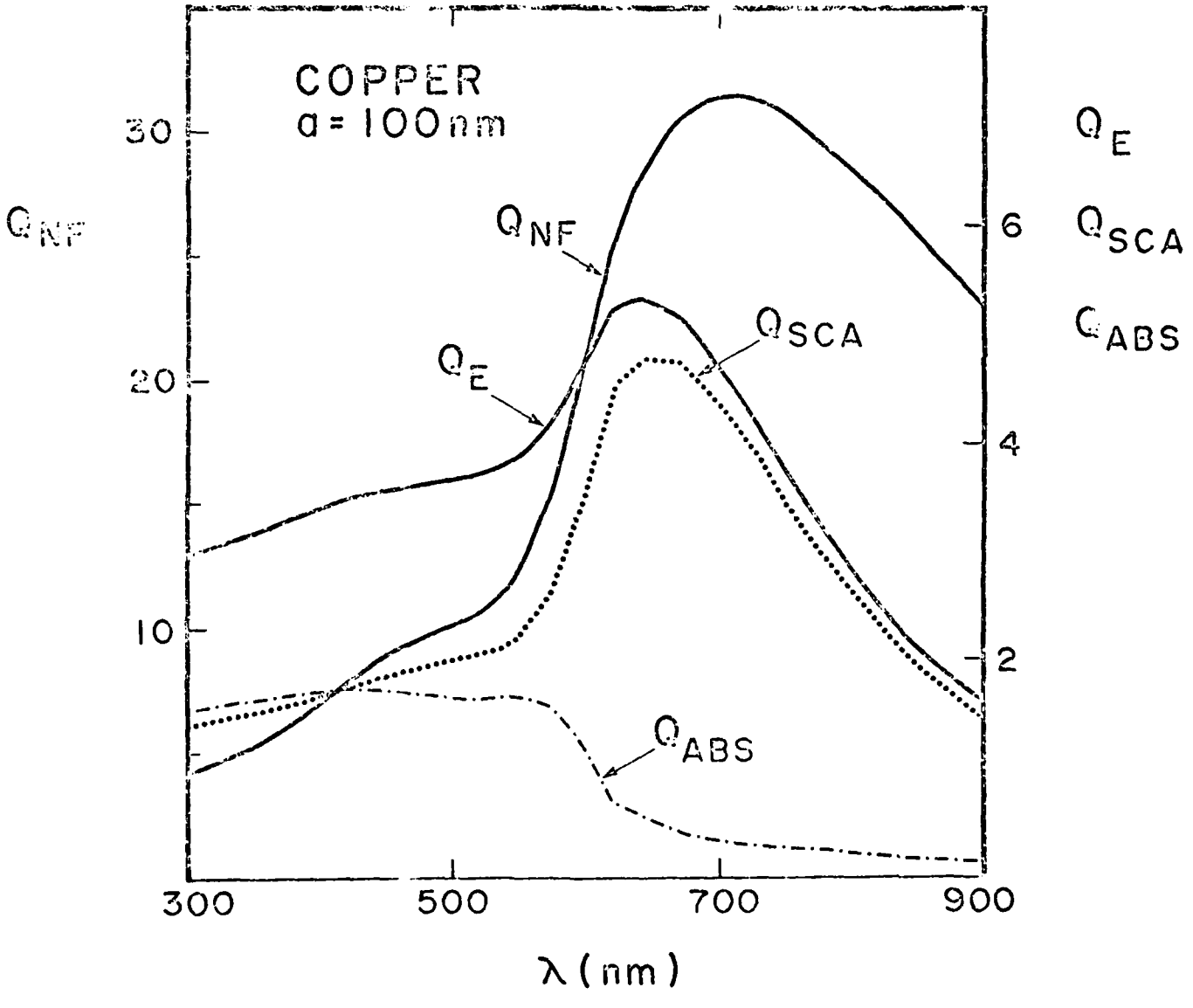

Fig. 13c

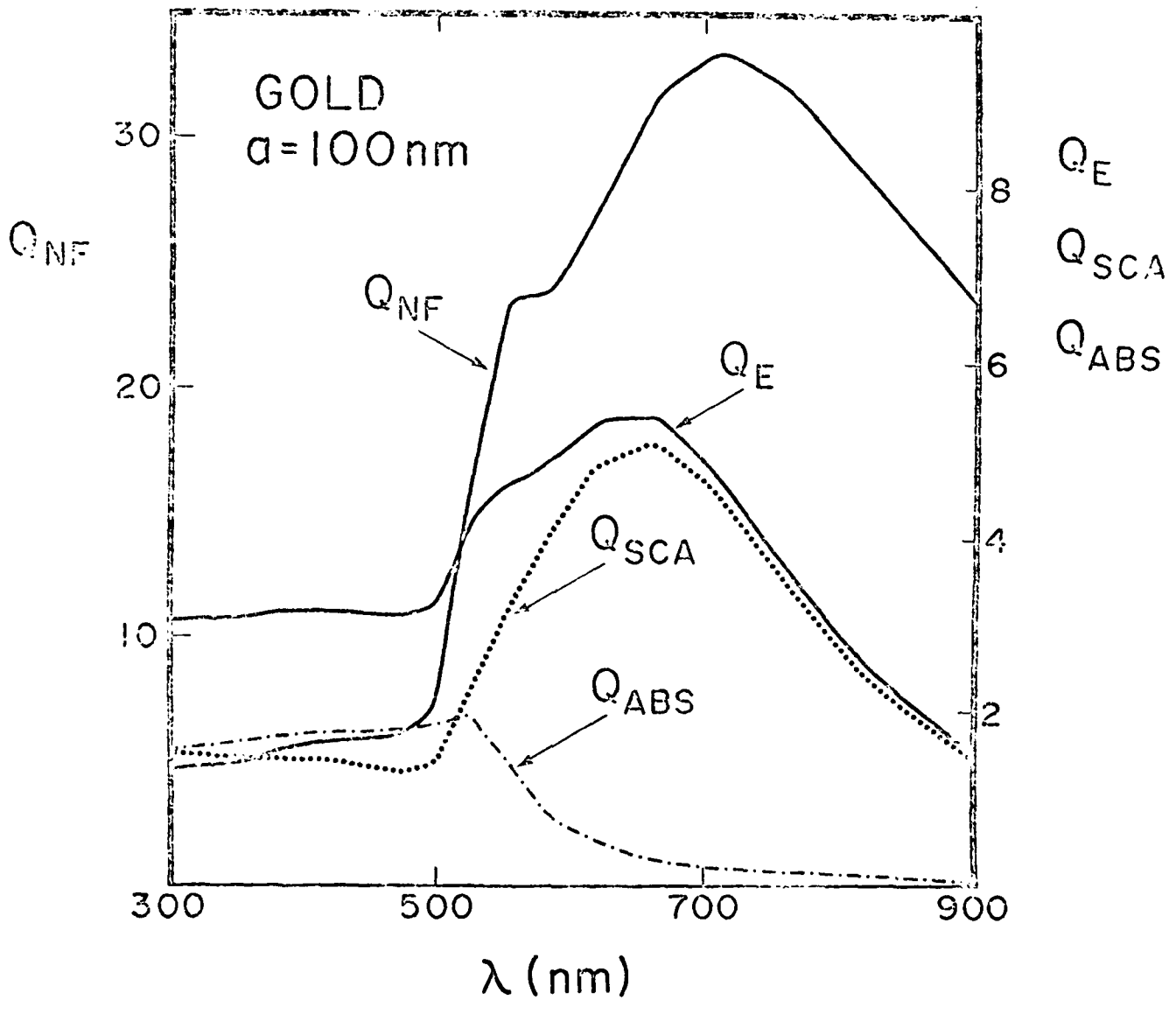

Fig. 14a

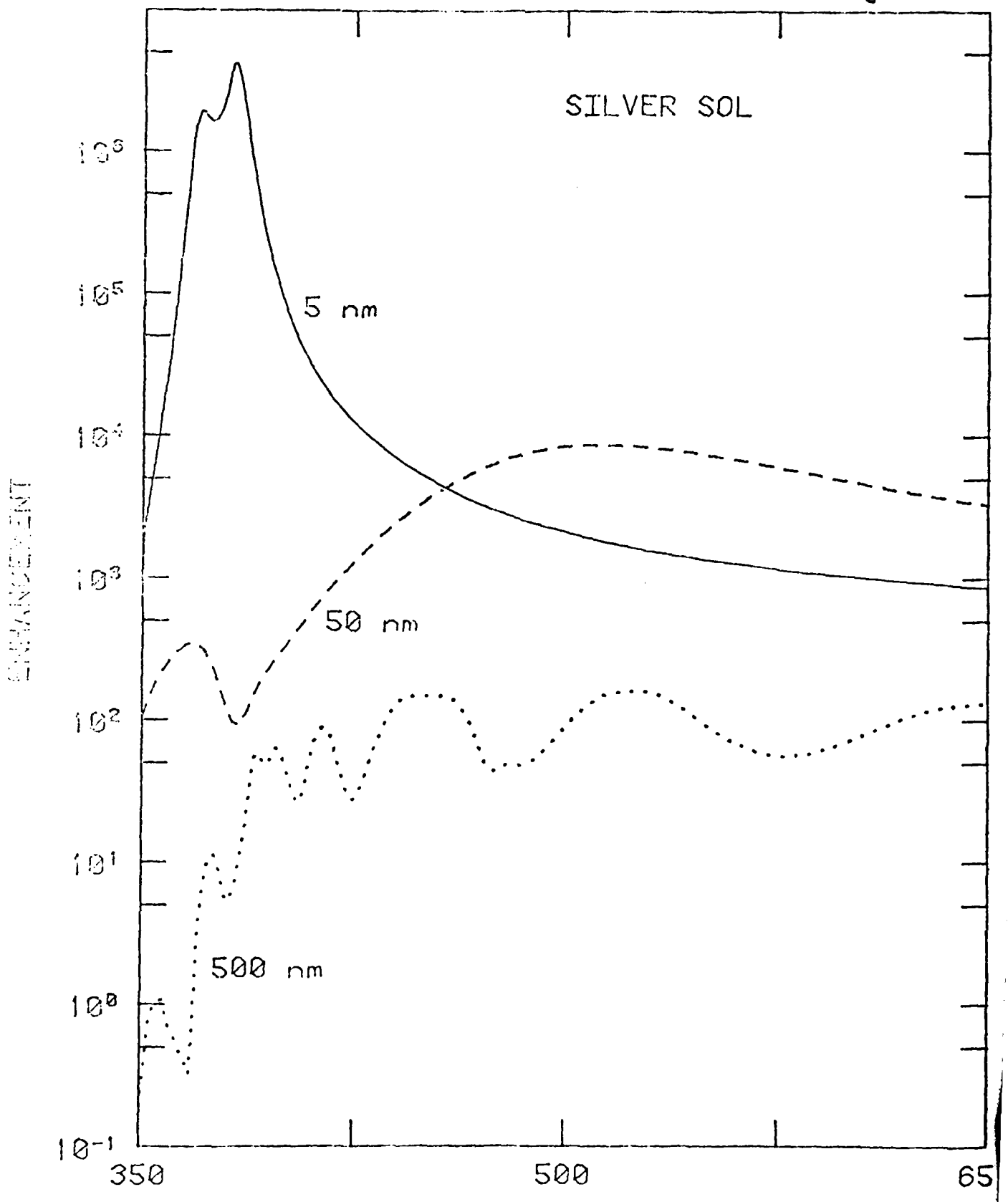
SILVER SOL
5 nm
50 nm
500 nm
ENHANCEMENT
10^6
10^5
10^4
10^3
10^2
10^1
10^0
10^{-1}
350
500
65
wavelength (nm)

Fig. 14b

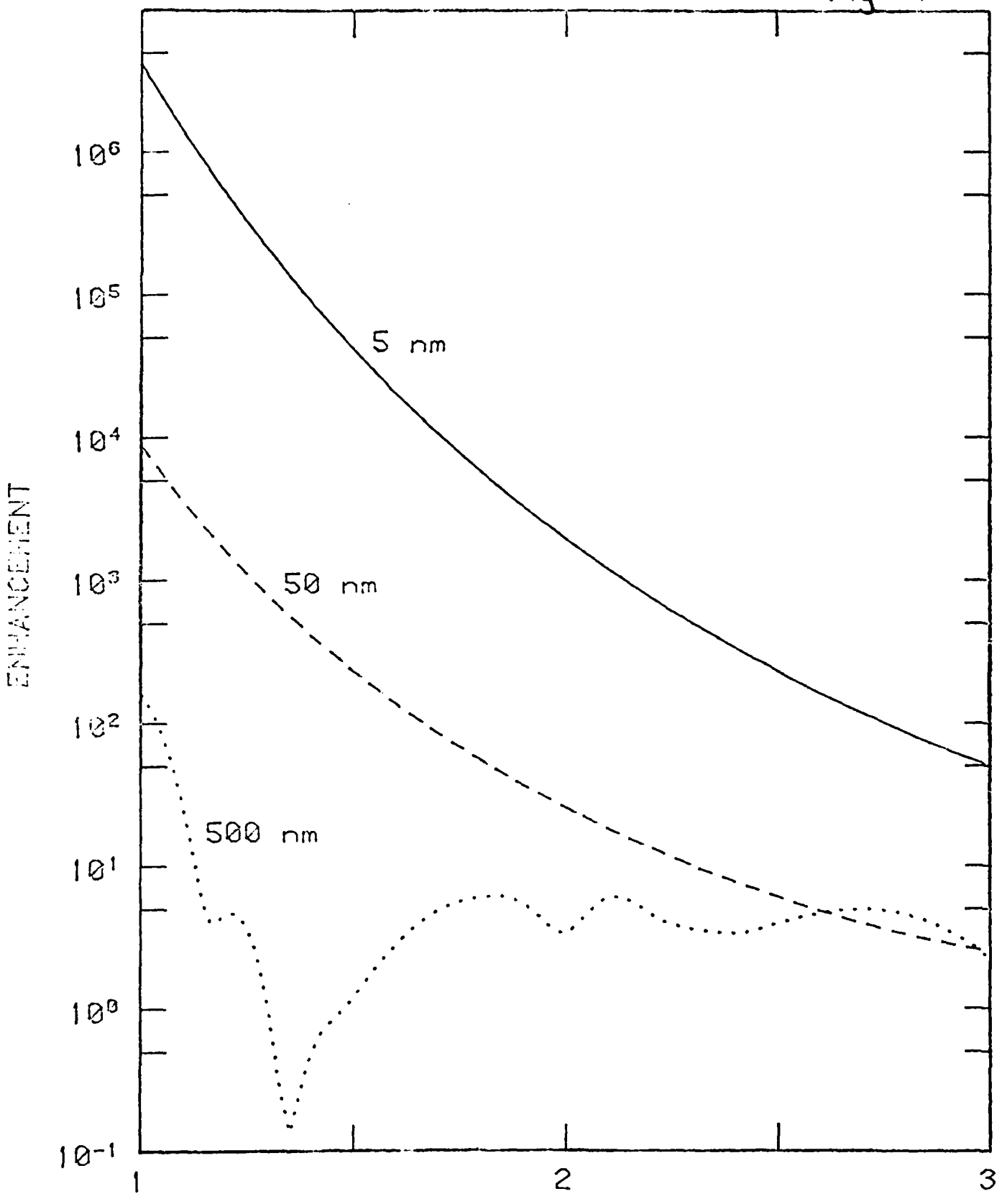
ENHANCEMENT
10^6
10^5
10^4
10^3
10^2
10^1
10^0
10^{-1}
5 nm
50 nm
500 nm
1
2
3
r'/a

Fig. 14c

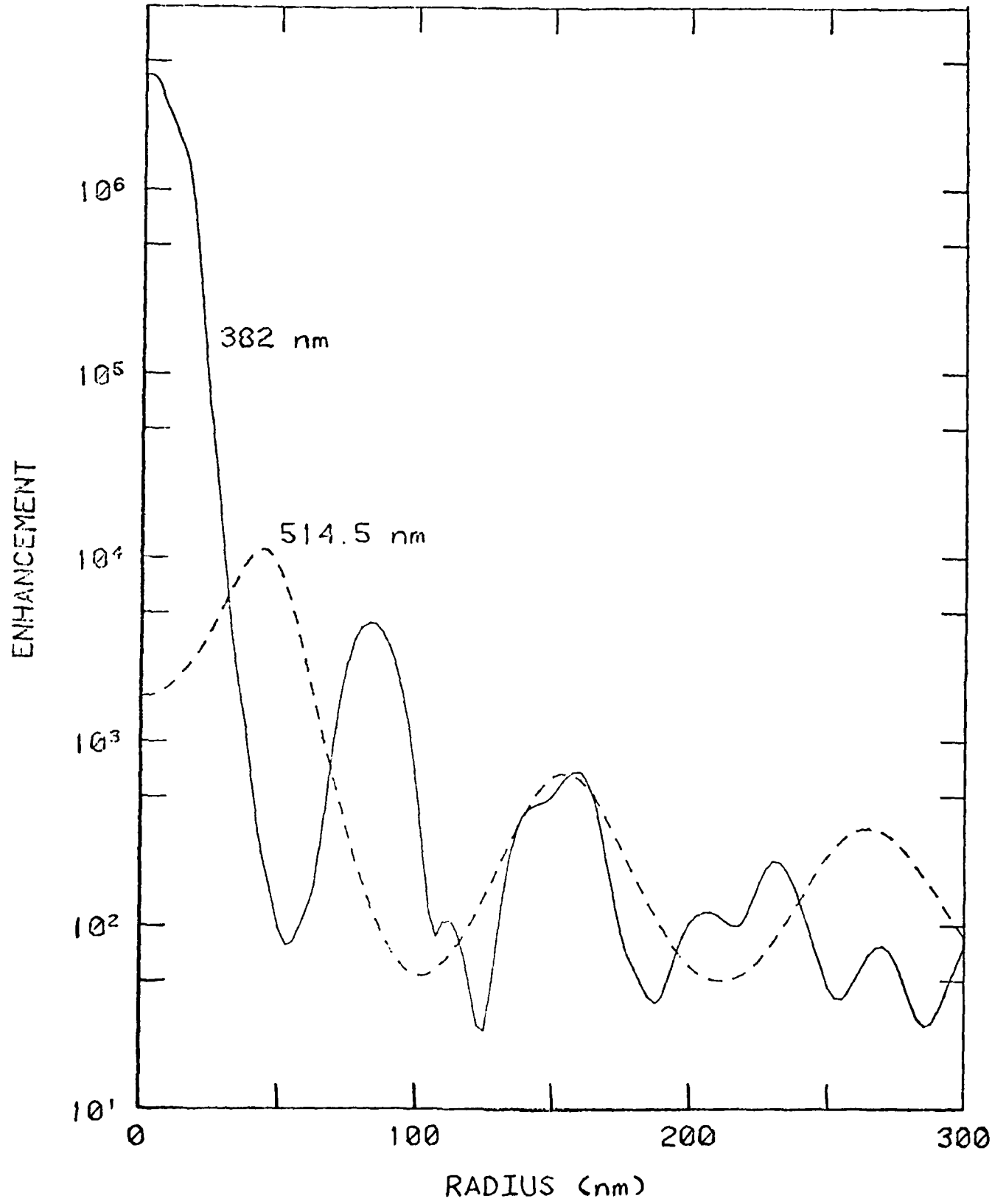
382 nm
514.5 nm
ENHANCEMENT
10^6
10^5
10^4
10^3
10^2
10^1
0
100
200
300
RADIUS (nm)

Fig. 15

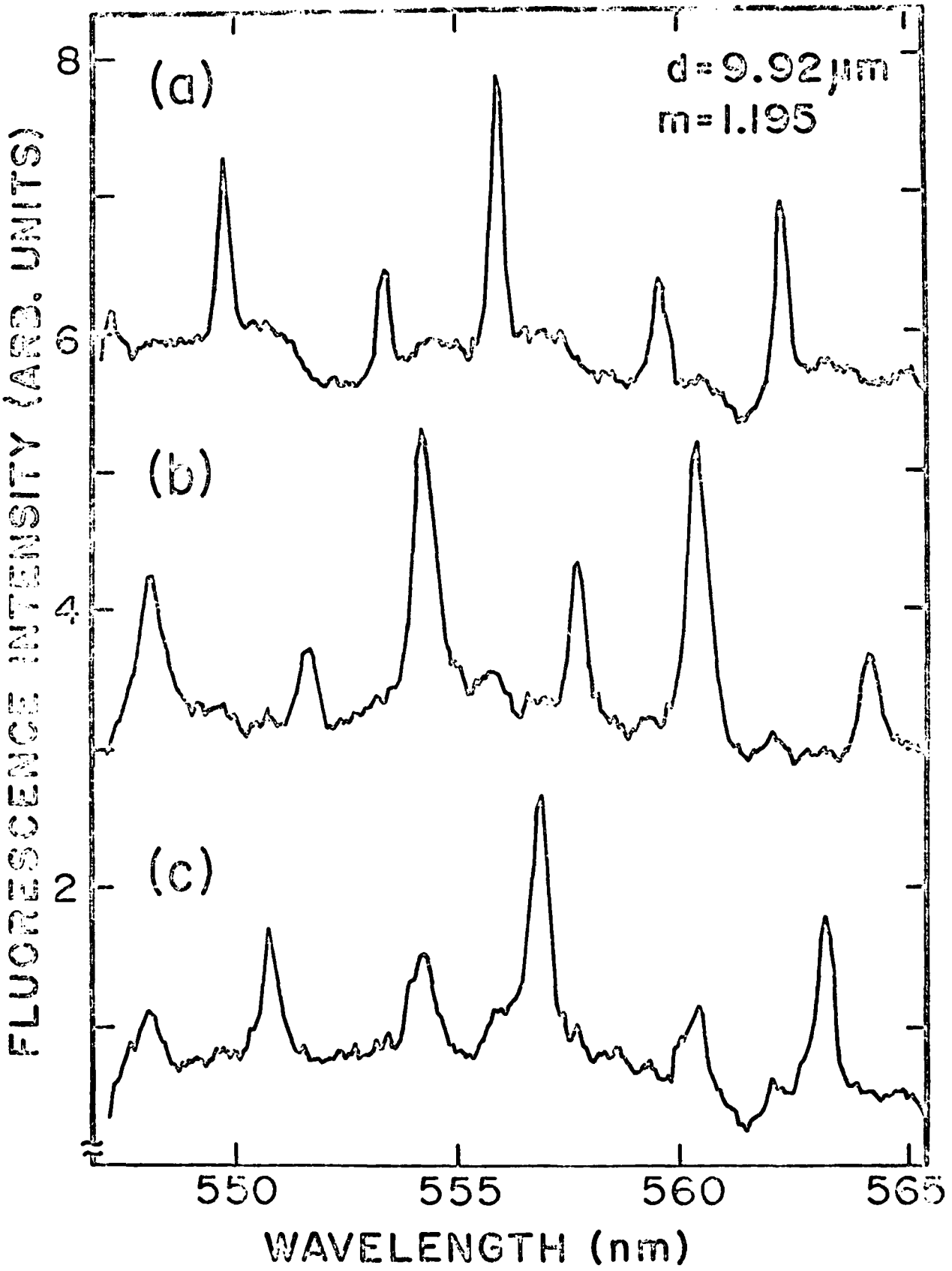
(a)
d = 9.92 μm
m = 1.195
(b)
(c)
FLUORESCENCE INTENSITY (ARB. UNITS)
8
6
4
2
550
555
560
565
WAVELENGTH (nm)

Fig. 16

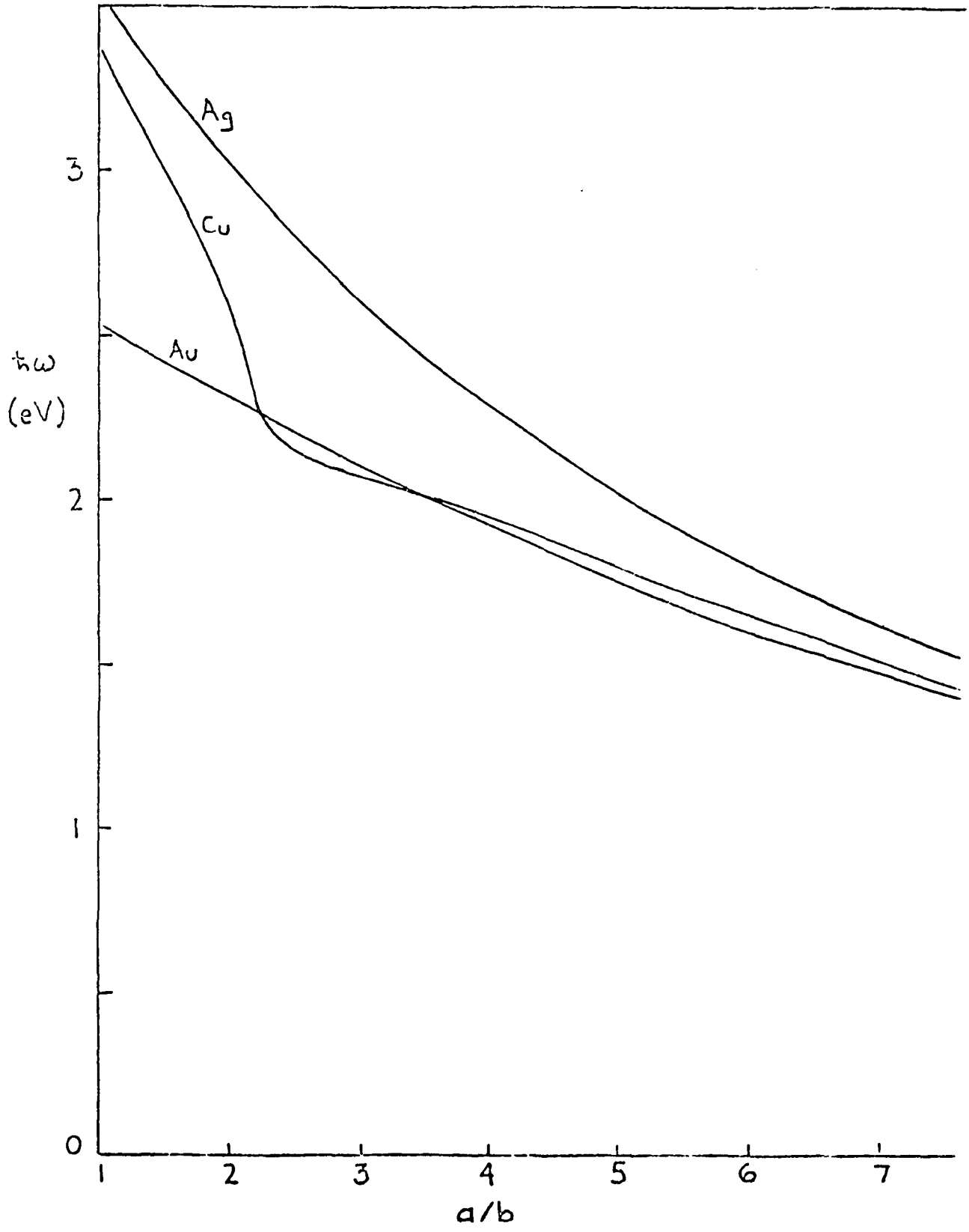

Fig. 17a

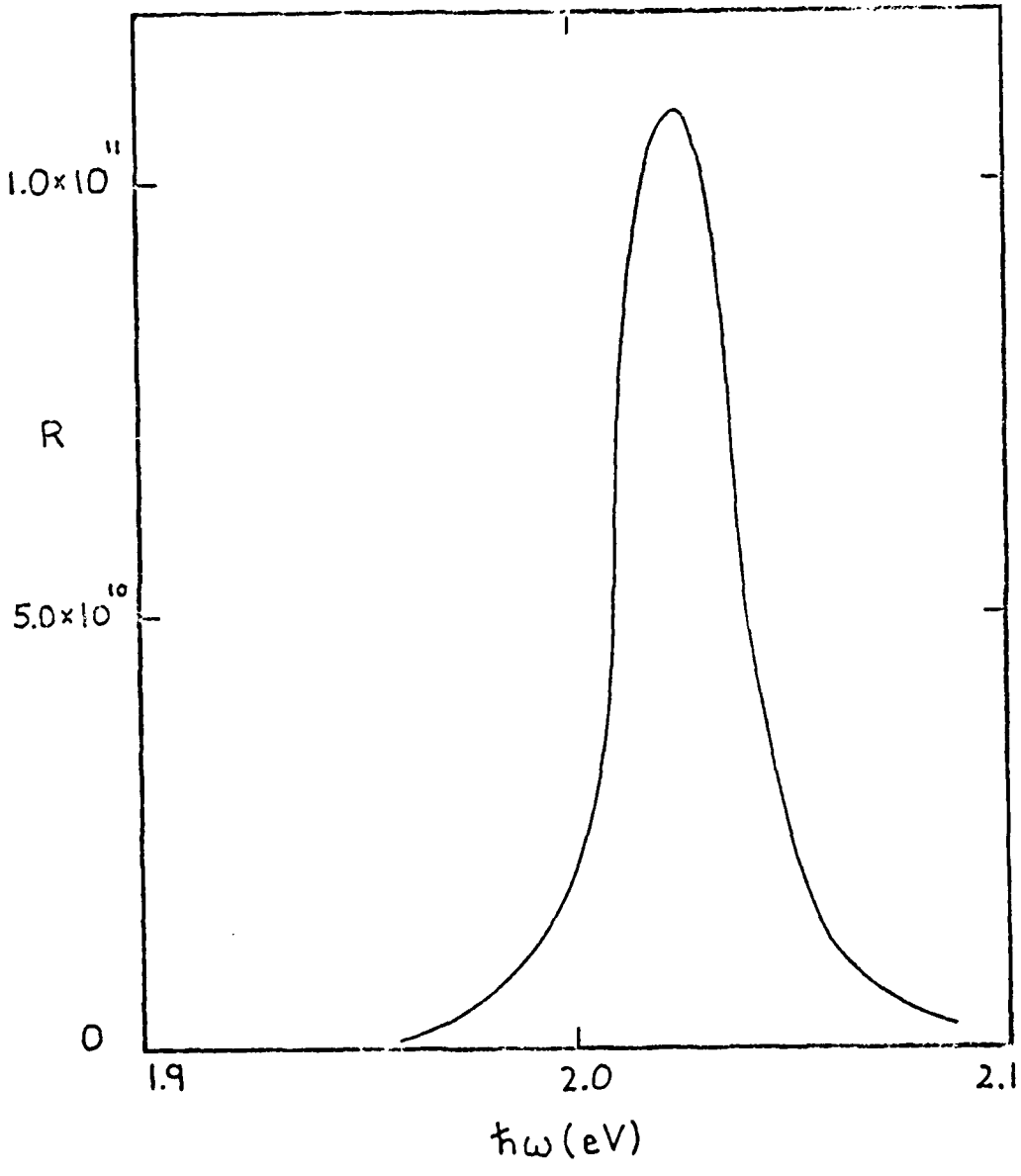

Fig. 17b

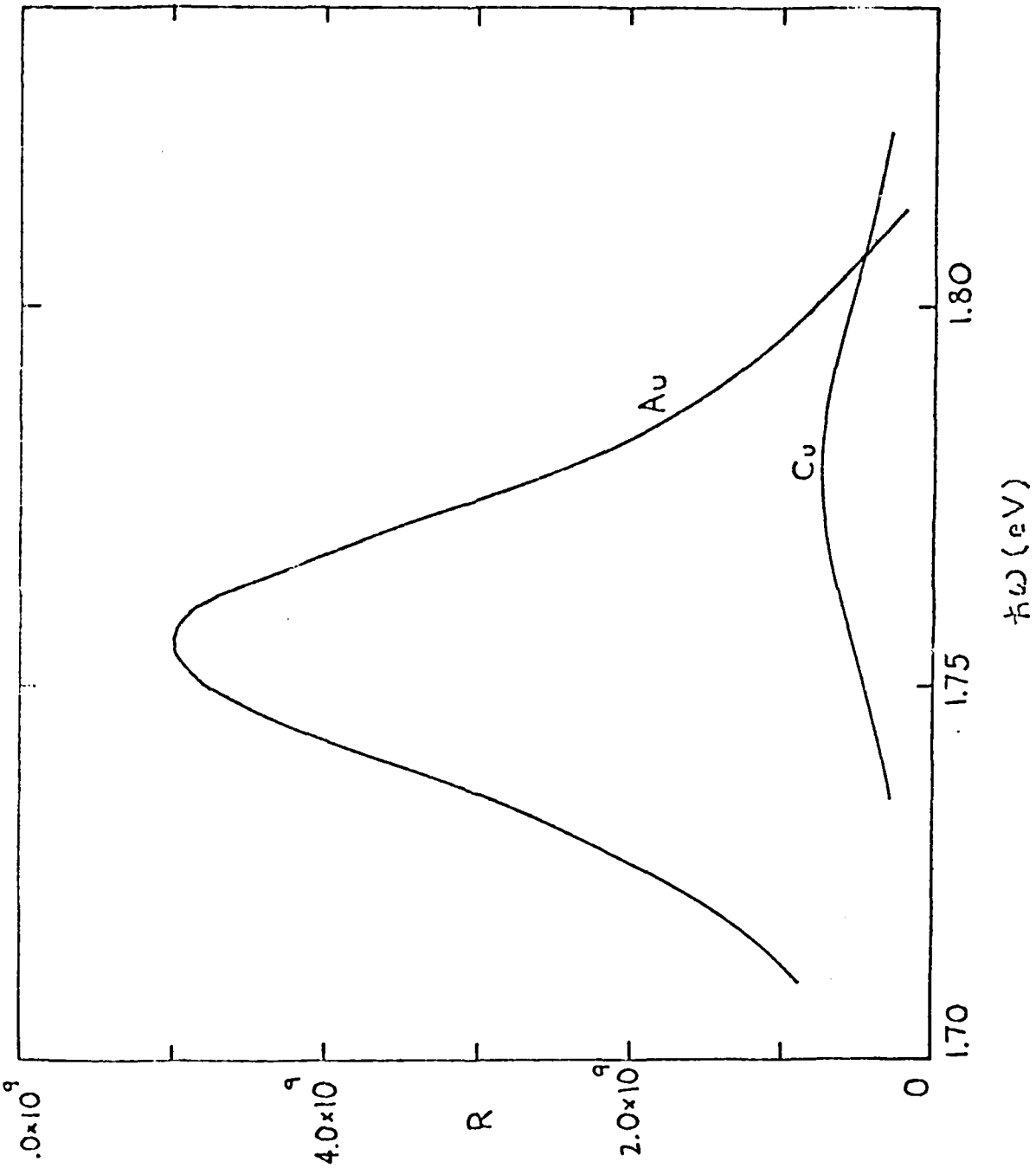

Fig. 13

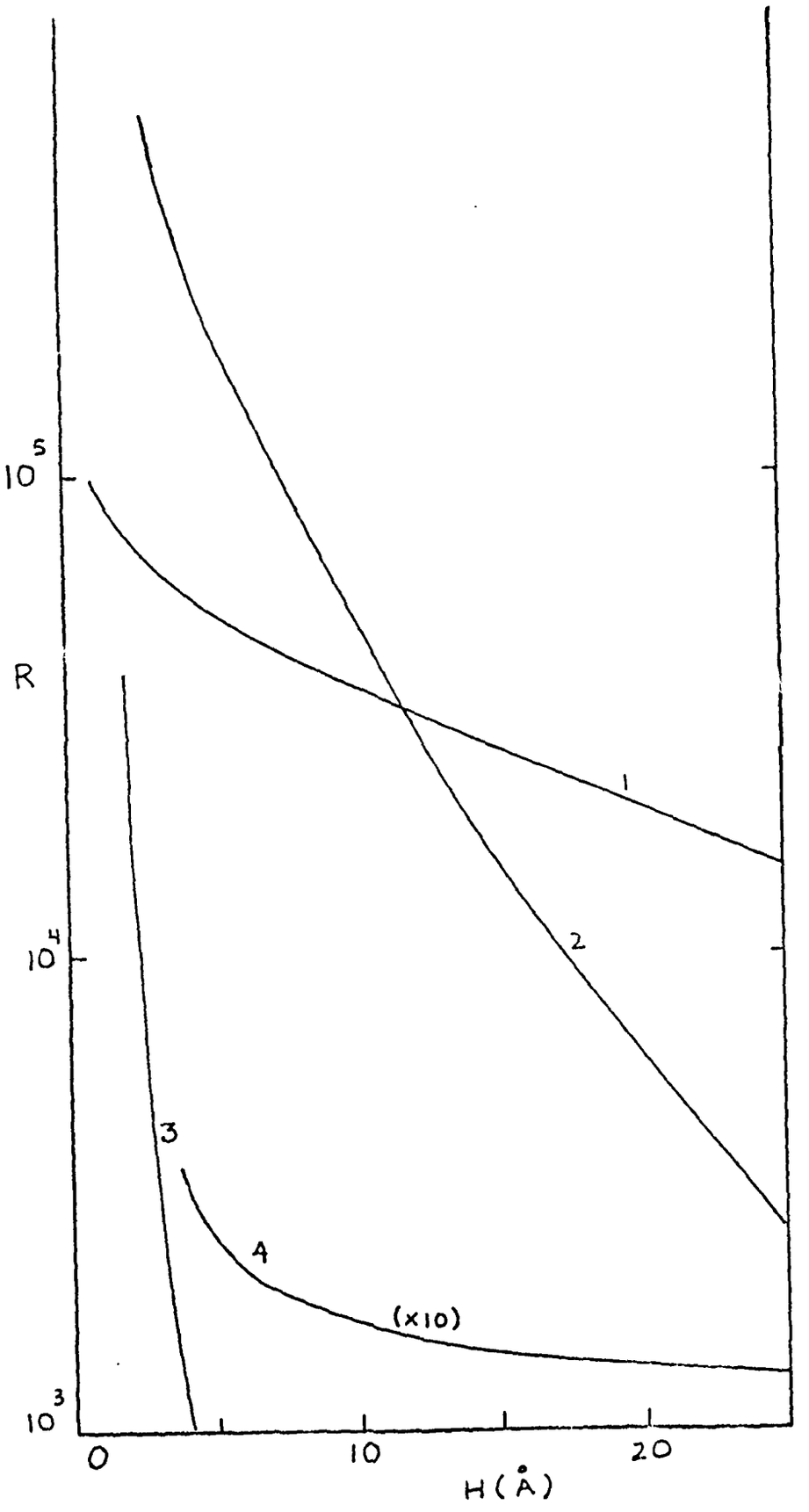

Fig. 19

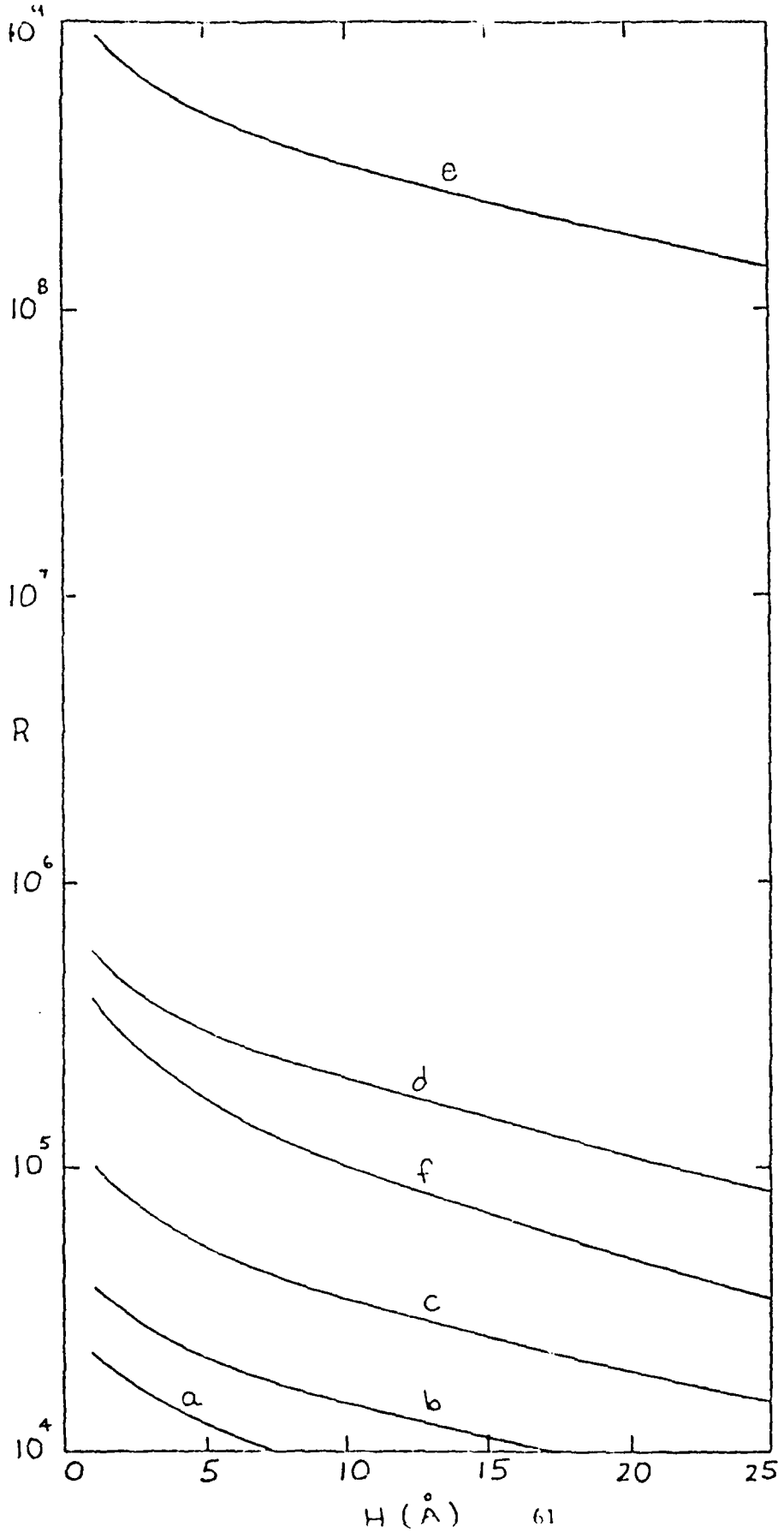

61

Fig. 20

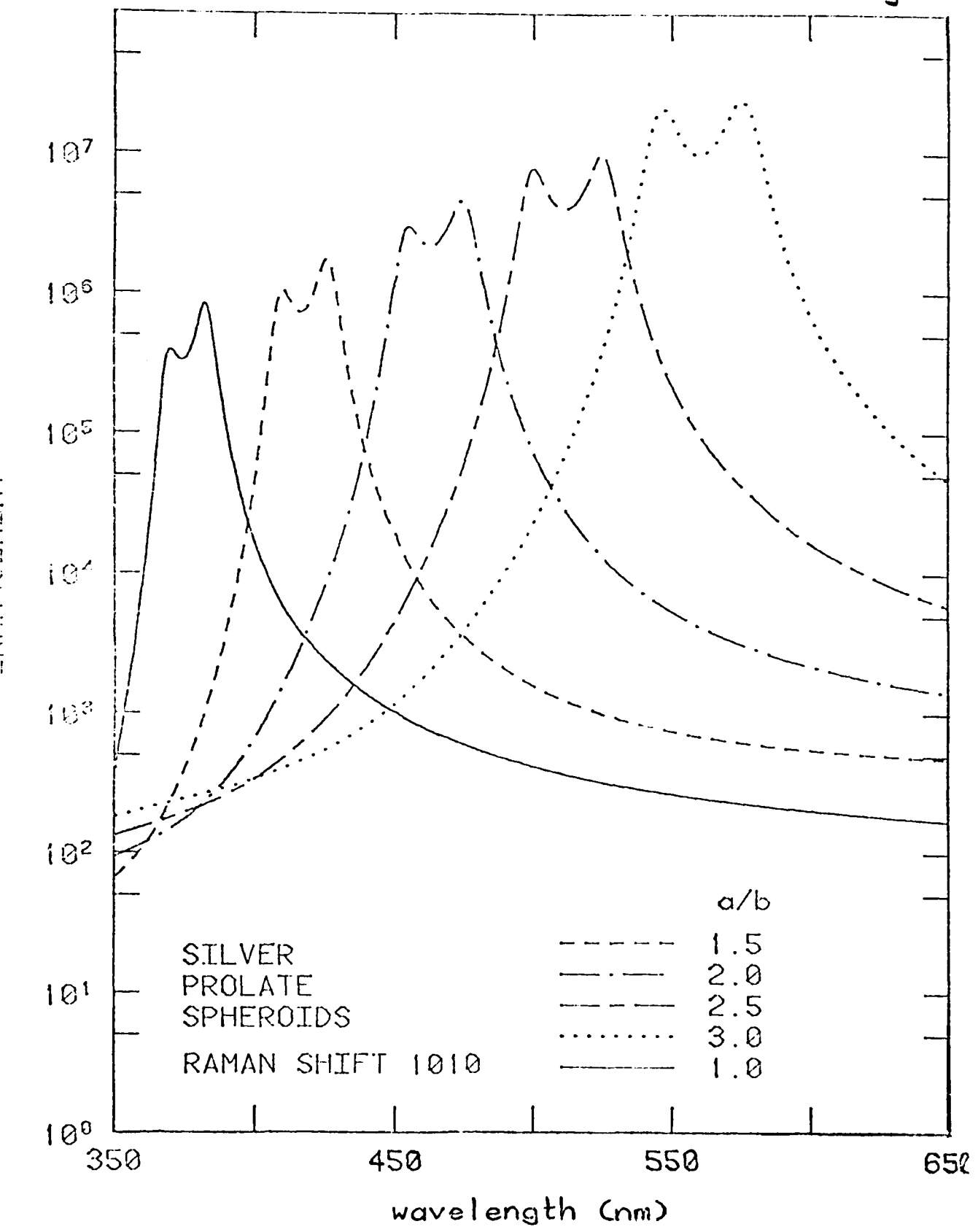
ENHANCEMENT
10^7
10^6
10^5
10^4
10^3
10^2
10^1
10^0
350
450
550
650
wavelength (nm)
SILVER
PROLATE
SPHEROIDS
RAMAN SHIFT 1010
a/b
1.5
2.0
2.5
3.0
1.0

Fig. 21

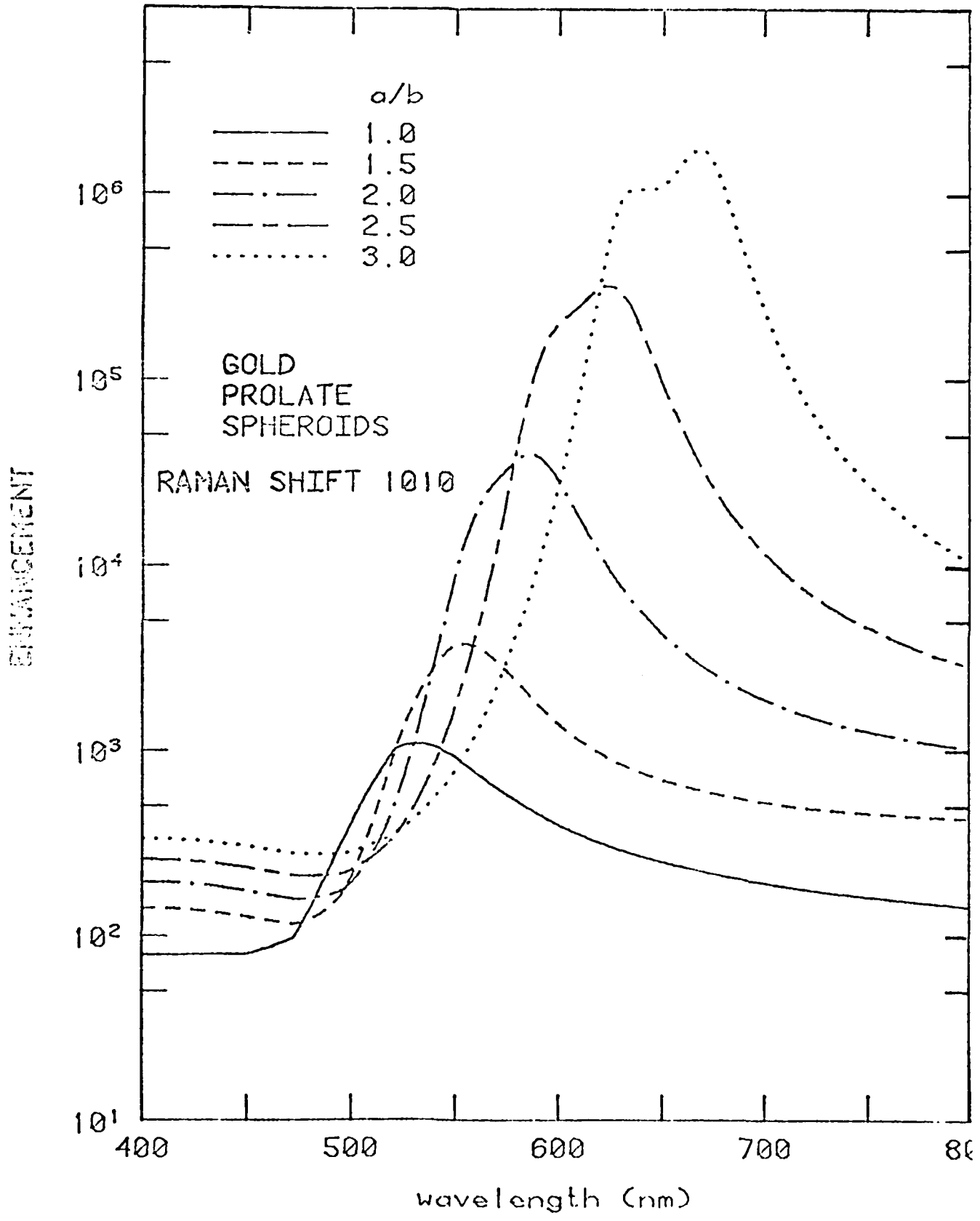
a/b
1.0
1.5
2.0
2.5
3.0
GOLD
PROLATE
SPHEROIDS
RAMAN SHIFT 1010
ENHANCEMENT
10⁶
10⁵
10⁴
10³
10²
10¹
400
500
600
700
wavelength (nm)

Fig. 22

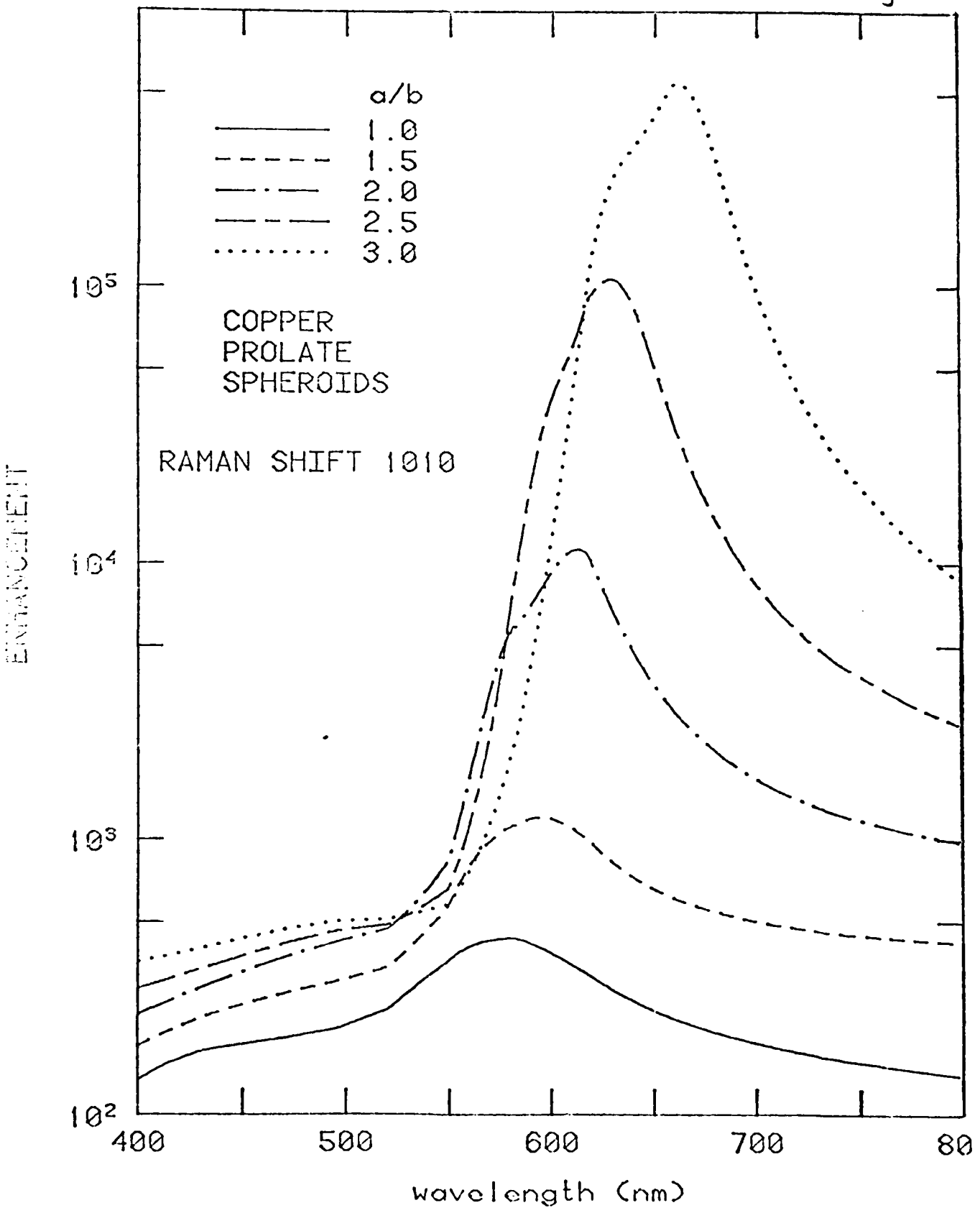
a/b
1.0
1.5
2.0
2.5
3.0
COPPER
PROLATE
SPHEROIDS
RAMAN SHIFT 1010
ENHANCEMENT
10⁵
10⁴
10³
10²
400
500
600
700
80
wavelength (nm)

Fig. 23

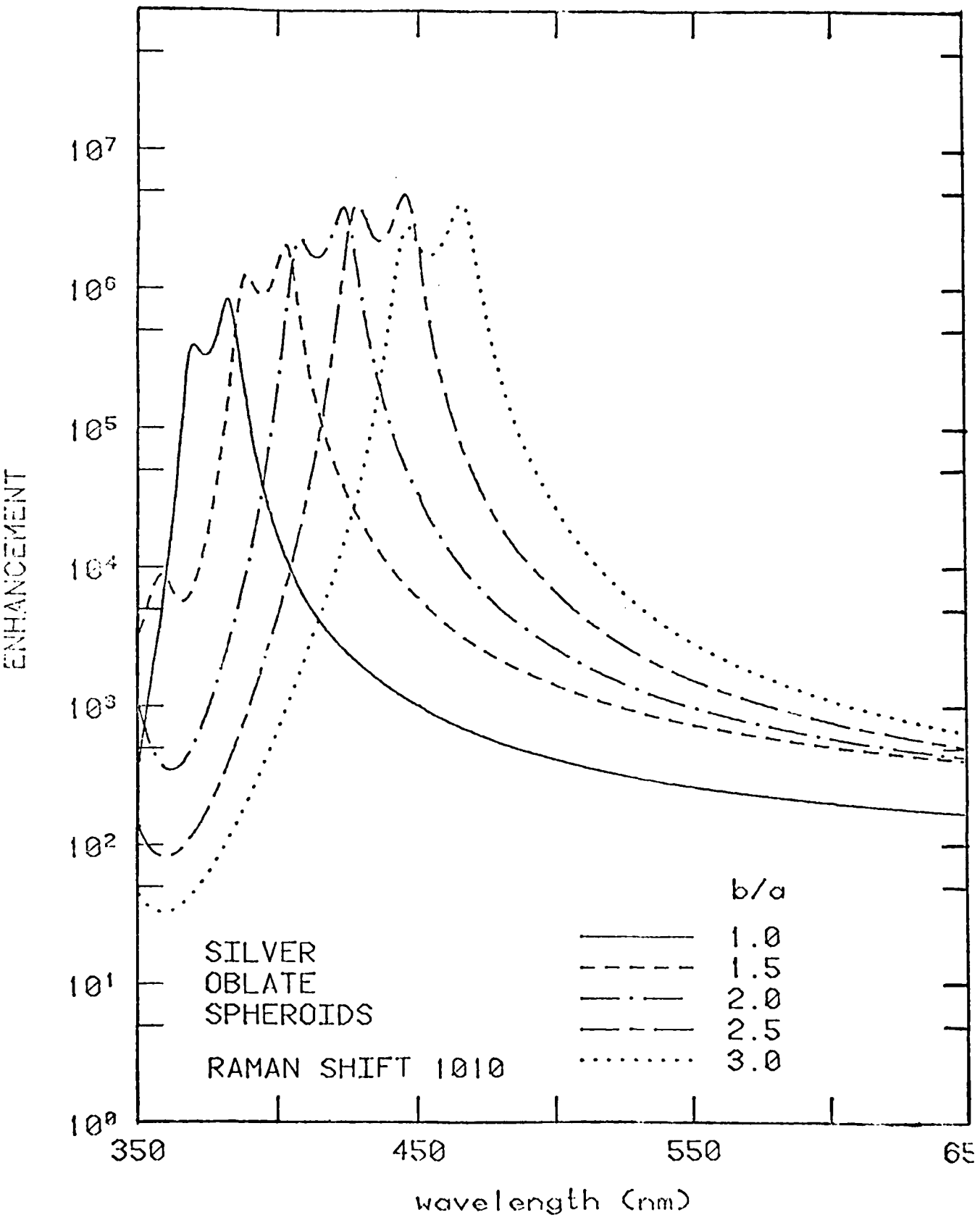
ENHANCEMENT
10^7
10^6
10^5
10^4
10^3
10^2
10^1
10^0
350
450
550
65
wavelength (nm)
SILVER
OBLATE
SPHEROIDS
RAMAN SHIFT 1010
b/a
1.0
1.5
2.0
2.5
3.0

Fig. 24

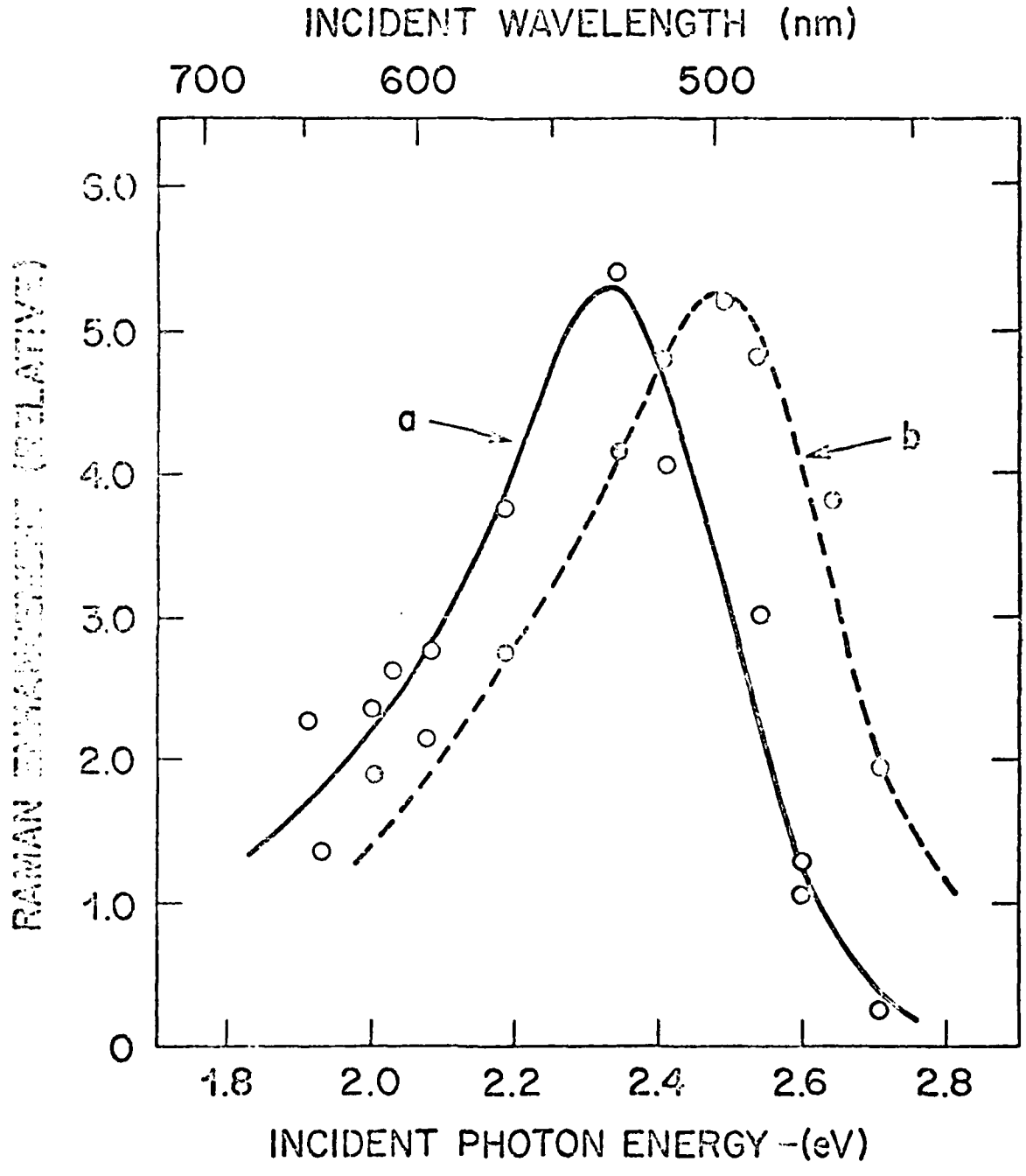
INCIDENT WAVELENGTH (nm)
700
600
500
6.0
5.0
4.0
3.0
2.0
1.0
0
a
b
1.8
2.0
2.2
2.4
2.6
2.8
INCIDENT PHOTON ENERGY -(eV)

Fig. 25

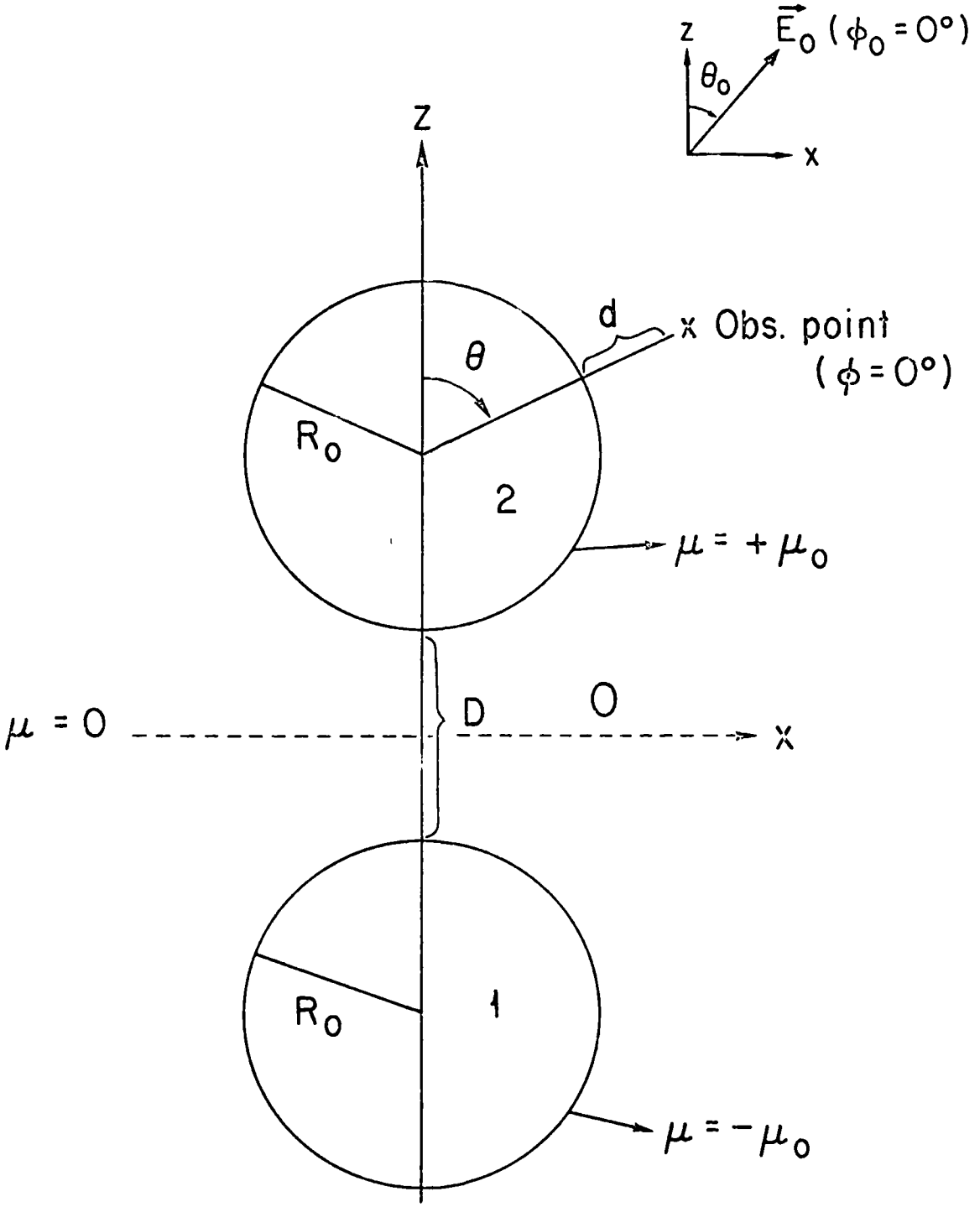
z
$\vec{E}_0$ ($\phi_0 = 0°$)
θ_0
x
Z
d
x Obs. point
($\phi = 0°$)
θ
R_0
2
$\mu = +\mu_0$
$\mu = 0$
D
O
x
R_0
1
$\mu = -\mu_0$

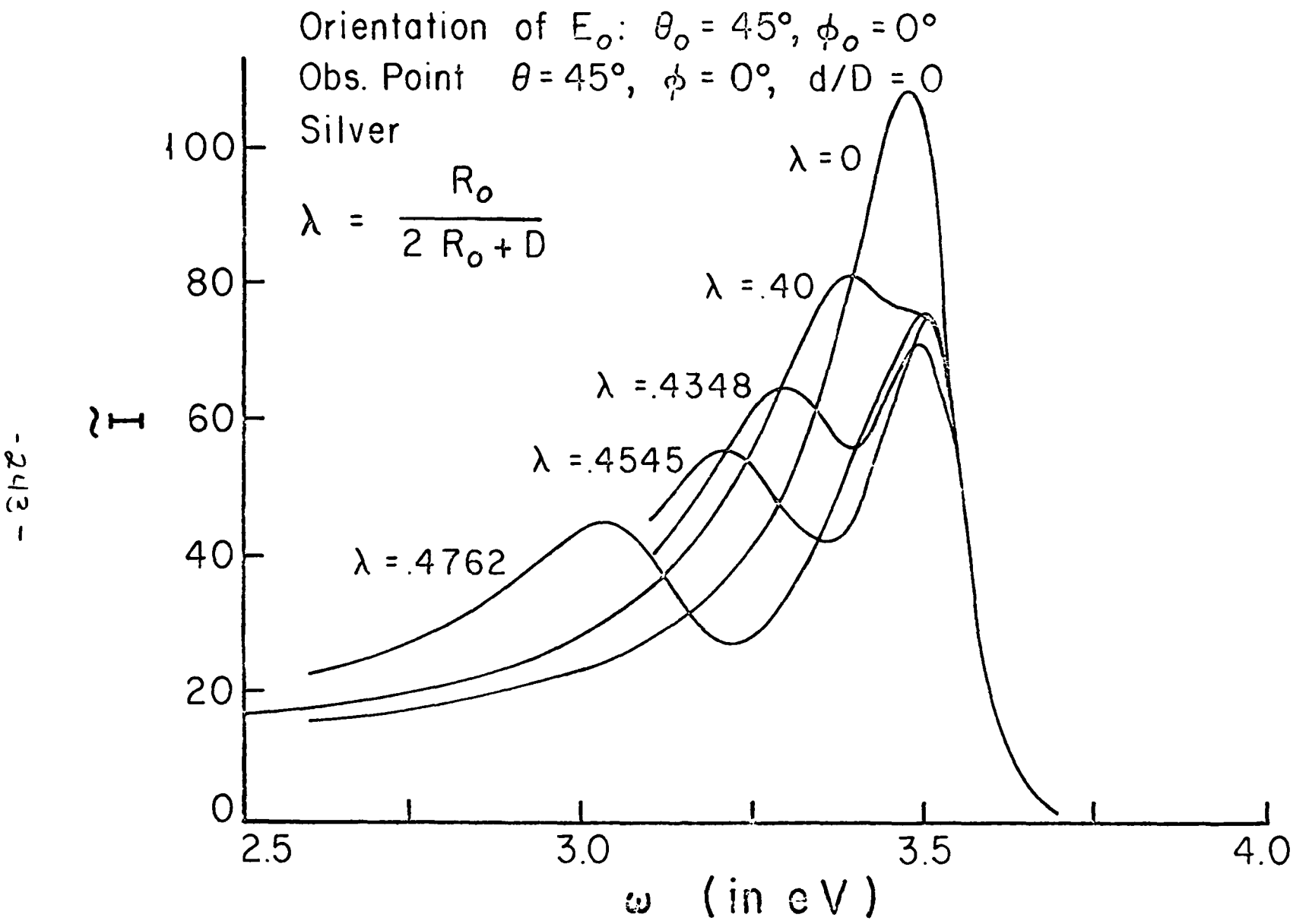
Orientation of E_o: $\theta_o = 45°$, $\phi_o = 0°$
Obs. Point $\theta = 45°$, $\phi = 0°$, d/D = 0
Silver
$\lambda = \frac{R_o}{2R_o + D}$
λ = 0
λ = .40
λ = .4348
λ = .4545
λ = .4762
I
100
80
60
40
20
0
2.5
3.0
3.5
4.0
ω (in eV)

Fig. 3a

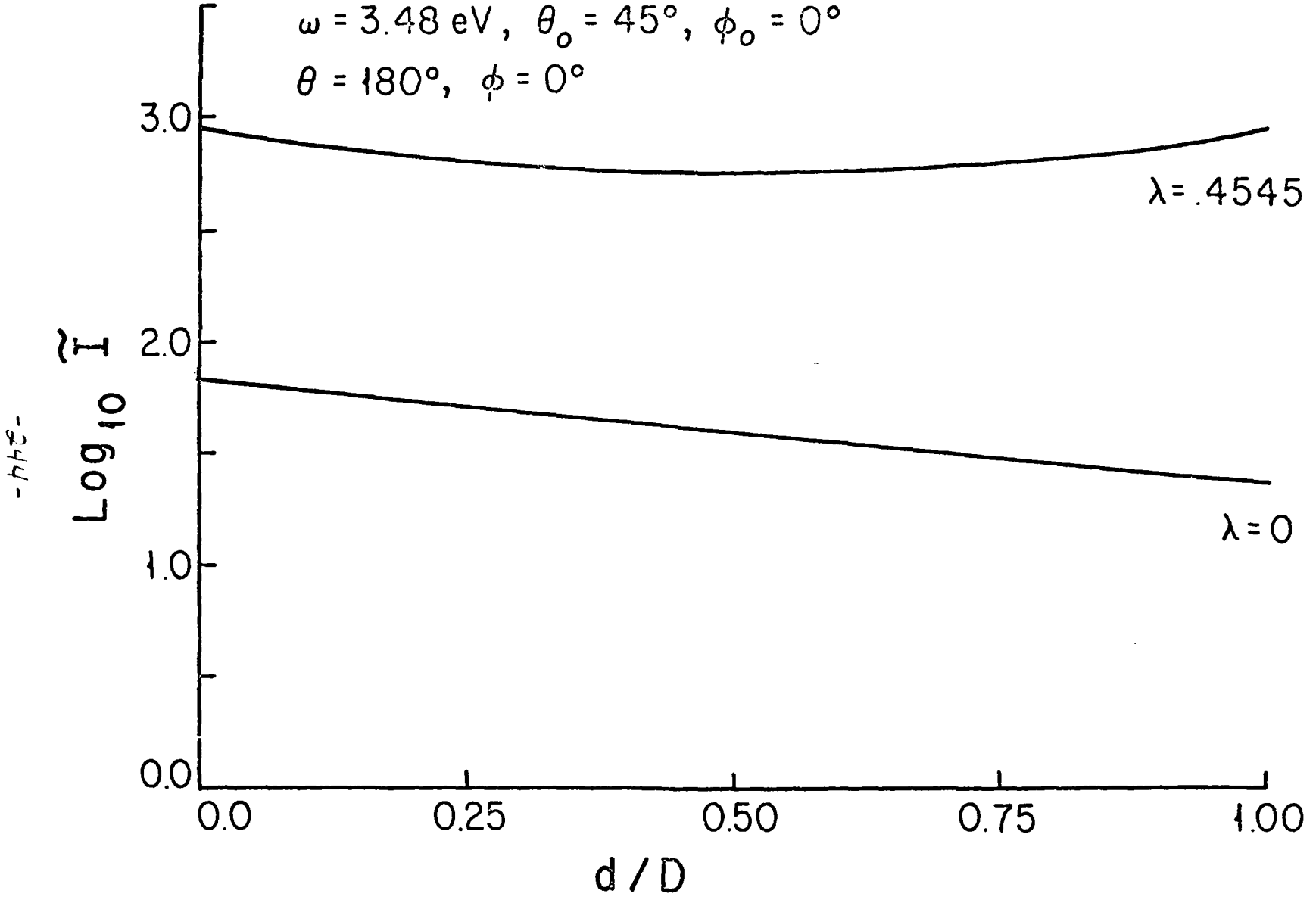

Fig. 27a

SURFACE SCIENCE 323 (19[illegible]) [illegible]

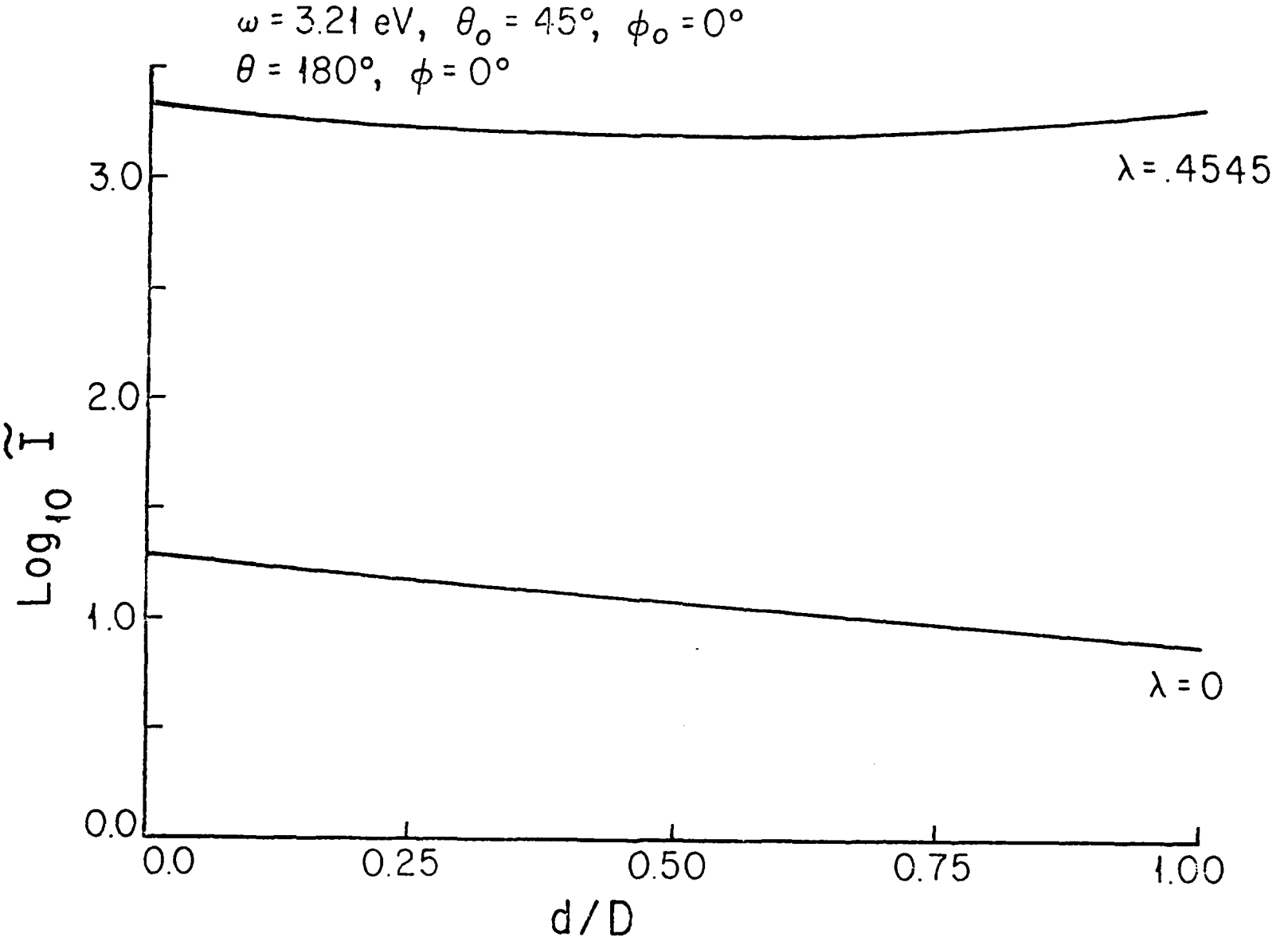
ω = 3.21 eV, θ0 = 45°, φ0 = 0°
θ = 180°, φ = 0°
λ = .4545
λ = 0
Log10 Ĩ
3.0
2.0
1.0
0.0
0.0
0.25
0.50
0.75
1.00
d/D

-345-

Fig. 2b

Fig. 29a

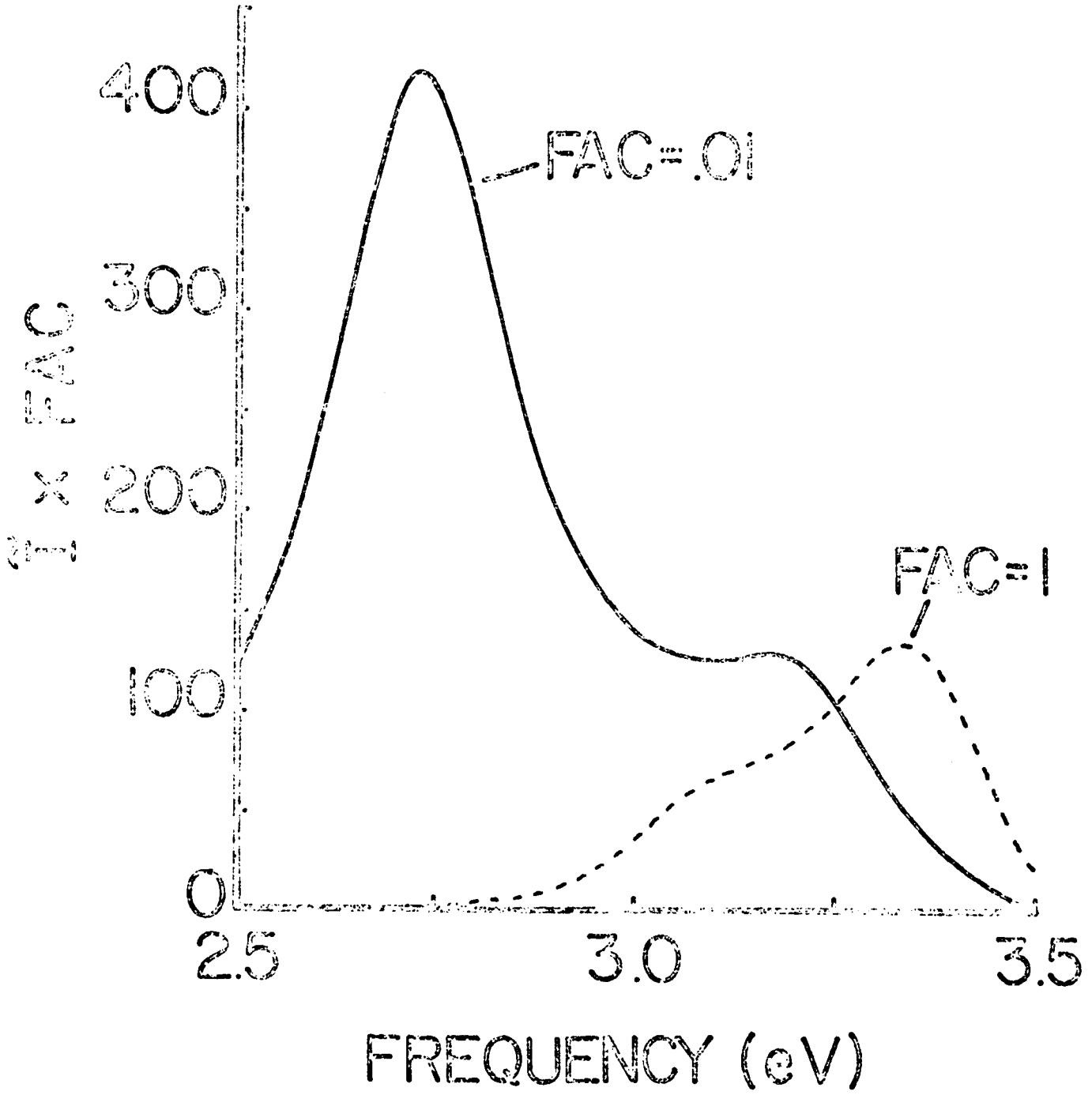

Fig. 28b

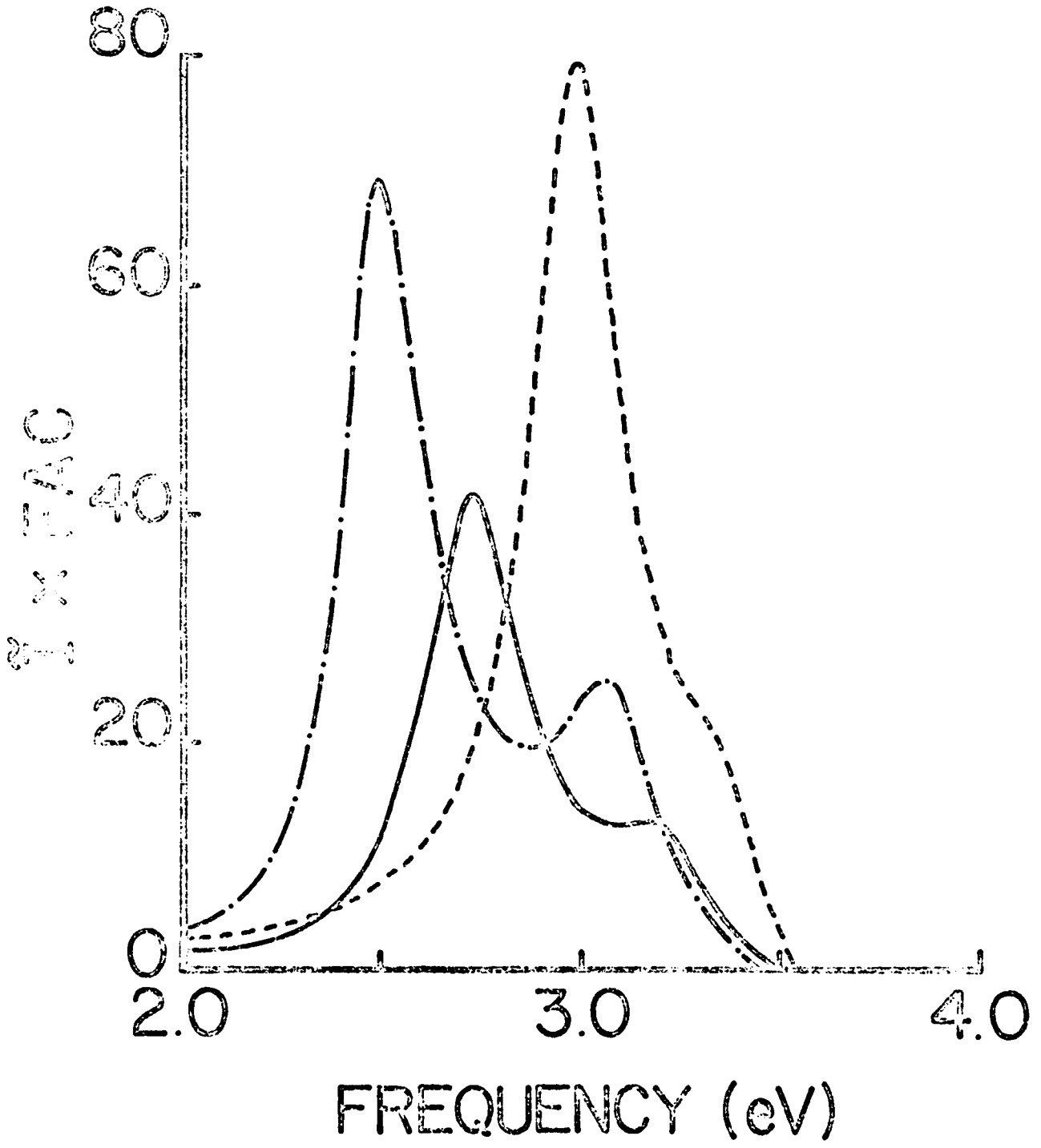

Fig. 29

Raman intensity
450
500
600
700
800
excitation wavelength / nm

Fig. 30

Ag/IM KCl in H_2O

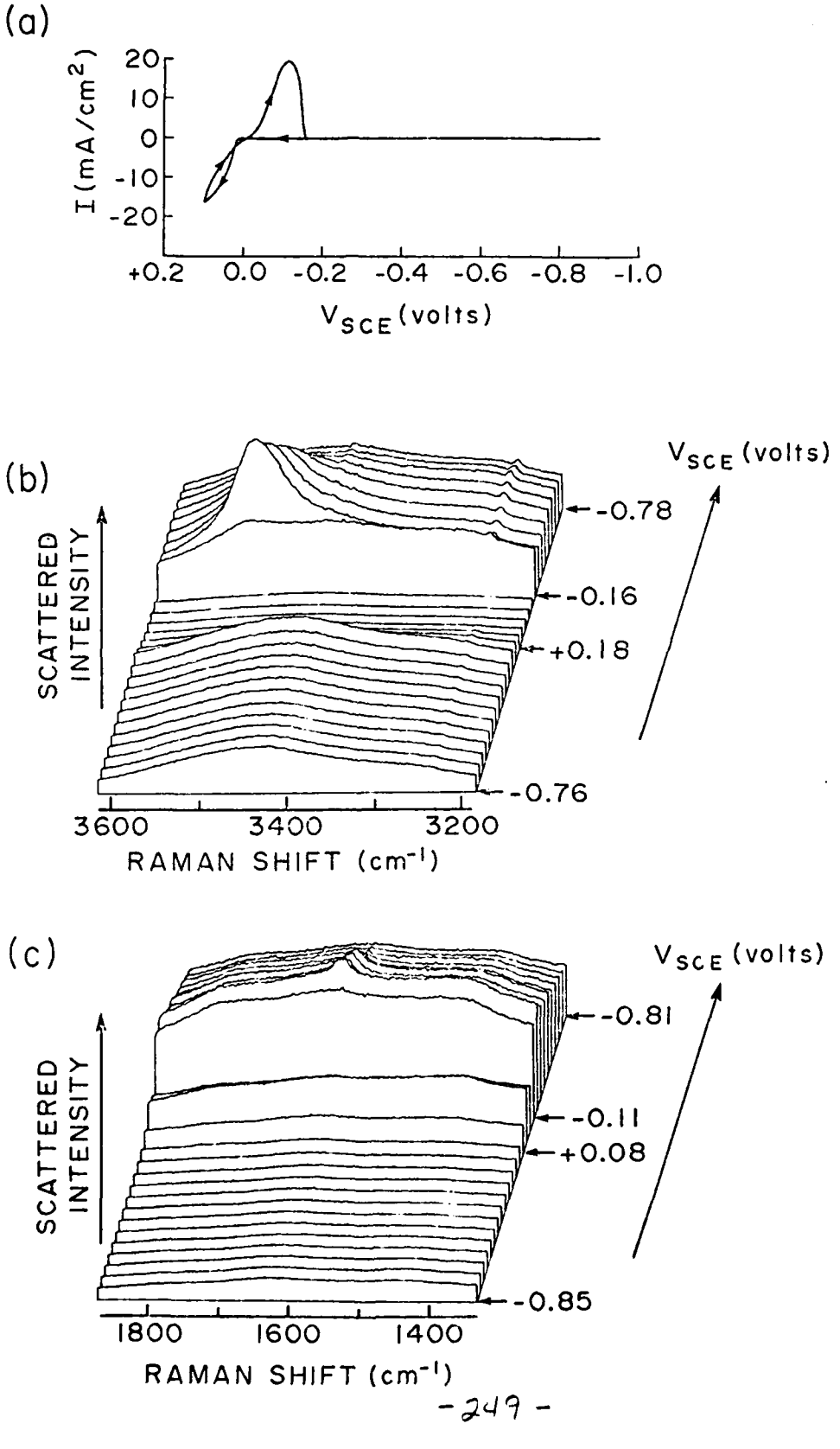

Ag/1M KBr in H_2O(50%)+D_2O(50%)

Fig. 31

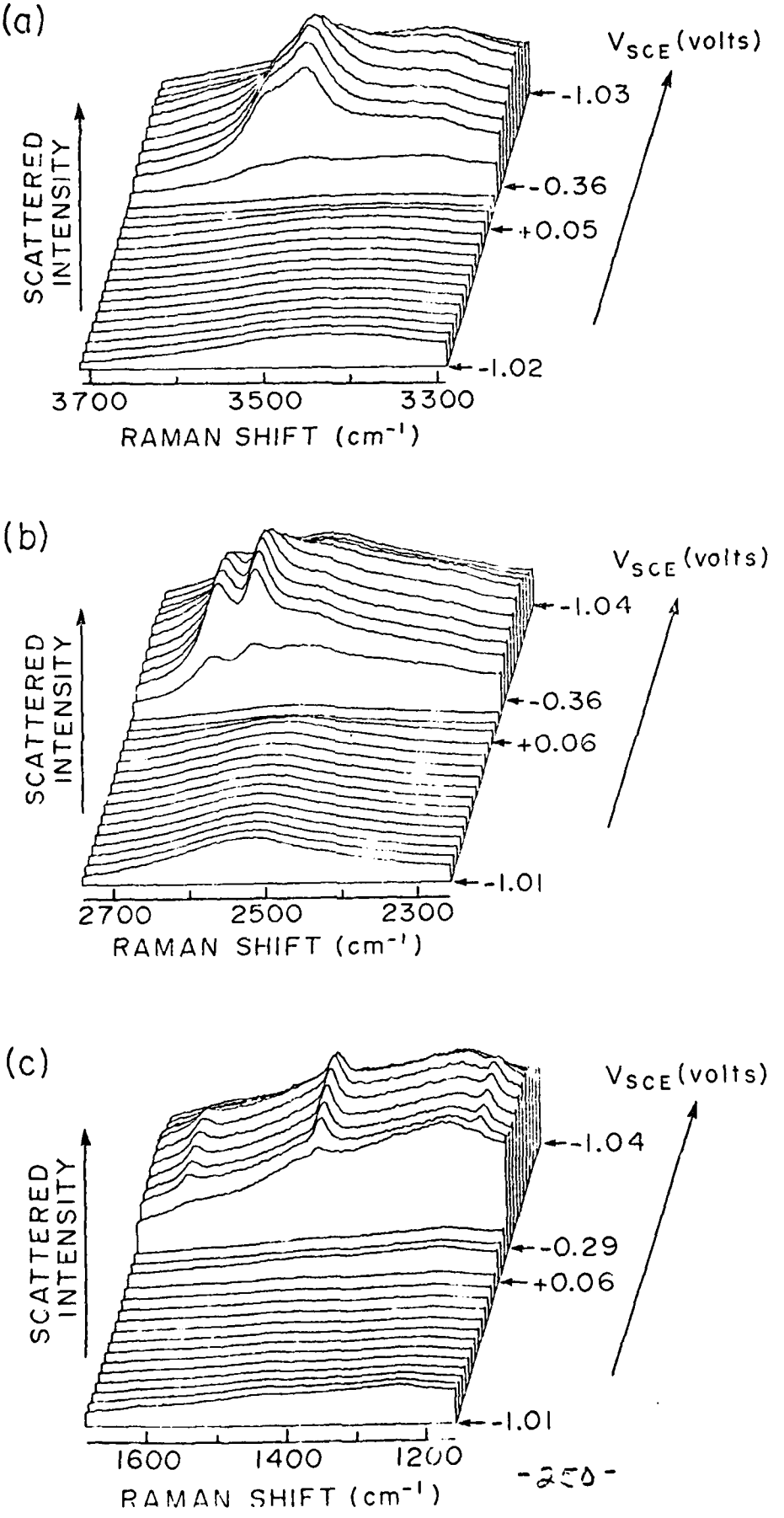

References

[1] R. Van Duyne, in Chemical and Biochemical Applications of Lasers, Vol. 4, Ed. C.B. Moore (Academic Press, New York, 1978).

[2] S. Efrima and H. Metiu, Israel J. Chem. 18, 17 (1979).

[3] E. Burstein, C.Y. Chen and S. Lundquist, in Light Scattering in Solids, ed. J.L. Birman, H.Z. Cummins and K.K. Rebane, Plenum Press, New York, 1979, p. 479.

[4] T.E. Furtak and J. Reyes, Surface Sci. 93, 351 (1980).

[5] A. Otto, Proc. 6th Solid-Vacuum Interface Conference, Delft, The Netherlands, May 7-9, 1980; Applied Surface Sci. 6, 308 (1980).

[6] R.K. Chang and T.F. Furtak, eds., Surface Enhanced Raman Scattering, Plenum, New York, 1981.

[7] J.D. Jackson, Classical Electrodynamics, J. Wiley, New York, 1975.

[8] J.A. Stratton, Electromagnetic Theory, McGraw-Hill,New York, 1941.

[9] W.R. Smythe, Static and Dynamic Electricity, 3rd edition, McGraw-Hill, New York, 1969.

[10] L.M. Landau and E.M. Lifshitz, Electrodynamics of Continuous Media, Pergamon, Oxford, 1971.

[11] M. Born and E. Wolf, Principles of Optics, 4th edition, Pergamon, New York, 1970.

[12] H. Hagstrum, Phys. Rev. 96, 336 (1954).

[13] R.P. Van Duyne, private communication.

[14] C-T. Tai, Dyadic Green's Functions in Electromagnetic Theory, Intext, San Francisco, 1971.

[15] R. Loudon, The Quantum Theory of Light, Clarendon, Oxford, 1973.

[16] W.H. Louisell, Quantum Statistical Properties of Radiation, Wiley, New York, 1973.

[17] W. Heitler, Quantum Theory of Radiation, 3rd ed, Oxford U. Press, 1954.

[18] R.M. Hammaker, S.A. Francis and R.P. Eischens, Spectrochim. Acta. 21, 1295 (1965); R.A. Shigeshi and D.A. King, Surface Sci. 58, 484 (1976); G.D. Mahan and A.A. Lucas, J. Chem. Phys, 68, 1344 (1978); J.C. Campuzano and R.G. Greenler, Surface Sci. 83, 301 (1979); M. Scheffler, Surface Sci. 81, 562 (1979); M. Moskovits and J.E. Hulse, Surface Sci. 78, 397 (1979); S. Efrima and H. Metiu, Surface Sci. 92, 433 (1980); 108, 329 (1981) and 109, 109 (1981); S. Efrima, Surface Sci. 110, 56 (1981).

[19] G.L. Eesley and J.R. Smith, Solid State Commun. 31, 815 (1979); I. Pockrand and A. Otto, Solid State Commun. 35, 861 (1980).

[20] J. Behringer in Molecular Spectroscopy, Vol. 2, The Chemical Society, London (1974).

[21] S. Efrima and H. Metiu, J. Chem. Phys. 70, 1939 (1979).

[22] H. Metiu, The use of reciprocity theorem in surface enhanced spectroscopy, unpublished.

[23] S. Efrima and H. Metiu, J. Chem. Phys. 70, 1602 (1979).

[24] S. Efrima and H. Metiu, J. Chem. Phys. 20, 2297 (1979).

[25] J.B. Valder and S. Ushioda, Phys. Rev. Letters 38, 1098 (1977) and references therein.

[26] S.G. Schultz, M. Janik-Czachor and R.P. Van Duyne, Surface Sci. 104, 419 (1981).

[27] G. Binning, H. Roher, Ch. Gerber and E. Weibel, Tunneling Through a Controllable Vacuum Gap, submieted to Phys. Rev. Lett.

[28](a) B. Pettinger and U. Wenning, Chem. Phys. Letters 56, 253 (1978).

(b) B. Pettinger, U. Wenning and D.M. Kolb, Ber. Bunsenges. Phys. Chem. 82, 1326 (1978).

[29] J.A. Harrison and H.R. Thirsk in Electroanalytical Chemistry Vol. 5, Ed. A.J. Bard (Dekker, N.Y. 1971) p. 67-148.

[30] D.M. Kolb and R. Kötz, Surface Sci. 64, 96 (1977).

[31] P.K. Aravind, R. Randell and H. Metiu, Chem. Phys. Lett. (in print).

[32] M. Udagawa, C-C. Chen, J. Hemminger and S. Ushioda, Phys. Rev. B23, 6843 (1981).

[33] J.E. Rowe, C.V. Shank, D.A. Zwemer and C.A. Murray, Phys. Rev. Lett, 44, 1770 (1980).

[34] T.H. Wood, D.A. Zwemer, C.V. Shank and J.E. Rowe, The Dependence of Surface Enhanced Raman Scattering on Surface Preparation: Evidence for an Electromagnetic Mechanism (preprint, 1981).

[35] A. Campion, J. Keenan Brown and V.M. Grizzle, Surface Sci. Lett. (submitted, 1981).

[36] R.R. Chance, A. Prock and R. Silbey, in Advances in Chemical Physics, ed. I. Prigogine and S.A. Rice (Wiley, N.Y. 1978) p. 1-65.

[37] K.H. Drexhage in Progress in Optics XII, ed. E. Wolf, North Holland, Amsterdam, (1974) p. 165.

[38] A. Adams, R.W. Rendell, W.P. West, H.P. Broida, P.K. Hansma and H. Metiu, Phys. Rev. B21, 5565 (1980).

[39] A. Adams, R.W. Rendell, R.W. Garnett, P.K. Hansma and H. Metiu, Optics Commun. 34, 417 (1980).

[40] A. Campion, A.R. Gallo, C.B. Harris, H.J. Robota and P.M. Whitmore, Chem. Phys. Lett. 73, 447 (1980).

[41] C.F. Eeagen, W.H. Webber, S.L. McCarthy and R.W. Terhune, Chem. Phys. Lett. 75, 274 (1980).

[42] I. Pockrand, A. Brillante and D. Mobius, Chem. Phys. Lett. 69, 499 (1980).

[43] P.M. Whitmore, H.J. Robota and C.B. Harris, J. Chem. Phys. (submitted, 1981).

[44] A. Rosetti and L.E. Brus, J. Chem. Phys. 73, 572 (1980).

[45] G. Korzeniewski, T. Maniv and H. Metiu, Chem. Phys. Lett. 73, 212 (1980).

[46] G. Korzeniewski, T. Maniv and H. Metiu, J. Chem. Phys. 76, xxxx (1982).

[47] W.H. Webber and G.W. Ford, Phys. Rev. Lett. 44, 7774 (1980).

[48] R. Fuchs and R.G. Barrera, Phys. Rev. B24, 2940 (1981).

[49] J. Arias, P.K. Aravind and H. Metiu, Chem. Phys. Lett. (in press).

[50] H. Raether, Excitation of Plasmons and Interband Transitions by Electrons, Springer, N.Y. 1980.

[51] J.W.S. Rayleigh, Proc. Roy. Soc. A79, 399 (1907); Philosoph. Mag. 14, 70 (1907).

[52] V. Celli, A. Marvin and F. Toigo, Phys. Rev. B, 11 1779 (1975).

[53] A. Marvin, F. Toigo and V. Celli, Phys. Rev. B, 11, 2777 (1975).

[54](a) A.A. Maradudin and D.L. Mills, Phys. Rev. B, 11, 1392 (1975).

(b) An error in this paper has been corrected by G.S. Agarwal, Phys. Rev. B, 14, 846 (1976) and (c) B. Laks and D.L. Mills, Phys. Rev. B, 20, 4962 (1979) and B, 21, 5175 (1980).

[55] E. Kroger and E. Kretschmann, Z. Physik, 237, 1 (1970); E. Kretschmann and E. Kroger, J. Opt. Soc. Amer. 65, 150 (1975).

[56] R. Petit, ed., Electromagnetic Theory of Gratings, Springer, Berlin, 1980.

[57] S.S. Jha, J.R. Kirtley and J.C. Tsang, Phys. Rev. B22, 3973 (1980).

[58] P.K. Aravind, E. Hood and H. Metiu, Surface Sci. 109, 95 (1981).

[59] T.S. Rahman and A.A. Maradudin, Phys. Rev. B21, 504 (1980).

[60] J.C. Tsang, J.R. Kirtley and J.A. Bradley, Phys. Rev. Lett. 43, 772 (1979).

[61] A. Girlando, M.R. Philpot, D. Heitman, J.D. Swalen and R. Santo, J. Chem. Phys. 72, 5187 (1980).

[62] P.N. Sanda, J.M. Warlaumont, J.E. Demuth, J.C. Tsang, K. Christmann and J.A. Bradley, Phys. Rev. Lett. 45, 1519 (1980).

[63] A. Adams, J. Moreland and P.K. Hansma, Surface Sci. 111, 351 (1981).

[64] A. Adams, J. Moreland, P.K. Hansma, L. Schlesinger, Phys. Rev. B (submitted).

[65] J. Callaway, Quantum Theory of the Solid State, Academic Press, New York, 1974.

[66] D.L. Mills at U.C. Irvine and H. Metiu at U.C. Santa Barbara.

[67] D.L. Mills, Phys. Rev. B12, 4036 (1975); A.A. Maradudin and W. Zierau, Phys. Rev. B14, 484 (1976); E. Kroeger and E. Kretschmann, Phys. Stat. Sol. 76b, 515 (1976).

[68] A. Otto, Z. Physik. 216; 398 (1968).

[69] E. Kretschmann, Z. Physik. 241 313 (1971); D.M. Kolb, J. Phys. (Paris) 38 167 (1977); E. Kretschmann, Opt. Commun. 26, 41 (1978); A. Brillante, I. Pockrand, M.R. Philpott and J.D. Swalen, Chem. Phys. Lett. 57, 395 (1978).

[70](a) M.R. Philpott, in "Topics in Surface Chemistry," E. Kay and P.S. Bagus, eds., Plenum, New York 1979, p. 329.

(b) A. Otto in "Optical Properties of Solids - New Developments" B.O. Seraphin ed. North-Holland, Amsterdam (1976) p. 677.

[71] Y.J. Chen, W.P. Chen and E. Burstein, Phys. Rev. Lett. 36, 1207 (1976); W.P. Chen, G. Ritchie and E. Burstein, Phys. Rev. Lett. 37, 993 (1976).

[72] B. Pettinger, A. Tadjeddine and D.M. Kolb, Chem. Phys. Lett. 66, 544 (1979).

[73] R. Dornhaus, R.E. Benner, R.K. Chang and I. Chabay, Surface Sci. 101, 367 (1980).

[74] Y.M. Gerbshtein, I.A. Merkulov and D.N. Mirlin, JETP Lett. 22, 35 (1974).

[75] W.H. Weber and C.F. Eagen, Optics Letters, 4, 236 (1979).

[76] R.E. Benner, R. Dornhaus and R.K. Chang, Optics Commun. 30, 145 (1979).

[77] C.F. Eeagen, W.H. Weber, S.L. McCarthy and R.W. Terhune, Chem. Phys. Lett. 75, 274 (1980).

[78] I. Pockrand, A. Brillante and D. Mobius, Nuovo Cimento, 63B, 350 (1981).

[79] Other experimental arrangements which study fluorescence by using metal films and ATR can be found in W. Lukosz and M. Meier, Optics Lett. 6, 251 (1981); W. Lukosz and R.E. Kunz, Opt. Commun. 31, 42 (1979); R.E. Kunz and W. Lukosz, Phys. Rev. B21, 4814 (1980); W. Lukosz, Phys. Rev. B22, 3030 (1980).

[80] I. Pockrand, J.D. Swalen, J. G. Gordon II and M.R. Philpott, Surface Sci. 74, 237 (1977).

[81] I. Pockrand, J.D. Swalen, R. Santo, A. Brillante, and M.R. Philpott, J. Chem. Phys. 69, 4001 (1978).

[82] I. Pockrand and J.D. Swalen, J. Opt. Soc. Am. 68, 1147 (1978).

[83] P. G. Sherman and M.R. Philpott, J. Chem. Phys. 68, 1729 (1978).

[84] J.G. Gordon II and S. Ernest, Surface Sci. 101, 499 (1980).

[85] A. Otto, Surface Sci. 101, 99 (1980).

[86] H. Kuhn, D. Mobius and H. Bucher, in: Techniques of Chemistry, Vol. 1. Physical Methods of Chemistry, part 2b, eds. A. Weissberger and B.W. Rossiter (Wiley-Interscience, New York, 1972) Ch.7.

[87] W.N. Hansen, J. Opt. Soc. Am. 58, 380 (1968).

[88] E. Burstein, C.Y. Chen, and S.L. Lundquist in: Light Scattering in Solids, Eds. J.L. Birman, H.Z. Cummins and K.K. Reband (Plenum, New York, 1979) p. 479).

[89] C.Y. Chen, I. Davoli and E. Burstein, Surface Sci. 101, 363 (1980).

[90] H.E. Bennett, J.M. Bennett, E.J. Ashley and R.J. Motyka, Phys. Rev. 165, 766 (1968).

[91] D. Beaglehole and O. Hundery, Phys. Rev. B2, 309 (1970).

[92](a) J.G. Endriz and W.E. Spicer, Phys. Rev. Letters, 24, 64 (1970);

(b) J.G. Endriz and W.E. Spicer, Phys. Rev. B4, 4144 (1971).

[93](a) J. Crowell and R.H. Ritchie, J. Opt. Soc. Am. 60, 795 (1970).
J.M. Elson and R.H. Ritchie, Phys. Status' Solidi B62, 461 (1974).

(b) E. Kretschmann, Z. Physik. 222, 412 (1969).

[94] P.K. Aravind and H. Metiu, Chem. Phys. Lett. 74, 301 (1980).

[95] S.L. McCarthy and J. Lambe, Appl. Phys. Lett. 30, 427 (1977);

[96] J. Lambe and S.L. McCarthy, Phys. Rev. Lett. 37, 923 (1976).

[97] D. Hone, B. Muhlschlegel and D. Scalapino, Appl. Phys. Lett. 33, 203 (1978); R.W. Rendell, D.J. Scalapino and B. Muhlschlegel, Phys. Rev. Lett. 41, 1746 (1978).

[98] P.K. Hansma and H.P. Broida, Appl. Phys. Lett. 32, 545 (1978); A. Adams, J.C. Wyss and P.K. Hansma, Phys. Rev. Lett. 42, 312 (1979).

[99] J. Kirtley, T.N. Theis and J.C. Tsang, Appl. Phys. Lett. (in press).

[100] B.J. Berne and R. Pecora, Dynamic Light Scattering, Wiley, N.Y. 1976.

[101] H. Metiu and G. Korzeniewski, J. Chem. Phys. 53, 483 (1978).

[102] T. Rahman and A. Maradudin, Phys. Rev. B21. 504 (1980).

[103] R.S. Sennett and G.D. Scott, J. Opt. Soc. Am. 40, 203 (1950).

[104] L.I. Maissel and R. Glang, Handbook of Thin Film Technology (McGraw Hill, N.Y. 1970).

[105] H. Abe, K. Manzel, W. Schulze, M. Moskovits and D.P. DiLella, J. Chem. Phys. 74, 792 (1981).

[106] P.K. Aravind and H. Metiu, J. Phys. Chem. (submitted).

[107] P.K. Aravind and H. Metiu, Surface Sci. (submitted).

[108] P.M. Morse and H.Feshbach, Methods of Theoretical Physics (McGraw Hill, New York, 1953) p. 1298.

[109] M. Kerker, The Scattering of Light, Academic Press, New York, 1969.

[110] D.-S. Wang, H. Chew and M. Kerker, Appl. Opt. 19, 2256 (1980).

[111] M. Kerker, D.-S. Wang and H. Chew, Appl. Opt. 19, 3373 (1980).

[112] S.L. McCall, P.M. Platzman and P.A. Wolff, Phys. Lett. 77A, 381 (1980).

[113] B.J. Messinger, K. Ulrich von Raben, R.K. Chang and P.W. Barber, Phys. Rev. B24, 649 (1981).

[114] J.I. Gersten, J. Chem. Phys. 72, 5779, 5780 (1980).

[115] J.I. Gersten and A. Nitzan, J. Chem. Phys. 73, 3023 (1980).

[116] F.J. Adrian, Chem. Phys. Lett. 78, 45 (1981).

[117](a) G.D. Mahan, Many-Particle Physics, Plenum Press, New York, 1981, Ch. 7; (b) S. Doniach and E.H. Sondheimer, Green's Functions for Solid State Physicists, Benjamin, Reading, Mass 1976.

[118] S. Flugge, Practical Quantum Mechanics, Springer, New York, 1974.

[119] J.E. Rowe, C.V. Shank, D.A. Zwemer and C.A. Murray, Phys. Rev. Letters. 44, 1770 (1980).

[120] D.A. Zwemer, C.V. Shank and J.E. Rowe, Chem. Phys. Letters. 73, 201 (1980).

[121] D.L. Allara, C.A. Murray and M. Rhinewine, Phys. Rev. Letters. 46, 57 (1981).

[122] P.K. Aravind, A. Nitzan and H. Metiu, Surface Sci. 110, 189 (1981).

[123] D.-S. Wang and M. Kerker, Phys. Rev. B. 24, 1777 (1981).

[124] J.A. Creighton, C.G. Blatchford and M.G. Albrecht, J. Chem. Soc., Faraday Trans. II, 75, 790 (1979).

[125] M. Kerker, O. Siiman, L.A. Bumm and D.-S. Wang, Appl. Optics, 19, 3253 (1980).

[126] H. Wetzel and H. Gerischer, Chem. Phys. Lett. 76, 460 (1980).

[127] K.U. von Raben, R.K. Chang and B.L. Laube, Chem. Phys. Lett. 79, 465 (1981).

[128] H. Abe, K. Manzel, W. Schultze, M. Moskovits and D.P. LiLella, J. Chem. Phys, 74, 792 (1981).

[129] D. Langbein, Theory of van der Walls Interactions, (Springer, New York, 1974).

[130] A. Creighton, private communication.

[131] A. Creighton, in Surface Enhanced Ranian Spectroscopy, eds. R.K. Chang and T. Furtak, Plenum, 1981 (to be published).

[132] P.K. Aravind and H. Metiu, unpublished.

[133] R.K. Chang, private communication.

[134] J. Turkevich, G. Garton and P.C. Stevenson, J. Colloid Sci. Suppl. 1, 26 (1954).

[135] For example: (a) H. Abe, W. Schultze and B. Tesche, Chem. Phys. 47, 2200 (1976); (b) C.G. Granquist and R.A. Buhrman, J. Appl. Phys. 47, 2200 (1976); N. Wada, Jap. J. Appl. Phys. 7, 1278 (1968); J.D. Eversole and H.P. Broida, J. Appl. Phys. 45, 596 (1974).

[136] T.H. Wood and M.V. Klein, J. Vac. Sci. Technol. 16, 459 (1980).

[137] M. Kerker, D.-S. Wang and H. Chew, Appl. Optics 19, 4159 (1980).

[138] Y. Nomura, Science Report ofTohoku University (Japan). 1-2, pp. 25-49 (quoted in Tai. Ref. 13).

[139] H. Chew, M. Kerker, D.D. Cooke, Phys. Rev. A16, 320 (1977).

[140] D.S. Jones, The Theory of Electromagnetism (Pergamon, New York, 1964).

[141] P.B. Johnson and R.W. Christy, Phys. Rev. B6, 4370 (1972).

[142] S. Efrima and H. Metiu, Surface Sci. 92, 417 (1980).

[143] G. Ritchie, C.Y. Chen and E. Burstein, private communication.

[144] J.P. Kratohvil, M.-P. Lee and M. Kerker, Appl. Optics, 17, 1978 (1978).

[145] M. Kerker, P.J. McNulty and H. Chew in Recent Developments in Aerosol Science, ed. D.T. Shaw (John Wiley & Sons, Inc., 1978).

[146] M. Kerker and S.D. Druger, Appl. Optics 18, 1172 (1979).

[147] M. Kerker, P.J. McNulty, M. Sculley, H. Chew and D.D. Cooke, J. Opt. Soc. Am. 68, 1676 (1978).

[148] P.J. McNulty, S.D. Druger M. Kerker and H.W. Chew, Appl. Optics 18, 1484 (1979).

[149] R.E. Benner, P.W. Barber, J.F. Owen and R.K. Chang, Phys. Rev. Lett. 44, 475 (1980).

[150] E.-H. Lee, R.E. Benner, J.B. Fenn and R.K. Chang. Appl. Opt. 17, 1980 (1978); R.K. Chang, private communication.

[151] J. Gersten and A. Nitzan, J. Chem. Phys. 75, 1139 (1981).

[152] A. Nitzan and L.E. Brus, J. Chem. Phys. 74, 5321 (1981).

[153] A. Nitzan and L.E. Brus, J. Chem. Phys. 75, 2205 (1981).

[154] H. Metiu (Unpublished)

[155] D.S. Wang and M. Kerker, Phys. Rev. B24, 1777 (1981).

[156] C.Y. Chen and E. Burstein, Phys. Rev. Lett. 45, 1287 (1980) E. Burstein, C.Y. Chen and S. Lundquist, Proc. US-USSR Symposium on Inelastic Light Scattering from Solids, eds. J.L. Birman, H.Z. Cummins and K.K. Rebane, (Plenum, 1979), p. 479; E. Burstein and C.Y. Chen, Proc. CII-th International Conference on Raman Spectroscopy, Ed. W.F. Murphy (North Holland, 1980), p. 346.

[157] M. Moskovits, J. Chem. Phys. 69, 4159 (1978); Solid State Commun. 32, 59 (1979).

[158] J. Mathew and R.L. Walker, Mathematical Methods of Physics, (Benjamin, Reading, Mass., 1970).

[159] A. Wokaun, J.P. Gordon and P.F. Liao, Radiation Damping in Surface Enhanced Raman Scattering, preprint.

[160] L.D. Landau and E.M. Lifshitz, The Classical Theory of Fields, (Pergamon, Oxford, 1965), Eq. (75.4).

[161] P.F. Liao, J.G. Bergman, D.S. Chemla, A. Wokaum, J. Melngailis, A.M. Hawryluk and N.P. Economu, Chem. Phys. Lett. 82, 355 (1981).

[162] J.G. Bergman, D.S. Chemla, P.F. Liao, A.M. Glass, A. Pinczuk, R.M. Hart and D.H. Olson, Optics Lett. 6, 33 (1980).

[163] D.A. Weitz, S. Garoff and T.J. Gramilla, Optics Lett. (submitted)

[164] C.Y. Chen and E. Burstein, Bull. Am. Phys. Soc. 25, 424 (1980).

[165] J.G. Bergman, D.S. Chemla, P.F. Liao, A.M. Glass, A. Pinczuk, R.M. Hart and D.H. Olson, Optics Lett. 6, 33 (1981).

[166] A.M. Glass, P.F. Liao, J.G. Bergman and D.H. Olson, Optics Lett. 5, 368 (1980).

[167] S. Garoff, D.A. Weitz, T.J. Gramila and C.D. Hanson, Optics Lett. 6, 245 (1981).

[168] S. Garoff, R.B. Stephens, C.D. Hanson and K. Sorenson, J. Luminescence (in print).

[169] D.A. Weitz, S. Garoff, C.D. Hanson, T.J. Gramila and J.I. Gersten, Fluorescent Lifetimes of Molecules on Silver Island Films, Optics Lett. (submitted).

[170] R.S. Sennett and G.D. Scott, J. Opt. Soc. Am. 40, 203 (1950).

[171] L.I. Maissel and R. Glang, Handbook of Thin Film Technology (McGraw-Hill, N.Y., 1970).

[172] U. Laor and G.C. Schatz, Chem. Phys. Lett. 82, 566 (1981).

[173] J.C. Garland and D.B. Tanner, Electrical Transport and Optical Properties of Inhomogeneous Media (Am. Inst. Phys., New York, 1978).

[174] J.M. Ziman, Models of Disorder (Cambridge U. Press, 1979).

[175] P.M. Morse and H. Feshbach, Methods of Mathematical Physics, (McGraw-Hill, New York, 1953).

[176] W.M. Gelbart in Correlation Functions and Quasiparticle Interactions in Condensed Matter, ed. J.W. Halley (Plenum, New York, 1978) p. 365.

[177] D.L. Jeanmaire and R.P. Van Duyne, J. Electroanal. Chem. 84, 1 (1977).

[178] M.G. Albrecht and J.A. Creighton, J. Am. Chem. Soc. 99, 5215 (1977).

[179] Earlier work has obtained Raman spectra of surface molecules but did not recognize the existence of the enhancement: M. Fleischmann, P.J. Hendra and A.J. McQuillan, Chem. Phys. Lett. 26, 163 (1974); R.L. Paul, A.J. McQuillan, P.J. Hendra and M. Fleischmann, J. Electroanal. Chem. 66, 248 (1975); A.J. McQuillan, P.J. Hendra, and M. Fleischmann, J. Electroanal. Chem. 65, 933 (1975); M. Fleischmann, P.J. Hendra, A.J. McQuillan, R.L. Paul and E.S. Reid, J. Raman. Spec. 4, 269 (1976). Commun. 32, 59 (1979).

[180] R.R. Smardewski, R.J. Coulton and J.S. Murday, Chem. Phys. Letters, 68, 53 (1979).

[181] (a) G.L. Eesley, Phys. Letters 81A, 193 (1981); (b) G.L. Eesley and J.M. Burkstrand, Phys. Rev. B24, 582 (1981).

[182] J. Pockrand and A. Otto, Solid State Commun. 35, 861 (1981).

[183] C.A. Murray, D.L. Allara and M. Rhinewine, Phys. Res. Lett. 46, 57 (1981).

[184] T.H. Wood and M.V. Klein, Solid State Commun. 35, 263 (1980).

[185] T.H. Wood, M.V. Kline and D.A. Zwemer, Surface Sci. 107, 625 (1981).

[186] H. Metiu, in Surface Enhanced Raman Scattering, eds. P.K. Chang and T.E. Furtak (Plenum, 1981), ch. I.

[187] G.L. Eesley, Phys. Rev. B24, Nov. 15 (1981).

[188] F. Fujimoto and K. Komaki, J. Phys. Soc. Japan 25, 1679 (1968); F. Fujimoto, K. Komaki and K. Ishida, J. Phys. Soc. Japan 23, 1186 (1967).

[189] E. Kretschmann, T.A. Calcott and E.T. Arakawa, Surface Sci. 91, 237 (1980).

[190] C.G. Blatchford, J.R. Campbell and J.A. Creighton, Surface Sci. 108, 411 (1981).

[191] A. Girlando, J.G. Gordon, D. Heitmann, M.R. Philpott, H. Seki and J.D. Swalen, Surface Sci. 101, 417 (1980).

[192] J.A. Creighton, M.G. Albrecht, R.E. Hester and J.A.D. Matthew, Chem. Phys. Lett. 55, 55 (1978).

[193] H. Seki and M.R. Philpott, J. Chem. Phys. 73, 5376 (1980); H. Seki, J. Vac. Sci. Tech. 18, 633 (1981); H. Seki, Surface Sci. (accepted); H. Seki, The role of direct surface interaction in surface enhanced Raman scattering by pyridine and CO on silver (preprint); H. Seki, Surface enhanced Raman scattering of pyridine on different silver surfaces (preprint).

[194] I. Pockrand and A. Otto, Solid State Commun. 38, 1159 (1981); I. Pockrand and A. Otto, Solid State Commun. 37, 109 (1981); I. Pockrand and A. Otto, Appl. Surface Sci. 6, 362 (1980); I. Pockrand, Chem. Phys. Lett. (in print); I. Pockrand, J. Billmann and A. Otto, J. Chem. Phys. (submitted). Other works are quoted in these references.

[195] (a) D. Pines, Elementary Excitations in Solids, W.A. Benjamin, New York, 1964. (b) D. Pines and P. Nozieres, The Theory of Quantum Liquids, W.A. Benjamin, New York, 1966.

[196] T. Maniv and H. Metiu, J. Chem. Phys. 72, 1996 (1980).

[197] T. Maniv and H. Metiu, Phys. Rev. B22, 4731 (1980).

[198] T. Maniv and H. Metiu, Fresnel formulas for the electromagnetic field for a jellium model with RPA, J. Chem. Phys. (1982).

[199] T. Maniv and H. Metiu, J. Chem. Phys. 76, 696 (1982).

[200] P.J. Feibelman, Phys. Rev. Lett. 34, 1092 (1975); Phys. Rev. B12, 1319, 4282 (1975); Phys. Rev. B14, 1762 (1976).

[201] G. Mukhopadhyay and S. Lundquist, Solid State Commun. 21, 629 (1977); Phys. Scripta. 17, 19 (1978).

[202] D.M. Newns, Phys. Rev. B1, 3304 (1970); D.E. Beck and V. Celli, Phys. Rev. B2, 2955 (1970).

[203] K.L. Kliewer and R. Fuchs, Phys. Rev. 172, 607 (1968); R. Fuchs and K.L. Kliewer, Phys. Rev. 185, 905 (1969); K.L. Kliewer and R. Fuchs, Adv. Chem. Phys. 27, 355 (1974); K.L. Kliewer, in Photo-emission and the Electronic Properties of Surfaces, edited by B. Feuerbacher, B. Fitton and R.F. Willis (Wiley, New York, 1978).

[204] P. R. Hilton and D.W. Oxtoby, J. Chem. Phys. 72, 6346 (1980).

[205] G.W. Ford and W.H. Weber, Surface Sci. 109, 451 (1981).

[206] W.E. Palke, Surface Sci. 97, L331 (1980).

[207] T. Maniv and H. Metiu, Chem. Phys. Lett. 79, 79 (1981).

[208] S.L. McCall and P.M. Platzman, Phys. Rev. B22, 1660 (1980).

[209] J.I. Gersten, R.L. Birke and J.R. Lombardi, Phys. Rev. Lett. 43, 147 (1979).

[210] E. Burstein, Y.J. Chen, C.Y. Chen, S. Lundquist and E. Tosatti, Solid State Commun. 29, 567 (1979).

[211] G.W. Robinson, Chem. Phys. Lett. 76, 192 (1980).

[212] T.K. Lee and J.L. Birman, Phys. Rev. B22, 5953, 5961 (1980).

[213] H. Ueba, J. Chem. Phys. 73, 725 (1980); H. Ueba and S. Ichimura, J. Chem. Phys. 74, 3070 (1981).

[214] M. Philpott, J. Chem. Phys. 62, 1812 (1975).

[215] P.W. Anderson, Phys. Rev. 124, 41 (1961); U. Fano, Phys. Rev. 124, 1866 (1961).

[216] J.E. Demuth and Ph. Avouris, Phys. Rev. Lett. 47, 61 (1981); Ph. Avouris and J.E. Demuth, 75, 4783 (1981); J.E. Demuth and P.N. Sanda, Phys. Rev. Lett. 47, 57 (1981).

[217] R. Naaman, S.J. Buelow, O. Cheshnousky and D.R. Herschbach, J. Phys. Chem. 84, 2692 (1980).

[218] G.W. Ford and W.H. Weber, Surface Sci. 110, L587 (1981).

[219] A.Z. Genack, personal communication.

[220] L.A. Sanchez, R.L. Birke and J.R. Lombardi, Chem. Phys. Lett. 79, 219 (1981).

[221] R.L. Birke, personal communication.

[222] L.A. Sanchez, R.L. Birke and J.R. Lombardi, A.C.S. Advances in Chemistry Series, to be published.

[223] B. Pettinger, M.R. Philpott and J.G. Gordon II, J. Chem. Phys, 74, 934 (1981).

[224] M. Fleischman, P.J. Hendra, I.R. Hill and M.E. Pemble, J. Electronal. Chem. 117, 243 (1981).

[225] B. Pettinger, M.R. Philpott and J.G. Gordon II, Surface Sci. (in print).

[226] R.K. Chang, personal communication.

[227] R. Dornhaus, M.B. Long, R.E. Benner and R.K. Chang, Surface Sci. 93, 240 (1980).

[228] R.E. Benner, R. Dornhaus, R.K. Chang and B.L. Laube, Surface Sci. 101, 341 (1980).

[229] E.M. Stuve, R.J. Madix and B.A. Sexton, Surface Sci. 111, 11 (1981).

[230] E. Yeager, W.E. O'Grady, M.Y.C. Wu and P. Hagaus, J. Electrochem. Soc. 125, 346 (1978).

[231] A.T. Hubbard, R.M. Ishikawa and J. Kalekaau, J. Electroanal. Chem. 86, 271 (1978); R.M. Ishikawa and A.T. Hubbard, J. Electroanal. Chem. 69, 317 (1976).

[232] R.N. Ross, J. Electroanal. Chem. 76,139 (1977); R.N. Ross, J. Electrochem. Soc. 126, 67 (1979).

[233] There is evidence that the layer formed by adsorption of molecules from solution undergoes phase transitions in which the orientation of the adsorbed molecules change (A.T. Hubbard, to be published). Such phase transitions have been observed in UHV by J. Demuth, K. Christmann and P.N. Sanda, Chem. Phys. Lett. 76, 201 (1980).


DAT
ILM